



STUDY REPORT

SR 288 (2013)

Update of New Zealand's Atmospheric Corrosivity Map

Z.W. Li, N.J. Marston and M.S. Jones



The work reported here was funded by BRANZ from the Building Research Levy.

© BRANZ 2013
ISSN: 1179-6197

Update of New Zealand's Atmospheric Corrosivity Map

BRANZ Study Report SR 288

Z.W. Li, N.J. Marston and M.S. Jones

Reference

Li ZW, Marston NJ and Jones MS. 2013. 'Update of New Zealand's Atmospheric Corrosivity Map'. BRANZ Study Report 288. BRANZ Ltd, Judgeford, New Zealand.

Abstract

Atmospheric corrosion testing was conducted at thirty-nine exposure sites across New Zealand. The corrosion rates of mild steel and hot dip galvanised zinc coated coupons were measured after one year of exposure, and were compared with those obtained in the original BRANZ surveys of the 1980s to determine whether atmospheric corrosion behaviour of metals has changed over the past three decades. No nationwide, universal trend was found in the results of this current work, as the changes in corrosion rates derived at different sites exhibited different relative behaviours. At a limited number of sites the new corrosion rate data for mild steel and/or zinc was significantly different from the old data. However, at most sites the new data appears to be comparable with the old data, indicating that a more complete atmospheric corrosion rate data set can be established by combining BRANZ previous and present studies.

The trends for typical climatic parameters (ambient temperature, rainfall, relative humidity, wind speed) over the past three decades were derived using data retrieved from NIWA's National Climate Database. At most exposure sites, the average annual ambient temperature had increased slightly, whilst relative humidity and wind speed decreased slightly. The variations in rainfall and wet days were complex and no uniform trend was found.

Correlations between the long- and short-term trends for individual climatic factors and changes in metal corrosion rates are discussed in detail in this report. However, it was not possible to establish a strong relationship between each climatic factor and metal corrosion rate. Overall, it wasn't possible to derive a clear relationship between variations in New Zealand climate over the past thirty years and atmospheric corrosion behaviour.

Based mainly on the one year corrosion rates of mild steel, measured in 2011 – 2012, the current pair of atmospheric corrosivity maps, shown in NZS 3404 and NZS 3604, appear to have limitations in their zone boundary definitions for some regions. Recommendations for adjustments to the zone boundaries defined by the map shown in NZS 3604 are given later in this report.

Keywords: Atmospheric corrosion; mild steel; zinc; mapping; climate change

Acknowledgments

This work was funded by the Building Research Levy. BRANZ also acknowledges MetService, NIWA and property owners for allowing the installation of exposure racks on their premises.

The PDFs of Figure 20 – North Island corrosivity zone map, Figure 22 – Auckland corrosivity zone map, Figure 23 – Wellington corrosivity zone map, and Figure 25 – Dunedin corrosivity zone map from the following New Zealand Standard NZS 3404.1:2009 – Steel Structures Standard – Part 1: Materials, fabrication, and construction had been provided by the Standards New Zealand under licence 001020. Please refer to the Standard for full details, available for purchase from www.standards.co.nz.

Contents

1. INTRODUCTION	1
2. LITERATURE REVIEW	1
2.1 Atmospheric Corrosion.....	1
2.1.1 Factors Affecting Atmospheric Corrosion	1
2.1.2 Atmospheric Corrosion Category.....	4
2.1.3 Atmospheric Corrosion Testing.....	4
2.1.4 Commonly Used Testing Materials	6
2.1.5 International Standard Classification.....	10
2.2 CLIMATE CHANGE.....	11
2.2.1 Global Prospective	11
2.2.2 New Zealand.....	11
3. ATMOSPHERIC CORROSIVITY OF NEW ZEALAND	12
3.1 1980s Surveys	12
3.2 Atmospheric Corrosivity Map in NZS 3604	13
3.3 Atmospheric Corrosivity Map in NZS 3404	13
4. OBJECTIVE OF CURRENT RESEARCH.....	13
5. EXPERIMENTAL.....	16
5.1 Retrieval of Climate Data	16
5.2 Atmospheric Corrosion Rate Measurement.....	16
5.2.1 Methodology	16
5.2.2 Sample.....	16
5.2.3 Exposure Site	17
5.2.4 Rack Installation.....	21
5.2.5 Corrosion Rate Measurement.....	22
6. RESULTS.....	23
6.1 Changes in Climatic Factors.....	23
6.1.1 Average Ambient Temperature	23
6.1.2 Rainfall and Wet Days.....	25
6.1.3 Relative Humidity.....	28
6.1.4 Solar Irradiation.....	30
6.1.5 Wind Speed	31
6.2 Atmospheric Corrosion.....	36
6.2.1 Corrosion Morphology	36

6.2.2	Corrosion Rate	49
7.	DISCUSSION.....	51
7.1	Effect of Starting Time	51
7.2	Effect of Climatic Factors	52
7.2.1	Ambient Temperature	52
7.2.2	Humidity.....	53
7.2.3	Rainfall	55
7.2.4	Wind Speed	58
7.2.5	Wind Direction	60
7.2.6	Solar Irradiation.....	60
7.3	Potential Impacts on Current Atmospheric Corrosivity Maps.....	60
7.3.1	Auckland Region	62
7.3.2	Wellington Region	63
7.3.3	Otago Region	65
7.3.4	Potential Adjustment to Current NZS 3604 Map	67
8.	SUMMARY	71
9.	REFERENCES	72
	APPENDIX.....	81

Figures

Page

Figure 1. Atmospheric corrosion zone definition for the North Island of New Zealand (NZS 3604:1999 (Left) and 2011 (Right)).....	14
Figure 2. Atmospheric corrosion zone definition for the South Island of New Zealand (NZS 3604:1999 (left) and 2011 (right))	15
Figure 3. Exposure rack carrying mild steel and hot dip galvanised steel coupons used in the present study.....	17
Figure 4. Atmospheric corrosion exposure sites in North Island except Wellington.....	18
Figure 5. Atmospheric corrosion exposure sites in Wellington region	19
Figure 6. Atmospheric corrosion exposure sites in Dunedin region.....	20
Figure 7. Atmospheric corrosion exposure sites in Greymouth and Invercargill regions.....	21
Figure 8. Atmospheric corrosion exposure rack installed at Metservice's weather station at Paraparaumu Airport	22
Figure 9. Composite series of annual mean air temperatures for Auckland from 1900 to 2009 (NIWA's result).....	23
Figure 10. Annual mean air temperatures for Auckland Airport from 1980 to 2010 (Linear fitting to these data derived a temperature increase trend of 0.0196 °C/year which is slightly higher than that of NIWA's composite series from 1900 to 2009) (BRANZ's result).....	23
Figure 11. Composite series of annual mean air temperatures for Wellington (Kelburn) from 1900 to 2009 (NIWA's result).....	24
Figure 12. Annual mean air temperatures for Wellington (Kelburn) from 1980 to 2010 (Linear fitting to these data derived a temperature increase trend of 0.0063 °C/year which is slightly lower than that of NIWA's composite series from 1900 to 2009) (BRANZ's result).....	24
Figure 13. Composite series of annual mean air temperatures for Musselburgh (Dunedin) from 1900 to 2009 (NIWA's result).....	25
Figure 14. Annual mean air temperatures for Dunedin Airport from 1980 to 2010 (Linear fitting to these data derived a temperature increase trend of 0.0117 °C/year which is slightly higher than that of NIWA's composite series from 1900 to 2009) (BRANZ's result).....	25
Figure 15. Annual rainfall and wet days at Auckland Airport from 1980 to 2010 (Linear fitting showed a very gentle decreasing trend for rainfall and a small increase for wet days)	26
Figure 16. Annual rainfall and wet days at Kelburn (Wellington) from 1980 to 2010 (Linear fitting to these data showed an increasing trend for rainfall and wet days).....	27
Figure 17. Annual rainfall and wet days at Dunedin Airport from 1980 to 2010 (Linear fitting to these data showed a small decreasing trend for rainfall and wet days)	28
Figure 18. Mean 9am annual relative humidity for Auckland Airport from 1980 to 2010	29
Figure 19. Mean 9am annual relative humidity for Kelburn from 1980 to 2010	29
Figure 20. Mean 9am annual relative humidity for Dunedin Airport from 1980 to 2010	30
Figure 21. Mean daily global radiation at Auckland Airport from 1980 to 2010	30
Figure 22. Mean daily global radiation at Kelburn from 1980 to 2010	31
Figure 23. Mean daily global radiation at Dunedin Airport from 1980 to 2010	31
Figure 24. Mean annual wind speed at Auckland Airport from 1980 to 2010.....	32
Figure 25. Mean annual wind speed at Kelburn from 1980 to 2010	32

Figure 26. Mean annual wind speed at Dunedin Airport from 1980 to 2010	33
Figure 27. Typical morphology of mild steel coupons after one year exposure at Waitoki	36
Figure 28. Cross-sectional morphology of mild steel coupons after one year exposure at Waitoki (200×)	37
Figure 29. Typical morphology of hot dip galvanised steel coupons after one year exposure at Waitoki	38
Figure 30. Typical morphology of mild steel coupons after one year exposure at Auckland Airport	39
Figure 31. Cross-sectional morphology of mild steel coupons after one year exposure at Auckland Airport (200×)	40
Figure 32. Typical morphology of hot dip galvanised steel coupons after one year exposure at Auckland Airport	40
Figure 33. Typical morphology of mild steel coupons after one year exposure at Gracefield, Lower Hutt	41
Figure 34. Cross-sectional morphology of mild steel coupons after one year exposure at Gracefield, Lower Hutt (200×)	42
Figure 35. Typical morphology of hot dip galvanised steel coupons after one year exposure at Gracefield, Lower Hutt	43
Figure 36. Typical morphology of mild steel coupons after one year exposure at Tiwai Point	44
Figure 37. Cross-sectional morphology of mild steel coupons after one year exposure at Tiwai Point (200×)	45
Figure 38. Inclusions of unknown composition found on the groundward surface of the mild steel samples exposed at Tiwai Point (400×)	45
Figure 39. Typical morphology of hot dip galvanised steel coupons after one year exposure at Tiwai Point	46
Figure 40. Typical morphology of mild steel coupons after one year exposure at Forbury, Dunedin	47
Figure 41. Cross-sectional morphology of mild steel coupons after one year exposure at Forbury, Dunedin (200×)	48
Figure 42. Typical morphology of hot dip galvanised steel coupons after one year exposure at Forbury, Dunedin	49
Figure 43. Corrosion zone boundary definition in NZS 3404 and NZS 3604 maps with the mild steel corrosion rates derived from the present study (2011 – 2012)	62
Figure 44. Corrosion zone boundary definition in NZS 3604 map for Wellington region	63
Figure 45. Corrosion zone boundary definition in NZS 3404 map for Wellington region with mild steel corrosion rates derived from the present study (2011 – 2012)	64
Figure 46. Corrosion zone boundary definition in NZS 3604 map for Otago region	66
Figure 47. Corrosion zone boundary definition in NZS 3404 map for Otago region with mild steel corrosion rates derived from the present study (2011 – 2012)	66

Tables

Page

Table 1. ISO 9223 Atmospheric corrosion classification (based on one year corrosion rates - g/m ²)	10
Table 2. Chemical composition of metallic coupons used in the present study (wt.%)	17
Table 3. Summary of changes in typical climatic factors observed at some exposure sites ..	34
Table 4. Corrosion rates of mild steel and hot dip galvanised zinc coating derived from BRANZ previous and present studies.....	49
Table 5. Changes in relative humidity (RH) and atmospheric corrosion rate	54
Table 6. Changes in rainfall and atmospheric corrosion rate.....	56
Table 7. Changes in wind speed and atmospheric corrosion rate	59
Table 8. Corrosion categories based on first year corrosion rate of mild steel.....	67
Table 9. Summary of one year atmospheric corrosion rate of mild steel, exposure site location and potential adjustment to NZS 3604 maps.....	68

1. INTRODUCTION

When a metal is exposed to the atmosphere, a thin aqueous layer will form through various interactions between atmospheric water vapour and the metal surface. This aqueous layer, containing dissolved gaseous and/or solid constituents from the atmosphere, provides suitable conditions for electrochemical processes. Coupling of these reactions results in attack of the metal surface. This process is commonly defined as atmospheric corrosion of metals [Syed 2006].

Under practical exposure conditions, the environment to which the metal is exposed is much more complicated. A wide variety of reactions can be involved in the corrosion processes, leading to various corrosion morphologies and failure modes. One typical model proposed to explore the chemistry of metal or metal oxide surfaces exposed to the atmosphere, and to perform theoretical mechanistic investigation of atmospheric corrosion process, is the so-called 'GILDES' computer model [Graedel 1996; Farrow et al., 1996].

Many structures and plant/infrastructure are exposed to the atmosphere, meaning that atmospheric corrosion accounts for the highest cost and metal loss among all corrosion forms. It is a major contributor (>50%) to overall corrosion induced costs, which have been estimated to be 2-6% of GDP for most developed countries [Anon 2002; Elisabete and Almeida 2005]. It was estimated that the total cost of corrosion to the U.S. economy exceeded \$1 trillion in 2012 [G2MT 2012]. In New Zealand, corrosion related costs are thought to be of the order of 2.5% of GDP [Boardman 2008]. Hence, research and testing aimed at developing a better understanding of monitoring and mapping atmospheric corrosivity are needed for the development, specification and selection of materials, protective coating systems and maintenance schemes.

The building and housing sector is a key component of the New Zealand economy and contributes 4-5% of GDP by employing 8% of the New Zealand workforce. The nation's housing stock is valued at approximately 600 billion dollars [Department of Building and Housing 2010]. Metallic components are widely used in building and construction for claddings, fastening and decorative purposes. Their resistance to corrosion from a variety of atmospheric environments is highly relevant to the New Zealand Building Code (NZBC) and relevant Standards. Updated knowledge is needed to ensure that any metallic components, products or structures, when chosen as acceptable or alternative solutions for building and construction, will meet or exceed the performance requirements of the NZBC, for use within the specified geographic environments.

2. LITERATURE REVIEW

2.1 Atmospheric Corrosion

2.1.1 Factors Affecting Atmospheric Corrosion

Atmospheric corrosion is mainly influenced by climatic parameters and atmospheric pollutants [Brown and Masters 1982].

2.1.1.1 Relative humidity

Relative humidity (RH) is closely related to the rate of atmospheric corrosion [Mansfeld 1979]. There is a critical threshold of RH, below which corrosion will not happen on a metal because there is insufficient moisture to create an electrolyte layer on the surface [McCafferty 2010]. This value is highly dependent on the surface condition of the metal and also the pollution level of the surrounding air. The primary critical relative humidity for a clean aluminium surface in unpolluted air is about 66%, which appears to be

virtually identical for all metals. If the metal is covered with any corrosion products, a second critical relative humidity may also exist. In the case of iron and steel, a tertiary critical humidity appears. At ~60% RH rusting commences at a very slow rate, but the corrosion rate increases sharply at 75-80% RH. This is probably due to capillary condensation of moisture within the rust layer. At ~90% RH the tertiary increase in corrosion rate is observed.

2.1.1.2 Temperature

Ambient temperature might not be very important for atmospheric corrosion and it is, perhaps, more important to consider the surface temperature of the metal. An increase in temperature will accelerate mass transportation and electrochemical reactions within the absorbed electrolyte. This will tend to accelerate corrosion processes at constant environmental humidity. That said, RH will normally decrease when the temperature is increased, leading to a decrease in time of wetness (ToW) and the overall corrosion rate [Roberge 1999]. Therefore, temperature tends to affect atmospheric corrosion in complex ways. Atmospheric corrosion of iron was found to peak at an ambient temperature around 38°C [Shaw and Andersson 2010]. Other metals, such as copper and zinc, have also shown certain temperature dependence [Al-Hazza and Al-Abdullatif 1995].

2.1.1.3 Atmospheric pollutants

Airborne pollutants, such as many gases, aerosols and solid particulates, when dissolved or suspended within the aqueous layer sitting on the metal surface, may affect corrosion through various mechanisms. For example, the moisture layer on the surface will become more conductive and, therefore, offer a lower resistance to oxygen diffusion. Consequently, electrochemical reactions that involve oxygen may take place more readily [Vargel 2004].

Chloride

Chlorides mainly come from the sea, road de-icing salts, dust binders and municipal incinerators. In coastal areas, the wind sweeping over the oceans can carry chloride-containing particles over tens or even hundreds of kilometres. Deposition of hygroscopic salts, such as NaCl and MgCl₂, can promote corrosion at lower relative humidities. Chlorides can also directly participate in electrochemical corrosion reactions by influencing the morphology and composition of the growing rust layer [Ghali 2010; Ma et al., 2009]. On ferrous metals, chloride ions are known to compete with hydroxyl ions to combine with ferrous cations, leading to the formation of unstable and soluble iron-chloride complexes, which have a lower passivation effect within surface films than stable iron-hydroxyl species. Studies have shown corrosion rates up to 2.75 times higher when chloride is present than when it is not [Suzuki and Robertson 2011]. A direct relationship between airborne salt level (salinity) or surface salt deposition and corrosion rate has been observed with many metals [Qu et al., 2002a].

Most cities in New Zealand are coastal, and many buildings are within 5 km of the sea. Measurements using salt candles installed at Oteranga Bay, Wellington, found that the chloride deposition rate could be as high as 3000 mg/m²/day and was also season dependent [Haberecht and Kane 1999]. Chloride may play an important role in the deterioration of various building and construction materials. Previous studies by BRANZ suggest that sea salt mediated corrosion rates at a distance of 20 km and more inland in New Zealand were higher than those obtained on continental land masses [Duncan and Balance 1988].

Sulphur dioxide

Sulphur dioxide (SO₂) is mainly released from the combustion of sulphur containing fossil fuels/coins and from metallurgical, petrochemical and pulp/paper-making

processes. In areas without significant industrial activities, the concentration of SO₂ in the air normally shows a seasonal variation; being much higher during winter than in summer. It has a high solubility in water (~2600 times more soluble than oxygen) and dissolves easily in the moisture layer on the metal surface to form sulphuric anhydride (H₂SO₃) and then sulphuric acid (H₂SO₄). The presence of sulphate ions on iron and steel leads to the formation of iron sulphate (FeSO₄), which can be hydrolysed to release sulphate ions. This is an auto-catalytic process [Badea et al., 2011]. The presence of SO₂ also leads to a decrease in the critical relative humidity for corrosion initiation. This, in effect, increases the corrosivity of a particular set of environment conditions. Therefore, sulphur dioxide can damage or accelerate the degradation, of many building materials, such as stone, concrete, metal and organic coatings [WBK & Associates Inc 2003].

In New Zealand, the main sources of sulphur dioxide are transport, coal-fired and diesel boilers. Monitoring indicates that the 1-hour maximum of SO₂ in Auckland and Christchurch could reach about 200-300 µg/m³. In other cities, e.g. Hamilton, Wellington and Dunedin, SO₂ levels are generally considered to be low. SO₂ levels at most cities have fallen in recent years, though sites near industrial sources, such as Woolston and Hornby in the Canterbury region, have occasionally recorded high levels [Ministry for the Environment 2007].

Nitrogen oxide

Nitrogen oxides (NO_x) are mainly released from combustion processes in power plants and vehicles. Most nitrogen oxides are emitted as nitric oxide (NO). Under solar irradiation and in the presence of moisture and catalysts, NO can be rapidly oxidised to nitrogen dioxide (NO₂). NO₂ is likely to be further oxidised to form nitric acid, though this process will be very slow. The detrimental effects of NO₂ on atmospheric corrosion of structural materials, particularly steel, copper and zinc, are not well characterised [Arroyave and Morcillo 1995].

In New Zealand, about 80-90% of nitrogen oxides are produced by transportation in all the main centres of population. Monitoring at a site near Khyber Pass Road, Auckland showed that the concentration of NO₂ could be higher than 400 µg/m³ (1-hour maximum) in the early 2000s. Nitrogen oxides emissions have increased slightly since 1998 in Auckland, due mainly to the increase in the number of diesel vehicles [Ministry for the Environment 2007].

Carbon dioxide

Carbon dioxide (CO₂), released mainly from combustion of coal and oil, was originally thought to be essential for atmospheric corrosion, according to the carbonic acid theory, but is currently considered of relatively minor importance. The solubility of CO₂ in water is relatively low. Moreover, in the presence of CO₂, zinc corrosion induced by NaCl could be partly inhibited [Falk et al., 1998; Lindström et al., 2000] and corrosion product layers containing protective carbonates are found on zinc exposed to atmospheres containing CO₂. A laboratory study also found that corrosion of aluminium was about 10-20 times faster in CO₂-free humid air compared to that in air containing ambient levels of CO₂ [Bengtsson Blücher et al., 2001].

Ozone

Ozone (O₃) of itself has little effect on the corrosion of metals. However, ozone has a high oxidising power. For example, it may change airborne H₂S to S, SO₂ and to SO₃. Thus, synergistic effects with other atmospheric pollutants, typically, SO₂ and NO₂, could become important at low levels. Several lab-scale studies have shown that atmospheric corrosion of copper and zinc could be enhanced by the presence of O₃ [Svensson and Johansson 1993a; Aastrup et al., 2000].

Auckland, Christchurch and Hamilton have the highest potential for ozone pollution during summer. The 1-hour maximum of Ozone levels at Musick Point, Auckland was about 140 $\mu\text{g}/\text{m}^3$ during the period of 1996-2005 [Ministry for the Environment 2007].

Hydrogen sulphide

Hydrogen sulphide (H_2S) is mainly emitted by oil refineries, paper-making industries and food processing plants. In New Zealand, it is often encountered within, and close to, geothermal areas. H_2S is extremely corrosive to most metals. In the presence of water, it may react with metal and/or its oxides to form sulphides and/or sulphates, as observed on copper [Lenglet et al., 1995; Tran et al., 2003].

Ammonia

Principal sources of ammonia (NH_3) are animals, fertiliser production plants and cleaning detergents. In the aqueous phase, NH_3 can establish equilibrium with NH_4^+ and increase the oxidation rate of $\text{S}(4^+)$ to $\text{S}(6^+)$. It may also affect the chemistry of atmospheric corrosion by neutralising acidic pollutants such as hydrochloric acid, nitric acid and sulphuric acid [Dehri et al., 2003].

Currently there is very little information about ambient ammonia concentrations and emission rates in New Zealand. The most common source of ammonia within New Zealand is likely to be from productive farmland [Ministry for the Environment 2000].

2.1.2 Atmospheric Corrosion Category

Atmospheric corrosion can be classified into dry, damp and wet categories, depending on the forms of water/moisture present on the metal surface. The damp and wet atmospheric corrosion classifications are characterised by the presence of a thin, invisible water film or by visible deposits of dew, rain and sea-spray on the metal surface, respectively. According to the nature and amount of airborne pollutants involved in corrosion, the atmospheric environments to which the metal is exposed can be categorised into four typical groups [Tullmin and Roberge 2000]:

- Rural: This environment features minimal amounts of aggressive pollutants. The deposition rate of SO_2 and NaCl is typically lower than 15 $\text{mg}/\text{m}^2/\text{day}$. Corrosion is induced primarily by interactions between temperature, moisture, oxygen, small amounts of SO_x and CO_2 from combustion processes, and probably NH_3 released from farm fertilizers. Arid and tropical types are two extreme cases in this category.
- Urban: Major airborne pollutants are oxides of sulphur and nitrogen from vehicles and domestic fuel emissions. The deposition rate of SO_2 is higher than 15 $\text{mg}/\text{m}^2/\text{day}$ and that of NaCl lower than this value. These oxides, through chemical interactions with dew or fog, can generate highly aggressive acids.
- Industrial: High concentrations of SO_x and NO_x are released from heavy industrial manufacturing processes. Chlorides, phosphates, hydrogen sulphate and ammonia may also be in this atmosphere at low concentrations.
- Marine: This environment is influenced by fine, airborne chloride particles (deposition rate of NaCl higher than 15 $\text{mg}/\text{m}^2/\text{day}$).

2.1.3 Atmospheric Corrosion Testing

2.1.3.1 Corrosion coupon

This is the simplest approach for atmospheric corrosivity evaluation. Clean metallic coupons of standardised composition, dimensions and configuration are exposed to the atmosphere of interest. The most widely used metallic samples include mild steel (or low carbon steel), zinc, copper and aluminium. These samples, fixed on purpose-built

exposure racks, normally face directly towards the Equator, at an angle of 5, 45, or 90°. After a certain time, samples are retrieved and characterised for morphology and composition of corrosion products and measurements are made of weight loss and/or pit density/depth. Corrosion rates measured after one-year exposure are commonly used to classify the atmospheric corrosivity. However, it is not uncommon for programs to run for 10 – 20 years or longer to generate more reliable data. The corrosion rates measured after short-term exposure provide critical information about the interactions between metal and its surrounding environment and are commonly used for classification of environmental aggressivity, while the results after longer exposure periods provide information about the protective character of the layer of corrosion products developed [Wypych 2003; Dean 2005; Lawson 2005].

2.1.3.2 CLIMAT

The CLIMAT test (Classify Industrial and Marine Atmospheres), also known as ‘Wire-on-Bolt’ technique, is a relatively simple method for determining the corrosivity of an atmosphere [ASTM G 116; Hack 2005]. This method uses a helical coil of material wrapped around a coarsely threaded bolt. The high surface area/weight ratio offered by this configuration provides a much higher sensitivity compared with a flat coupon. Exposure times can, therefore, be significantly reduced, typically to 3 months. Wrapping aluminium wire onto copper or steel bolts provides the highest sensitivity in industrial and marine environments respectively. The percentage weight loss of the aluminium wires are commonly expressed as the industrial and marine corrosion indexes (ICI and MCI) respectively. This test can also detect seasonal variation of atmospheric corrosivity, which would be harder with testing using corrosion coupons.

However, the CLIMAT method does have several limitations for the assessment of atmospheric corrosivity:

- It only provides comparative corrosivity information and an indication of relative atmospheric corrosion severity. Five levels, commonly known as Negligible, Moderate, Moderately Severe, Severe and Very Severe, are defined depending upon the average percent weight loss measured with the aluminium wires. However, these corrosion indices are not correlated with the corrosion categories identified in international or national standards (e.g. ISO 9223, AS/NZS 2312 and AS/NZS 2728). Further, correlations between these corrosivity levels and the actual corrosion rates of metal have not been explored and/or established.
- Although weight loss percentages can be derived for the aluminium wires, they don’t reflect the actual corrosion rates of aluminium when exposed to the atmosphere due to the significantly altered sample configuration and galvanic corrosion effects. Thus, this technique cannot provide any accurate information regarding deterioration behaviour, corrosion rate and failure mechanism of metallic components when exposed to the atmosphere concerned. However, reliable corrosion rates are always needed for specification of materials, surface protection systems and maintenance schemes. Also, a clear understanding of deterioration behaviour is critical to materials selection for certain applications. For example, pitting is commonly observed with metals relying on passivation. Although it leads to very small weight loss or thickness reduction, it is very hazardous for exterior building claddings.

2.1.3.3 Sensors

Electrochemical sensors, which measure electrical current and/or potential in real time and in a highly sensitive manner, have been utilised to measure or monitor atmospheric corrosion. The operating principles or techniques behind these sensors typically include electrochemical impedance spectroscopy (EIS), zero resistance ammetry (ZRA), electrochemical noise (EN) and linear polarisation resistance (LPR) [Hladky et

al., 1986; Diwan et al., 1998; Roberge et al., 2000; Shitanda et al., 2009; Nyrkova et al., 2012]. The quartz crystal microbalance (QCM) is another approach that uses the frequency response of a piezoelectric crystal to mass changes for atmospheric corrosion measurement [Olsson and Landolt 2005]. However, these sensors have difficulties in monitoring long-term atmospheric corrosivity and these derived results might not be able to reflect deterioration of large components exposed to real world situations. Interpretation of results also requires intensive skills and background knowledge.

2.1.4 Commonly Used Testing Materials

2.1.4.1 Carbon steel

Mild steel (or carbon steel) is widely used for plant and/or infrastructure due to its low cost and relatively good mechanical properties. As a result, the phenomena and mechanisms associated with the atmospheric corrosion of mild steel have been extensively researched. Quantification of its degradation kinetics in different atmospheric environments is also fundamental to the development of methodologies and/or standards that can be used to determine the aggressivity of atmospheres and to predict the service life of metallic structures [Morcillo et al., 2011].

When exposed to a dry and clean atmosphere, a stable, thin and relatively protective film will be formed on the surface of carbon steel through interactions of oxygen, water and iron [Graedel and Frankenthal 1990]. When exposed to near-neutral aqueous environments, this film will change into green rust which can be subsequently transformed into a fragile, brownish layer composed of iron oxides and/or hydroxides. For example, after 13 years of exposure in Spain, lepidocrocite (γ -FeOOH), goethite (α -FeOOH), magnetite (Fe_3O_4) and/or maghemite (γ - Fe_2O_3) were detected in the rust layer.

In marine atmospheres, however, corrosion rates are higher and akaganeite (β -FeOOH) has been found in considerable proportions [de la Fuente et al., 2011; Oh et al., 1999; Kamimura et al., 2002; Asami and Kikuchi 2003; Cook 2005]. Sulphates and chlorides were detected in the inner adherent strata of the rust, probably as a consequence of ion migration.

Environmental humidity plays a major role in the atmospheric corrosion of carbon steel. A moisture layer sitting on the metal surface provides a suitable environment for many chemical and electrochemical processes to proceed. The presence of hygroscopic chloride salts, such as NaCl and MgCl_2 , also increases electrolyte conductivity and enables the formation of this moisture layer at much lower environmental RH levels.

Absorption of SO_2 into the surface aqueous layer will acidify the corrosive media and produce FeSO_4 , which undergoes hydrolysis reactions to form oxyferric hydroxides and probably regenerates H_2SO_4 [Yamashita et al., 1994]. If NaCl particles are present on a carbon steel surface, these two pollutants will work synergistically at RH levels which have generally been considered too low to start SO_2 induced corrosion. The corrosion rate of carbon steel with NaCl and SO_2 at 90% RH has been shown to be approximately 14 times higher than that caused by NaCl alone [Ericsson 1978]. On the other hand, long-term atmospheric exposure tests indicated that in the presence of SO_2 in a marine environment, the phase transformation from γ -FeOOH to stable, protective amorphous α -FeOOH could be promoted to some extent, leading to lower corrosion rates compared with those exposed to pure marine environments [Singh et al., 2008].

Other pollutants, including NO_x , O_3 , organic acids and particulate matter can also affect the atmospheric corrosion of carbon steel, even at low concentrations.

Corrosion rates of mild steel in different environments can generally be summarised as follows:

- Rural: 4-65 $\mu\text{m}/\text{year}$;
- Urban: 23-71 $\mu\text{m}/\text{year}$;
- Industrial: 26-175 $\mu\text{m}/\text{year}$; and
- Marine: 26-104 $\mu\text{m}/\text{year}$.

In New Zealand, the first year corrosion rate of mild steel could be ranged from 2 to 600 $\mu\text{m}/\text{year}$, according to BRANZ previous field test [Duncan and Corder 1991]. The extremely high corrosion rates were generally found in the geothermal regions.

2.1.4.2 Zinc

Zinc and its alloys have been used in strip form for roofing on a large scale in Europe and elsewhere since about 1960. One of the biggest uses of zinc is in making coatings for steel, as zinc will corrode preferentially to give cathodic protection to iron. Globally, some 4 million tonnes of zinc are used annually to protect around 100 million tonnes of steel. This represents almost half the total world consumption of zinc. Building and construction industries use at least two thirds of all the coated steel strips produced, mainly for roofing and cladding applications [Wall 1998].

Atmospheric corrosion of zinc occurs via several critical steps [Graedel 1989a]. At the very beginning, zinc reacts with oxygen to form a thin layer of zinc oxide, ZnO (zincite). In the presence of water, zincite promptly transforms into hydroxides. After extended exposure in mildly polluted atmospheres with CO₂, zinc carbonate and hydrozincite (Zn₅(OH)₆(CO₃)₂) may form. In moderately polluted atmospheres zinc hydroxyl sulphates, such as Zn₄SO₄(OH)₆·nH₂O, and in marine sites basic chlorides, such as simonkolleite [Zn₅(OH)₈Cl₂·H₂O] have been found.

SO₂ can significantly affect atmospheric corrosion of zinc [Manning 1988]. In environments with high concentrations of SO₂, the corrosion products formed may have high contents of zinc sulphate, which has a relatively high solubility in aqueous solutions. It, therefore, provides limited protection to the underlying substrate. Consequently, no decline in corrosion rate with exposure time was observed. Even in environments containing low, but measureable SO₂ concentrations, the decrease in corrosion rate with time could also be small. A linear corrosion kinetic behaviour has been verified in long-term exposure tests [de la Fuente et al., 2007].

O₃ may oxidise loosely bound, four-valent sulphur and increase the deposition rate of SO₂ on zinc and, therefore, increase the corrosion rate of this metal. O₃ alone has negligible effect on the corrosion of zinc [Svensson and Johansson 1993a].

NO₂ also has a limited effect on zinc corrosion. However, a synergistic effect with a combination of NO₂ and SO₂ has been identified at 90-95% RH. NO₂ could catalyse the oxidation of SO₂ to sulphate [Svensson and Johansson 1993a]. The increased formation of sulphate and hydrogen ions leads to the dissolution of solid corrosion products and then to an increased rate of metal dissolution.

The deposition of solid particulates can accelerate zinc corrosion, particularly via localised corrosion mechanisms, since partially dissolved components can increase the conductivity of the surface layer [Almeida et al., 2000a; Qu et al., 2004; Qu et al., 2005]. Here, the effects of different particulates were investigated at 85% RH and 40°C. The mass loss decreased in the order NH₄Cl > NaCl > Na₂SO₄ > (NH₄)₂SO₄; that is chlorides were more corrosive than sulphates. This was attributed to the greater hygroscopicity of chlorides compared to sulphates. Furthermore, corrosion rates influenced by NaCl deposition increased with humidity and the maximum was observed between 70 and 80% RH [Lobnig et al., 1996]. The amount of NaCl deposition also

affected the zinc corrosion rate. Initially, the corrosion rate increased with the deposition, but it decreased with moderate to high deposition. The authors concluded that zincite and hydrozincite could react with aggressive chloride ions to form simonkolleite which could provide some protection and reduce aggressive soluble chlorides [Almeida et al., 2000b; Chen et al., 2006].

The co-existence of NaCl particles and SO₂ in the surface layer can accelerate the initial atmospheric corrosion rate of zinc since:

- the conductivity of the surface aqueous film will be quickly enhanced by sulphate formation, and electrochemical corrosion will accelerate more rapidly in the presence of NaCl [Qu et al., 2002b]; and
- the formation of insoluble chloride compounds will be prevented [Chen et al., 2008].

However, the presence of SO₂ slows down the corrosion of zinc somewhat at higher concentrations of NaCl, due to the formation of sodium zinc chlorohydroxysulphate [NaZn₄Cl(OH)₆SO₄·6H₂O] or zinc chlorohydroxysulphate [Zn₄Cl₂(OH)₄SO₄·5H₂O] [Svensson and Johansson 1993b].

Ambient concentrations of CO₂ could inhibit NaCl induced corrosion of zinc, although in the absence of NaCl, CO₂ enhanced the corrosion rate of zinc slightly, due to acidification of the surface electrolyte. The corrosion rate of zinc at 22°C was 3-4 times smaller in air containing 350 ppm CO₂ compared with CO₂-free air in the presence of 70 µg/cm² NaCl particles [Lindström et al., 2000].

Atmospheric corrosion of zinc is also seasonally dependent [Xu et al., 2002]. The highest rates were traditionally reported in winter but recently, higher rates have been found in summer in Japan and in September in the United States. The winter maximum has been attributed with some confidence to the winter maximum in the atmospheric SO₂ concentration, and, perhaps, also with a greater tendency for surfaces to remain wet.

The corrosion rates of zinc in different environments are given in the literature as follows:

- Rural: 0.2-3 µm/year;
- Urban: 2-16 µm/year;
- Industrial: 2-16 µm/year; and
- Marine: 0.5-8 µm/year.

In New Zealand, the first year corrosion rate of zinc coating on steel was ranging from 0.1 to 20 µm/year, while after 10 years of exposure, the corrosion rate was much lower, 0.1-2.5 µm/year [Duncan and Cordner 1991; Haberecht et al., 1999]. High corrosion rates were normally observed in severe marine and geothermal environments.

2.1.4.3 Aluminium

Aluminium is a light-weight metal. It has a long history of structural and also non-structural applications [Mazzolani 2004]. Architectural applications of aluminium and its alloys in the built environment mainly include frames, facades, roof and wall claddings, windows, doors, balconies and conservatories.

Corrosion of aluminium occurs principally at physical defects, e.g. segregation of residual impurities and grain boundaries, and manifests as deep pits rather than as uniform surface recession.

In industrial environments, sulphur-containing compounds will be heavily involved in the corrosion processes of aluminium, and aluminium sulphate hydrate is the most

abundant corrosion product. Lab testing has confirmed that SO₂ can enhance aluminium corrosion due to acidification of the surface electrolyte that destabilises the alumina passive film [Bengtsson-Blücher et al., 2005]. In the presence of SO₂, other oxidising agents such as O₃ and H₂O₂ may also play a role in the atmospheric corrosion of aluminium. In lab experiments with high concentrations of NO₂, an acceleration of aluminium corrosion was found in humid air. However, in the simultaneous presence of NO₂ and SO₂ the reported corrosion rates were both higher and lower than that produced by SO₂ alone.

Chlorides in the atmosphere can cause significant localised corrosive attack to aluminium, though no specific compounds containing chloride and aluminium have yet been clearly identified on corroded aluminium. This might be because the solubility of the chloride-containing products prevents large build-ups. If trace CO₂ was present in the atmosphere, corrosion induced by chlorides could be somewhat inhibited. Some authors believe that CO₂ could neutralise the alkaline solution formed in the cathodic areas and solid carbonates could be formed [Bengtsson Blücher et al., 2006].

Aluminium corrodes rather slowly under most atmospheric conditions due to the formation of a continuous and uniform passive film with low solubility over a relatively wide pH range (4 – 8.6) [Vargel 2004]. However, accelerated corrosion does occur in marine and some urban environments with high levels of pollutants. The following ranges of corrosion rates have been reported [Graedel 1989b]:

- Rural: <0.1 µm/year;
- Urban: ~1 µm/year; and
- Marine: 0.4-0.6 µm/year.

Short and long term atmospheric exposure tests conducted in New Zealand showed that certain aluminium alloys performed very well in most regions with very low uniform corrosion rates, though their surfaces might suffer from pitting attack, particularly in the presence of chloride [Fahy 1980 & 1983; Duncan & Corder 1991].

2.1.4.4 Copper

Copper has been used as a water-proof roofing material since ancient times, giving many old buildings their greenish roofs and domes. It is simple to use and offers natural beauty and extreme durability. Architects today are taking advantage of the flexibility of copper as a distinctive external covering for many building elements, including roof slopes, cladding, soffits, fascias, flashings, gutters and downpipes.

Copper is not very chemically active in air. A freshly exposed surface will be oxidised slowly and a very thin layer will be formed through interactions with oxygen and water within a few days or weeks. The corrosion products are mainly composed of cupric and cuprous oxides, as well as cuprous hydroxides. This changes the colour from reddish brown to dark brown or black [Oesch and Faller 1997]. With extended exposure, a greenish-blue patina with a layered structure can be developed on the top of the oxide layer through various reactions with gaseous pollutants, ionic constituents of aerosol particles or ions in precipitation. Constituents detected in patina commonly include copper sulphate brochantite (Cu₄SO₄(OH)₆), antlerite (Cu₃SO₄(OH)₄), posnjakite (Cu₄SO₄(OH)₆·2H₂O), copper sulphides, copper chlorides (e.g. atacamite (Cu₂Cl(OH)₃)) and nitrates (e.g. gerhardite (Cu₂NO₃(OH)₃)) [Krätschmer et al., 2002].

The influence of SO₂ on copper corrosion is complex and not clearly understood [Anon 1991; Oesch and Heimgartner 1996]. Decreased atmospheric pollution levels including SO₂ appear to increase the time for the development of a green patina [FitzGerald et al., 2006] while acid rain, caused by high SO₂ concentrations, led to dissolution of patina in several countries [FitzGerald et al., 1998]. A corrosion-stimulating effect was found for a certain combination of SO₂, wind speed and time of wetness. Generally, the

presence of NO₂ could exert a corrosion-inhibiting effect. However, since a correlation between NO₂ and O₃ exists, the effect of NO₂ could be interpreted as a positive effect of O₃ or a combination of both.

A critical threshold for atmospheric salinity, approximately 20 mg/m²/day of Cl⁻, seems to differentiate copper corrosion behaviour in pure marine atmospheres. Below this threshold, copper behaves as in rural atmospheres. Above this threshold, corrosion accelerates notably [Morcillo et al.]. In metropolitan areas, the deposition of fine dust particles influences the corrosion rate of copper. The most abundant ions detected are SO₄²⁻ and NH₄⁺, with the ratio being between that of NH₄HSO₄ and (NH₄)₂SO₄. Several lab tests have demonstrated that exposures to (NH₄)₂SO₄ produced patinas with at least some of the characteristics of naturally grown patina [Lobnig et al., 1993; Lobnig et al., 1994]. The size of particles may also affect the corrosion rate. According to simulated atmospheric corrosion tests, smaller particles result in a higher corrosion rate than larger particles at equal amounts of deposition, due to the higher surface coverage of the smaller particles [Chen 2005].

The patina grown on copper is dense and protective in nature. Therefore, its surface presence could lead to a continuing decrease in corrosion rate with increasing exposure time. This is the main reason why copper is widely used as a building and construction material. The following ranges of corrosion rates in different environments have been reported for copper:

- Rural: 0.2-0.6 µm/year;
- Urban: 0.9-2.2 µm/year;
- Industrial: 1.5-2.5 µm/year; and
- Marine: 0.7-1.5 µm/year [de la Fuente et al., 2008].

2.1.5 International Standard Classification

The classification of the corrosivity of an atmosphere is important for specifying materials and corrosion protection measures to ensure adequate service life of metallic structures. The International Organisation for Standardisation (ISO) assesses the corrosivity of a specific environment by assuming that the atmospheric corrosivity is mainly determined by time of wetness and levels of atmospheric corrosive pollutants. Once the wetness, sulphur dioxide and chloride classes of a given environment are identified, the corrosivity class can be established and the rate of corrosion of the different materials can be estimated using the ISO guidelines. This was also supported by the largest ever worldwide exposure program known as ISOCORRAG [ISO 9223, 1991; ISO 9224, 1991; ISO 9225, 1991; Knotkova et al., 2010]. Five corrosivity categories have been identified based on corrosion rates of metals.

Table 1. ISO 9223 Atmospheric corrosion classification (based on one year corrosion rates - g/m²)

Category	Description	Mild Steel	Zinc	Aluminium	Copper
C1	Very low	<10	<0.7	~0	<0.9
C2	Low	10 – 200	0.7 – 5	<0.6	0.9 – 5
C3	Medium	201 – 400	5.01 – 15	0.6 – 2	5.01 – 12
C4	High	401 – 650	15.01 – 30	2.01 – 5	12.01 – 25
C5	Very high	651 – 1500	30.01 – 60	5.01 – 10	25.01 – 50

2.2 Climate Change

2.2.1 Global Prospective

Observations over past decades suggest that the world's climate is changing [Jackson 2009; Graßl 2009]. In addition to natural causes (e.g. changes in the Earth's orbit, the Sun's radiation intensity, the circulation of the ocean and the atmosphere, and volcanic activity) human activities have increased atmospheric concentrations of carbon dioxide (CO₂), methane (CH₄), nitrous oxide (N₂O) and other gases in trace amounts, enhancing greenhouse effect in the atmosphere [Serreze 2009]. Consequently, the world's climate will undergo significant change by 2030 and profound change by 2080 [Mullan et al., 2006]. It is very likely that all land regions will warm in the 21st century, according to IPCC assessment [Christensen et al., 2010].

Besides the warming-up of the climate, other climatic parameters also show changes. For example, average annual precipitation for the contiguous USA has increased by nearly 10% over the course of the 20th century [Roberge 2010]. A statistical model of daily precipitation was applied to summer data collected from eight countries: Australia, Canada, China, Mexico, Norway, Poland, the former Soviet Union and the USA. It was shown that the changes in mean monthly precipitation totals tend to have the most influence on the heavy precipitation rates in these countries. The increase in the probability of heavy precipitation is four times the increase in mean precipitation. Observations also showed that in each country (except China) mean summer precipitation had increased by at least 5% in the past century.

Increasing trends in specific humidity have been observed over most of the globe, with the main exceptions being Australia and parts of the Southern Ocean. The broad pattern of trends in specific humidity can be well explained by temperature trends.

2.2.2 New Zealand

Climate change and its direct and indirect impacts on the New Zealand built environment is an important topic of research at BRANZ. Efforts have been made to identify options for adaptation through cross-disciplinary assessments of building's vulnerability to climate changes [Bengtsson et al., 2007].

2.2.2.1 Average ambient temperature

Analysis clearly shows that mean air temperature in New Zealand is increasing, with an amplitude somewhat larger than that of the surrounding oceans [Christensen et al., 2007]. However, the magnitude of New Zealand temperature increase is likely to be only about two-thirds of the global mean temperature increase. This is largely because its climate is controlled by the South Pacific and Southern Ocean, which respond slowly to global temperature changes. NIWA's "Seven-Station" temperature series analysis revealed that the New Zealand wide warming trend is about 0.9°C/century. However the 100-year trend has increased slightly at some sites and decreased slightly at others. In addition, the highest temperature increase in New Zealand is likely to be in the north of the country (e.g. Auckland, 1.53°C/century) and the least warming in the east of the South Island, especially in winter (e.g. Dunedin, 0.58°C/century) [Ministry for the Environment 2001; Mullan et al., 2010].

2.2.2.2 Rainfall and wet days

Rainfall is projected to increase in the west of the country (especially South Island) and decrease in many eastern regions [Christensen et al., 2007]. The frequency and magnitude of extremely heavy rainfall events could increase in many areas, even where the annual average rainfall undergoes little change, although it cannot be ruled out that no discernible increase could still occur [Reisinger et al., 2010].

2.2.2.3 Relative humidity

In past decades most New Zealand cities had the lowest RH during summer, due to the frequent combination of warm sunny conditions and longer days (maximum potential for drying) and the highest RH in winter, due to colder, cloudier and more unsettled damper conditions (minimum potential for drying). The mean 9am annual RH was found to be very close to 80% for most cities.

2.2.2.4 Sea level

Sea levels are expected to rise under global warming. During the 20th century, local sea levels in New Zealand have risen between 10 and 25 cm [Ministry for the Environment 2001]. Under the projected further temperature increases, sea level rise during the 21st century could be between 1 and 4 times as fast as during the 20th century. Analysis showed that the sea level at the port of Auckland remained almost static for the past 25 years, but increased markedly 5-7.5 cm during 1999 – 2000. However, uncertainties are large in consideration of New Zealand landmass uplift due to the removal of glacial ice-caps and plate tectonic movements over short and long time frames. Sea levels around New Zealand are, therefore, not expected to rise gradually, but to exhibit stepwise changes, which can locally offset or enhance the long-term sea level rise projected under global warming [Ministry for the Environment 2001].

2.2.2.5 Solar irradiation

Ultraviolet (UV) radiation over New Zealand increased by 12% between 1989 and 1999. This is associated with the depletion of stratospheric ozone [McKenzie et al., 1999]. Data since the late 1990s suggests that UV in New Zealand most likely showed a decreasing trend. However, greenhouse gas emissions could promote ozone depletion and delay the expected recovery of the ozone layer over New Zealand by 15 to 20 years, and increase UV levels slightly [Ministry for the Environment 2001].

2.2.2.6 Wind speed

The past and future change in wind (prevailing direction and speed) have been analysed by NIWA [Mullan et al., 2006]. The results indicated that the wind speed is showing a slight change, though it may increase by a few percent as predicted by other models. The wind speed changes differ in different places. For example, Hamilton has a high wind speed change when compared with other cities, though wind speed in this region is generally low. Similarly, the change in prevailing wind direction is fairly small. This possibly results from the fact that the predominant winds at many places in New Zealand are determined by the mountain ranges. In winter, the pressure gradient is predicted to increase over the South Island, thus an increase of mean wind speed is likely [Christensen et al., 2007].

3. ATMOSPHERIC CORROSIVITY OF NEW ZEALAND

3.1 1980s Surveys

New Zealand's territory consists of a group of islands in the south-west Pacific Ocean. Its climate is warm and humid with prevailing westerly winds flowing across the land from over the Tasman Sea. These winds can carry a large amount of sea salt great distances inland, and so pose potentially significant atmospheric corrosion problems for buildings and infrastructure.

In 1987, BRANZ started a project to study the atmospheric corrosivity of New Zealand by measuring the corrosion rates of mild steel, galvanised steel (zinc) and aluminium coupons exposed at 168 meteorological sites [Cordner 1990; Duncan and Cordner

1991]. Corrosion rates of mild steel after one-year of exposure varied from 18 to 4800 g/m²/year and from 9 to 5300 g/m²/year after two-year exposure. Corrosion rates of galvanised steel derived after one year of exposure typically ranged from 0.7 to 141 g/m²/year and 0.5 to 76 g/m²/year after two years. All the extremely high corrosion rates were found with those coupons exposed in geothermal areas. A clear correlation between corrosion rate and distance from the coast was also evident from these measurements, indicating that atmospheric corrosivity is also highly related to the deposition rate of chloride-containing salt particles.

Corrosion of aluminium in most areas of New Zealand was extremely low. Surface averaged corrosion rates of about 2.6 g/m²/year were found at a number of severe marine sites. At one industrial site a rate of 1.3 g/m²/year was recorded. Aluminium also appeared to be markedly more durable than galvanised steel in geothermal regions. However, localised corrosion forms, such as pitting corrosion, which are more detrimental to the performance of aluminium, were not fully characterised within this study.

3.2 Atmospheric Corrosivity Map in NZS 3604

These corrosion rate data (especially those derived from mild steel coupons) were used to establish an atmospheric corrosivity map, used in NZS 3604 [NZS 3604, 1999 & 2011]. Climatic factors, such as prevailing wind, were also taken into consideration. In this map, New Zealand's territory was covered by five corrosion zones according to the corrosivity of the atmosphere, i.e. Zones 1 to 4 and a sea spray zone. When NZS 3604 was reviewed in 2010, these zones were replaced by three zones (B, C & D) as defined within the relevant ISO standards (see Figures 1 and 2). These maps showed that most of New Zealand was of low corrosivity, with a band of medium corrosivity around the coast reaching up to 10 kms inland.

3.3 Atmospheric Corrosivity Map in NZS 3404

The first-year macro-climate corrosion rates of carbon steel at different sites in New Zealand was derived theoretically, using six equations that are a function of meteorological variables, e.g. average annual daily temperature, time of wetness, annual rainfall and distance from the coast [El Sarraf and Mandeno 2008; El Sarraf and Clifton 2011]. The data was then modified with a series of multipliers, depending mainly on distance from the coast and geographic location, to establish a final atmospheric corrosivity map that is shown in NZS 3404 [NZS 3404, 2009]. In this map, New Zealand was covered by five zones, i.e. Zones 1, 2, 3, 4 (Taupo Volcanic Zone) and a sea spray zone. The corrosion rate ranges used to define these zones are similar to those used in NZS 3604:1999. A comparison between this map and that in NZS 3604 reveals differences in zone boundary definitions in some regions.

4. OBJECTIVE OF CURRENT RESEARCH

Atmospheric corrosivity mapping is fundamental to the specification and selection of materials for buildings in different geographic locations, to ensure that they meet the durability requirement of the New Zealand Building Code and relevant building standards when used as acceptable or alternative solutions. After 25 years of use, it is advisable to check the on-going credibility of the only experimentally collected metal atmospheric corrosion rate data set, and to determine whether the atmospheric corrosivity map shown in NZS 3604 is still reliable. This work was also intended to explore possible changes in climatic conditions in New Zealand during the past three decades and their potential influence on materials deterioration. Outputs from this study are intended to move towards a single, accurate atmospheric corrosivity map based on an updated, complete data set, to avoid confusion for practitioners.

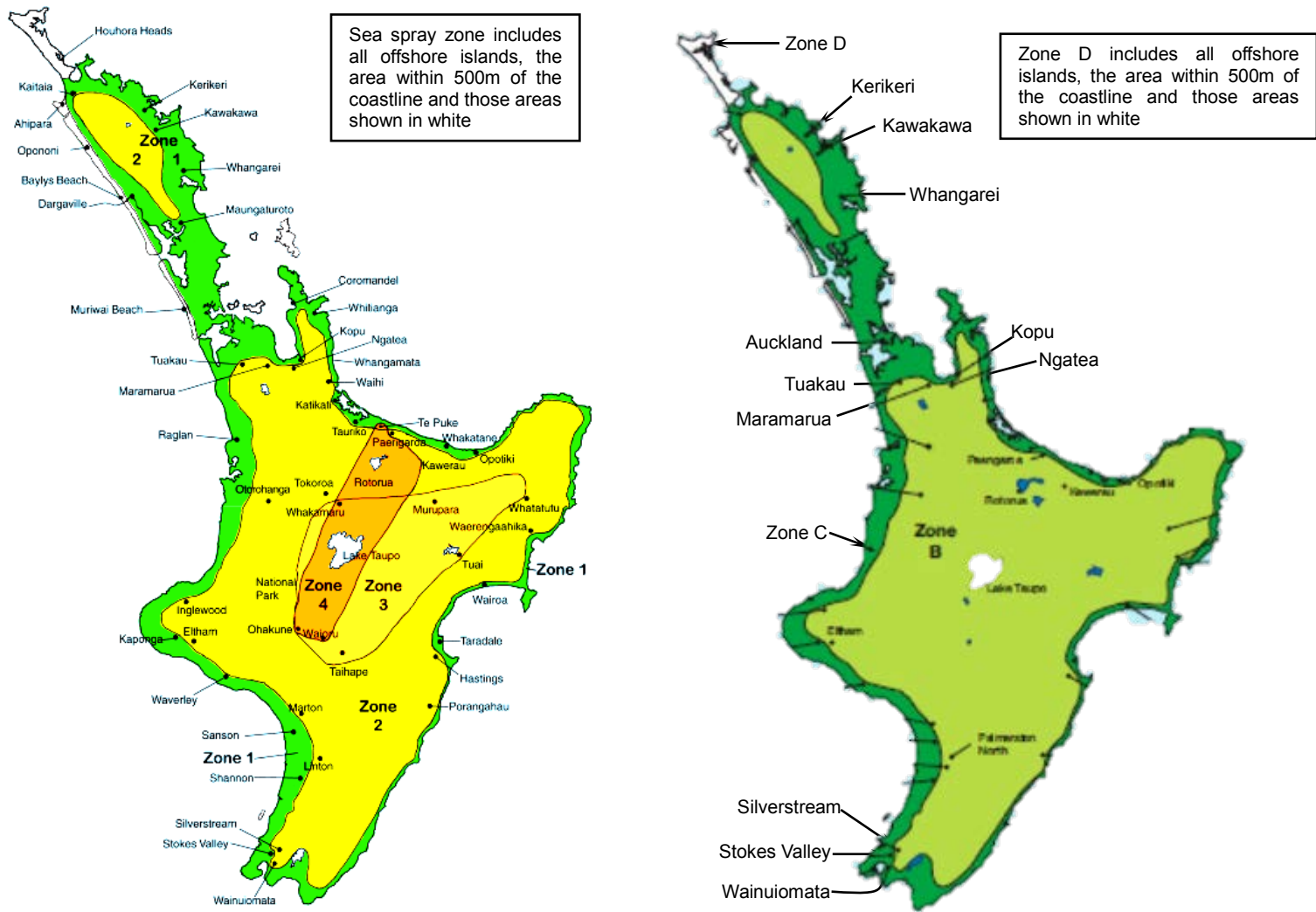


Figure 1. Atmospheric corrosion zone definition for the North Island of New Zealand (NZS 3604:1999 (Left) and 2011 (Right))

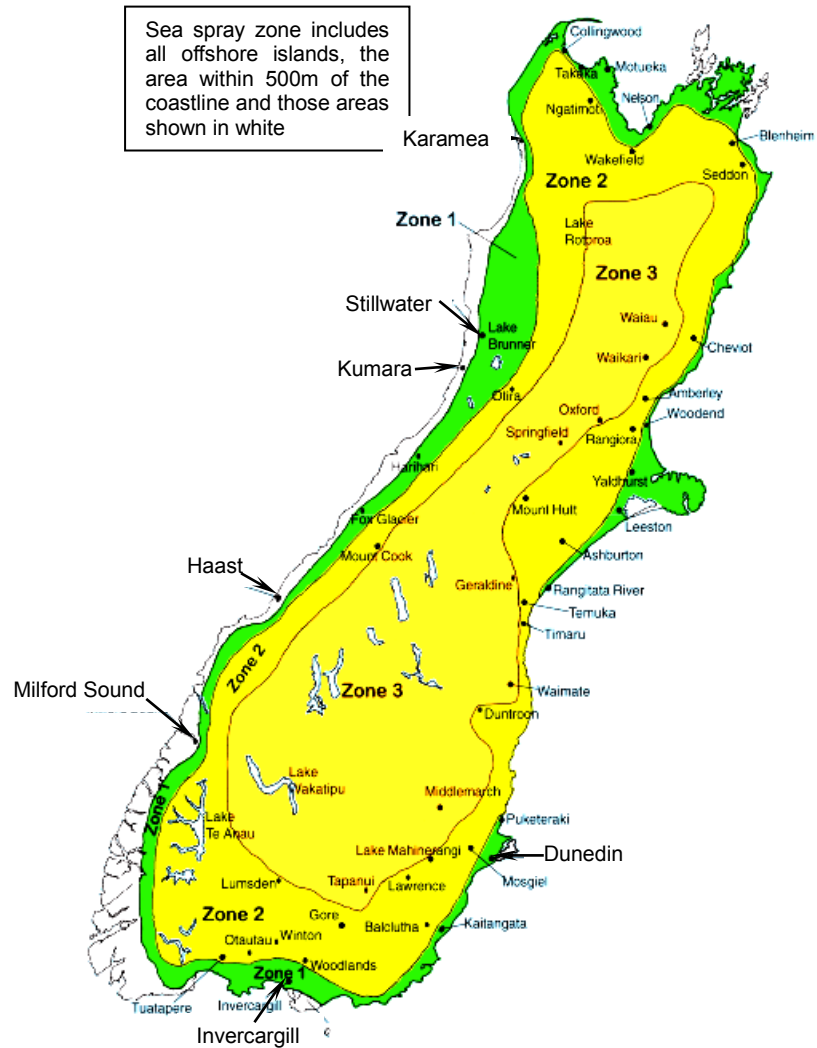


Figure 2. Atmospheric corrosion zone definition for the South Island of New Zealand (NZS 3604:1999 (left) and 2011 (right))

5. EXPERIMENTAL

5.1 Retrieval of Climate Data

Climate data, including average ambient temperature, rainfall, wet days (defined as daily precipitation > 1 mm), relative humidity, average wind speed and mean daily global radiation, were retrieved from NIWA's CliFlo database (<http://cliflo.niwa.co.nz/>). Their changing trends in the period of 1980 – 2010 were analysed using linear regression fitting. Comparisons of climatic parameters between 1987 – 1988 and 2011 – 2012 were also made with the purpose of determining whether a significant difference in environmental conditions existed between the two periods of field exposure testing.

5.2 Atmospheric Corrosion Rate Measurement

5.2.1 Methodology

A comprehensive literature survey by BRANZ indicated that most atmospheric corrosivity monitoring and mapping activities were based on:

- direct measurements of metal corrosion rates in the environment of interest [Santana et al., 2001; Natesan et al., 2006; Shalaby et al., 2006; Natesan et al., 2008];
- classification using meteorological data and deposition rates of atmospheric contaminants [Sica et al., 2007]; or
- classification using corrosion rate, together with meteorological parameters and deposition rates of atmospheric contaminants [de Rincón et al., 1998].

This current study used the first methodology, i.e. direct measurement of corrosion rates of standardised metallic samples exposed to atmosphere of interest for one year. This method was also used in BRANZ's study of 1980s. The first year corrosion rates were then used to classify atmospheric corrosivity according to the ISO corrosion categories.

5.2.2 Sample

Standard specimens of mild steel (~150 × 100 × 3 mm) and hot dip galvanised steel (~150 × 100 × 0.5 mm) were prepared and used in the present study. Chemical compositions for these materials are given in Table 2. These samples were the retained, unused, samples from BRANZ' testing in the 1980s and were stored in a well-sealed cabinet located in a room with constant temperature and humidity [Duncan and Cordner 1991]. As it is generally believed that even small differences in composition, dimension and surface finish of the samples exposed could affect the accuracy of the corrosion rates derived, this meant that the experimental error from material variation was minimised.

Prior to exposure, the surface of the mild steel coupons was grit blasted to SA3 grade, the surface finish used in the 1980s testing. The hot dip galvanised steel samples were immersed into a solution containing ammonium chloride to remove the thin oxide film formed on the zinc surface during storage. The accurate size of each coupon was then measured with an electronic calliper for the calculation of exposed surface area. Prior to exposure rack construction, the exposed surfaces of these samples were cleaned with acetone, fully dried with hot air, and then weighed to 0.01 g using an electronic balance. These coupons were sealed in plastic bags, shipped to the selected exposure sites and mounted onto the light-weight exposure racks made of aluminium extrusions using nylon bolts and washers (see Figure 3).

Table 2. Chemical composition of metallic coupons used in the present study (wt.%)

Metal	Element							
	C	N	Al	Si	P	S	Ti	V
Mild Steel	0.18	0.003	0.007	0.04	0.027	0.014	0.005	0.002
	Cr	Mn	Ni	Cu	Mo	Sn	Nb	Fe
	0.03	0.69	0.02	0.03	<0.001	<0.001	<0.001	Bal.
Galvanised Steel	Mg	Al	Cu	Sn	Pb	Zn		
	<0.01	0.32	<0.01	<0.01	0.10	Bal.		

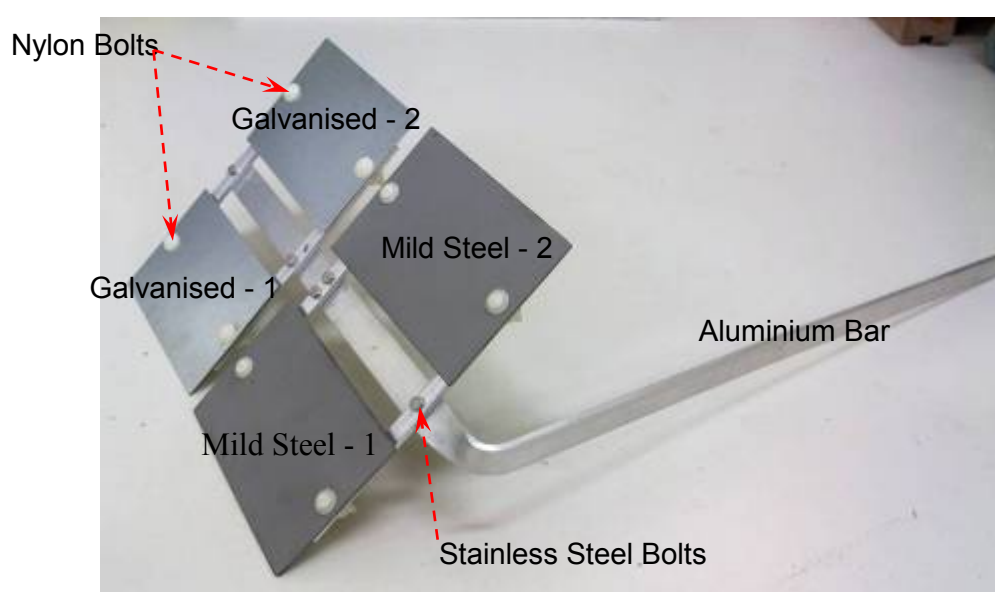


Figure 3. Exposure rack carrying mild steel and hot dip galvanised steel coupons used in the present study

5.2.3 Exposure Site

The present study selected sites in consideration of:

- a direct comparison of corrosion rate data between the present and previous BRANZ tests can be made.
- where the atmospheric corrosion zone boundaries defined by the maps shown in NZS 3404 and NZS 3604 didn't agree with each other, and

In total, thirty-nine exposure sites were selected. Most sites were located within Auckland, Waikato, Wellington, Dunedin and Invercargill. Christchurch was not included into this pilot study due to the devastating earthquakes that occurred in 2010 and 2011. To ensure sample security, exposure racks were installed within weather stations operated by MetService and NIWA, airports, private gardens of residential buildings and on fenced farm land. Maps showing the locations of these sites are given in Figures 4 to 7.

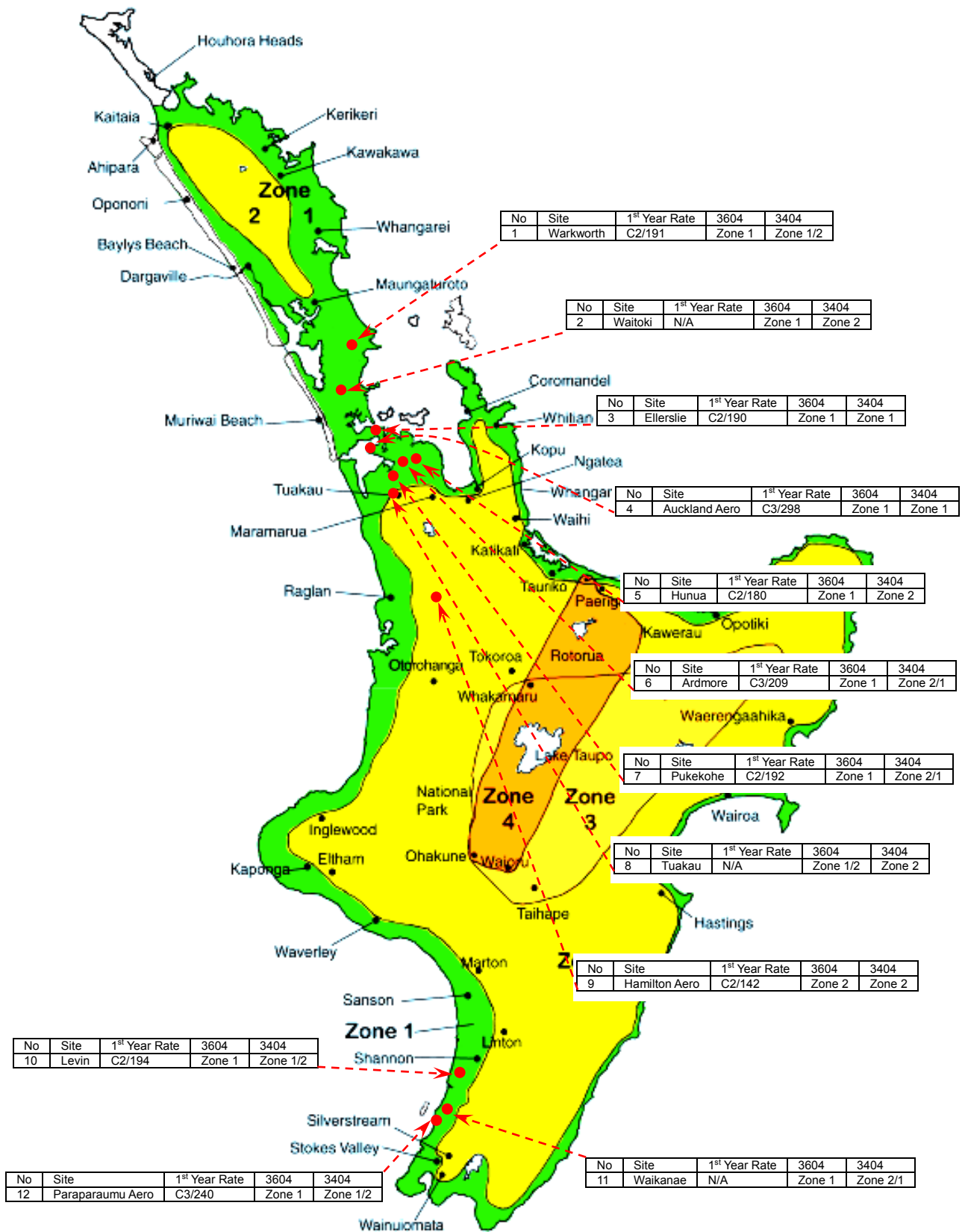


Figure 4. Atmospheric corrosion exposure sites in North Island except Wellington

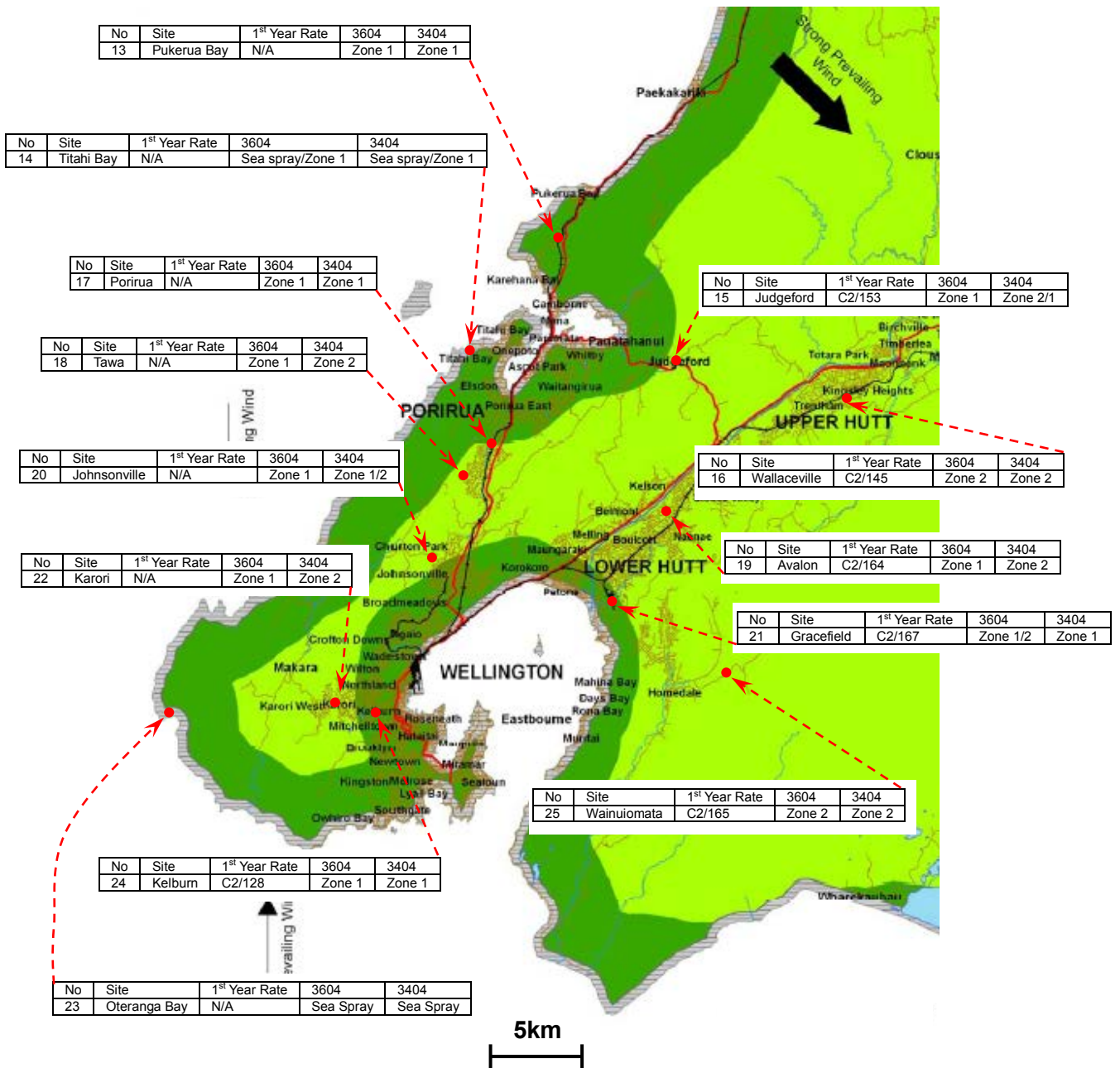


Figure 5. Atmospheric corrosion exposure sites in Wellington region

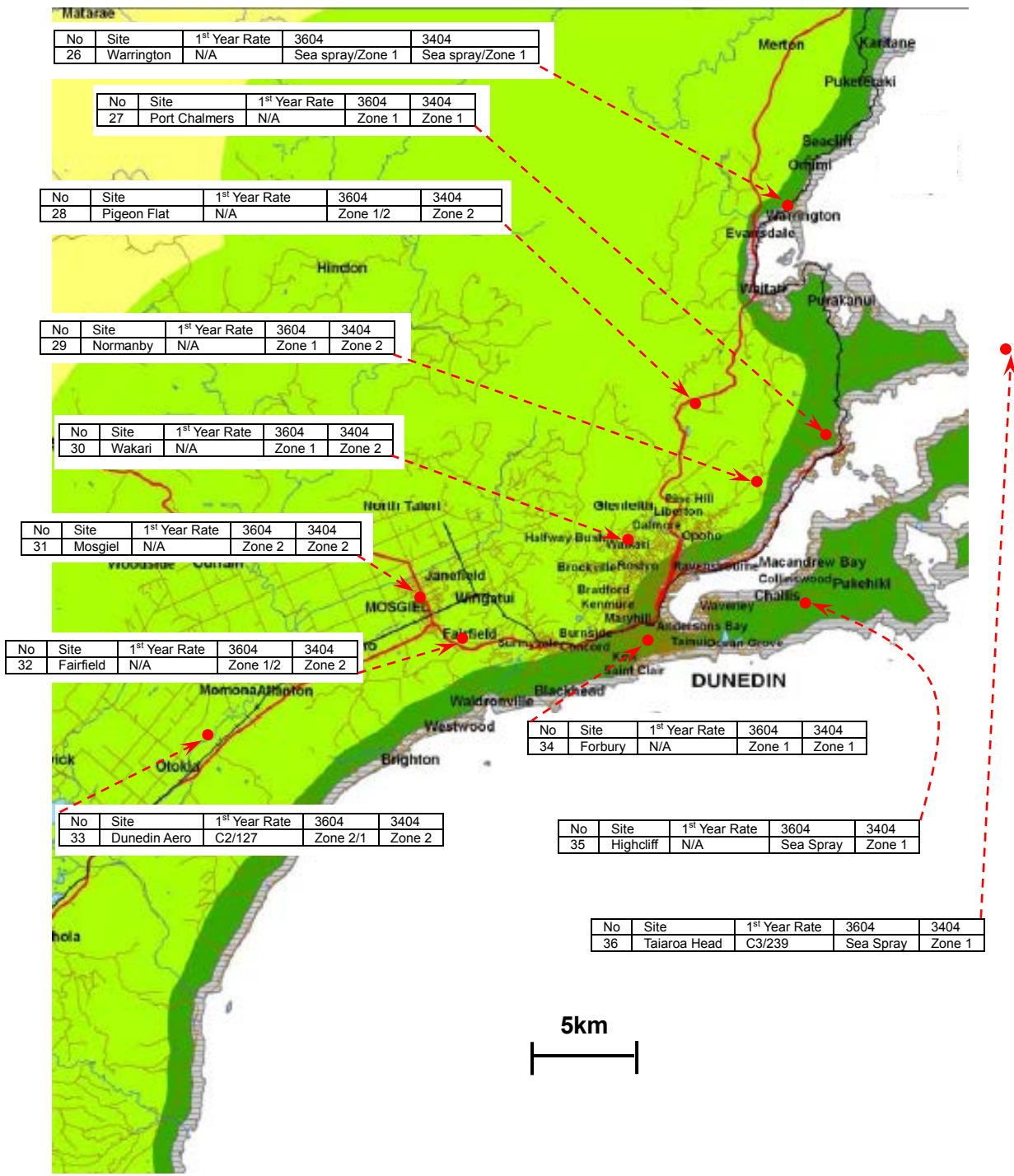


Figure 6. Atmospheric corrosion exposure sites in Dunedin region



Figure 7. Atmospheric corrosion exposure sites in Greymouth and Invercargill regions

5.2.4 Rack Installation

Most of the exposure racks were installed during September and October of 2011 by BRANZ, MetService and NIWA. These racks were placed (where practical)

approximately 1.8 m above the ground, facing north at a 45° angle. This installation was very similar to that used in the BRANZ surveys in the 1980s, since atmospheric corrosion was found to be heavily dependent on exposure angle and orientation [Vera et al., 2003]. A typical example of the installed exposure rack is shown in Figure 8.



Figure 8. Atmospheric corrosion exposure rack installed at MetService's weather station at Paraparaumu Airport

5.2.5 Corrosion Rate Measurement

After one year of atmospheric exposure, these coupons were retrieved from the exposure sites. Their surface morphology was examined visually and microscopically. The corrosion products were then cleaned thoroughly following the procedures recommended by ASTM G1:

- Mild steel: 0.5 L/L hydrochloric acid (HCl, specific gravity = 1.19) + 3.5 g/L hexamethylenetetramine (C₆H₁₂N₄) at 20-25°C; and
- Hot dip galvanised steel: 100 g/L ammonium chloride (NH₄Cl) at 70°C.

Before immersion in the cleaning solution, the corrosion products, particularly the loosely attached rust layer on the surface of mild steel samples, was removed using a wooden spatula under flowing water. The chemical solution was also agitated magnetically during the cleaning process. This was to accelerate the removal of rust and to make the cleaning period as short as possible. The sample surface condition was inspected regularly during this process. The mild steel samples were also frequently taken out of the chemical solution to manually remove the partially dissolved rust layer. This practice ensured that the steel samples were not unnecessarily attacked by the cleaning solution. The completely cleaned samples were then washed with distilled water, rinsed with acetone, and dried with hot air. They were then weighed again to obtain mass losses, thus enabling corrosion rates to be quantified.

A mild steel sample and a hot dip galvanised steel sample of the same chemical composition, dimensions and surface finish were also immersed into the same chemical solutions for the same periods. Their mass losses due to chemical etching were recorded. The mass loss per surface area was calculated for correction of the corrosion rates derived.

6. RESULTS

6.1 Changes in Climatic Factors

6.1.1 Average Ambient Temperature

The trends of change in average temperature derived from NIWA's composite temperature series for Auckland, Wellington and Dunedin in the last 100 years [Mullan et al., 2010], and those obtained by BRANZ's analysis using the climatic data in the last 30 years are given in Figures 9 to 14. In general, BRANZ's results agree with NIWA's findings, i.e. the average air temperature of New Zealand increased slowly in past decades at most sites. The exact amplitudes revealed by these two analyses are slightly different due to differences in weather station location and length of time period analysed.

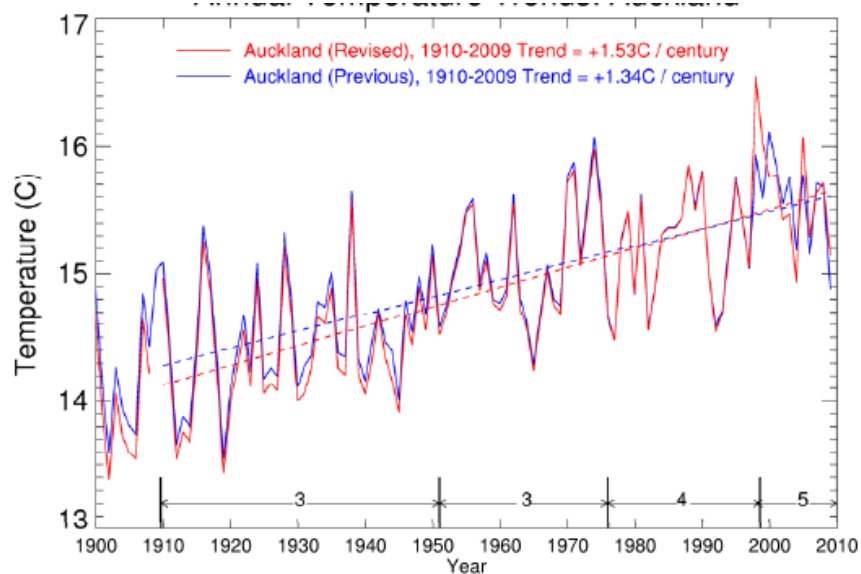


Figure 9. Composite series of annual mean air temperatures for Auckland from 1900 to 2009 (NIWA's result)

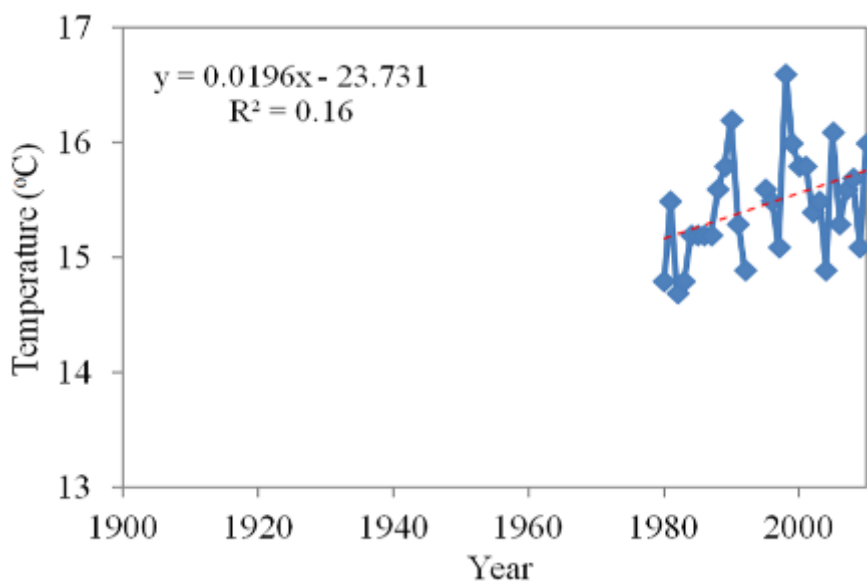


Figure 10. Annual mean air temperatures for Auckland Airport from 1980 to 2010 (Linear fitting to these data derived a temperature increase trend of 0.0196 °C/year which is slightly higher than that of NIWA's composite series from 1900 to 2009) (BRANZ's result)

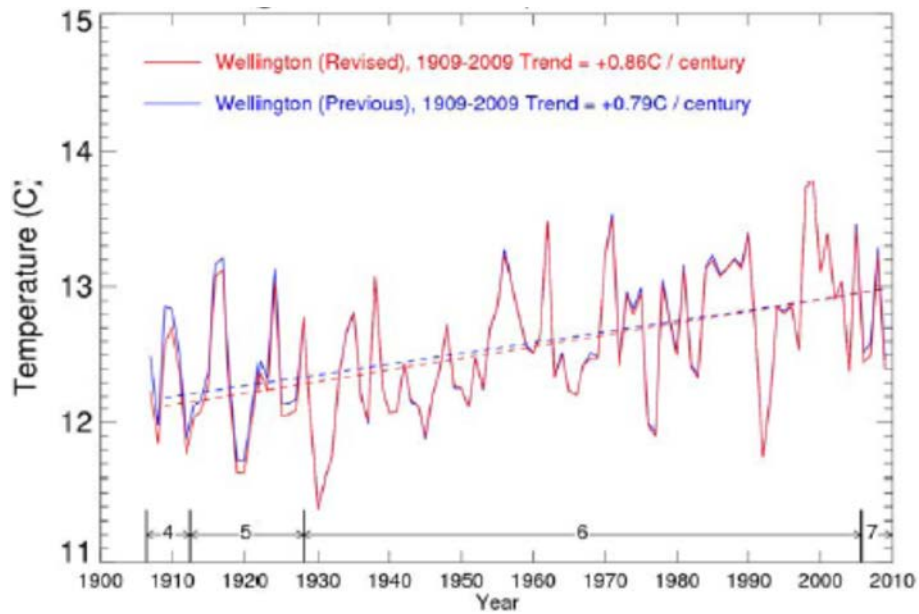


Figure 11. Composite series of annual mean air temperatures for Wellington (Kelburn) from 1900 to 2009 (NIWA's result)

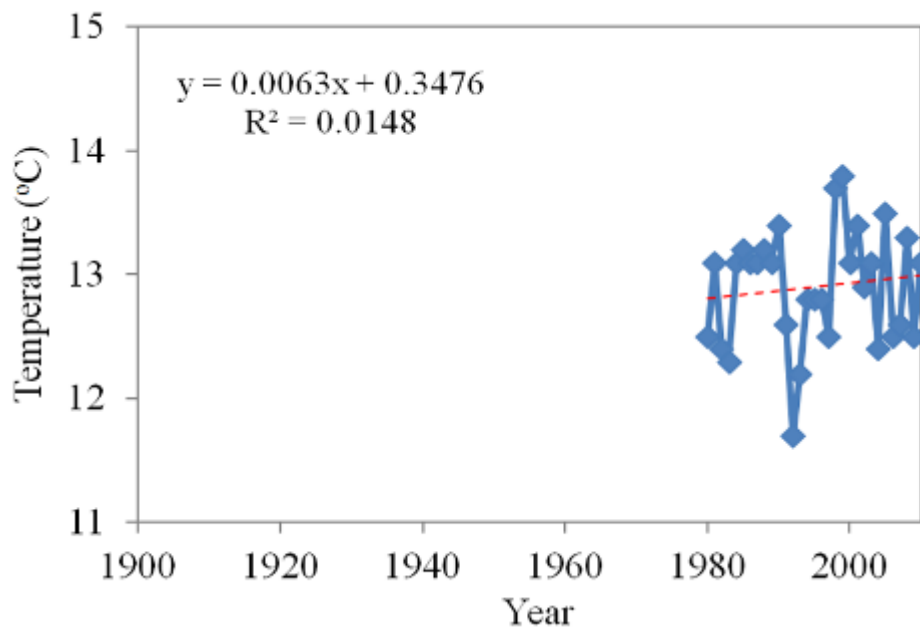


Figure 12. Annual mean air temperatures for Wellington (Kelburn) from 1980 to 2010 (Linear fitting to these data derived a temperature increase trend of 0.0063 °C/year which is slightly lower than that of NIWA's composite series from 1900 to 2009) (BRANZ's result)

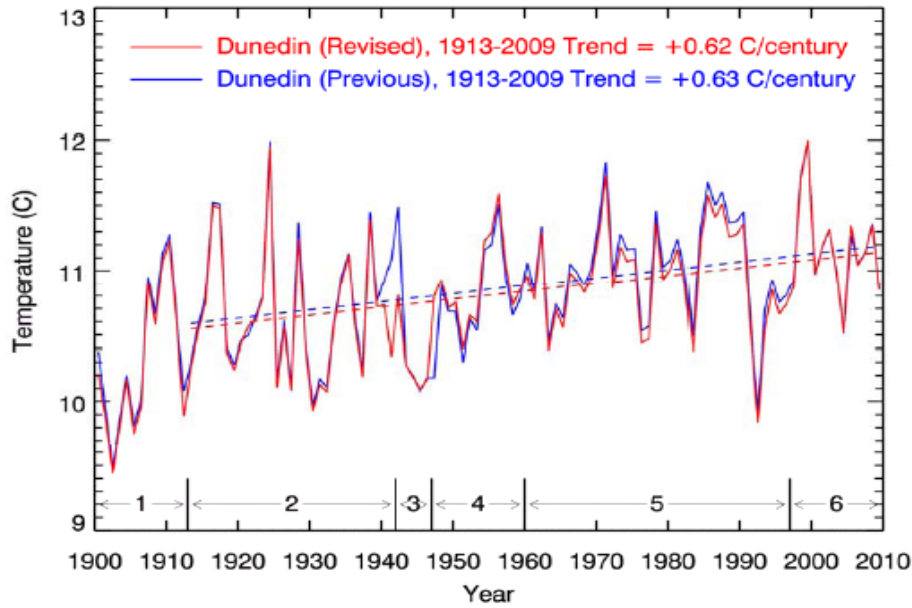


Figure 13. Composite series of annual mean air temperatures for Musselburgh (Dunedin) from 1900 to 2009 (NIWA's result)

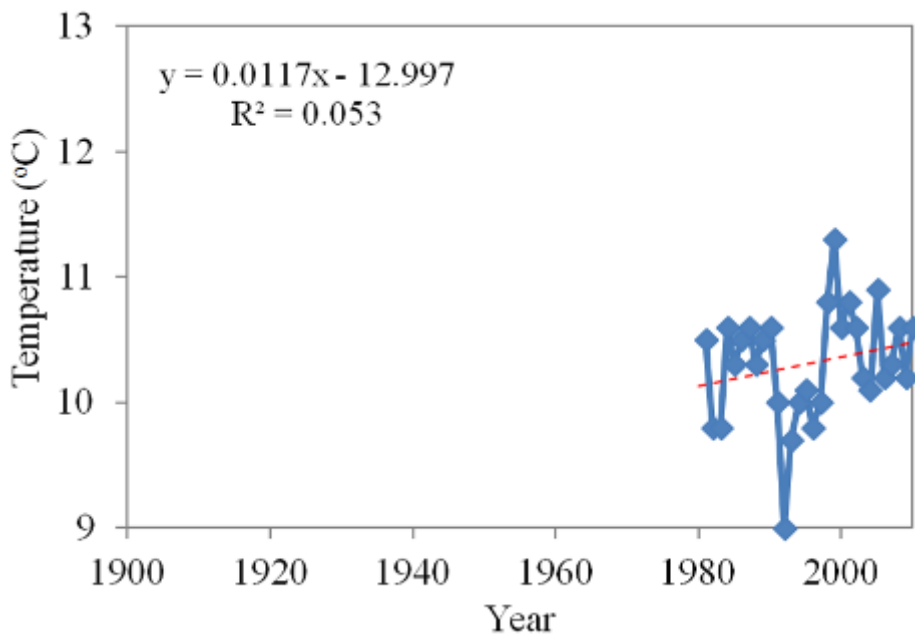


Figure 14. Annual mean air temperatures for Dunedin Airport from 1980 to 2010 (Linear fitting to these data derived a temperature increase trend of 0.0117 °C/year which is slightly higher than that of NIWA's composite series from 1900 to 2009) (BRANZ's result)

The temperature change trends for other exposure sites selected for the present atmospheric corrosion study are also given in the Appendix of this report.

6.1.2 Rainfall and Wet Days

In Figures 15 to 17, the changing trends of rainfall and wet days in the last thirty years at Auckland, Wellington and Dunedin are given. The changing trend for other sites is given in the Appendix. The analysis showed that most sites had a decreasing trend of rainfall. The annual wet days (daily rainfall > 1 mm) exhibited a similar trend in most sites.

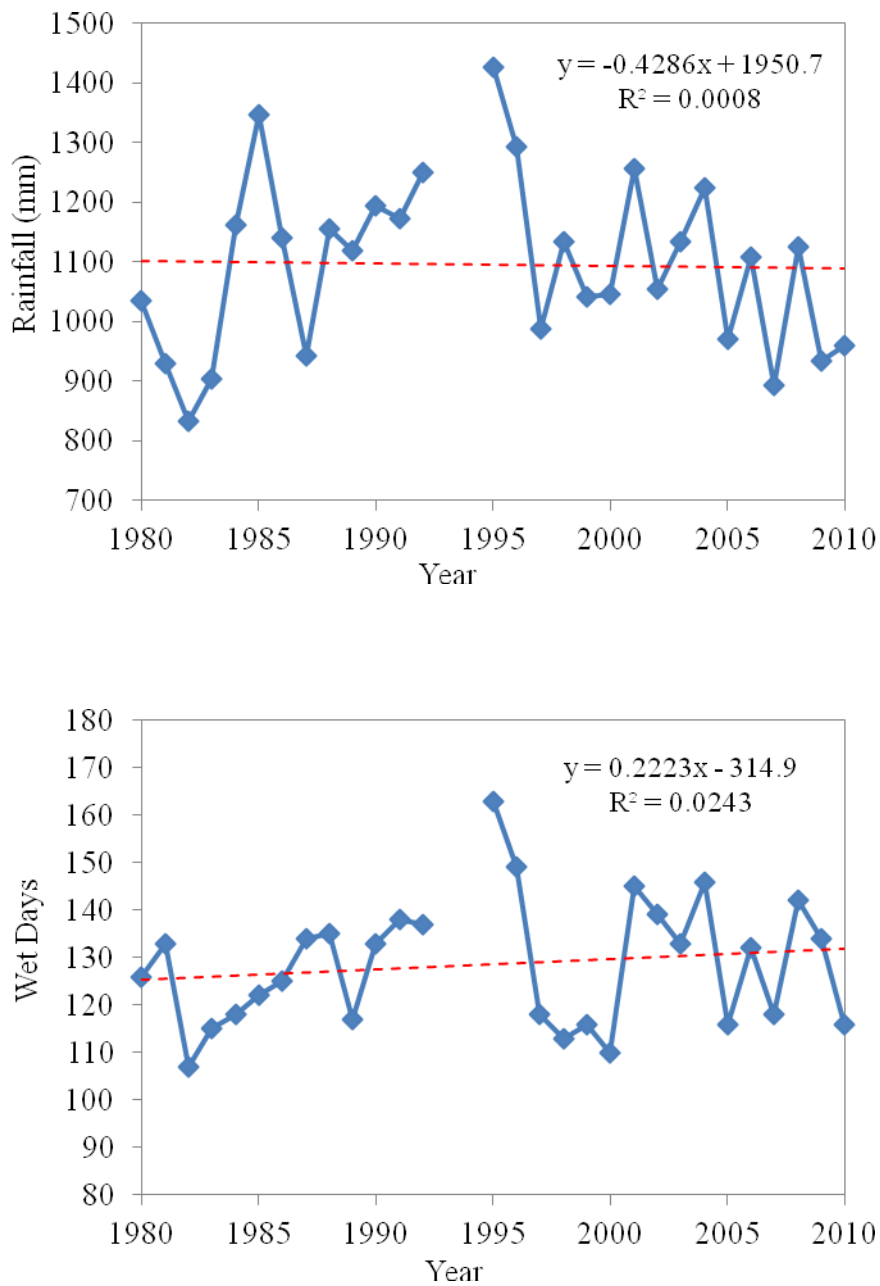


Figure 15. Annual rainfall and wet days at Auckland Airport from 1980 to 2010 (Linear fitting showed a very gentle decreasing trend for rainfall and a small increase for wet days)

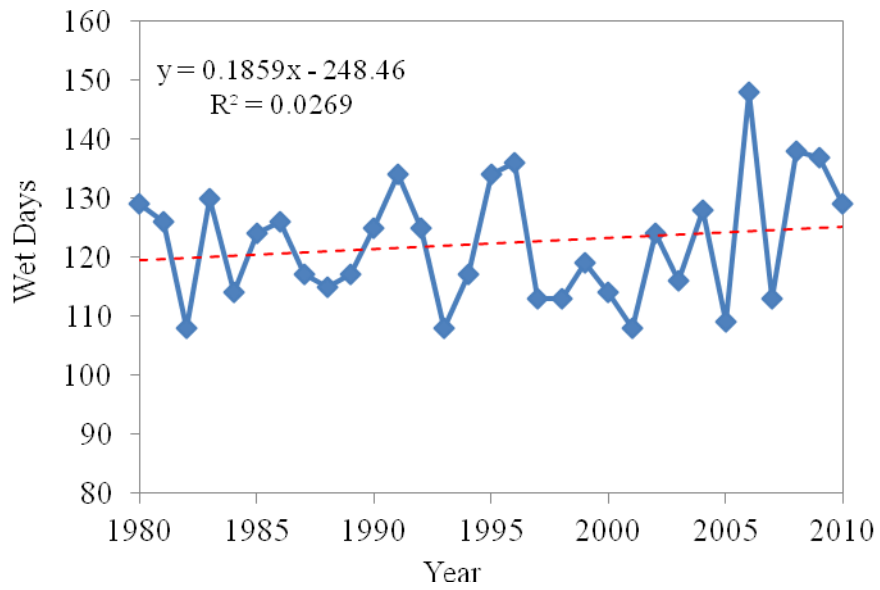
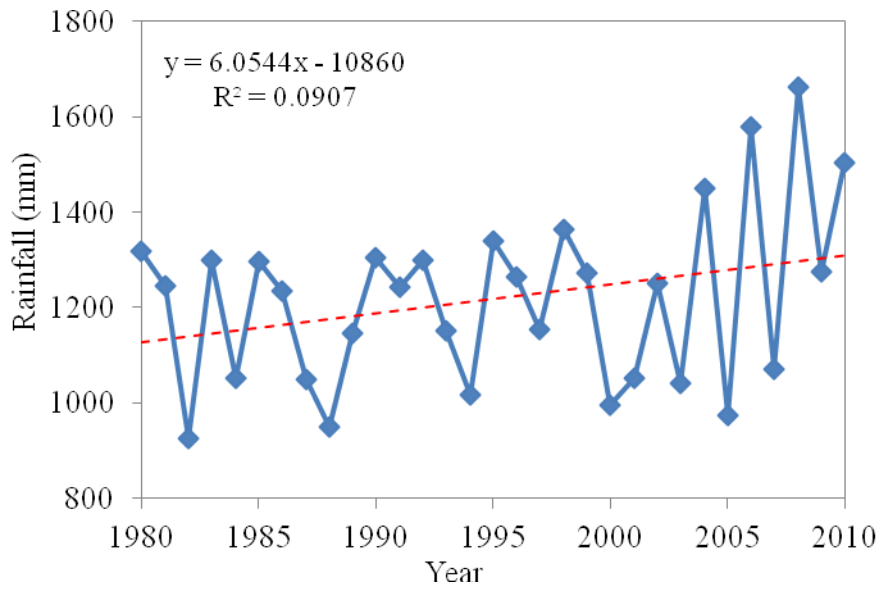


Figure 16. Annual rainfall and wet days at Kelburn (Wellington) from 1980 to 2010 (Linear fitting to these data showed an increasing trend for rainfall and wet days)

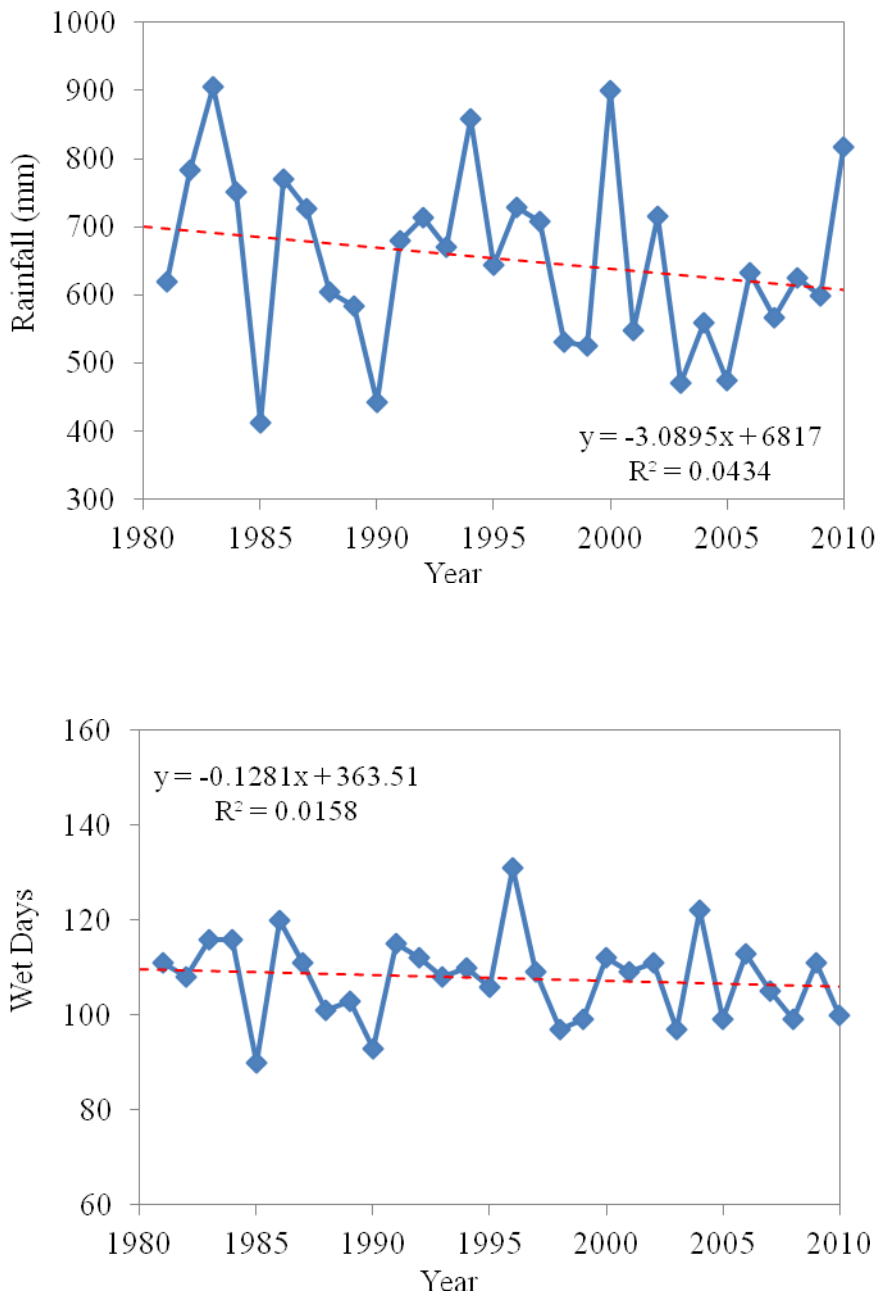


Figure 17. Annual rainfall and wet days at Dunedin Airport from 1980 to 2010 (Linear fitting to these data showed a small decreasing trend for rainfall and wet days)

6.1.3 Relative Humidity

The changing trend of the mean 9am annual RH in the past three decades selected for the present atmospheric corrosion study was analysed using the data retrieved from the NIWA's National Climate Database (CliFlo). The results for three exposure sites in Auckland, Wellington and Dunedin are presented in Figures 18 to 20 respectively, while the results for other sites are shown in the Appendix.

It can be seen that the RH trends at these sites are very complicated, but it is quite clear that significant changes in RH are not occurring. Meanwhile, rainfall analysis indicated a higher rainfall in western regions and a lower rainfall in eastern regions.

This behaviour was not found in the RH data. NIWA believe that long-term RH variations were not closely related to rainfall in the current climate. Considering the amplitude of future temperature increase, mean relative humidity could show a modest reduction in most places [Mullan et al., 2006].

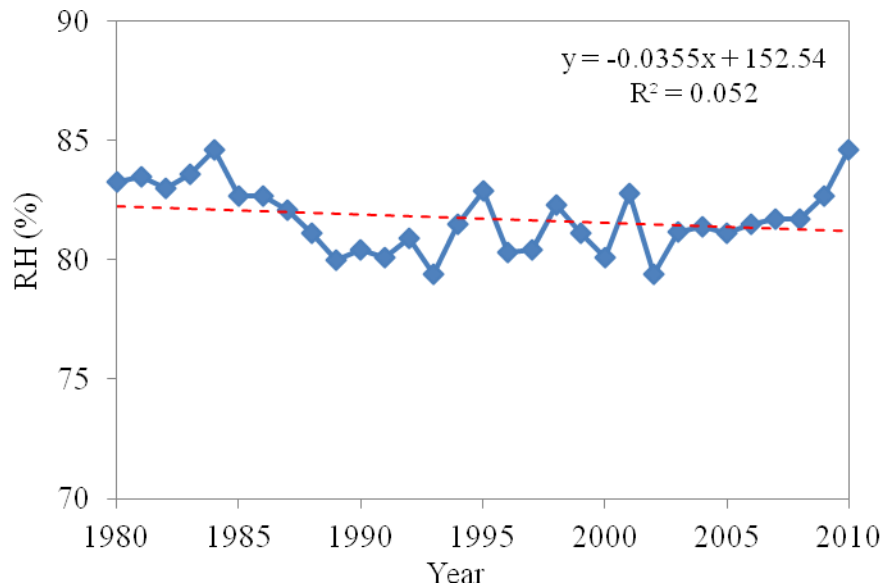


Figure 18. Mean 9am annual relative humidity for Auckland Airport from 1980 to 2010

Linear fitting showed a marginally decreasing trend of relative humidity in this period. However, it appeared that the relative humidity was decreasing from around 1985, levelling off till 2005, and then increasing gradually.

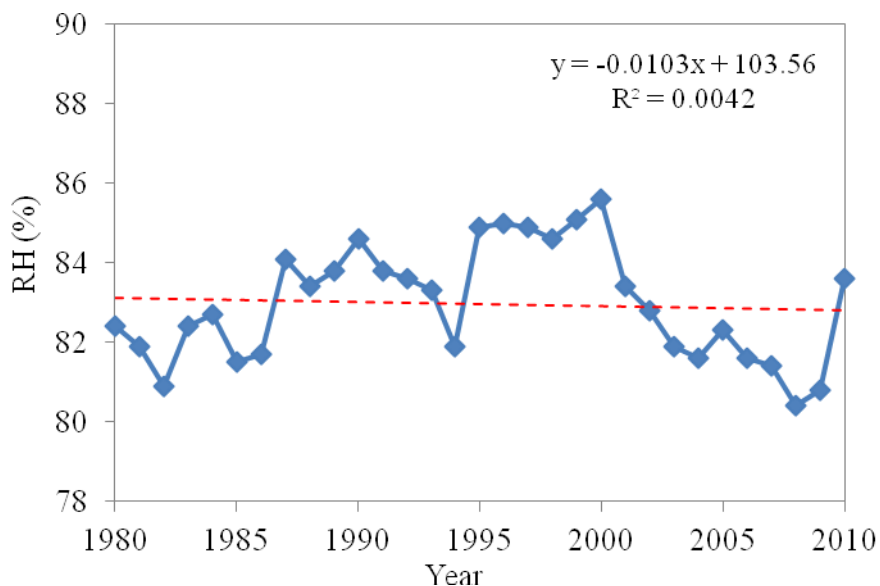


Figure 19. Mean 9am annual relative humidity for Kelburn from 1980 to 2010

The mean 9am annual RH at this site was also high: all above 80%. In the first 20 years, it was generally increasing slowly. After the year 2000, a decreasing trend was observed. Linear fitting of the overall data for the last 30 years exhibited a slightly decreasing trend.

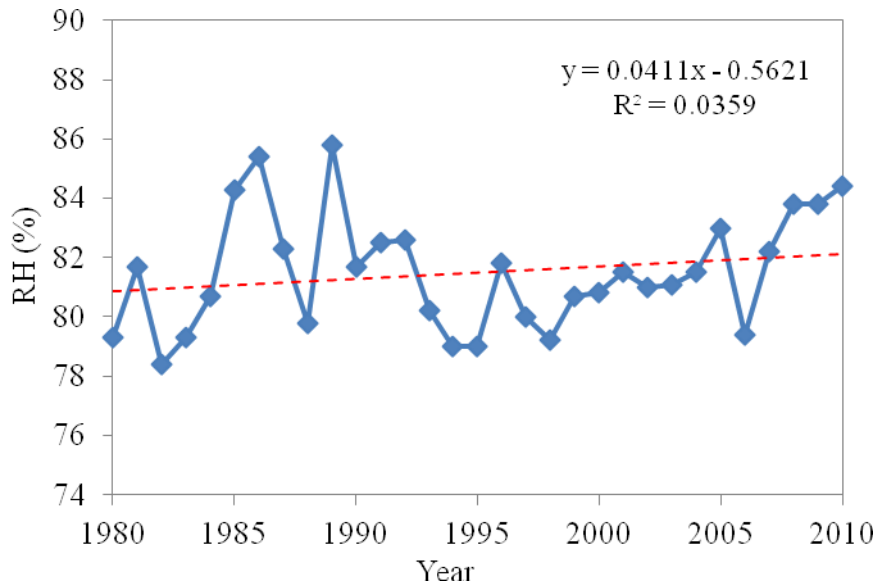


Figure 20. Mean 9am annual relative humidity for Dunedin Airport from 1980 to 2010

The mean 9am annual RH at this site showed a complicated trend during the last 30 years. From 1980 to 1989, the RH was generally increasing. It generally decreased from 1989 to 1998, and then increased slowly. Overall, linear fitting of the data for the last 30 years exhibited a slightly increasing trend.

6.1.4 Solar Irradiation

NIWA's CliFlo database provides mean daily global radiation data. Global radiation is the total short-wave radiation from the sky falling onto a horizontal surface on the ground. It includes both the direct solar radiation and the diffuse radiation resulting from reflected or scattered sunlight. However, this data set is only available for very limited number of exposure sites used in the present study. The changing trends for Auckland, Kelburn (Wellington) and Dunedin were analysed and are given in Figures 21-23. The changing trends for other sites, including Invercargill, Levin, Pukekohe and Tiwai Point, are given in the Appendix.

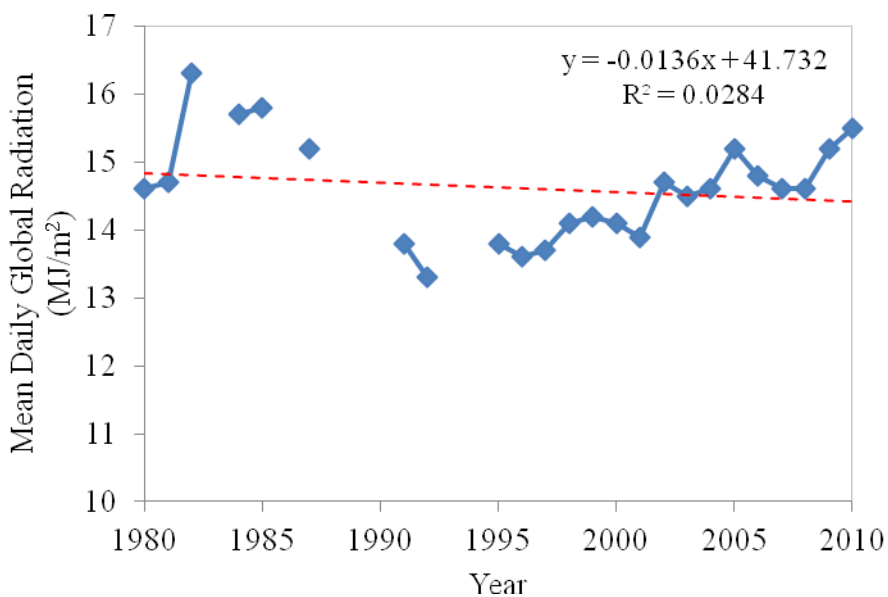


Figure 21. Mean daily global radiation at Auckland Airport from 1980 to 2010

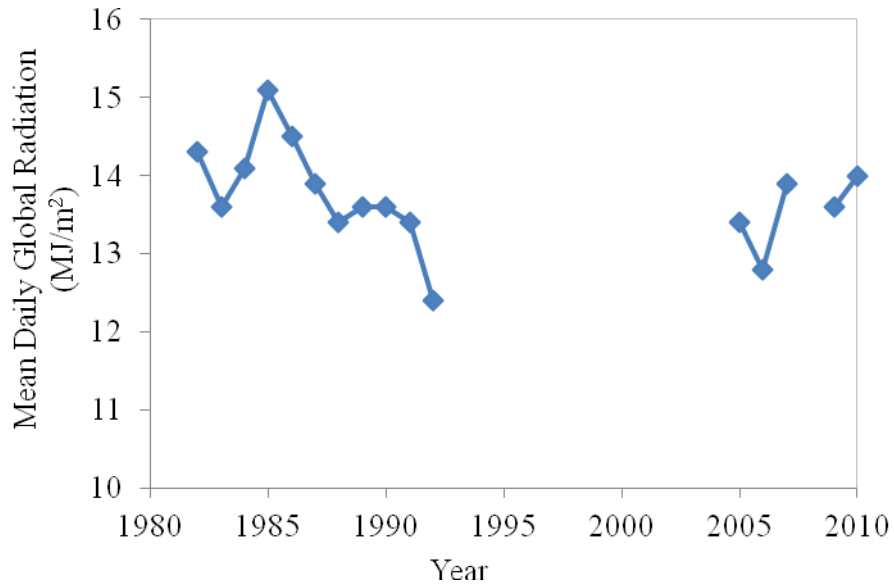


Figure 22. Mean daily global radiation at Kelburn from 1980 to 2010

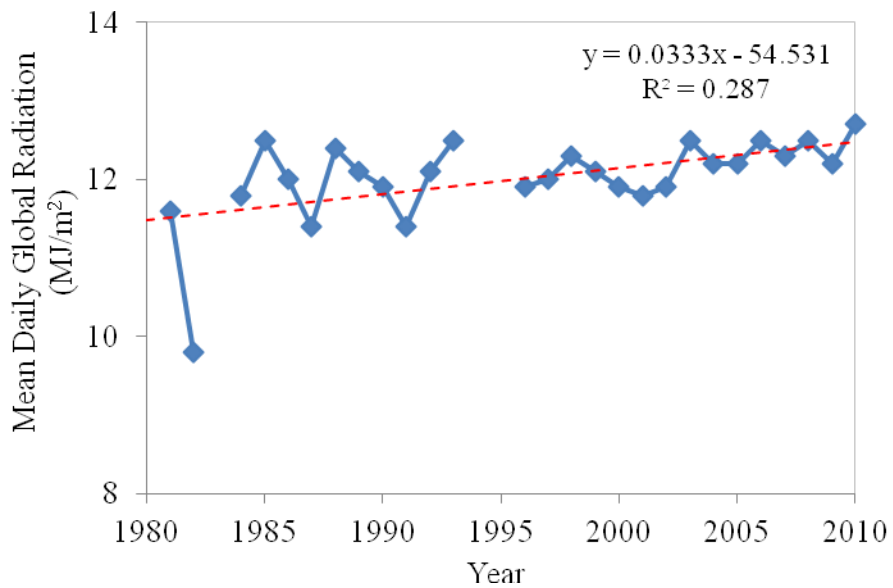


Figure 23. Mean daily global radiation at Dunedin Airport from 1980 to 2010

6.1.5 Wind Speed

The changes of wind speed at Auckland, Wellington and Dunedin sites are shown in Figures 24 to 26. The results for other sites used for the present atmospheric study are given in the Appendix.

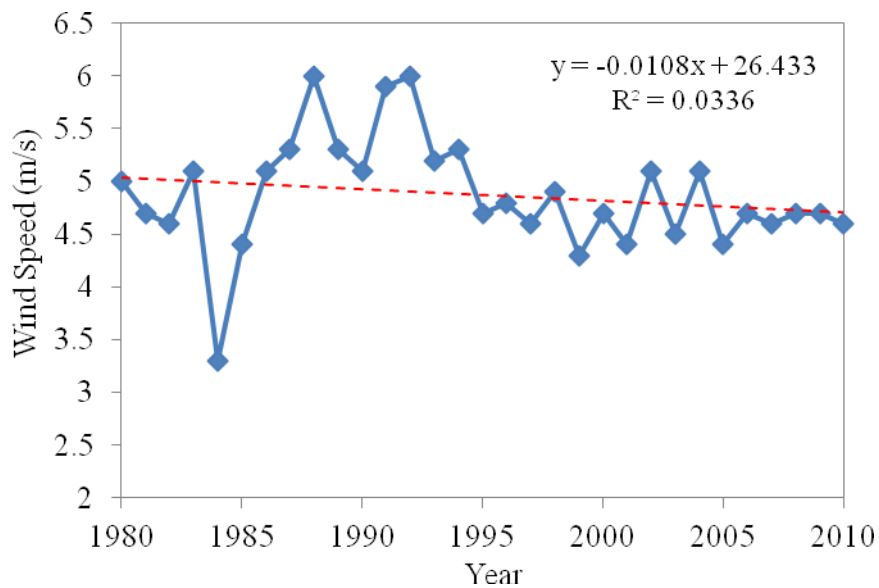


Figure 24. Mean annual wind speed at Auckland Airport from 1980 to 2010

The wind speed at Auckland Airport showed a relatively large variation in 1980s and 1990s, around 20% in amplitude. During the period of 1995 to 2010, the annual wind speed was reasonably stable at ~4.5 m/s. A linear fitting of the data collected in the past three decades shows a gentle decreasing trend at this site.

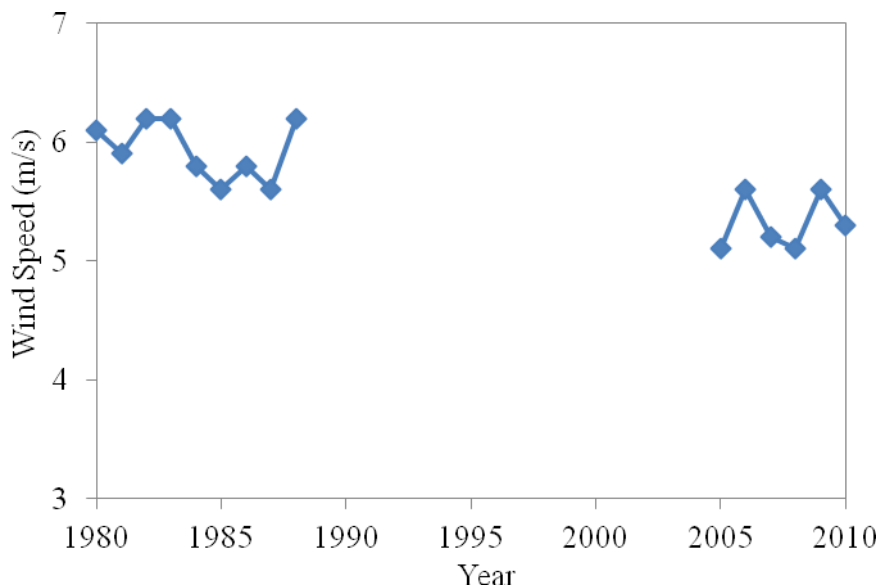


Figure 25. Mean annual wind speed at Kelburn from 1980 to 2010

Wind speed data for Kelburn (Wellington) is only available for the periods 1980 – 1988 and 2005 – 2010. Wind speed at this site was higher than 5 m/s, particularly in 1980s. This value is the highest within the sites where wind speed data are available for this analysis.

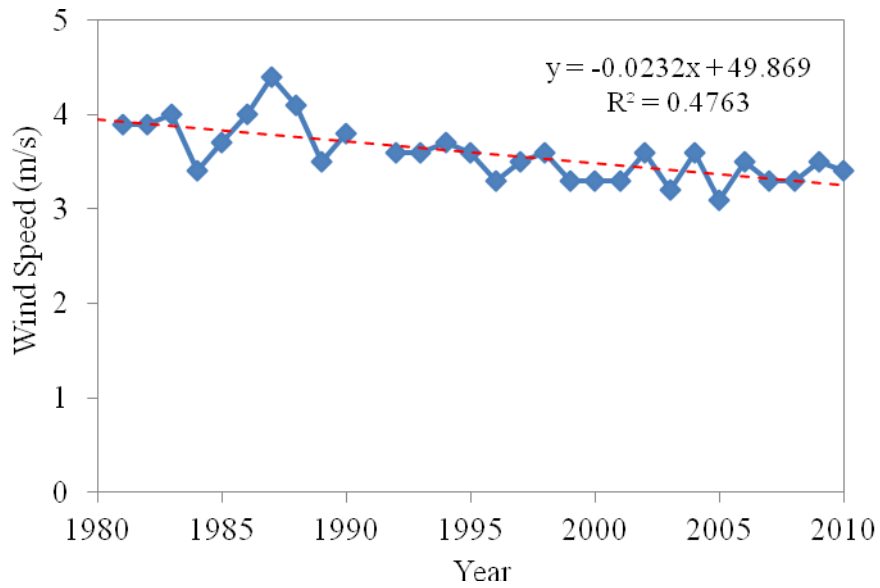


Figure 26. Mean annual wind speed at Dunedin Airport from 1980 to 2010

Dunedin Airport annual mean wind speed shows a gently decreasing trend over the past 30 years, from 4 m/s to ~3.2 m/s. However, during the period 1995 to 2010 the wind speed was reasonably stable.

The trends for changes in temperature, precipitation, humidity, wet days and wind speed derived from BRANZ's analysis of climatic data retrieved from NIWA's CliFlo database for the last 30 years are summarised in Table 3. The results from comparisons between the separate climatic factors in the periods of 1987 – 1988 and 2011 – 2012 are also given.

Table 3. Summary of changes in typical climatic factors observed at some exposure sites

Exposure Site	Long-Term Change (1980 – 2010)					Two-Year Comparison (2011 – 2012 minus 1987 – 1988)				
	Temperature	RH	Rainfall	Wet Days	Wind Speed	Temperature	RH	Rainfall	Wet Days	Wind Speed
Ardmore Airport	0.0084 °C/y	-0.0896 %/y	1.84 mm/y	0.50 day/y	×	0.2 °C	-6.5	2.5 mm	-0.6 day	×
Auckland Airport	0.0196	-0.0355	-0.43	0.22	-0.01 m/s/y	0.2	2.4	15.2	-0.2	-0.9
Dunedin Airport	0.0117	0.04	-3.09	-0.13	-0.02	0.2	2.3	-2.2	-0.1	-0.9
Dunedin Botanic Garden	×	×	-3.00	×	×	×	×	3.9	×	×
Greymouth	0.0202	-0.0269	0.22	-0.14	×	0.7	-1.1	-22.6	-1.8	×
Hamilton Airport	0.0194	0.0075	3.13	0.33	-0.01	0.1	2.2	27.6	0.5	×
Invercargill Airport	0.0086	-0.0188	-0.95	-0.10	-0.01	-0.2	0.8	-5.6	-1.3	-0.7
Judgeford	×	×	3.15	×	×	×	×	10.8	×	×
Karori	×	×	0.02	×	×	×	×	×	×	×
Kelburn	0.0063	-0.0103	6.05	0.19	×	-0.3	-0.9	23.6	2.5	-0.8
Levin	0.0296	0.095	-4.35	-0.13	×	-0.1	-2.9	6.1	0.6	0.4
Mosgiel	×	×	-1.67	-0.11	×	×	×	4.6	1.3	×
Musselburgh	0.0015	-0.046	-6.95	-0.80	-0.03	-0.3	-4.0	-2.7	-0.4	-1.1
Paraparaumu	0.0141	-0.138	-1.84	-0.34	-0.02	0	-3.1	9.7	0.1	-0.6
Pukekohe	0.0142	0.26	-4.78	-0.38	0.04	0	2.8	1.5	-1.6	-0.1
Taiaroa Head	×	-0.147	-9.67	×	×	×	×	×	×	×
Tawa	×	×	-0.30	×	×	×	×	×	×	×
Titahi Bay	×	×	×	×	×	×	×	×	×	×
Tiwai Point	-0.0045	0.0257	-1.29	0.13	-0.007	-0.1	1.8	-18.8	-1.0	-1.1
Waikanae	×	×	3.06	0.02	×	×	×	16.3	0	×
Wainuiomata	×	×	-2.23	×	×	×	×	×	×	×

Exposure Site	Long-Term Change (1980 – 2010)					Two-Year Comparison (2011 – 2012 minus 1987 – 1988)				
	Temperature	RH	Rainfall	Wet Days	Wind Speed	Temperature	RH	Rainfall	Wet Days	Wind Speed
Wallaceville	0.0114	0.0434	-0.90	0.10	×	-0.6	2.4	0.5	-0.4	×
Warkworth	0.0066	0.086	-0.07	-0.26	-0.004	-0.3	1.6	-8.8	-0.9	×

Note:

- Slope of the linear fitting was used for long-term trend analysis
- Averaged monthly data in the two year period was used for the two-year comparison
- Dunedin Botanic Garden Weather Station: Close to exposure sites at Wakari and Normanby
- Musselburgh Weather Station: Close to exposure sites at Forbury and Highcliff
- “×”: Data not available or incomplete

6.2 Atmospheric Corrosion

6.2.1 Corrosion Morphology

New Zealand's atmospheric environment is reasonably clean and free of heavy industrial pollution in most regions. The exposure sites used in this atmospheric corrosion testing can be roughly classified into several categories: marine, rural, industrial (with marine influence) and urban (with marine influence). Morphological characterisations of the exposed specimens showed that corrosion products formed on the metallic coupons were somewhat different, either in thickness or in scale structure (macro or micro) with a dependency on the environmental classification. This was particularly true with the mild steel samples. This is in agreement with Morcillo et al., who also observed that the composition of the rust layer formed on mild steel varied according to the type of atmosphere [Morcillo et al., 2011].

6.2.1.1 Waitoki (Rural)

This site, located in the northern part of the Auckland region, is within a farming area. Both sides of the mild steel sample were uniformly rusted after one year exposure (Figure 27). However, the groundward surface seemed to have more small-sized dark-brown, particle-like features. Under higher magnifications (Optical Microscopy) it could be seen that the corrosion product layers formed on both sides were relatively thick and had a large number of physical defects, such as cracks, pores and protrusions. Similarly, observations at low magnifications revealed more dark protrusions on the groundward surface.

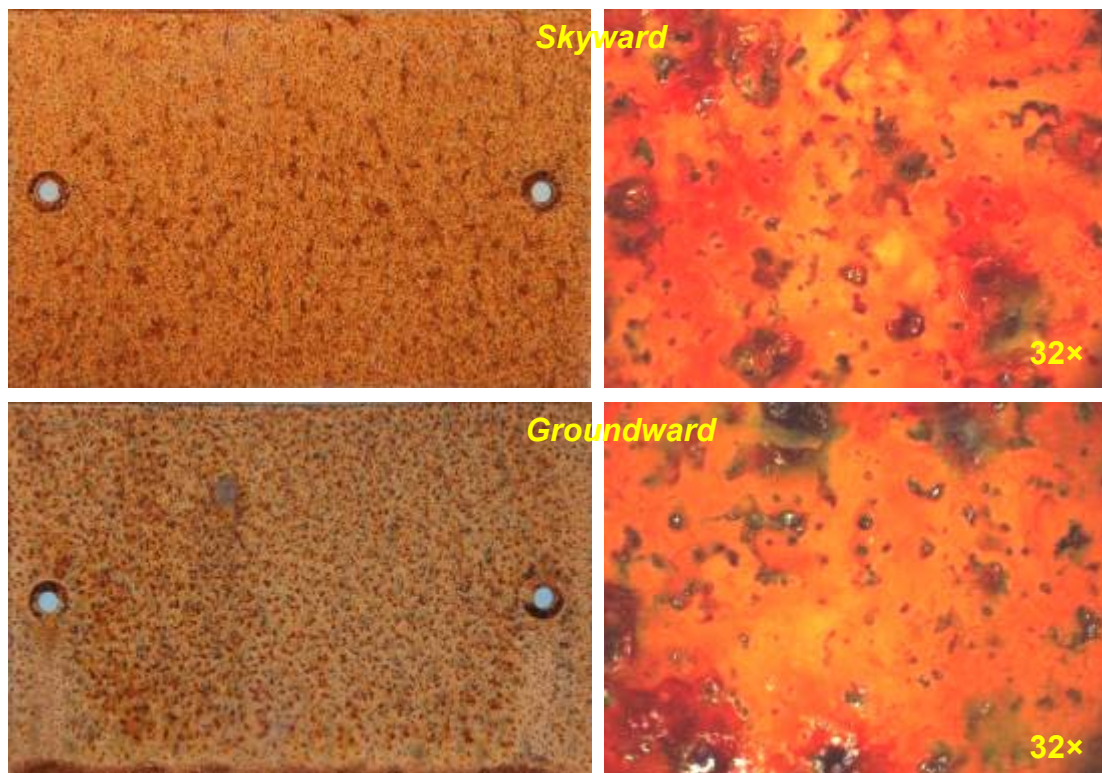


Figure 27. Typical morphology of mild steel coupons after one year exposure at Waitoki

Cross-sectional characterisation revealed an irregular layer with distinct sub-layers on both skyward and groundward faces (Figure 28). The top most layer was relatively thin and exhibited a red/brown colour which was consistent with the optical surface characterisation. The inner layer appeared to be thicker (50-100 μm) and was grey in

colour. The colour difference indicated that the composition and/or phase structure of these two sub-layers might be different. In addition, long, near-horizontal cracks were easily observed in the inner sub-layer, rendering the corrosion layer prone to spalling.

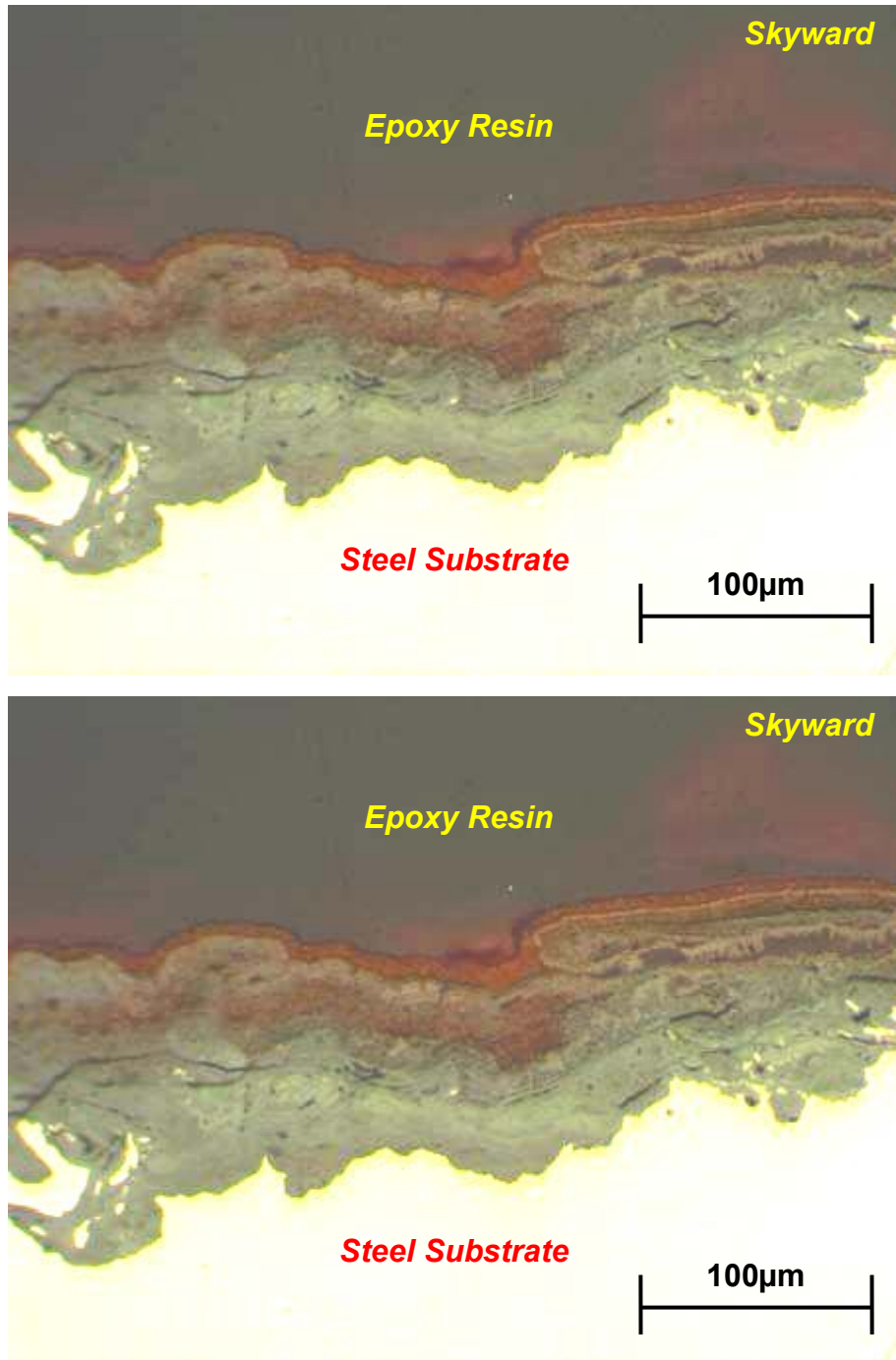


Figure 28. Cross-sectional morphology of mild steel coupons after one year exposure at Waitoki

No serious deterioration was found on the hot dip galvanised zinc coated samples, though some small patches, white in colour, could be identified on the groundward surface (Figure 29). At higher magnifications, dark coloured patches and small white spots or patches could be seen on both surfaces. No rust, or rust-like spots, were

observed on either surface, indicating that the deterioration of the zinc coating was superficial.

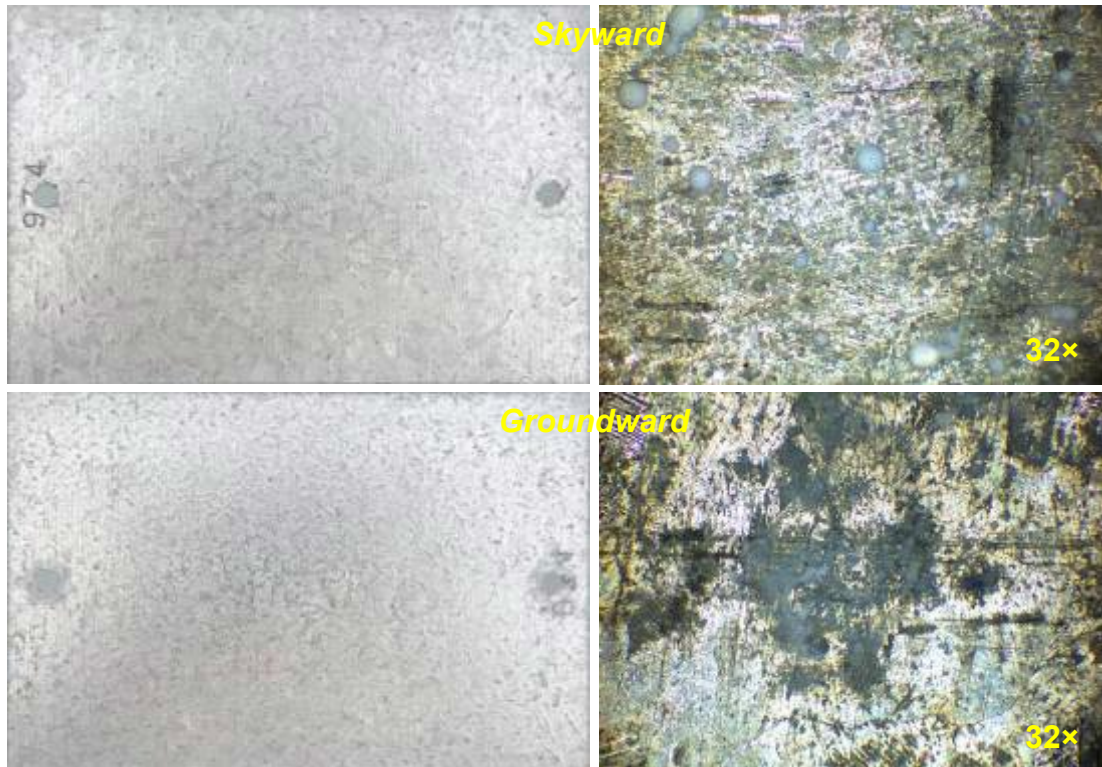


Figure 29. Typical morphology of hot dip galvanised steel coupons after one year exposure at Waitoki

6.2.1.2 Auckland Airport (Marine)

This site, within the Auckland Airport, was very close to the sea. After one year of exposure, the mild steel samples were uniformly, severely corroded (Figure 30). Cross-sectional images also indicated that the corrosion product layer could be divided into two or three sub-layers based on their colour and morphology (Figure 31). However, it appeared that although a distinct red/brown top layer like that observed on the samples exposed at Waitoki was formed, it was much thinner. Therefore, a grey sub-layer comprised the main part of the corrosion product layer remaining on the sample surface. The groundward side suffered even more serious corrosive attack than the skyward. The top part of the iron-rich rust layer was relatively loose, partly detached and spalled off. This led to obvious thickness recession of the steel substrate. This could also be seen under higher magnifications. Cross-sectional images confirmed that the grey corrosion product layer remaining was extremely thick (~200 μm) and had some long cracks and pores (Figure 31).

Relatively serious material deterioration was observed on the hot dip galvanised zinc coating samples as well (Figure 32). This presented in the formation of a large number of small-sized white spots on both surfaces, especially in the areas close to the four edges and the formation of relatively thick, continuous, cloud-like patches covering large areas. Light brown spots or patches were also found on the skyward and groundward faces. The source of this brown material could not be identified. It might be from the underlying steel substrate due to local breakdown of the zinc coating, but possibly could come from the iron-rich corrosion products formed on the nearby mild steel coupons due to wind transfer.

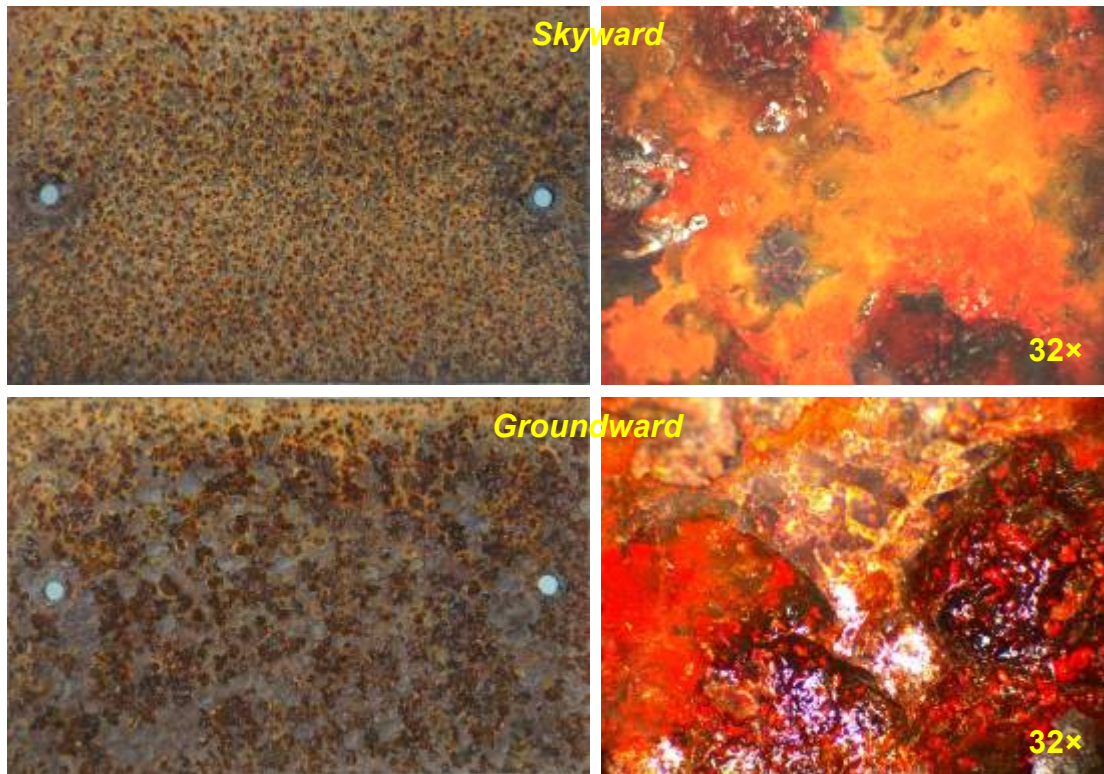
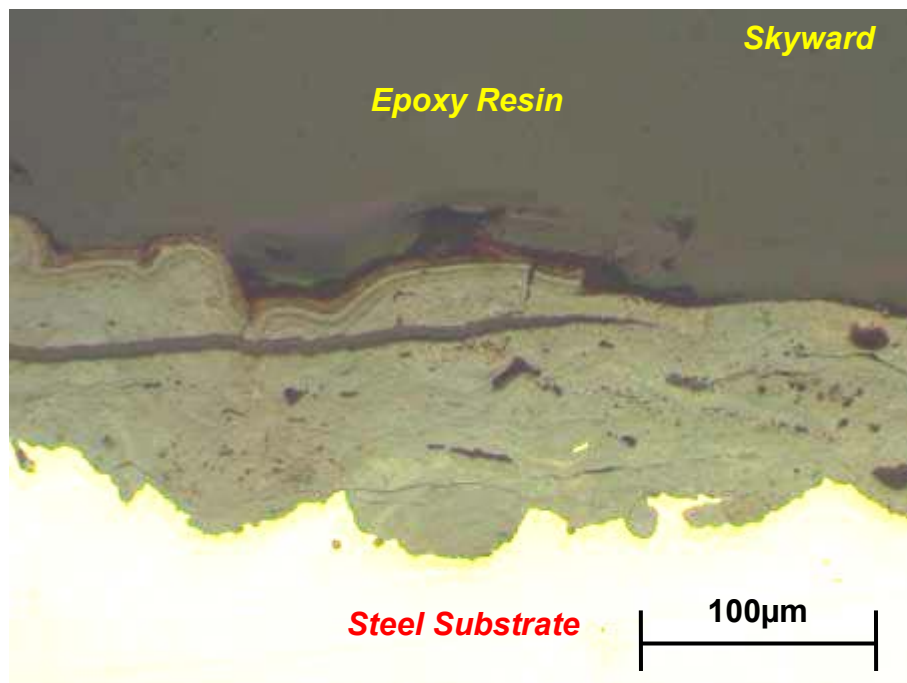


Figure 30. Typical morphology of mild steel coupons after one year exposure at Auckland Airport



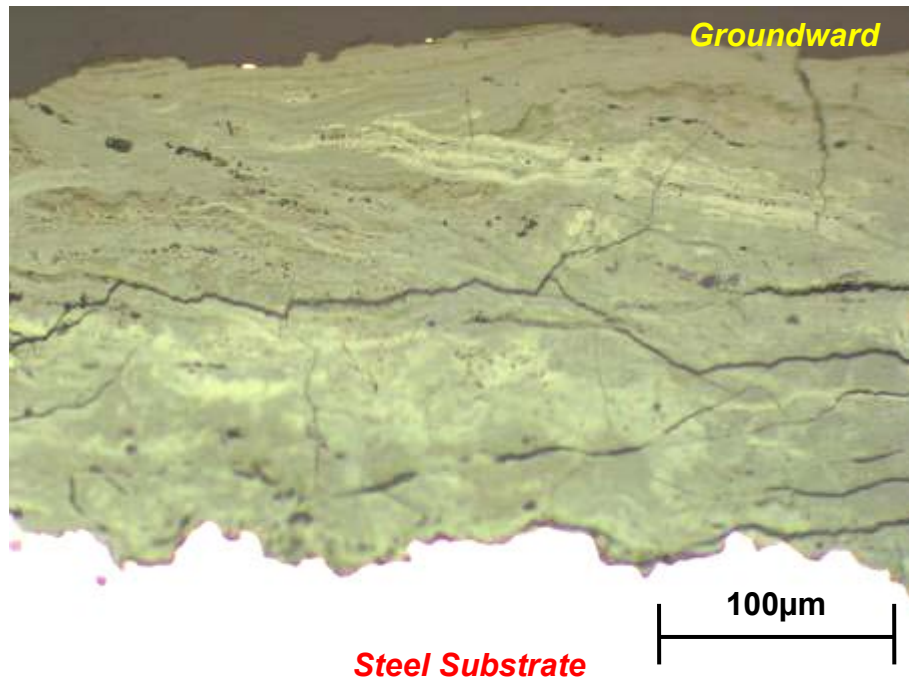


Figure 31. Cross-sectional morphology of mild steel coupons after one year exposure at Auckland Airport

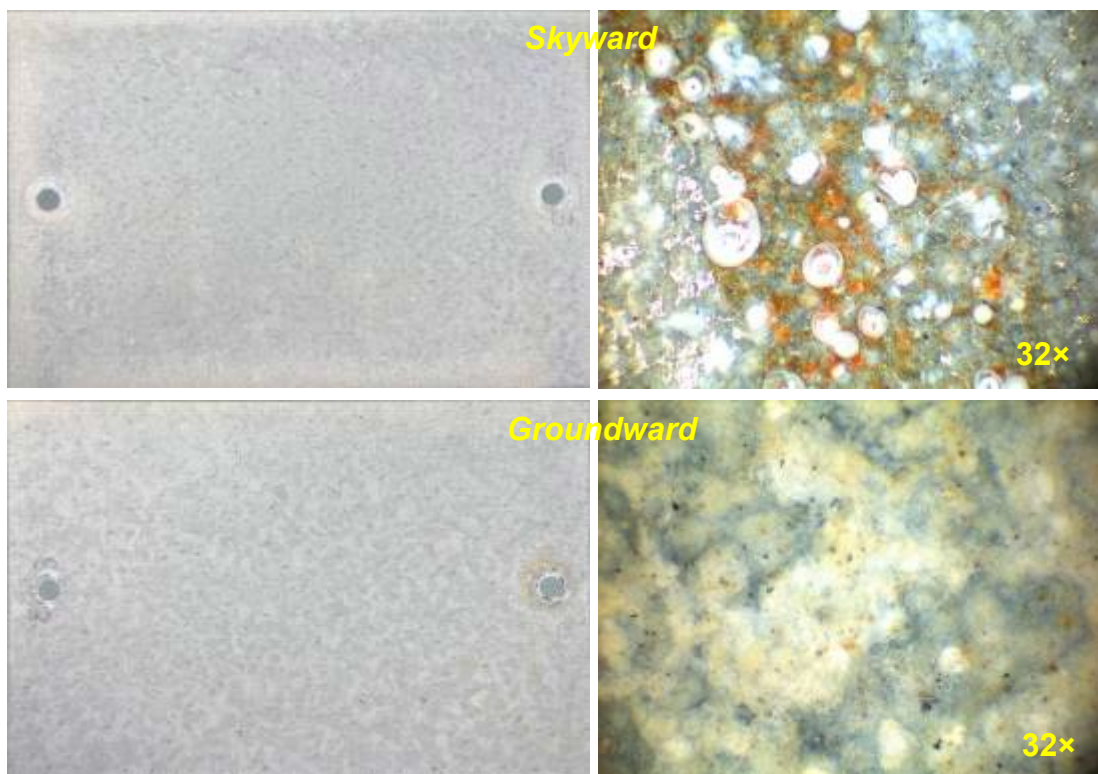


Figure 32. Typical morphology of hot dip galvanized steel coupons after one year exposure at Auckland Airport

6.2.1.3 Gracefield (Light Industrial + Marine)

This site was within the industrial area of Lower Hutt, Wellington. That said, heavy industrial emissions were most likely absent in this area. This site, a few meters away from a road with relatively heavy traffic, was also about 2 km away from the northeast coast of the Wellington Harbour. After one year of exposure, the mild steel samples were uniformly corroded. The groundward face suffered more serious corrosive attack when compared with the skyward side (Figure 33). Observations at higher magnifications showed that the corrosion product layer had a large number of pits and dark coloured protrusions and/or inclusions. The groundward face had more dark coloured protrusions/inclusions. This explained why the groundward side exhibited a darker colour than the skyward side when examined at low magnifications. It is supposed that the more serious corrosion on the groundward side is related to accumulation of salts (especially containing chloride), dirt and/or other particulates from the road which cannot be easily removed by rain.

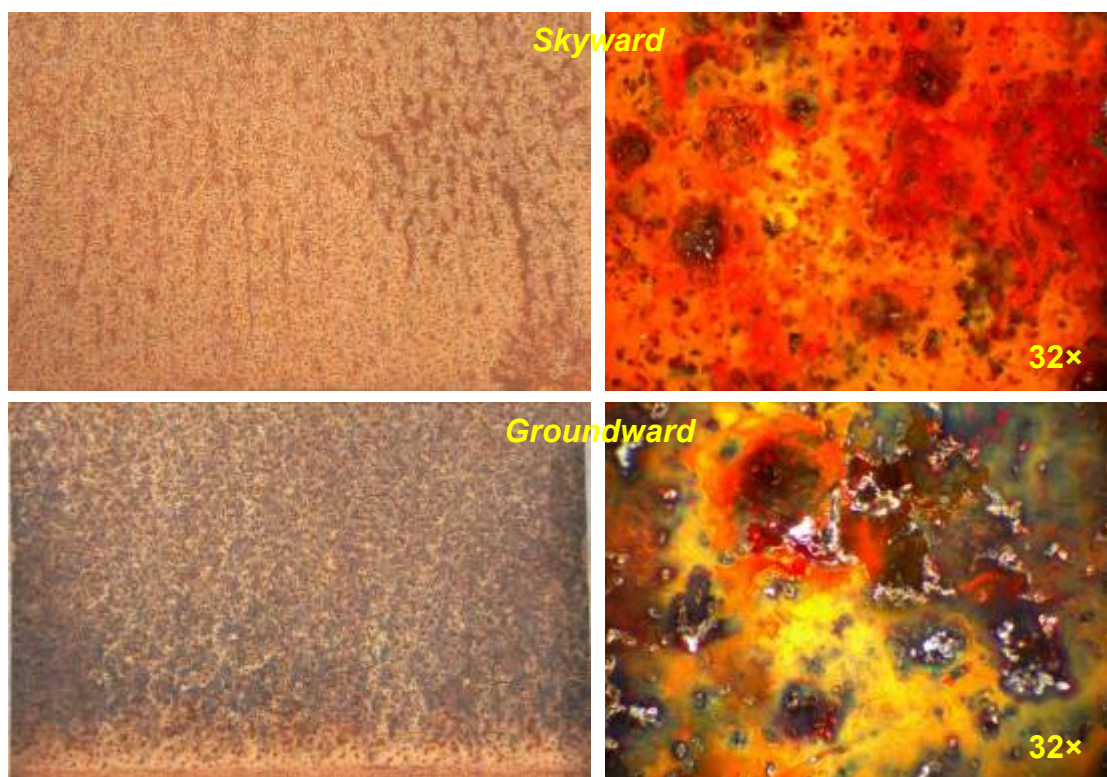


Figure 33. Typical morphology of mild steel coupons after one year exposure at Gracefield, Lower Hutt

Observation of the polished cross-sections revealed a non-uniform layer on the sample surface (Figure 34). The top most part was covered with a red/brown layer which was somewhat similar to that found on the samples exposed at Waitoki, a rural environment. However, its thickness was highly variable, 5-15 μm , especially on the skyward face. The corrosion products immediately adjacent to the steel substrate were grey and had some vertical/horizontal cracks and pores. This sublayer was much thicker ($\sim 60 \mu\text{m}$) on the groundward face.

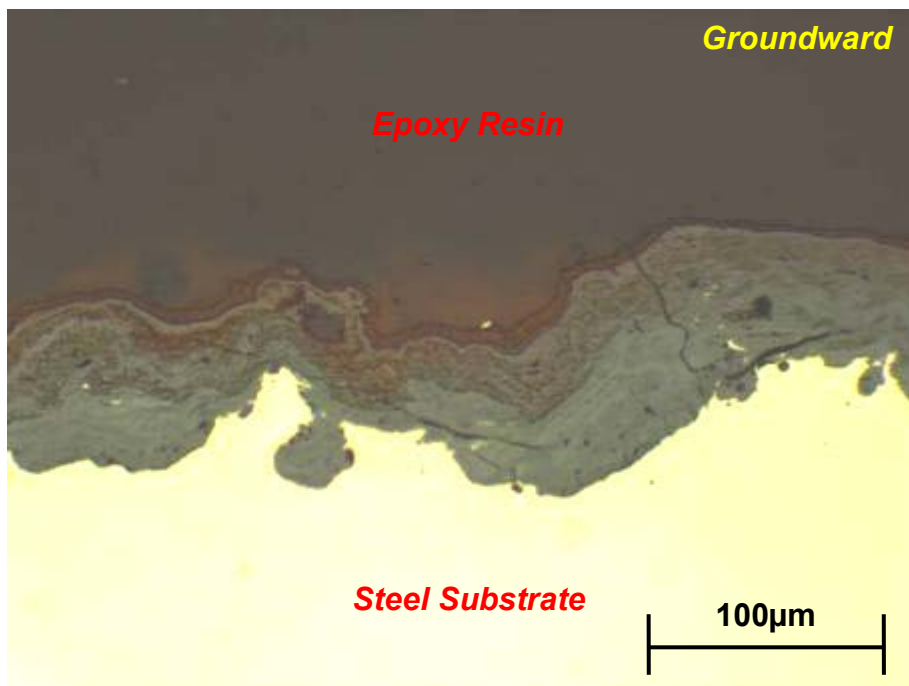
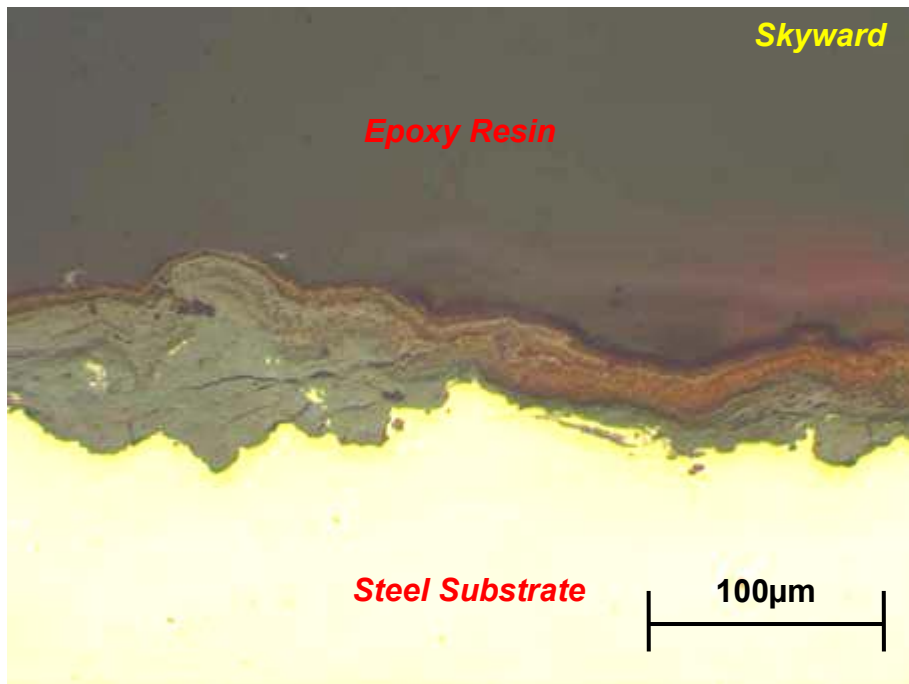


Figure 34. Cross-sectional morphology of mild steel coupons after one year exposure at Gracefield, Lower Hutt

No serious material deterioration was observed on the hot dip galvanised zinc coated samples (Figure 35). However, lots of white particles/spots of varying sizes were formed on the skyward face. Darkening of the zinc coating could also be seen at higher magnifications. On the groundward face, less white spots were found but whitening of some spangles was identified.

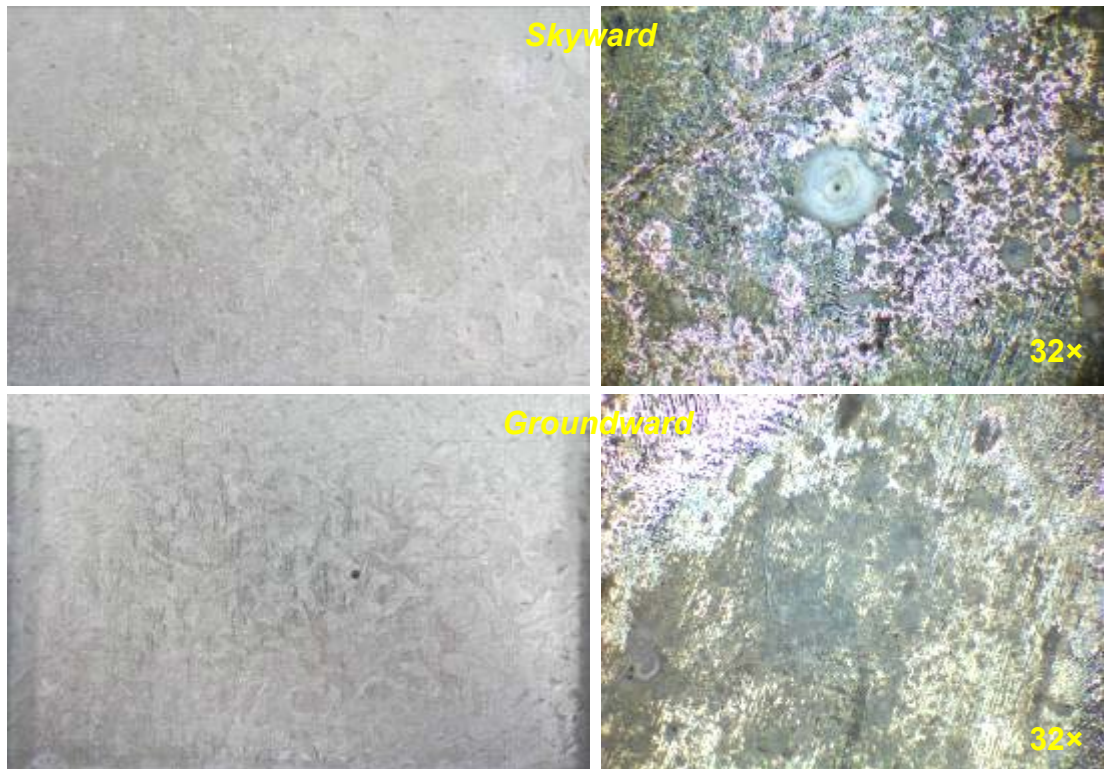


Figure 35. Typical morphology of hot dip galvanised steel coupons after one year exposure at Gracefield, Lower Hutt

6.2.1.4 Tiwai Point (Industrial + Marine)

Tiwai Point lies at the entrance to the Bluff Harbour on the southern coast of the South Island. The site was within the NIWA weather station that was close to the New Zealand Aluminium Smelters factory. The atmospheric environment of this site is influenced by both industrial emissions derived from the aluminium smelter and marine generated chlorides.

It was not surprising to find that after one year of exposure, the surfaces of the mild steel samples were uniformly covered with red-brown iron-rich rust layers (Figure 36). The corrosion product layer on the groundward face appeared to be rough. Characterisation at higher magnifications revealed the presence of many cracks, pores and protrusions. Some inclusions that appeared to be somewhat different from typical iron-rich rust were also found on this surface. Observations on cross-sections also revealed a multi-layered structure (Figure 37). The top most layer was red/brown coloured and relatively thin (15-20 μm). This layer seemed to have a stratified structure and could be found on most areas. Under this layer, a much thicker but irregular layer was present (20-120 μm). It was grey in colour and relatively dense, though horizontal and vertical cracks could be found within it. Inclusions observed in the surface characterisations were also identified from the cross-sectional images. These materials were sitting on the top of the rust layer and appeared to be quite different from the corrosion products of mild steel and the steel substrate. Since this site is very close to the aluminium smelter, they might be aluminium-based particles released from the aluminium production processes.

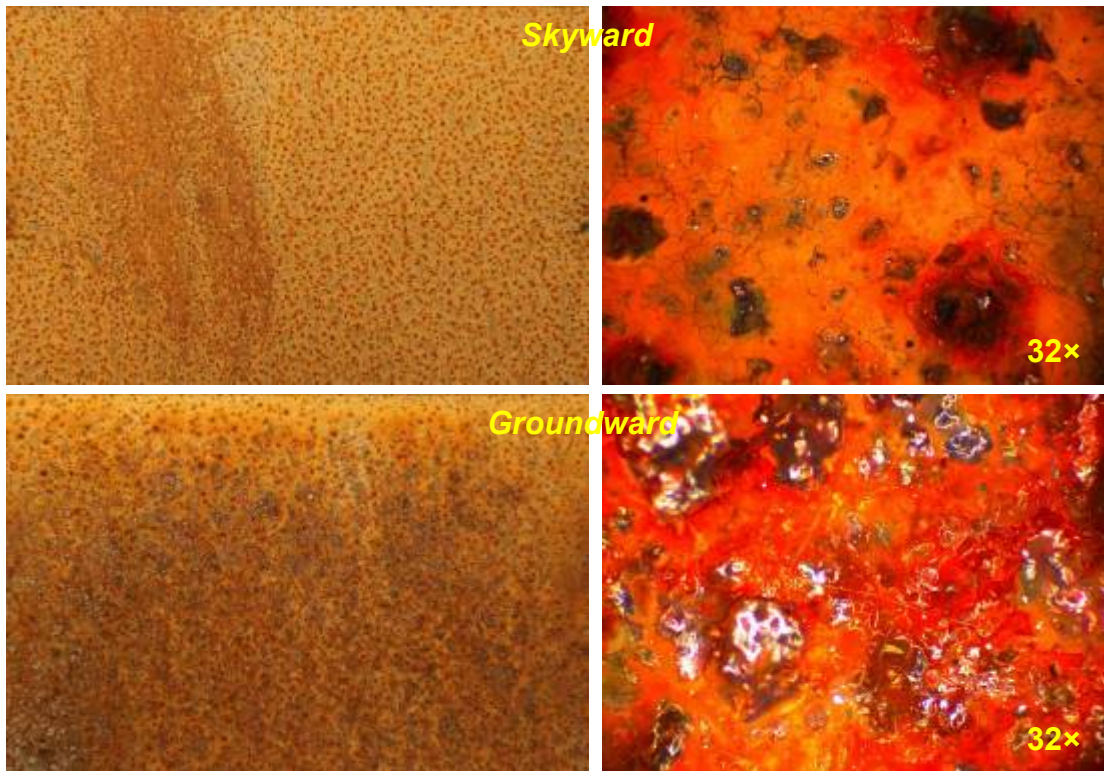
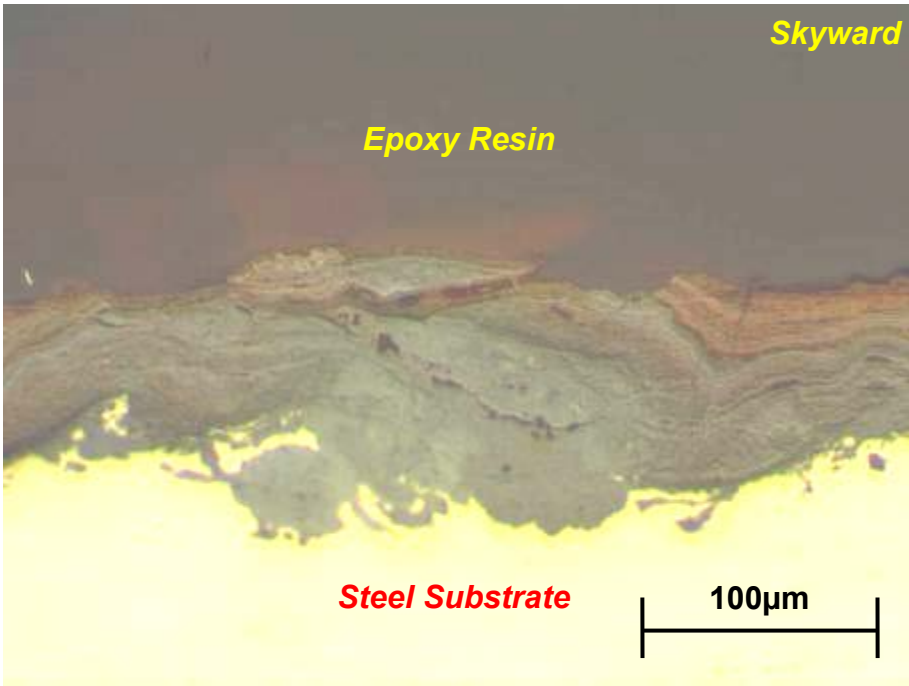


Figure 36. Typical morphology of mild steel coupons after one year exposure at Tiwai Point



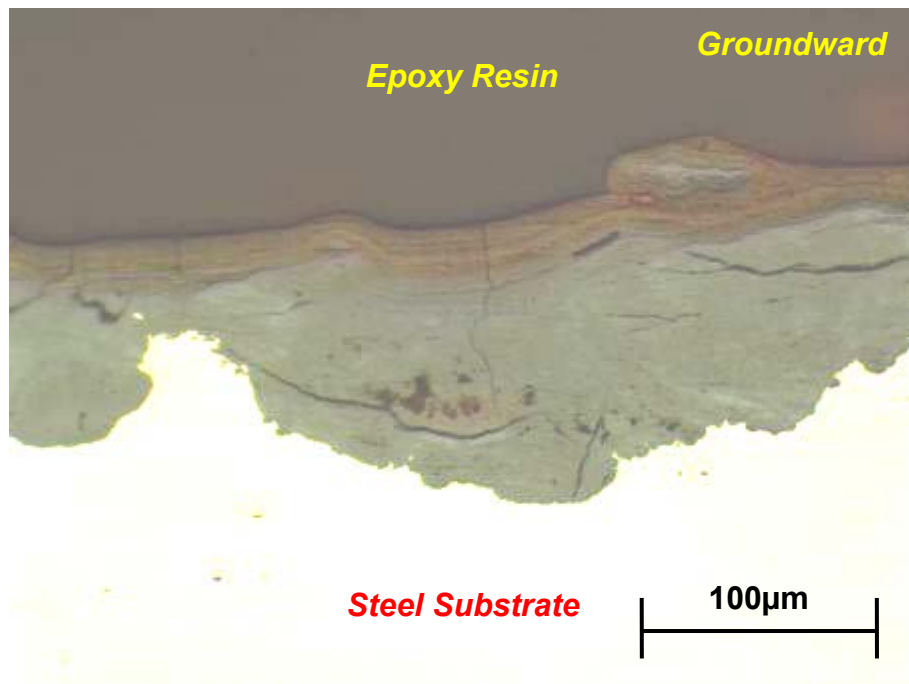


Figure 37. Cross-sectional morphology of mild steel coupons after one year exposure at Tiwai Point

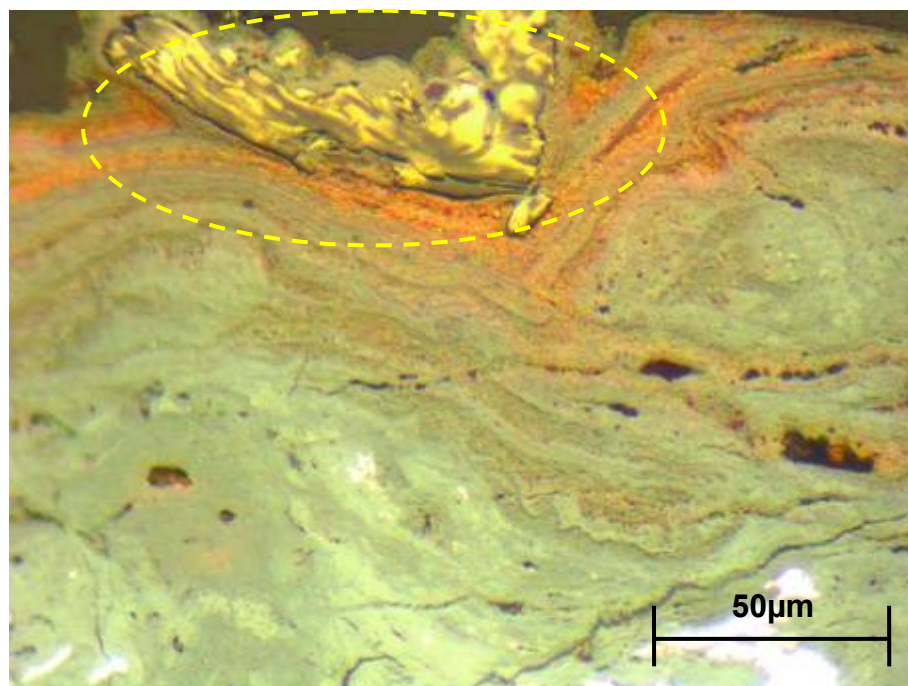


Figure 38. Inclusions of unknown composition found on the groundward face of the mild steel samples exposed at Tiwai Point

Deterioration of the galvanised zinc coating was not serious and showed mainly as darkening (Figure 39). White spots or particles commonly observed on samples exposed at other sites were not seen either. The coating on the groundward side appeared to be attacked more severely, especially in the areas along the edges. A relatively thick layer composed of white and/or grey, densely packed corrosion products was observed.

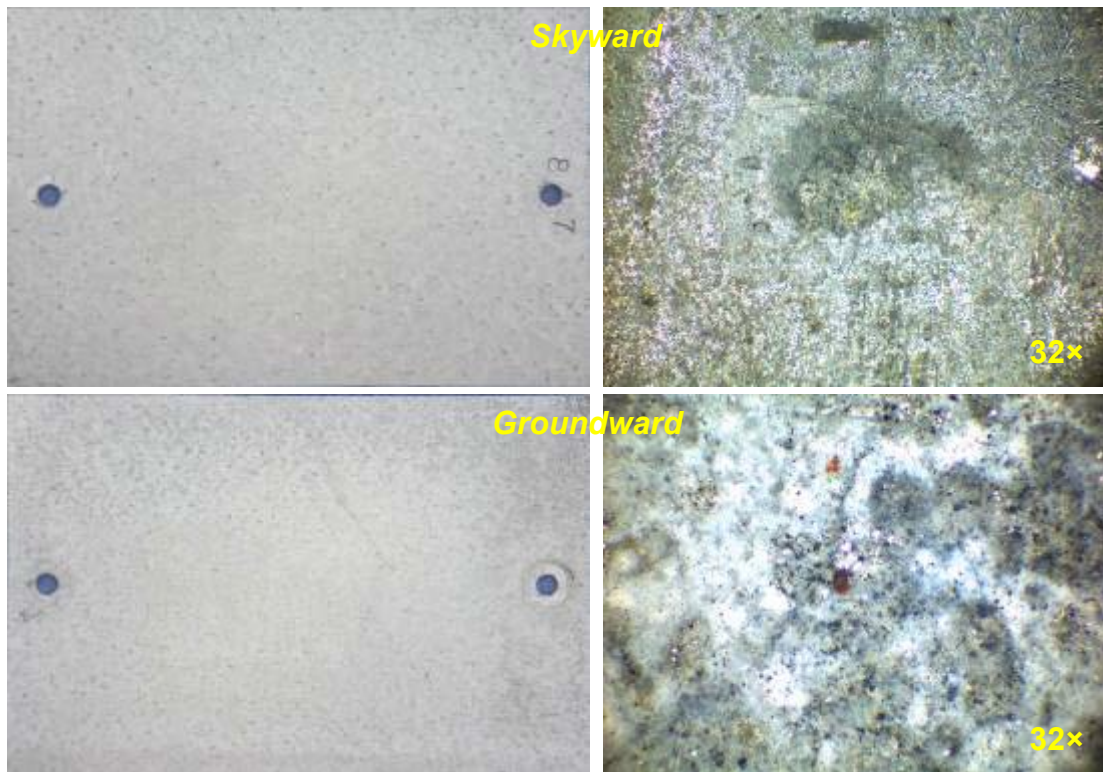


Figure 39. Typical morphology of hot dip galvanised steel coupons after one year exposure at Tiwai Point

6.2.1.5 Forbury (Urban + Marine)

Atmospheric pollution for this site would be mainly from traffic although it may also be influenced by airborne salt brought from the sea (~1.5 km distant) with the prevailing wind from the southwest.

The skyward surfaces of the mild steel samples were uniformly corroded after one year of exposure at this site. Corrosion on the groundward faces appeared to be more advanced with the lower half more dark coloured. This was supported by the optical microscope characterisations that revealed more relatively large, dark protrusions (Figure 40). Cross-sectional characterisation revealed the formation of a two-layered structure: a red/brown top layer and an irregular grey bottom layer. In some areas, the top-most red/brown layer was thicker than the underlying grey layer. However, at most locations, the red/brown layer was absent and the grey layers appeared to be a dominant part of the corrosion product remaining on the steel surface (Figure 41). The protection ability of the growing corrosion product layer was limited since it had lots of physical defects that could provide fast routes for ingress and/or transportation.

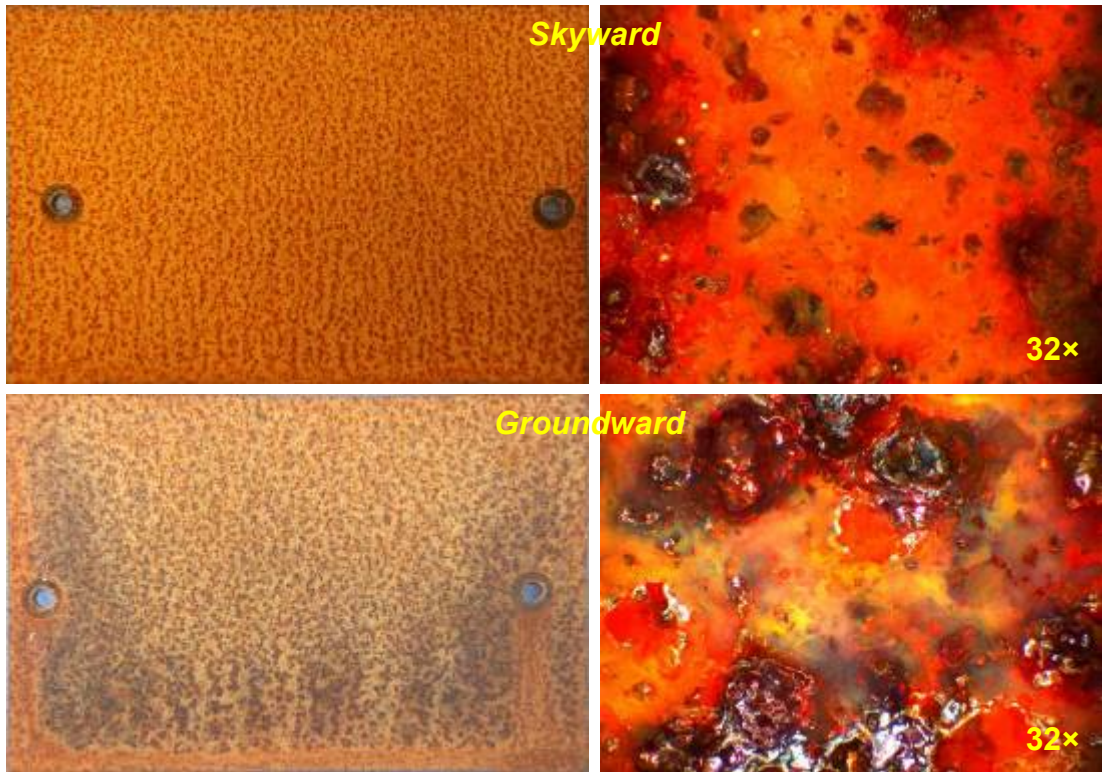
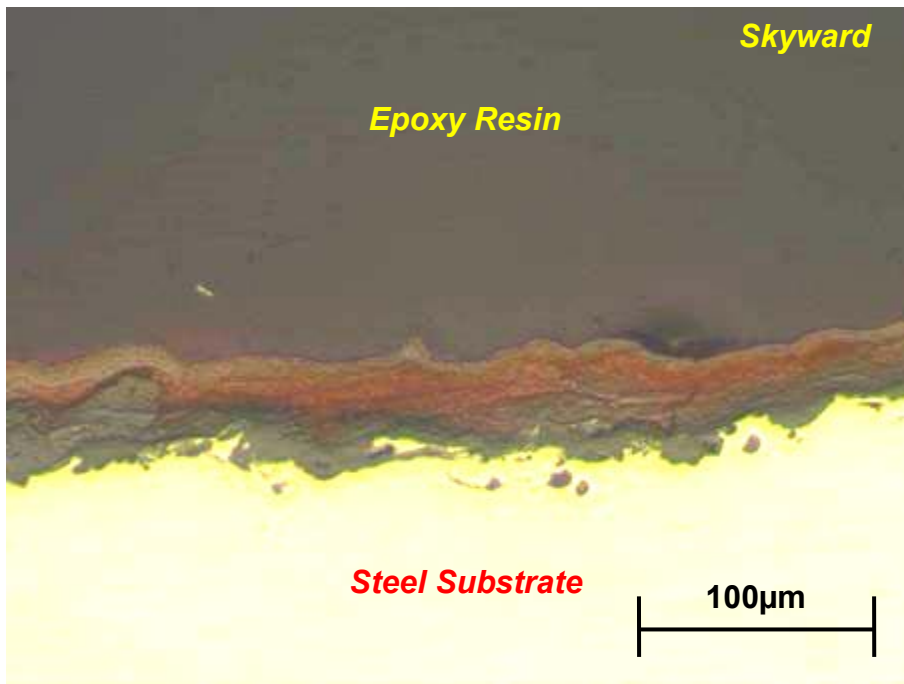


Figure 40. Typical morphology of mild steel coupons after one year exposure at Forbury, Dunedin



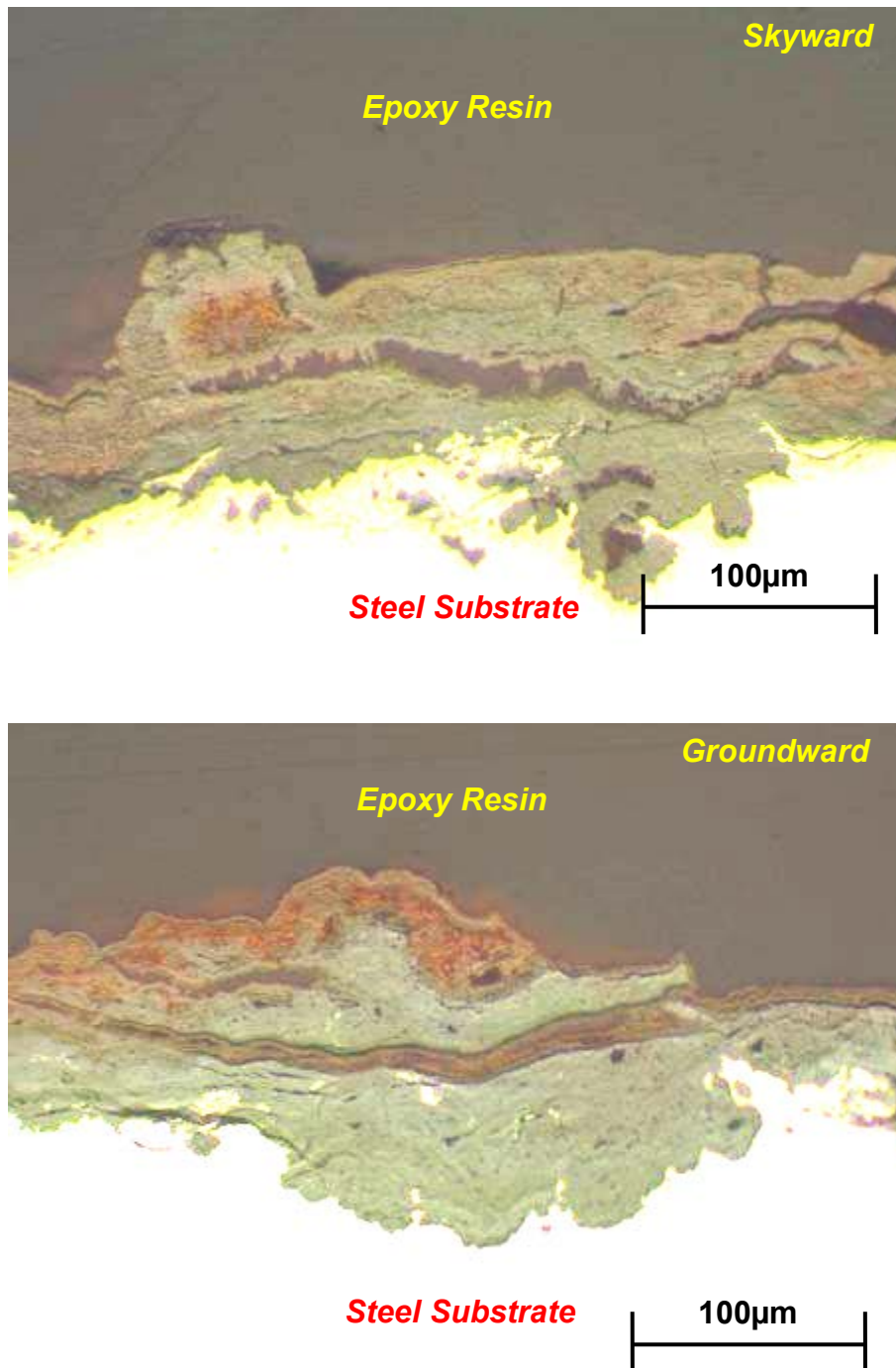


Figure 41. Cross-sectional morphology of mild steel coupons after one year exposure at Forbury, Dunedin

Some small, white spots/particles were observed on the skyward face of the zinc coating, while whitening of some spangles was seen on the groundward face. Optical microscopy revealed darkening of the zinc and the formation of some small, shallow pits (Figure 42).

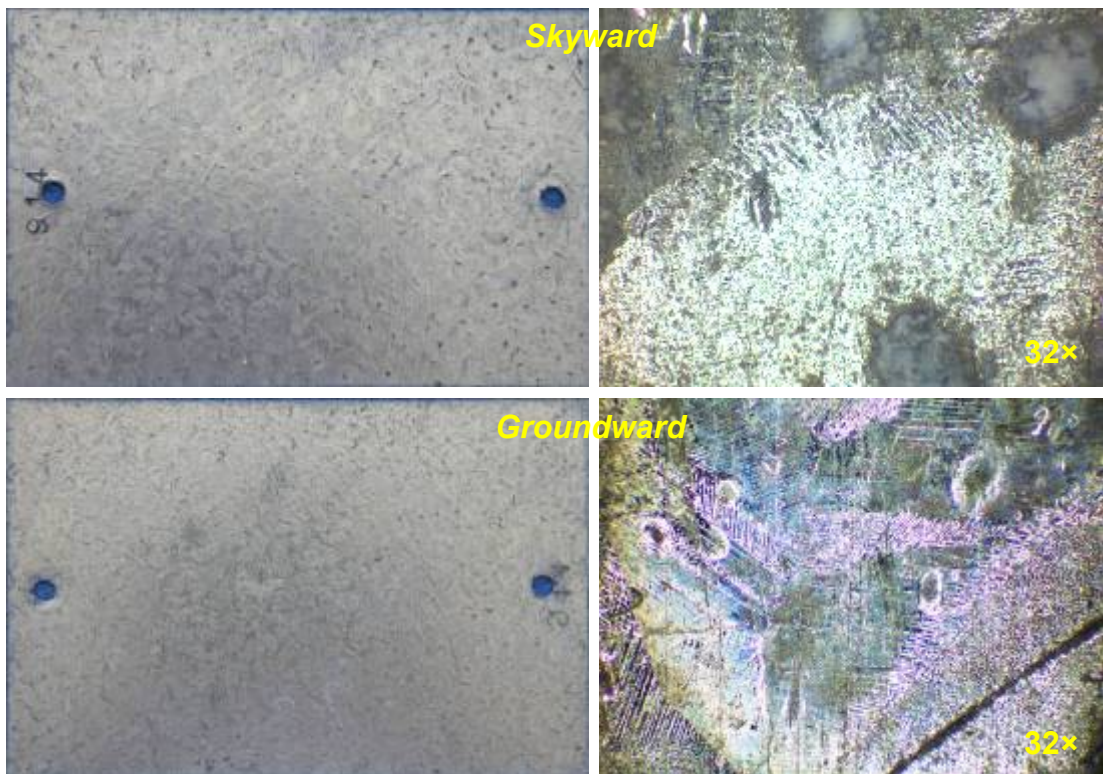


Figure 42. Typical morphology of hot dip galvanised steel coupons after one year exposure at Forbury, Dunedin

6.2.2 Corrosion Rate

The corrosion rates of mild steel and hot dip galvanised zinc coating after one-year exposure at different sites were calculated based on mass loss measurements. The corrosion rates derived from the present study were then compared, where possible, with those of the study carried out in the 1980s by BRANZ (see Table 4).

Table 4. Corrosion rates of mild steel and hot dip galvanised zinc coating derived from BRANZ previous and present studies

Exposure Site	Corrosion Rate (g/m ² /year)				Change in Corrosion Rate (2011 – 2012 vs. 1987 – 1988)	
	1987 – 1988		2011 – 2012		MS	HDG
	MS	HDG	MS	HDG		
Warkworth	191	5.7	-	-	N/A	N/A
Waitoki	-	-	194	3.0	N/A	N/A
Ellerslie	190	3.2	180	4.3	-5%	+34%
Auckland Airport	298	13.0	491	33.3	+65%	+156%
Hunua	180	4.1	155	4.0	-14%	-2%
Ardmore	209	3.5	166	4.7	-21%	+34%
Pukekohe	192	4.1	-	-	N/A	N/A
Tuakau	-	-	139	2.6	N/A	N/A
Hamilton Airport	142	3.5	165	3.3	+16%	-6%

Exposure Site	Corrosion Rate (g/m ² /year)				Change in Corrosion Rate (2011 – 2012 vs. 1987 – 1988)	
	1987 – 1988		2011 – 2012			
	MS	HDG	MS	HDG	MS	HDG
Levin	194	4.0	184	5.3	-5%	+33%
Waikanae	-	-	166	4.3	N/A	N/A
Paraparaumu	240	9.1	187	6.7	-22%	-26%
Pukerua Bay	-	-	167	3.3	N/A	N/A
Titahi Bay	-	-	225	8.6	N/A	N/A
Porirua/Tawa	-	-	206	6.7	N/A	N/A
Tawa	-	-	180	4.7	N/A	N/A
Johnsonville	-	-	208	4.7	N/A	N/A
Gracefield	167	7.0	159	5.3	-5%	-24%
Judgeford	153	5.5	171	4.7	+12%	-15%
Wallaceville	145	4.1	151	2.3	+4%	-44%
Wainuiomata	165	4.1	169	3.3	+2%	-20%
Avalon	164	5.1	153	2.3	-7%	-55%
Kelburn	128	2.5	-	-	N/A	N/A
Karori	-	-	211	5.3	N/A	N/A
Oteranga Bay	-	-	692	33.1	N/A	N/A
Warrington	-	-	128	1.0	N/A	N/A
Port Chalmers	-	-	168	4.3	N/A	N/A
Normanby	-	-	151	4.7	N/A	N/A
Pigeon Flat	-	-	149	2.0	N/A	N/A
Wakari	-	-	146	1.6	N/A	N/A
Forbury	-	-	162	3.0	N/A	N/A
Taiaroa Head	239	4.4	301	5.0	+26%	+14%
Highcliff	-	-	250	5.7	N/A	N/A
Fairfield	-	-	129	0.6	N/A	N/A
Mosgiel	-	-	120	3.6	N/A	N/A
Dunedin Airport	127	1.7	130	1.3	+2%	-24%
Greymouth	511	9.1	342	9.3	-33%	+2%
Invercargill	253	4.0	217	4.3	-14%	+8%
Tiwai Point	341	15.4	300	4.7	-12%	-69%

Note: As mentioned in the Experimental Section, measurement and acquisition of atmospheric corrosion rates to study the potential effects of climate change on material deterioration was not the only objective of this study. Some exposure sites were chosen in areas where the atmospheric corrosion zone boundaries, defined by the maps shown in NZS 3404 and NZS 3604, didn't agree with each other. At some of these sites, a direct comparison of corrosion rate data between the present and previous BRANZ tests cannot be made.

At Auckland Airport, the one year corrosion rate was significantly increased with mild steel from 298 to 491 g/m²/year (an increase of 65%) and zinc from 13 to 33.3 g/m²/year (an increase of 156%). At Avalon, the mild steel corrosion rates measured in previous and present studies were quite similar, while the zinc corrosion rate decreased 55% from 5.1 to 2.3 g/m²/year. At Greymouth, the one year mild steel corrosion rate decreased 33% from 511 to 342 g/m²/year, while the zinc corrosion rate appeared to be unchanged. At Tiwai Point, the mild steel corrosion rate slightly decreased, while the zinc corrosion rate decreased markedly from 15.4 to 4.7 g/m²/year. At other exposure sites where comparisons could be made, changes in corrosion rate (decreases or increases) were also found. These sites include Ellerslie, Hunua, Ardmore, Levin, Paraparaumu Airport, Gracefield, Tairua Head and Invercargill Airport. It was common to find that the changing trend and extent for mild steel and zinc were not always the same and this almost certainly could be explained by the different corrosion mechanisms of mild steel and zinc.

7. DISCUSSION

7.1 Effect of Starting Time

The starting condition (season) of field atmospheric corrosion exposure tests is believed to play a relatively important role in corrosion process and then rate, as the composition and structure of the first layer of corrosion products formed could be significantly affected and, therefore, the protection ability of the growing layer of corrosion products [Syed 2006; Parekh et al., 2012]. However, it is very hard to keep the starting conditions of different exposure tests the same, even at one exposure site, since the climatic conditions, such as ambient temperature, rainfall, environmental humidity and wind speed are not predictable and cannot be completely duplicated.

The starting dates for most samples tested in previous BRANZ survey were within June of 1987. Due to constraints in experimental schedule, most samples in the present study were exposed from middle September and early October 2011. It would then be interesting to see whether the results obtained in these two studies are comparable.

Two sample sets were established at BRANZ's Judgeford campus. One set was exposed from 22 June 2011 to 22 June 2012 while the other set was exposed from 14 September 2011 to 14 September 2012. After one year of exposure, the corrosion rates of these two sample sets were measured to be 164 and 158 g/m²/year. The difference was less than 5%. This result potentially indicates that the starting time has some limited influences on atmospheric corrosion results.

A closer look at climate data of the first 30 days of the current and the previous field exposures at some sites revealed that:

- The ambient temperature in September – October 2011 could be several degrees Celsius higher than that in June – July 1987. This increase might have a positive influence on the corrosion rate;
- The 9am RH in September – October 2011 was, in general, slightly lower than that in June – July 1987. This might decrease ToW and then slow down the corrosion process;
- Precipitation provides surface wetness but can also remove pollutants from the metal surface. There was no consistent trend for rainfall comparison at different exposure sites although the September – October 2011 period might have had a larger number of days without rain.

As such, the initial exposure condition and the initiation of corrosion on the samples exposed in 2011 – 2012 could be either similar to, or different from, that on the samples

exposed in 1987 – 1988, if the potential effects of individual climatic factors on atmospheric corrosion were considered.

Although the composition and phase structure of the corrosion products formed in the initial stage could be changed due to any changes in the starting condition, it is currently unknown to what extent this change can affect the corrosion rates derived after reasonably long exposures. Parekh et al measured the corrosion rates of mild steel, zinc and aluminium with exposure starting points in both the summer and winter seasons. The results of this study indicated that, although the corrosion rate trend was different for samples exposed in different seasons, after one year of exposure the total corrosion rates appeared to be rather similar [Parekh et al., 2012].

7.2 Effect of Climatic Factors

Atmospheric corrosion is controlled by the presence and chemistry of a thin aqueous layer, and by the chemical/phase composition and microstructure of the corrosion products growing on the metal surface. Obviously, any changes in climatic parameters could influence atmospheric chemistry/composition and then atmospheric corrosion processes and kinetics, directly or indirectly [Grøntoft 2011].

Under most atmospheric conditions, wet-dry cycles will happen on metal surfaces. During the night, a moisture layer forms as the surrounding temperature drops, particularly if any contaminants have been deposited, and as the ambient and surface relative humidity increases. During the day, the surface temperature of the metal increases due to solar heating. This leads to a decrease of the surface RH. Consequently, the moisture layer will thin and eventually disappear through evaporation. Surface contaminants may be blown away, be washed off or be retained on the surface, depending on microclimatic conditions. Thus, in determining the effects of climate change on atmospheric corrosion, the effects of climate change on humidity variation, pollutant transportation, pollutant deposition/retention on surfaces and wetting/drying of contaminated surfaces should be considered.

Analysis showed that in the past three decades, New Zealand's climate had undergone a gradual change. In the following sections, the potential correlation between the changes in individual climatic factor and metal corrosion rate will be discussed.

7.2.1 Ambient Temperature

The ambient temperature at the atmospheric exposure site is believed to play a role in determining the corrosivity of an environment since it can affect the surface temperature of the metal concerned [Larsen 2012]. The metal surface temperature directly affects: time of wetness (ToW); drying rate of the electrolyte layer; and, hence, the duration of the electrochemical reactions occurring on the metal surface. Therefore, it can exert various influences on atmospheric corrosion behaviour and kinetics. Generally, an increase in the ambient temperature would tend to increase the metal surface temperature. However, other factors, such as the thermal capacity of metal, its orientation with respect to the sun, the intensity of solar radiation and wind speed/direction will affect the metal surface temperature as well.

An increase in temperature will be expected to increase mass transportation and diffusion, therefore increasing the rate of diffusion-influenced electrochemical reactions, leading to accelerated corrosive attack on the metal. Thus, if the RH of the surrounding environment was kept constant, the increase in temperature would lead to a higher corrosion rate. However, an increase of temperature, partly due to solar irradiation, will generally lead to a decrease of the RH and also a decrease of the ToW. Consequently, the corrosion rate tends to be decreased. The interactions are clearly complex, but the effect of temperature on atmospheric corrosion actually has a maximum for many

materials. The decreasing part of the trend is due to the true time of wetness [Barton 1976; Tidblad et al., 1998].

From a global perspective, the most direct consequence of climate change is an increase in ambient temperature. From Table 3, 12 of the 14 exposure sites, where reasonably complete ambient temperature data set can be obtained, showed an increase in averaged annual ambient temperature in the long-term trend. However, it should be mentioned that the increase of temperature was normally at the level of 0.01-0.03°C per year. In addition, the comparison of the ambient temperature between the periods of 1987 – 1988 and 2011 – 2012 showed that no large increase of temperature occurred at most exposure sites used for the present study.

From Table 4, it is clear that atmospheric corrosion rates for both mild steel and the galvanised steel samples exhibited relatively complex changing behaviours. Increased, decreased and equivalent corrosion rates were observed for sites where comparisons between tests in the 1980s and 2010s were possible. This indicated that the exact influences of ambient temperature cannot be considered alone and it must be realised that atmospheric corrosion is a process governed by many factors, including both environmental- and materials-based aspects.

The current results indicate that the slight temperature change at most sites over the last two decades has had a very limited direct influence on metal corrosion processes. Some researchers actually believe that climate change induced warming is unlikely to have a significant effect on corrosion of most materials, even though they might have a positive temperature coefficient of corrosion rate. An increase of 2 K in temperature would be expected to increase corrosion rate for only about 0.6% [Cole and Paterson 2010; Nguyen et al., 2012]. However, it is possible that changes in ambient temperature, though gradual and small, may still exert an influence on other climatic factors, directly or indirectly. These factors may affect atmospheric corrosion processes of metals. Unfortunately, these complex correlations cannot be explored in detail as limited information is currently available.

7.2.2 Humidity

A comparison between Table 3 (climate) and Table 4 (corrosion rate) revealed that:

- At Ardmore, the annual RH at 9am exhibited a slight decrease in the long-term trend and a relatively obvious decrease in the two-year period comparison (2011 – 2012 vs. 1987 – 1988). Meanwhile, the mild steel corrosion rate decreased by approximately 20%.
- At Auckland Airport, the annual RH at 9am exhibited a very slight decrease in the long-term trend and a slight increase in the two-year period comparison (2011 – 2012 vs. 1987 – 1988). Meanwhile, the mild steel corrosion rate increased significantly, by approximately 65%.
- At Dunedin Airport, the annual RH at 9am exhibited a very slight increase in the long-term trend and a slight increase in the two-year period comparison (2011 – 2012 vs. 1987 – 1988). Meanwhile, the mild steel corrosion rate remained unchanged (130 vs. 127 g/m²/year).
- At Greymouth, the annual RH at 9am exhibited a very slight decrease in the long-term trend and the two-year period comparison (2011 – 2012 vs. 1987 – 1988). Meanwhile, the mild steel corrosion rate decreased by approximately 33%.
- At Hamilton Airport, the annual RH at 9am was almost unchanged over the long-term, but showed a slight increase in the two-year period comparison (2011 – 2012 vs. 1987 – 1988). Meanwhile, the mild steel corrosion rate increased slightly, by approximately 16%.

- At Invercargill Airport, the annual RH at 9am exhibited a very slight decrease in the long-term trend and a very slight increase (almost unchanged) in the two-year period comparison (2011 – 2012 vs. 1987 – 1988). Meanwhile, the mild steel corrosion rate decreased by approximately 14%.
- At Levin, the annual RH at 9am exhibited a slight increase in the long-term trend and a slight decrease in the two-year period comparison (2011 – 2012 vs. 1987 – 1988). Meanwhile, the mild steel corrosion rate remained almost unchanged (184 vs. 194 g/m²/year).
- At Paraparaumu Airport, the annual RH at 9am exhibited a relatively obvious decrease in the long-term trend and a slight decrease in the two-year period comparison (2011 – 2012 vs. 1987 – 1988). Meanwhile, the mild steel corrosion rate decreased by approximately 22%.
- At Taiaroa Head, the annual RH at 9am exhibited a relatively obvious decrease in the long-term trend (the two-year period comparison cannot be made). Meanwhile, the mild steel corrosion rate increased by approximately 26%.
- At Tiwai Point, the annual RH at 9am exhibited a very slight increase in the long-term trend and a slight increase in the two-year period comparison (2011 – 2012 vs. 1987 – 1988). Meanwhile, the mild steel corrosion rate decreased by approximately 12%.
- At Wallaceville, the annual RH at 9am exhibited a very slight increase in the long-term trend and the two-year period comparison (2011 – 2012 vs. 1987 – 1988). Meanwhile, the mild steel corrosion rate remained almost unchanged (151 vs. 145 g/m²/year).

Table 5. Changes in relative humidity (RH) and atmospheric corrosion rate of mild steel

Exposure Site	Long-Term Trend (1980 – 2010)	Two-Year Comparison (2011 – 2012 minus 1987 – 1988)	Change in Corrosion Rate (2011 – 2012 vs. 1987 – 1988)
Ardmore	-0.0896 %/year	-6.5	-20%
Auckland Airport	-0.0355	2.4	+65%
Dunedin Airport	0.04	2.3	+2%
Greymouth	-0.0269	-1.1	-33%
Hamilton Airport	0.0075	2.2	+16%
Invercargill Airport	-0.0188	0.8	-14%
Levin	0.095	-2.9	-5%
Paraparaumu Airport	-0.138	-3.1	-22%
Taiaroa Head	-0.147	N/A	+26%
Tiwai Point	0.0257	1.8	-12%
Wallaceville	0.0434	2.4	+4%

These observations indicate that the long-term trend of RH of the atmosphere has a relatively poor correlation with the corrosion rate derived from short-term exposures. However, it appeared that a slightly better correlation between the short-term (two-year period) comparison of RH and the one year mild steel corrosion rate is present in the current measurements. For example, at Ardmore and Auckland Airport, the change in

RH was similar to the change in corrosion rate. At Dunedin Airport, Levin and Wallaceville, RH exhibited a slight change while the mild steel corrosion rate appeared to be unchanged. That said, at Greymouth and Paraparaumu Airport, the mild steel corrosion rate obviously decreased while the RH only showed a slight change.

Environmental humidity is regarded as one of the most important factors for atmospheric corrosion since it directly affects the formation of a surface moisture layer that will participate and/or assist mass transfer, electrochemical reaction and corrosion process [Nguyen et al., 2012]. If water or moisture was the only medium involved in the metal corrosion process, a lower RH could lower the fraction of the metal surface wetted and, hence, a smaller area of metal surface would be affected. This would tend to decrease the corrosion rate. However, humidity is not the only factor and, in most cases; various gaseous and solid pollutants that deposit onto the metal surface will be involved directly in the atmospheric corrosion processes. Consequently, pH and concentration of pollutant dissolved in the surface electrolyte layer play a more important role. A decrease of RH together with a decreased fraction of surface wetted would then lead to a local increase of pollutant concentration. This favours a higher local corrosion rate, albeit over a relatively short time scale.

Most exposure sites used in the present study were within the marine influenced regions of New Zealand. Therefore, airborne salt particles will contribute to the material's deterioration. Changes in environmental RH may also induce changes in the size of airborne salt particles. Other researchers have found that corrosion may not initiate on steel surfaces covered with deliquescent NaCl particles having diameters less than $\sim 45 \mu\text{m}$, since small droplets may contain oxygen above the critical level necessary to passivate the steel surface [Li and Hihara 2010]. Therefore, RH changes will affect the nature, morphology and severity of corrosion attack with the involvement of chloride-containing particles.

It should also note that the 9am RH value at these exposure sites was quite high, typically around 80%. Based on this, the atmospheric environment can be classified as humid. A significant change in corrosion rate with RH alone would be difficult to categorically discern in this range. Furthermore, the data accumulated on averaged RH at 9am could not reflect the actual, complete wetting and drying behaviour occurring on a metal surface during the day and night periods. Therefore, it would give a relatively limited indication of how environmental humidity can influence atmospheric corrosion of metals. It is expected that time of wetness (ToW) would be a more reliable measure for analysis of atmospheric corrosion in regard to water or moisture on a metal surface. However, this data set is not available.

7.2.3 Rainfall

A comparison between Table 3 (climate) and Table 4 (corrosion rate) revealed that:

- At Ardmore, the rainfall exhibited a very slight increase on the long-term trend and the two-year period comparison (2011 – 2012 vs. 1987 – 1988). Meanwhile, the mild steel corrosion rate decreased by approximately 20%.
- At Auckland Airport, the rainfall was almost unchanged on the long-term trend but showed an increase in the two-year period comparison (2011 – 2012 vs. 1987 – 1988). Meanwhile, the mild steel corrosion rate increased by approximately 65%.
- At Dunedin Airport, the rainfall exhibited a slight decrease on the long-term trend and a very slight decrease in the two-year period comparison (2011 – 2012 vs. 1987 – 1988). Meanwhile, the mild steel corrosion rate remained unchanged (130 vs. 127 g/m²/year).
- At Greymouth, the rainfall was almost unchanged in the long-term trend but showed an obvious decrease in the two-year period comparison (2011 – 2012 vs.

1987 – 1988). Meanwhile, the mild steel corrosion rate decreased by approximately 33%.

- At Hamilton Airport, the rainfall exhibited a slight increase in the long-term trend and an obvious increase in the two-year period comparison (2011 – 2012 vs. 1987 – 1988). Meanwhile, the mild steel corrosion rate increased by approximately 16%.
- At Invercargill Airport, the rainfall exhibited a very slight decrease in the long-term trend and a slight decrease in the two-year period comparison (2011 – 2012 vs. 1987 – 1988). Meanwhile, the mild steel corrosion rate decreased by approximately 14%.
- At Levin, the rainfall exhibited a slight decrease on the long-term trend and a slight increase in the two-year period comparison (2011 – 2012 vs. 1987 – 1988). Meanwhile, the mild steel corrosion rate remained almost unchanged (184 vs. 194 g/m²/year).
- At Paraparaumu Airport, the rainfall exhibited a very slight decrease in the long-term trend but a relatively obvious increase in the two-year period comparison (2011 – 2012 vs. 1987 – 1988). Meanwhile, the mild steel corrosion rate decreased by approximately 22%.
- At Taiaroa Head, the rainfall exhibited an obvious decrease in the long-term trend (the short-term changing trend was not available). Meanwhile, the mild steel corrosion rate increased by approximately 26%.
- At Tiwai Point, the rainfall exhibited a very slight decrease in the long-term trend and an obvious decrease in the two-year period comparison (2011 – 2012 vs. 1987 – 1988). Meanwhile the mild steel corrosion rate decreased by approximately 12%.
- At Wallaceville, the rainfall showed no obvious change in the long-term trend and in the two-year period comparison (2011 – 2012 vs. 1987 – 1988). Meanwhile, the mild steel corrosion rate remained unchanged (151 vs. 145 g/m²/year).

Table 6. Changes in rainfall and atmospheric corrosion rate of mild steel

Exposure Site	Long-Term trend (1980 – 2010)	Two-Year Comparison (2011 – 2012 minus 1987 – 1988)	Change in Corrosion Rate (2011 – 2012 vs. 1987 – 1988)
Ardmore	1.84 mm/year	2.5 mm	-20%
Auckland Airport	-0.43	15.2	+65%
Dunedin Airport	-3.09	-2.2	+2%
Greymouth	0.22	-22.6	-33%
Hamilton Airport	3.13	27.6	+16%
Invercargill Airport	-0.95	-5.6	-14%
Levin	-4.35	6.1	-5%
Paraparaumu Airport	-1.84	9.7	-22%
Taiaroa Head	-9.67	N/A	+26%
Tiwai Point	-1.29	-18.8	-12%
Wallaceville	-0.90	0.5	+4%

It can be seen that the long-term trend of rainfall was very poorly correlated with the change in one year mild steel corrosion rate. However, it appeared that the two-year period comparison (2011 – 2012 vs. 1987 – 1988) might have a slightly better correlation with the trend of the first year atmospheric corrosion rates of mild steel found in this work. For example, at Auckland Airport, an increase was observed for both rainfall and corrosion rate. At Dunedin Airport, Invercargill Airport, Levin and Wallaceville, data analyses revealed a reasonably stable trend for both rainfall and corrosion rate. However, at Ardmore, Greymouth and Paraparaumu Airport, the one year mild steel corrosion rate decrease was obvious in the period of 2011 – 2012, while the rainfall did not show an obvious change in the same period.

Rainfall is very important for initialisation and development of corrosion on a metal surface, although its exact influence is not fully understood as yet. It is generally accepted that rain will maintain the humidity of the air above the critical humidity. If rain was retained in pockets or crevices of the corrosion product layer, it may accelerate corrosion by supplying continued wetness in these localised areas [Cole and Ganther 2006; Cole and Paterson 2007]. Further, regular washing of the sample surface could partially remove corrosion products, consequently fresh metal surface would be exposed to further corrosive attack.

It is interesting to note that the annual rainfall had a certain degree of correlation with the atmospheric corrosion rate of mild steel at some exposure sites. For example, the annual rainfalls for Dunedin Airport, Ardmore and Greymouth were around 700, 1000 and 2000 mm, while the corrosion rates were measured to be 127, 209 and 511 g/m²/year for the period of 1987-1988 and 130, 166 and 342 g/m²/year for the period of 2011 – 2012, respectively. However, at one exposure site, an increase of the annual rainfall does not always imply a higher corrosion rate will be seen.

The exposure sites used in the present study have diversified environments and the atmospheric corrosivity will be affected by many environmental factors, particularly the presence, deposition and concentration of airborne pollutants and/or solid particles. For example, mild steel had a corrosion rate of 491 and 166 g/m²/year at Auckland Airport and Ardmore, respectively. The annual rainfalls at these two exposure sites were very similar. The much higher metal corrosion rate at Auckland Airport could be partially explained by the heavier influence of airborne salt (e.g. NaCl) particles since the exposure rack installed at this site was just a few meters from the sea.

Mild steel had a corrosion rate of 491 and 342 g/m²/year at Auckland Airport and Greymouth, respectively. The annual rainfalls at these two sites were quite different, ~1000 mm at Auckland Airport and >2000 mm at Greymouth. Although the exposure rack was further from the sea at Greymouth (i.e. less severe airborne salt influence on the corrosion) this observation could still indicate that rain may have a beneficial effect on corrosion resistance. In other tests, atmospheric corrosion has been observed to be more severe and localised on surfaces that were not periodically washed by rain. Rain can clean the metal surface and, thus, remove accumulated dust and/or corrosive deposits. BRANZ measured the corrosion rates of mild steel samples installed at different angles (5, 45 and 90°) on one exposure rack. The sample with minimal drainage (5°) always exhibited the highest corrosion rate. Rain washing effects are particularly noticeable in marine environments if sufficient rain falls onto an inclined surface [Ganther et al., 2011]. However, if the amount of rainfall is extremely limited, pollutants deposited may redistribute on the metal surface, but their total load will remain the same. Experimental and theoretical work indicates that the amount of rainfall required for surface cleaning to begin was between 0.8 and 1.2 mm, while 1.3 and 3.7 mm of rain were required to totally clean a surface. Pollutants were reduced to 10% of their original concentrations after a rainfall of 1.5 mm [Cole and Paterson 2007].

Wet days at these exposure sites were also analysed. A wet day is defined by NIWA as the number of days during which the daily total precipitation is greater than 1 mm. This amount could be expected to have a cleaning effect on a metal surface. In general, the changes in rainfall and wet days were similar but a difference could still be found at some exposure sites. In other words, a higher rainfall does not always mean a larger number of wet days. This would make the understanding of rainfall effects on corrosion rate more complicated. A larger rainfall with a smaller number of wet days may indicate less frequent cleaning of the pollutants deposited onto a corroding surface. This will not necessarily lead to a lower corrosion rate.

7.2.4 Wind Speed

Wind, or more accurately, prevailing wind, is another climatic factor that should be considered during atmospheric corrosion testing and result analysis [Klassen and Roberge 2001; Schweitzer 2006]. Some studies have indicated that when wind speed was incorporated into atmospheric corrosion modelling, better predicted results and/or better correlations could be produced [Oesch and Heimgartner 1996]

The wind speed data set is incomplete in NIWA's CliFlo database, and limited data was available for analysis at several exposure sites used in the present study.

A comparison between Tables 3 and 4 yields the following findings.

- At Auckland Airport, the wind speed exhibited a very slight decrease in the long-term trend and a relatively obvious decrease in the two-year period comparison (2011 – 2012 vs. 1987 – 1988; ~1 m/s decrease). Meanwhile, the mild steel corrosion rate increased significantly by approximately 65%.
- At Dunedin Airport, the wind speed exhibited a slight decrease in the long-term trend and a relatively obvious decrease in the two-year period comparison (2011 – 2012 vs. 1987 – 1988; ~1 m/s decrease). Meanwhile, the mild steel corrosion rate remained unchanged (130 vs. 127 g/m²/year).
- At Hamilton Airport, the wind speed exhibited a very slight decrease in the long-term trend. Meanwhile, the mild steel corrosion rate increased by approximately 16%.
- At Invercargill Airport, the wind speed exhibited a very slight decrease in the long-term trend and a relatively obvious decrease in the two-year period comparison (2011 – 2012 vs. 1987 – 1988; ~0.7 m/s decrease). Meanwhile, the mild steel corrosion rate decreased by approximately 14%.
- At Levin, the wind speed exhibited a slight increase in the two-year period comparison (2011 – 2012 vs. 1987 – 1988). Meanwhile the mild steel corrosion rate was almost unchanged (184 vs. 194 g/m²/year).
- At Paraparaumu Airport, the wind speed exhibited a slight decrease in the long-term trend and in the two-year period comparison (2011 – 2012 vs. 1987 – 1988). Meanwhile, the mild steel corrosion rate decreased by approximately 22%.
- At Tiwai Point, the wind speed was almost unchanged in the long-term trend and exhibited a relatively obvious decrease in the two-year period comparison (2011 – 2012 vs. 1987 – 1988; ~1 m/s decrease). Meanwhile, the mild steel corrosion rate decreased by approximately 12%.

These observations demonstrate that when a decrease in wind speed was observed, a decrease in the one year mild steel corrosion rate could be expected. This is particularly true for the results derived from the short period comparisons (2011 – 2012 vs. 1987 – 1988) at Invercargill Airport, Paraparaumu Airport and Tiwai Point. At Levin, a slight increase of the wind speed was observed together with an almost unchanged

corrosion rate. Overall, these observations indicate that wind speed might be related to the one year corrosion rate of mild steel during atmospheric exposure.

Table 7. Changes in wind speed and atmospheric corrosion rate of mild steel

Exposure Site	Long-Term Trend (1980 – 2010)	Two-Year Comparison (2011 – 2012 minus 1987 – 1988)	Change in Corrosion Rate (2011 – 2012 vs. 1987 – 1988)
Auckland Airport	-0.01 m/s/year	-0.9 m/s	+65%
Dunedin Airport	-0.02	-0.9	+2%
Hamilton Airport	-0.01	N/A	+16%
Invercargill Airport	-0.01	-0.7	-14%
Levin	N/A	0.4	-5%
Paraparaumu Airport	-0.02	-0.6	-22%
Tiwai Point	-0.007	-1.1	-12%

At Auckland Airport, Invercargill Airport and Tiwai Point, the averaged wind speed was normally ranging from 4 to 6 m/s and the wind speed decrease was around 1 m/s in the two-year period comparisons. At Dunedin Airport, the wind speed was normally less than 4 m/s. An obvious change in the corrosion rate of mild steel was not observed with a decrease of 1 m/s in wind speed. It appeared that a critical wind speed, around 5 m/s, might exist and influence atmospheric corrosion. In other studies, a critical velocity, close to 3 m/s (or larger than 3-5 m/s) seemed to exist for saline winds. In addition, coastal atmospheric salinity notably increased, and a considerable effect on atmospheric corrosion could be observed [Morcillo et al., 2000; Feliu et al., 2001]. It has also been proposed that in order for corrosion to develop, salt aerosol must impinge onto a metal surface and this can only happen when the wind speed is above a certain minimum [Klassen et al., 2002].

As discussed in the previous sections, atmospheric corrosion is heavily dependent on the presence of a water/moisture film on the metal surface. The velocity and direction of the wind will affect the formation and persistence of this film on the metal surface. More importantly, airborne pollutants and solid dusts/particles, when dissolved into this water film, can generally increase its aggressivity and accelerate the corrosion processes. A lower wind speed would favour the retaining of the moisture layer on the metal surface and accumulation of more pollutants. This tends to result in a higher corrosion rate and this might be the case for Auckland Airport. However, different trends were observed at some sites in this study as well. Generally, the atmosphere in New Zealand is relatively clean and most regions are basically free of heavy industrial emission. Corrosion of metal, when exposed to the open atmosphere, is supposed to be mainly governed by pollutants in solid form, such as dust and salt particles. Transportation over long distances and accumulation of these pollutants on metal surfaces would be favoured by stronger winds.

Most airborne salt particles in New Zealand are sourced from the sea. Salt production in the ocean and airborne salinity are highly dependent on white-cap activity and local wind speeds, with the latter playing a more important role [Nguyen et al., 2012]. Computational modelling has shown that salt production at a wind speed of 15 m/s can be an order of magnitude higher than that at 5 m/s [Cole et al., 2003]. For the transport of salt from the open ocean to inland areas, the wind speed is by far the most important

physical variable. A higher wind speed normally leads to a larger distance of travel and a higher salt concentration.

However, corrosion of metal will be controlled by the concentration of salt deposited onto its surface at those times when a moisture layer is present. It is apparent that winds with a speed exceeding a critical value have the ability to blow dry salt off metal surfaces [Cole et al., 2004]. Thus, a higher wind speed may carry more pollutants over a longer distance, but it may also have a cleaning or even drying effect on a corroding metal surface, which may benefit corrosion resistance.

7.2.5 Wind Direction

The direction of the prevailing wind is also very important for atmospheric corrosion, especially in marine or polluted environments [Morcillo et al., 2000; Santana Rodríguez et al., 2003; Slamova et al., 2012]. In this study, the mild steel corrosion rate measured at Greymouth decreased significantly from 511 to 342 g/m²/year. The exposure rack was installed by the same technician at the same site as used in the 1980s study. Analysis of the long and short-term data revealed very slight changes in climatic factors at this exposure site. Therefore, this huge difference in corrosion rate might be related to a change in wind direction. Unfortunately, wind direction data is not available from the NIWA's national climate database for the period of 2011 – 2012.

The influence of pollutant transportation with the prevailing wind might be limited over long distances and would be highly dependent on geographic features over the route. A closer look at the mild steel corrosion rates obtained within the Otago region showed that an obvious increase or decrease of metal deterioration rate along the common wind direction was absent. This might be a result of the barrier effect of mountains, forest bands and vegetation coverage on the wind route. Some pollutants could be effectively blocked by these physical barriers. However, it did appear that a gradual decrease of corrosion rate with the distance from the coastline existed, and this could be explained by the carriage of sea-salt inland from the ocean [Duncan and Balance 1988; Feliu et al., 1999].

7.2.6 Solar Irradiation

Light of certain wavelengths can stimulate photo-sensitive corrosion reactions on steel and copper. Potential interactions between ultra-violet (UV) light, airborne chlorides and oxidising agents such as ozone may produce reactive species that can be transported to the surface of susceptible metals and then be involved in corrosion processes. It has been found that UV induced photo-dissociation of ozone can generate reactive atomic oxygen which can react with silver (Ag) rapidly to form Ag₂O, leading to a more severe attack on the Ag surface [Chen 2010]. On the other hand, UV irradiation has been proved to be capable of suppressing pit generation and enhancing the passivity of AISI 304 stainless steel in solutions containing chlorides [Macdonald et al., 1996; Moussa and Hocking 2001]. In addition, solar heating can affect ToW.

Data on solar irradiation is not available for most exposure sites used in the present study. Though limited data was retrieved from NIWA'S CliFlo database for Auckland Airport, Kelburn and Dunedin Airport, these data sets are incomplete and the long-term changing trend could not be derived with confidence.

7.3 Potential Impacts on Current Atmospheric Corrosivity Maps

Two atmospheric corrosivity maps are currently used in two discrete New Zealand standards: NZS 3404 and NZS 3604. As noted in the previous sections, these two maps were established using different methods.

Theoretical equations, defined as a function of meteorological variables, e.g. average annual daily temperature, time of wetness and annual rainfall, were used by NZS 3404

to produce first-year carbon steel macroclimate corrosion rates for regions at different distances from the sea. The raw data, after modification with a series of multipliers, was then used to determine the atmospheric corrosivity of a specific site or a geographic region, and to establish the atmospheric corrosivity map shown in NZS 3404.1:2009 [El Sarraf and Clifton 2011]. Meanwhile, BRANZ data used to determine atmospheric corrosivity was measured with mild steel and hot dip galvanised zinc coated coupons, exposed at more than 100 sites spread across New Zealand in the 1980s [Duncan and Cordner 1991]. The atmospheric corrosivity map shown in NZS 3604 was then established by considering actual metal corrosion rates and the prevailing wind.

A comparison of these two maps shows that their corrosion zone boundaries are not the same. Hence, some exposure sites used in the present study were selected from the regions where these two maps didn't agree with each other, for example, Auckland, Wellington and Dunedin. This provides an experimental approach to investigate whether the current maps are correctly defining the atmospheric corrosivity.

Some exposure sites were also chosen so that the latest corrosion rates could be compared directly with those collected about 25 years ago. Results analysis shows that significant changes in corrosion rates of mild steel or zinc were only observed at a limited number of sites. Overall, the new atmospheric corrosion rates were comparable to the old rates. Hence, the data obtained in this study can be incorporated with BRANZ previous data. This makes the data set more complete, especially for those regions where limited atmospheric corrosion testing had been done previously.

Based mainly on the mild steel corrosion rates obtained during the period of 2011 – 2012, potential changes to the zone boundaries for current atmospheric corrosivity maps can be recommended. These are detailed in the following sections. However, it must be noted that a proper interpretation of the results should take account of:

- The present testing was finished within 2011 – 2012, with a time gap of approximately 25 years from BRANZ previous surveying in the 1980s. It is not easy to reproduce metal atmospheric corrosion rate measurements. Many factors, typically including material (chemical composition, dimensions and surface finish), climate, atmospheric pollution, starting season and exposure period, can influence corrosion results. Atmospheric chemistry and composition could change due to variations in climatic variables over the long periods involved. Although the changing trends of individual climatic parameters and their correlations with variations in metal corrosion rates have been investigated in the present study, a clear understanding of New Zealand climate change and its potential influences on metal atmospheric corrosion has not been achieved.
- The methods used to generate the atmospheric corrosion rate data used for the maps in NZS 3404 and NZS 3604 are quite different. The experimental approach used by BRANZ (and in NZS 3604) measures metal corrosion rate and determines atmospheric corrosivity directly. The results derived might only reflect the corrosivity of the test sites accurately in the specified time period. Although the data used by NZS 3404 map is also defined as the first-year carbon steel corrosion rate, it appears to represent a statistical result since the climate data input into the theoretical modelling equations was based on an average of a 30-year period (1971 – 2000). The data, therefore, is not the same as the data used in the NZS 3604 map and collected in the present study. Further, the accuracy of the theoretically derived atmospheric corrosion rates heavily relies upon sufficient data and a clear understanding of the influences of individual climatic variables on metal corrosion. Several multipliers were then used to modify the predicted data to minimise its discrepancies with BRANZ experimental data, but differences still exist for several regions.

7.3.1 Auckland Region

Corrosion rate data was available for seven sites in the Auckland region. The corrosion rate numbers obtained in this study have been put onto the two maps to show their differences directly (Figure 43).

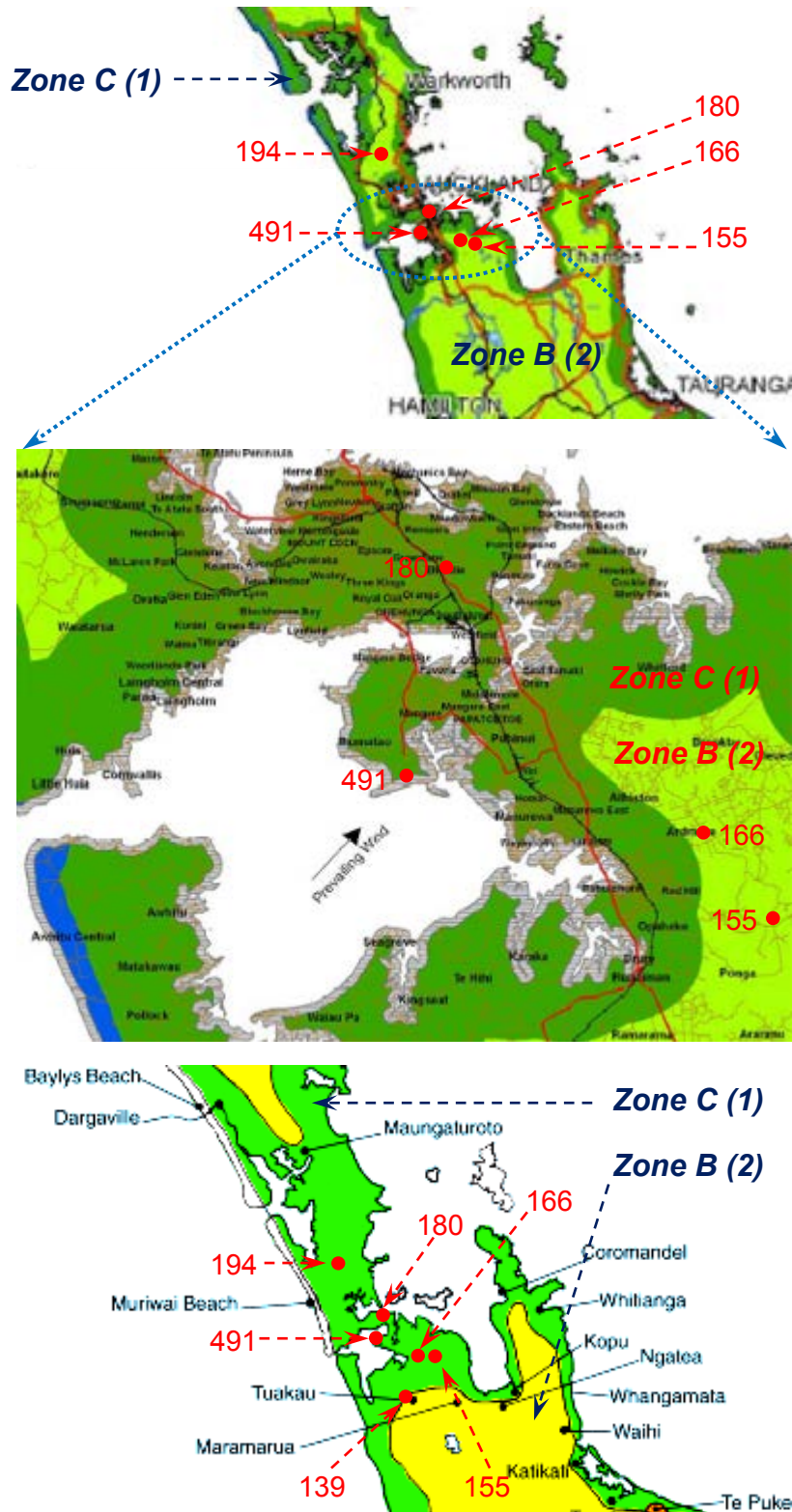


Figure 43. Corrosion zone boundary definition in NZS 3404 and NZS 3604 maps with the mild steel corrosion rates derived from the present study (2011 – 2012)

Major differences in boundary locations between the two maps exist in the northern part of Auckland. Zone 1 (or Zone C) covers a larger area in the NZS 3604 map than in the NZS 3404 map. Zone 1 (or Zone C) locations, according to ISO 9223, AS/NZS 2312 and AS/NZS 2728, would exhibit a one-year mild steel corrosion rate ranging from 201 to 400 g/m²/year.

Only one exposure site was selected within the area that was defined as Zone 2 by the map in NZS 3404 and as Zone 1 (or Zone C) by the map in NZS 3604. This site, at Waitoki, was a reasonably open, flat and rural environment surrounded mainly by farm land. After one year of exposure, the mass loss of the mild steel coupon was measured to be 194 g/m²/year. This value is very close to 200 g/m²/year and sits on the boundary between Zone 1 (or Zone C) and Zone 2 (or Zone B), and risk to infrastructure could be reduced by classifying this exposure site into Zone 1 (or Zone C).

A slight difference was also seen in the southern region of Auckland. This basically covered the areas of Drury, Pukekohe, Hunua and Tuakau. Similar to the northern area, Zone 1 (or Zone C) of the NZS 3604 map covered a larger area than that of the NZS 3404 map. The corrosion rates obtained at Ardmore, Hunua and Tuakau ranged from 139 to 166 g/m²/year. This indicates that the area classified as Zone 1 (or Zone C) in the NZS 3604 map could be reduced, particularly when the prevailing wind from the south-west direction is considered. The south end of Zone 1 (or Zone C) could be moved slightly north.

The mild steel corrosion rate at Ardmore was measured to be 209 and 166 g/m²/year in previous and present BRANZ studies, respectively. At Hunua, which is close to Ardmore, the mild steel had a corrosion rate of 155 g/m²/year in 2011 – 2012 measurement, i.e. decreased slightly, when compared with that obtained in the 1980s. Geographically, the Hunua Ranges at the east of Hunua and Ardmore is a range covered by forest and vegetation. This may block the salt-laden wind from the east coast, possibly leading to a recession of the boundary of Zone 1 (or Zone C) to the east in this area.

7.3.2 Wellington Region

Similar to the observations in the Auckland region, Zone 1 (or Zone C) in the map of NZS 3604 covered a larger area than that of NZS 3404. Wellington city was completely classified as Zone 1 by the NZS 3604 (Figure 44).

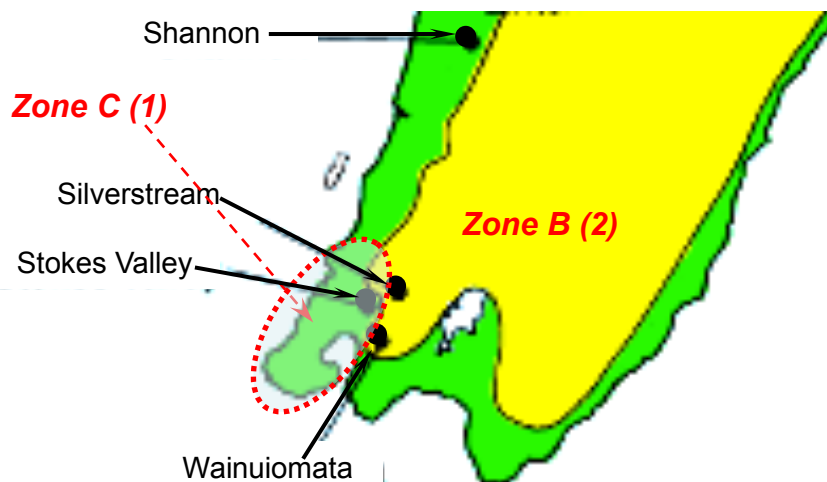


Figure 44. Corrosion zone boundary definition in NZS 3604 map for Wellington region

Atmospheric corrosion measurements were carried out at several sites in Porirua, Tawa, Johnsonville and Karori. All these sites were located in Zone 2 (or Zone B) defined by the map of NZS 3404. Corrosion rates of mild steel coupons were derived as 196, 180, 208 and 211 g/m²/year, respectively, during the period of 2011 – 2012. These numbers are at the lower end of the corrosion rate range of Zone 1 (or Zone C; 201 – 400 g/m²) or the higher end of Zone 2 (or Zone B; 10 – 200 g/m²/year). Further, the corrosion rates of hot dip galvanised zinc coated coupons were derived as 6.7, 4.7, 4.7 and 5.3 g/m²/year, respectively. These numbers are also at the lower end of the corrosion rate range of Zone 1 (5.01 – 15 g/m²/year) or the higher end of Zone 2 (0.7 – 5 g/m²/year). The mild steel corrosion rates were put onto the current atmospheric corrosivity map, as shown in Figure 45, for direct comparison. Please note that the coupons exposed at the Pukerua Bay site were slightly sheltered from the weather by the building and trees in the back yard.

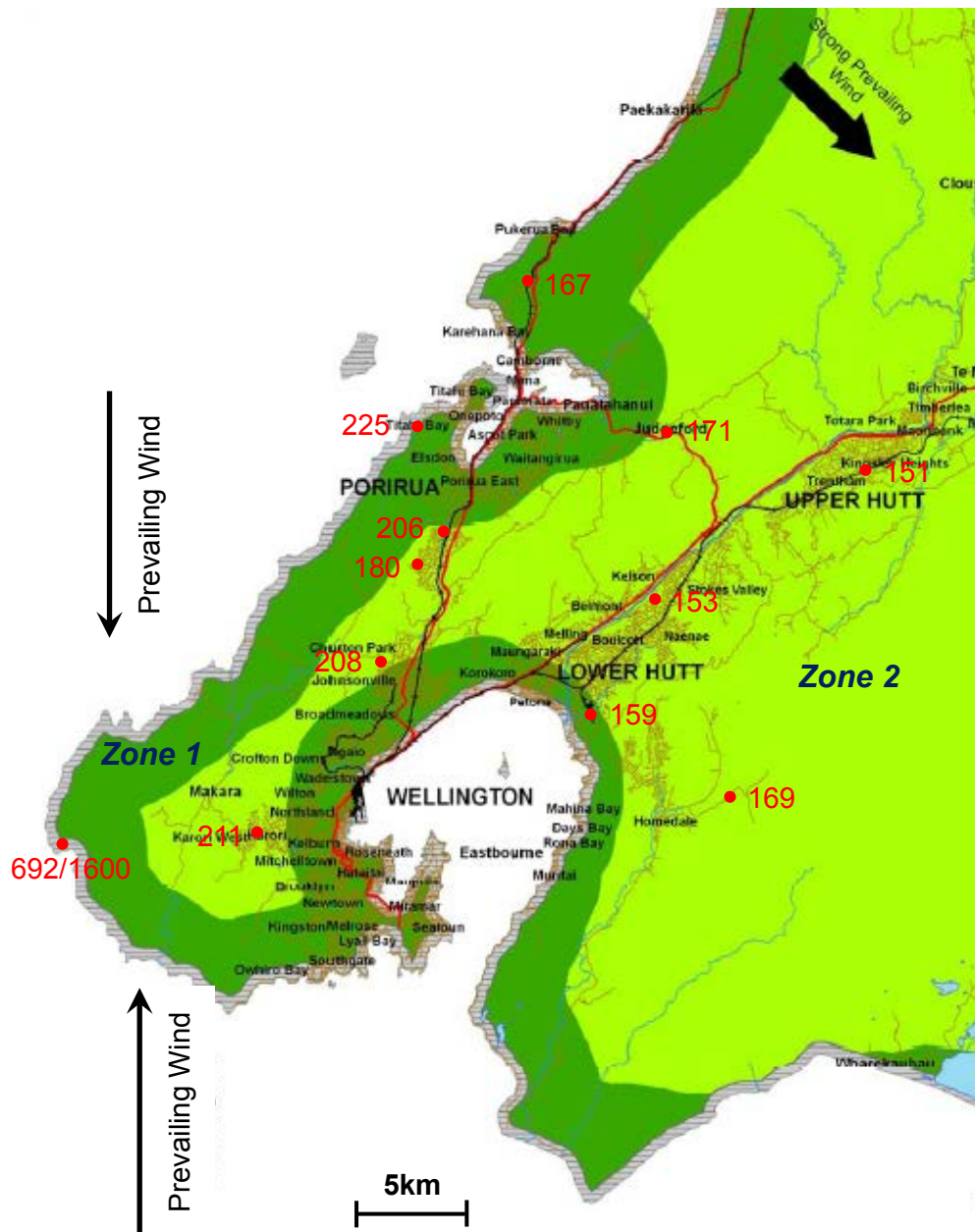


Figure 45. Corrosion zone boundary definition in NZS 3404 map for Wellington region with mild steel corrosion rates derived from the present study (2011 – 2012)

These results indicate that the atmospheric corrosivity in the Wellington city region might be slightly higher than that derived for NZS 3404 by calculations. This is particularly true for the region extending from Karori to Tawa. Although it is protected by hills and mountain ranges on the south-west, the strong prevailing wind from the north-west direction and slightly weaker prevailing wind from the north and south directions can affect its atmospheric environment significantly. It should also be noted that the south-west coast is extremely aggressive. The mild steel coupon, after one year exposure at the Oteranga Bay, lost 692 g/m² (This value is not completely reliable as the exposure rack was broken during exposure. BRANZ previous study at this site found a mild steel corrosion rate at a level of 1600 g/m²/year at this location [Holcroft 1998; Haberecht and Kane 1999]). This mass loss rate is significantly higher than that obtained in other highly corrosive areas, such as Muriwai Beach, Auckland (440 g/m²/year in BRANZ's study in the 1980s) and would be classified into corrosion category E according to ISO 9223. Salt particles from the rough ocean might be brought a long way inland by the strong winds in Wellington region.

Meanwhile, in the Lower Hutt and Upper Hutt regions, there were less marked differences between the corrosion zone boundaries of the two maps. The mild steel corrosion rates at Avalon, Wallaceville and Wainuiomata were around 150-160 g/m²/year. The zinc coating coupons also exhibited a relatively low corrosion rate, typically ranging from 2 to 3 g/m²/year. Atmospheric corrosivity could be classified into corrosion category C2 according to ISO 9223, i.e. Zone 2 according to NZS 3404 or Zone B according to NZS 3604.

It is interesting to note that the site at Wainuiomata had a mild steel corrosion rate of 169 g/m²/year, although it was located within a reserve and park area and was far from the sea (approximately 8 km from the Wellington Harbour). This might be related to the geographic features of Wainuiomata, which is a small basin. This may result in the sample having a higher ToW, due to extended shading. Unfortunately, meteorological data was not available for this site for comparison with sites nearby.

Gracefield, located on the north-east side of the Wellington Harbour, had a corrosion rate of 159 and 5.3 g/m²/year for mild steel and zinc during the period of 2011 – 2012, respectively. This site was within the Seaview industrial area, with the presence of light manufacturing, engineering workshops, paint manufacture, hazardous waste processor, freight storage, oil and fuel tank farms and wastewater treatment plant [Davy and Day 2001]. Heavy atmospheric emissions were most likely absent in this area. Volatile organic compounds, lead and arsenic were detected in the air but their levels are likely to have decreased significantly since 2004 due to improvements in process control. Meanwhile, particulate matters identified in this area were soil, marine aerosol, road dust and coarse sulphate [Mitchell 2012]. Due to heavy traffic on the road close to the exposure rack, deposition of particulates on the sample surface might be heavy. Classification based on zinc corrosion rate was C3 (Zone 1 or C) which is higher than that based on the corrosion rate of mild steel (C2) (Zone 2 or B). This might be a result of different mechanisms for different materials exposed to the same environment.

7.3.3 Otago Region

The corrosion zone boundary differences between the maps of NZS 3404 and NZS 3604 were mainly in the areas spanning from the north-east to the south-west and on the Otago Peninsula. Zone 1 (or Zone C) in the map of NZS 3604 covered a larger area than that of NZS 3404, while the Peninsula was considered to be quite aggressive towards metallic materials by the map in NZS 3604 (Figures 46 and 47).

A very limited amount of atmospheric exposure testing had been done in this region in BRANZ study of the 1980s. Exposure sites only included Dunedin Airport, Musselburgh and Taiaroa Head. In the present study, measurements were carried out at more sites where discrepancies were obvious between NZS 3404 and NZS 3604 maps. For

example, Pigeon Flat, Normanby, Wakari, Mosgiel and Fairfield were located in Zone 2 of the map in NZS 3404, but in Zone 1 (or Zone C) of the map in NZS 3604.

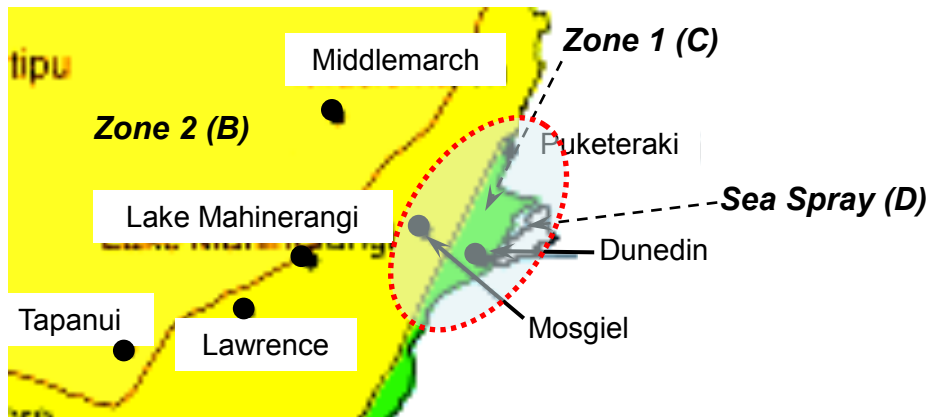


Figure 46. Corrosion zone boundary definition in NZS 3604 map for Otago region



Figure 47. Corrosion zone boundary definition in NZS 3404 map for Otago region with mild steel corrosion rates derived from the present study (2011 – 2012)

Corrosion rates of mild steel coupons were derived as 149, 151, 146, 120 and 129 g/m²/year at Pigeon Flat, Normanby, Wakari, Mosgiel and Fairfield during the period of 2011 – 2012, respectively. These numbers are within the typical range of corrosion rates observed within Zone 2 (or Zone B) (10 – 200 g/m²/year). Further, the corrosion rates of zinc coated coupons at these sites were derived as 2.0, 4.7, 1.6, 3.6 and 0.6 g/m²/year, respectively. These numbers are also within the corrosion rate range of Zone 2 (or Zone B) (0.7 – 5 g/m²/year).

After one year exposure at Highcliff and Taiaroa Head, the mild steel coupons showed a mass loss of 250 and 301 g/m², respectively. These numbers are within the typical range of Zone 1 (or Zone C), 201 – 400 g/m²/year. Similarly, the corrosion rates of zinc at these two sites, 5.7 and 5.0 g/m²/year, can be classified into Zone 1 (or Zone C). These results imply that the atmospheric environment of the Otago Peninsula was more corrosive than that of the urban area, but classification into Zone D, as in the map in NZS 3604, might not be appropriate based on current measurements.

The prevailing wind in the Otago region is along the south-west – north-east direction. An obvious change in corrosion rate with distance in this direction was not found, probably as a result of the blocking effect offered by the ranges in the north-east. A comparison of the corrosion rates obtained at Forbury, Fairfield and Mosgiel showed that the distance from the coast was playing some role in the material deterioration.

7.3.4 Potential Adjustment to Current NZS 3604 Map

NZS 3404 and NZS 3604 have a slightly different classification of atmospheric corrosivity. In NZS 3604:2011, Zone 2 and 3 defined in NZS 3604:1999 were combined to form Zone B. The sea spray zone was re-defined as Zone D. Zone E, of much higher corrosivity, was combined too. Corrosion zone definitions, based on the first-year corrosion rate of mild steel used in these two standards, are given in Table 8.

Table 8. Corrosion categories based on first year corrosion rate of mild steel

Standard	Corrosion Category			
	Zone 3	Zone 2	Zone 1	Sea Spray Zone
NZS 3404:2009				
g/m ² /year	<100	100 – 200	200 – 320	>320
µm/year	<12.5	12.5 – 25	25 – 40	>40
NZS 3604:1999	Zone 3	Zone 2	Zone 1	Sea Spray Zone
g/m ² /year	10 – 80	80 – 200	200 – 400	>400
µm/year	1.25 – 10	10 – 25	25 – 50	>50
NZS 3604:2011	Zone B		Zone C	Zone D (E)
g/m ² /year	10 – 200		200 – 400	>400
µm/year	1.25 – 25		25 – 50	>50

In Table 9, one year corrosion rates for mild steel coupons, location of the exposure site, and atmospheric corrosion category classification, based on maps of NZS 3404 and NZS 3604, are summarised. Potential changes to zone boundaries in NZS 3604 map, based on one year corrosion rates for mild steel measured during the period of 2011 – 2012, are also given. Again, it must be noted that, although the corrosion rates measured at most sites are still comparable to those collected about 25 years ago, significant changes in corrosion of mild steel or zinc have been observed at a limited number of sites and the mechanism behind this is not yet clearly understood.

Table 9. Summary of one year atmospheric corrosion rate of mild steel, exposure site location and potential adjustment to NZS 3604 maps

Exposure Site	Location in Atmospheric Corrosivity Map		One Year Mild Steel Corrosion Rate (g/m ² /year) (2011 – 2012)	Corrosivity Category Based on One Year Mild Steel Corrosion Rate (2011 – 2012)			Map Adjustment?
	NZS 3604:1999 (2011)	NZS 3404:2009		NZS 3604:1999	NZS 3604:2011	NZS 3404:2009	NZS 3604:2011
Warkworth	Zone 1 (C)	Zone 1/2	N/A	-	-	-	-
Waitoki	Zone 1 (C)	Zone 2	194	Zone 2	Zone B	Zone 2	N
Ellerslie	Zone 1 (C)	Zone 1	180	Zone 2	Zone B	Zone 2	N
Auckland Airport	Zone 1/Sea Spray (C/D)	Zone 1/Sea Spray	491	Sea Spray	Zone D	Sea Spray	N
Hunua	Zone 1 (C)	Zone 2	155	Zone 2	Zone B	Zone 2	Y
Ardmore	Zone 1 (C)	Zone 2/1	166	Zone 2	Zone B	Zone 2	Y
Pukekohe	Zone 1	Zone 2/1	N/A	-	-	-	-
Tuakau	Zone 1/2 (C/B)	Zone 2	139	Zone 2	Zone B	Zone 2	Y
Hamilton Airport	Zone 2 (B)	Zone 2	165	Zone 2	Zone B	Zone 2	N
Levin	Zone 1 (C)	Zone 1/2	184	Zone 2	Zone B	Zone 2	N
Waikanae	Zone 1 (C)	Zone 2/1	166	Zone 2	Zone B	Zone 2	N
Paraparaumu Airport	Zone 1 (C)	Zone 1/2	187	Zone 2	Zone B	Zone 2	N
Pukerua Bay	Zone 1 (C)	Zone 1	167	Zone 2	Zone B	Zone 2	N
Titahi Bay	Sea Spray/Zone 1 (D/C)	Sea Spray/Zone 1	225	Zone 1	Zone C	Zone 1	N
Porirua/Tawa	Zone 1 (C)	Zone 1/2	206	Zone 1	Zone C	Zone 1	N
Tawa	Zone 1 (C)	Zone 2	180	Zone 2	Zone B	Zone 2	N
Johnsonville	Zone 1 (C)	Zone 2	208	Zone 1	Zone C	Zone 1	N
Gracefield	Zone 1/2 (C/B)	Zone 1/2	159	Zone 2	Zone B	Zone 2	P

Exposure Site	Location in Atmospheric Corrosivity Map		One Year Mild Steel Corrosion Rate (g/m ² /year) (2011 – 2012)	Corrosivity Category Based on One Year Mild Steel Corrosion Rate (2011 – 2012)			Map Adjustment?
	NZS 3604:1999 (2011)	NZS 3404:2009		NZS 3604:1999	NZS 3604:2011	NZS 3404:2009	NZS 3604:2011
Judgeford	Zone 1 (C)	Zone 2/1	171	Zone 2	Zone B	Zone 2	P
Wallaceville	Zone 2 (B)	Zone 2	151	Zone 2	Zone B	Zone 2	N
Wainuiomata	Zone 2	Zone 2	169	Zone 2	Zone B	Zone 2	P
Avalon	Zone 1 (C)	Zone 2	153	Zone 2	Zone B	Zone 2	Y
Kelburn	Zone 1 (C)	Zone 1	N/A	-	-	-	-
Karori	Zone 1 (C)	Zone 2	211	Zone 1	Zone C	Zone 1	N
Oteranga Bay	Sea Spray (D)	Sea Spray	692	Sea Spray	Zone E	Sea Spray	N
Warrington	Sea Spray / Zone 1 (D/C)	Sea Spray / Zone 1	128	Zone 2	Zone B	Zone 2	N
Port Chalmers	Zone 1 (C)	Zone 1	168	Zone 2	Zone B	Zone 2	N
Normanby	Zone 1 (C)	Zone 2	151	Zone 2	Zone B	Zone 2	Y
Pigeon Flat	Zone 1/2 (C/B)	Zone 2	149	Zone 2	Zone B	Zone 2	Y
Wakari	Zone 1 (C)	Zone 2	146	Zone 2	Zone B	Zone 2	Y
Forbury	Zone 1 (C)	Zone 1	162	Zone 2	Zone B	Zone 2	N
Taiaroa Head	Sea Spray (D)	Zone 1	301	Zone 1	Zone C	Zone 1	Y
Highcliff	Sea Spray (D)	Zone 1	250	Zone 1	Zone C	Zone 1	Y
Fairfield	Zone 1/2 (C/B)	Zone 1	129	Zone 2	Zone B	Zone 2	Y
Mosgiel	Zone 1/2 (C/B)	Zone 2	120	Zone 2	Zone B	Zone 2	P
Dunedin Airport	Zone 2/1 (B/C)	Zone 2	130	Zone 2	Zone B	Zone 2	P
Greymouth	Sea Spray (D)	Sea Spray	342	Zone 1	Zone C	Sea Spray	N
Invercargill	Zone 1 (C)	Zone 1	217	Zone 1	Zone C	Zone 1	N

Exposure Site	Location in Atmospheric Corrosivity Map		One Year Mild Steel Corrosion Rate (g/m ² /year) (2011 – 2012)	Corrosivity Category Based on One Year Mild Steel Corrosion Rate (2011 – 2012)			Map Adjustment?
	NZS 3604:1999 (2011)	NZS 3404:2009		NZS 3604:1999	NZS 3604:2011	NZS 3404:2009	NZS 3604:2011
Airport							
Tiwai Point	Sea Spray (D)	Sea Spray / Zone 1	300	Zone 1	Zone C	Zone 1	Y

Note:

- Y: Corrosion zone boundary adjustment might be necessary
- N: Corrosion zone boundary adjustment might NOT be necessary
- P: Corrosion zone boundary adjustment PROBABLY necessary, but further investigation is needed
- Recommendations for potential corrosion zone boundary adjustments are given for the atmospheric corrosivity map, shown in NZS 3604:2011. The main reason is that this map was established using experimentally measured mild steel corrosion rates, which are highly comparable to those derived from the present study (2011 – 2012).
- Recommendations for potential corrosion zone boundary adjustment are not given to the atmospheric corrosivity map, shown in NZS 3404:2009. The data used to establish this map was produced by theoretical modelling equations involving mainly climatic variables. Although the raw data was further modified with a series of correction factors defined by the distance from the sea and the specific geographic locations to minimise its difference to BRANZ experimental data, discrepancies still exist in some regions. This could be a result of: (1) climate data used was based on a 30-year period from 1971 to 2000, and (2) geographic features and/or local emission/pollution may affect the applicability of the factors used for data correction. In consideration of the strengths and weaknesses of the two approaches used to generate data for atmospheric corrosivity determination, it might not be appropriate to directly use data derived from short-term exposure tests to make any changes to a map based on theoretical calculations of statistical data over a long period.

8. SUMMARY

Atmospheric corrosion testing was carried out at 39 sites; most of which were located within the Auckland, Wellington and Dunedin regions. One year corrosion rates were derived and then compared with those obtained from BRANZ's studies in the 1980s. An obvious change in atmospheric corrosion rate for mild steel or zinc was found at several sites. At Auckland Airport, a much larger mass loss rate for mild steel and for zinc was recorded in the period of 2011 – 2012, when compared with those collected in the period of 1987 – 1988. Meanwhile, significant decreases in the corrosion rates for mild steel and for zinc were found at Greymouth and Tiwai Point. At other exposure sites, although changes in corrosion rates were observed, it appeared that most of the new corrosion rate data was still comparable with the old data.

Changes in the degradation behaviour of materials exposed to the atmosphere could be induced by many factors. The contribution from material can be eliminated since samples of the same chemical composition, dimensions and surface finish were used in the present and past studies.

Climatic factor information, including ambient temperature, rainfall, humidity, wind speed and solar irradiation, were retrieved from NIWA's National Climate Database. Their trends over the past three decades (1980 – 2010) were derived. At most exposure sites, the average annual ambient temperature increased slightly, meanwhile relative humidity and wind speed decreased slightly. The variations in rainfall and wet days were complex and no uniform trend was found.

To investigate the mechanisms for changes in metal atmospheric corrosion behaviour, the correlations between the changing trends of a single climatic parameter and mild steel corrosion rate were explored. It appeared that the difference between the periods of 1987 – 1988 and 2011 – 2012 for a single climatic factor might be more useful for understanding of the changes in metal corrosion behaviour. However, atmospheric corrosion is a result of extremely complicated interactions between the material, climate and environmental pollution. Influences of some factors on atmospheric corrosion are not clearly understood as yet and cannot be quantified from the present study. In consequence, it was not possible to establish a strong relationship between each climatic factor and metal corrosion rate. Overall, it wasn't possible to achieve a clear understanding of the effects of variations in New Zealand's climate over the past thirty years, based on atmospheric corrosion behaviour.

Atmospheric corrosion testing was also carried out in some areas where the atmospheric corrosivity maps in NZS 3404 and NZS 3604 disagree with each other in their zone boundaries. Based mainly on the one year corrosion rate data derived from this study, it was found that both maps might have areas where the corrosivity of the atmospheric environment was not accurately defined. Recommendations for potential adjustments to zone boundaries of the atmospheric corrosivity map shown in NZS 3604 in some regions have been given.

It is suggested that testing should be continued to (1) complete a more thorough update of the atmospheric corrosion rate data set produced by BRANZ's surveys of the 1980s, (2) generate additional data for targeted growth areas (e.g. north and south parts of Auckland and Christchurch) where limited testing has been carried out previously.

This study, together with the research to follow, will make a step towards producing a map with accurately defined corrosion zone boundaries, by reconciling experimental and theoretic data and mapping techniques. This will contribute to minimising the impacts on New Zealand buildings and to the identification of suitable options for

adaptation through cross-disciplinary assessments of a building's vulnerability to the environment.

9. REFERENCES

- Aastrup T, Wadsak M, Leygraf C and Schreiner M. 2000. In Situ Studies of the Initial Atmospheric Corrosion of Copper – Influence of Humidity, Sulfur Dioxide, Ozone, and Nitrogen Dioxide. *Journal of the Electrochemical Society* **147**(7):2543-2551
- Al-Hazza MI and Al-Abdullatif MO. 1995. Atmospheric Corrosion Behaviour of Some Steel Alloys. Research Report LGP-2-45, King Saud University, Riyadh, Saudi Arabia
- Almeida E, Morcillo M and Rosales B. 2000a. Atmospheric Corrosion of Zinc, Part 1: Rural and Urban Atmospheres. *British Corrosion Journal* **35**(4):284-288
- Almeida E, Morcillo M and Rosales B. 2000b. Atmospheric Corrosion of Zinc, Part 2: Marine Atmospheres. *British Corrosion Journal* **35**(4):289-296
- Anon. 1991. UN/ECE International Cooperative Programme on Effect on Materials, Reports 5 and 8, Swedish Corrosion Institute, Stockholm, Sweden
- Anon. 2002. Corrosion Costs and Preventive Strategies in the United States. U.S. Department of Transportation, Federal Highway Administration, and NACE International, FHWA-RD-01-157, USA
- Arroyave C and Morcillo M. 1995. The Effect of Nitrogen Oxides in Atmospheric Corrosion of Metals. *Corrosion Science* **37**(2):293-305
- Asami K and Kikuchi M. 2003. In-depth Distribution of Rusts on a Plain Carbon Steel and Weathering Steels Exposed to Coastal-industrial Atmosphere for 17 Years. *Corrosion Science* **45**:2671-2688
- ASTM International. 1999 (2010). ASTM G116 – Standard Practice for Conducting Wire-on-Bolt Test for Atmospheric Galvanic Corrosion. ASTM, West Conshohocken, PA 19428-2959, USA
- ASTM International. 2003 (2011). ASTM G1 – Standard Practice for Preparing, Cleaning, and Evaluating Corrosion Test Specimens. ASTM, West Conshohocken, PA 19428-2959, USA
- Badea GE, Setel A, Sebesan M, Cret P, Lolea M and Covaci H. 2011. Corrosion Study in Atmospheric Environment. 17th Building Services, Mechanical and Building Industry Days – Urban Energy Conference, 13-14 October 2011. Debrecen, Hungary. pp111-117
- Boardman M. 2008. The Cost of Corrosion in the New Zealand Electricity Industry. <http://www.linetech.co.nz/documents/mike%20boardman%202008.pdf>
- Barton K. 1976. *Protection against Atmospheric Corrosion: Theories and Methods*, John Wiley & Sons
- Bengtsson Blücher D, Lindström R, Svensson JE and Johansson LG. 2001. The Effect of CO₂ on the NaCl-Induced Atmospheric Corrosion of Aluminium. *Journal of the Electrochemical Society* **148**(4):B127-131
- Bengtsson Blücher D, Svensson JE and Johansson LG. 2005. Influence of ppb Levels of SO₂ on the Atmospheric Corrosion of Aluminium in the Presence of NaCl. *Journal of the Electrochemical Society* **152**(10):B397-404
- Bengtsson Blücher D, Svensson JE and Johansson LG. 2006. The Influence of CO₂, AlCl₃·6H₂O, MgCl₂·6H₂O, Na₂SO₄ and NaCl on the Atmospheric Corrosion of Aluminium. *Corrosion Science* **48**:1848-1866

- Bengtsson J, Hargreaves R and Page IC. 2007. Assessment of the Need to Adapt Buildings in New Zealand to the Impacts of Climate Change. BRANZ Study Report No. 179. BRANZ Ltd, Judgeford, Wellington, New Zealand
- Brown PW and Masters LW. 1982. Factors Affecting the Corrosion of Metals in the Atmosphere. In *Atmospheric Corrosion*, edited by W.H. Ailor, John Wiley, New York
- Chen YY, Chung SC and Shih HC. 2006. Studies on the Initial Stages of Zinc Atmospheric Corrosion in the Presence of Chloride. *Corrosion Science* **48**:3547-3564
- Chen ZY. 2005. The Role of Particles on Initial Atmospheric Corrosion of Copper and Zinc. Doctoral Thesis, Royal Institute of Technology, SE-100 44 Stockholm, Sweden
- Chen ZY, Persson D and Leygraf C. 2008. Initial NaCl-particle Induced Atmospheric Corrosion of Zinc - Effect of CO₂ and SO₂. *Corrosion Science* **50**:111-123
- Chen ZY, Liang D, Ma G, Frankel GS, Allen HC and Kelly RG. 2010. Influence of UV Irradiation and Ozone on Atmospheric Corrosion of Bare Silver. *Corrosion Engineering, Science and Technology* **45**(2):169-180
- Christensen JH, Hewitson B, Busuioc A, Chen A, Gao X, Held I, Jones R, Kolli RK, Kwon WT, Laprise R, Magaña Rueda V, Mearns L, Menéndez CG, Räisänen J, Rinke A, Sarr A and Whetton P. 2007. Regional Climate Projections. In: *Climate Change 2007: The Physical Science Basis*. Contribution of Working Group I to the Fourth Assessment Report of the Intergovernmental Panel on Climate Change [Solomon, S., D. Qin, M. Manning, Z. Chen, M. Marquis, K.B. Averyt, M. Tignor and H.L. Miller (eds.)]. Cambridge University Press, Cambridge, United Kingdom and New York, NY, USA
- Cole IS, Paterson DA and Ganther WD. 2003. Holistic Model for Atmospheric Corrosion, Part 1 – Theoretical Framework for Production, Transportation and Deposition of Marine Salts. *Corrosion Engineering, Science and Technology* **38**(2):129-134
- Cole IS, Lau D, Chan F and Paterson DA. 2004. Experimental Studies of Salts Removal from Metal Surfaces by Wind and Rain. *Corrosion Engineering, Science and Technology* **39**(4):333-338
- Cole IS and Ganther WD. 2006. Experimental Determination of Time Taken for Openly Exposed Metal Surfaces to Dry. *Corrosion Engineering, Science and Technology* **41**(2):161-167
- Cole IS and Paterson DA. 2007. Holistic Model for Atmospheric Corrosion, Part 7 - Cleaning of Salt from Metal Surfaces. *Corrosion Engineering, Science and Technology* **42**(2):106-111
- Cole IS, Azmat NS, Kanta A and Venkatraman M. 2009. What Really Controls the Atmospheric Corrosion of Zinc? Effect of Marine Aerosols on Atmospheric Corrosion of Zinc. *International Materials Reviews* **54**(3):117-133
- Cole IS and Paterson DA. 2010. Possible Effects of Climate Change on Atmospheric Corrosion in Australia. *Corrosion Engineering, Science and Technology* **45**(1):19-26
- Cook DC. 2005. Spectroscopic Identification of Protective and Non-protective Corrosion Coatings on Steel Structures in Marine Environments. *Corrosion Science* **47**:2550-2570
- Cordner RJ. 1990. Atmospheric Corrosion Survey of New Zealand. *British Corrosion Journal* **25**(2):115-118
- Davy P and Day P. 2001. Petone-Seaview Ambient Air Quality Monitoring Strategy 2001-2003. Wellington Regional Council, Publication No. WRC/RINV-T-01/40, Wellington, New Zealand

- Dean SW. 2005. Chapter 11 – Atmospheric. In *Corrosion Tests and Standards: Application and Interpretation*. Edited by Robert Baboian. ASTM International, West Conshohocken, PA, USA
- Dehri I, Sözüsağlam H and Erbil M. 2003. EIS Study of the Effect of High Levels of NH₃ on the Deformation of Polyester-coated Galvanised Steel at Different Relative Humidities. *Progress in Organic Coatings* **48**:118-123
- de la Fuente D, Castaño JG and Morcillo M. 2007. Long-term Atmospheric Corrosion of Zinc. *Corrosion Science* **49**:1420-1436
- de la Fuente D, Simancas J and Morcillo M. 2008. Morphological Study of 16-year Patinas Formed on Copper in a Wide Range of Atmospheric Exposures. *Corrosion Science* **50**:268-285
- de la Fuente D, Díaz I, Simancas J, Chico B and Morcillo M. 2011. Long-term Atmospheric Corrosion of Mild Steel. *Corrosion Science* **53**:604-617
- Department of Building and Housing. 2010. New Zealand Housing Report 2009/2010: Structure, Pressures and Issues. Wellington, New Zealand. www.dbh.govt.nz
- de Rincón OT, Rincón Paz AA, de Romero MF, Sánchez MA, Hernandez de Rincón AI, del Rasario Prato M and de Laguna MF. 1998. A New Version of Atmospheric Corrosiveness Maps. *Materials Performance* **37**(12):48-53
- Diwan R, Veselyi S, Bhattacharya P, Raman A and Lee RU. 1998. Testing of Sensors for Atmospheric Corrosion. CORROSION 98, NACE International. 22-27 March 1998. San Diego Ca, USA
- Duncan JR and Balance JA. 1988. Marine Salts Contribution to Atmospheric Corrosion. In *Degradation of Metals in the Atmosphere*, ASTM STP 965, edited by S.W. Dean and T.S. Lee, American Society of Testing and Materials, Philadelphia, USA, pp316-326
- Duncan JR and Cordner RJ. 1991. Atmospheric Corrosion Rates over Two Years Exposure at 156 Sites in New Zealand. *IPENZ Transactions* **18**(1):1-13
- El Sarraf R and Mandeno W. 2008. Sustainable Durability Design, 4th Metal's Industry Conference, HERA, 29-30 October 2008. Manukau City, Auckland, New Zealand
- El Sarraf R and Clifton GC. 2011. New Zealand Steelwork Corrosion and Coatings Guide, HERA Report R4-133:2011. New Zealand Heavy Engineering Research Association, Manukau, Auckland 2104, New Zealand
- Elisabete M and Almeida M. 2005. Minimisation of Steel Atmospheric Corrosion: Updated Structure of Intervention. *Progress in Organic Coatings* **54**:81-90
- Ericsson R. 1978. The Influence of Sodium Chloride on the Atmospheric Corrosion of Steel. *Materials and Corrosion* **29**(6):400-403
- Fahy FW. 1980. Atmospheric Corrosion of Anodized Aluminium Exposed over a Twelve Year Period in New Zealand. *British Corrosion Journal* **15**:203-207
- Fahy FW. 1983. Atmospheric Corrosion of Anodized Aluminium Exposed over a Twelve Year Period in the Main Centers of New Zealand. *British Corrosion Journal* **18**:179-183
- Falk T, Svensson JE and Johnsson LG. 1998. The Role of Carbon Dioxide in the Atmospheric Corrosion of Zinc. *Journal of the Electrochemical Society* **145**(1):39-44
- Farrow LA, Graedel TE and Leygraf C. 1996. Gildes Model Studies of Aqueous Chemistry. II. The Corrosion of Zinc in gaseous Exposure Chambers. *Corrosion Science* **38**(12):2181-2199
- Feliu S, Morcillo M and Chico B. 1999. Effect of Distance from Sea on Atmospheric Corrosion Rate. *Corrosion* **55**(9):883-891

- Feliu S, Morcillo M and Chico B. 2001. Effect of State of Sea on Atmospheric Corrosion in Coastal Zones. *British Corrosion Journal* **36**(2):157-160
- FitzGerald KP, Nairn J and Atrens A. 1998. The Chemistry of Patination. *Corrosion Science* **40**(12):2029-2050
- FitzGerald KP, Nairn J, Skennerton G and Atrens A. 2006. Atmospheric Corrosion of Copper and the Colour, Structure and Composition of Natural Patinas on Copper. *Corrosion Science* **48**:2480-2509
- G2MT LLC. 2012. <http://www.g2mt.com/?s=cost+of+corrosion>. Accessed on 04 September 2012
- Ganther WD, Cole IS, Helal AM, Chan W, Paterson DA, Trinidad G, Corrigan P, Mohamed R, Sabah N and Al-Mazrouei A. 2011. Towards the Development of a Corrosion Map for Abu Dhabi. *Materials and Corrosion* **62**(11):1066-1073
- Ghali E. 2010. *Corrosion Resistance of Aluminium and Magnesium Alloys: Understanding, Performance, and Testing*. John Wiley & Sons, Inc., Hoboken, New Jersey
- Graedel TE. 1989a. Corrosion Mechanisms for Zinc Exposed to the Atmosphere. *Journal of the Electrochemical Society* **136**(4):193C-203C
- Graedel TE. 1989b. Corrosion Mechanisms for Aluminium Exposed to the Atmosphere. *Journal of the Electrochemical Society* **136**(4):204C-212C
- Graedel TE. 1996. Gildes Model Studies of Aqueous Chemistry. I. Formulation and Potential Applications of the Multi-regime Model. *Corrosion Science* **38**:2153-2180
- Graedel TE and Frankenthal RP. 1990. Corrosion Mechanisms for Iron and Low Alloy Steels Exposed to the Atmosphere. *Journal of the Electrochemical Society* **137**(8):2385-2394
- Graßl H. 2009. Scenarios of Climate Change. *The European Physical Journal Special Topics* **176**:5-12
- Grøntoft T. 2011. Climate Change Impact on Building Surfaces and Façades. *International Journal of Climate Change Strategies and Management* **3**(4):374-385
- Haberecht PW and Kane CD. 1999. Determining the Chloride Deposition Rate, Chloride Aerosol Flux and the Corrosion Rates in Subfloor Building Conditions in a Severe Marine Environment. Australasian Corrosion Association Annual Conference, 21-24 November 1999. Sydney, Australia
- Haberecht PW, Kane CD and Meyer SJ. 1999. Environmental Corrosivity in New Zealand: Results after 10 Years Exposure. 14th International Corrosion Congress, September 26 – October 1, 1999. Cape Town, South Africa
- Hack HP. 2005. Chapter 20 – Galvanic. In *Corrosion Tests and Standards: Application and Interpretation*. Edited by Robert Baboian. ASTM International, West Conshohocken, PA, USA
- Hladky K, Sussex GAM and Cox WM. 1986. CRE Atmospheric Corrosion Monitoring. CAPCIS, Bainbridge House Laboratories, Granby Row, Manchester M1 2PW, UK
- Holcroft G. 1998. Ventilation, Salt Ingress, Timber Moisture and Corrosion Rates in Model Coastal Subfloor Spaces. *Corrosion and Materials* **23**(2-3):7-11
- International Organisation of Standardisation. 1991. ISO 9223 - Corrosion of Metals and Alloys – Classification of Atmospheres. ISO, Geneva, Switzerland

- International Organisation of Standardisation. 1991. ISO 9224 - Corrosion of Metals and Alloys – Guiding Values for the Corrosivity Categories of Atmospheres. ISO, Geneva, Switzerland
- International Organisation of Standardisation. 1991. ISO 9225 - Corrosion of Metals and Alloys – Corrosivity of Atmospheres – Methods of Measurement of Pollution. ISO, Geneva, Switzerland
- Jackson SC. 2009. Parallel Pursuit of Near-Term and Long-Term Climate Mitigation. *Science* **326**:526-527
- Kamimura T, Nasu S, Tazaki T, Kuzushita K and Morimoto S. 2002. Mössbauer Spectroscopic Study of Rust Formed on a Weathering Steel and a Mild Steel Exposed for a Long Term in an Industrial Environment. *Materials Transactions* **43**:694-703
- Klassen RD and Roberge PR. 2001. The Effects of Wind on Local Atmospheric Corrosivity. CORROSION 2001. 11-16 March 2001. Houston, Tx, USA
- Klassen RD, Roberge PR, Lenard DR and Blenkinsop GN. 2002. Corrosivity Patterns near Sources of Salt Aerosols. In *Outdoor Atmospheric Corrosion*, STP 1421. Edited by H.E. Townsend. ASTM, West Conshohocken, PA, USA. pp19-33
- Knotkova D, Kreislova K and Dean SW. 2010. ISOCORRAG – International Atmospheric Exposure Program: Summary of Results. ASTM International, West Conshohocken, PA 19428-2959, USA
- Krätschmer A, Odnevall Wallinder I and Leygraf C. 2002. The Evolution of Outdoor Copper Patina. *Corrosion Science* **44**:425-450
- Larsen KR. 2012. NASA Launches Study of Corrosion Exposure Testing. *Materials Performance* **51**(9):28-32
- Lawson HH. 2005. Chapter 28 – Outdoor Atmospheres. In *Corrosion Tests and Standards: Application and Interpretation*. Edited by Robert Baboian. ASTM International, West Conshohocken, PA, USA
- Lenglet M, Lopitiaux J, Leygraf C, Odnevall I, Carballeira M, Noualhaguet JC, Guinement J, Gautier J and Boissel J. 1995. Analysis of Corrosion Products Formed on Copper in Cl₂/H₂S/NO₂ Exposure. *Journal of the Electrochemical Society* **142**(11):3690-3696
- Li SX and Hihara LH. 2010. Atmospheric Corrosion Initiation on Steel from Predeposited NaCl Salt Particles in High Humidity Atmospheres. *Corrosion Engineering, Science and Technology* **45**(1):49-56
- Lindström R, Svensson JE and Johansson LG. 2000. The Atmospheric Corrosion of Zinc in the Presence of NaCl – The Influence of Carbon Dioxide and Temperature. *Journal of the Electrochemical Society* **147**(5):1751-1757
- Lobnig RE, Frankenthal RP, Siconolfi DJ and Sinclair JD. 1993. The Effect of Submicron Ammonium Sulfate Particles on the Corrosion of Copper. *Journal of the Electrochemical Society* **140**(7):1902-1907
- Lobnig RE, Frankenthal RP, Siconolfi DJ, Sinclair JD and Stratmann M. 1994. Mechanism of Atmospheric Corrosion of Copper in the Presence of Submicron Ammonium Sulfate Particles at 300 and 373 K. *Journal of the Electrochemical Society* **141**(11):2935-2941
- Lobnig RE, Siconolfi DJ, Psota-Kelty L, Grundmeier G, Frankenthal RP, Stratmann M and Sinclair JD. 1996. Atmospheric Corrosion of Zinc in the Presence of Ammonium Sulfate Particles. *Journal of the Electrochemical Society* **143**(5):1539-1546

- Ma YT, Li Y and Wang FH. 2009. Corrosion of Low Carbon Steel in Atmospheric Environments of Different Chloride Content. *Corrosion Science* **51**:997-1006
- Macdonald DD, Sikora E, Balmas MW and Alkire RC. 1996. The Photo-inhibition of Localized Corrosion on Stainless Steel in Neutral Chloride Solution. *Corrosion Science* **38**(1):97-103
- Manning M. 1988. Corrosion of Building Materials due to Atmospheric Pollution in the United Kingdom. In *Air Pollution, Acid Rain and the Environment*. Edited by Kenneth Mellanby. Elsevier Science Publishers Ltd. England
- Mansfeld F. 1979. Atmospheric Corrosion Rates, Time-of-Wetness and Relative Humidity. *Materials and Corrosion* **30**(1):38-42
- Mazzolani F. 2004. Competing Issues for Aluminium Alloys in Structural Engineering. *Progress in Structural Engineering and Materials* **6**:185-196
- McCafferty E. 2010. *Introduction to Corrosion Science*. Springer, New York, Dordrecht, Heidelberg, London
- McKenzie R, Conner B and Bodeker G. 1999. Increased Summertime UV Radiation in New Zealand in Response to Ozone Loss. *Science* **285**:1709-1711
- Ministry for the Environment. 2000. Effects of Air Contaminants on Ecosystems and Recommended Critical Levels and Critical Loads. Air Quality Technical Report No.15. Review of the Ambient Air Quality Guidelines. Wellington, New Zealand
- Ministry for the Environment. 2001. Climate Change Impacts on New Zealand. Climate Change Group, Ministry for the Environment, PO Box 10 362, Wellington, New Zealand. <http://www.mfe.govt.nz/publications/climate/impacts-report/impacts-report-jun01.pdf>
- Ministry for the Environment. 2007. Chapter 7 – Air. Environment New Zealand 2007. Wellington, New Zealand. <http://www.mfe.govt.nz/publications/ser/enz07-dec07/index.html>
- Mitchell T. 2012. Air Quality in the Wellington Region: State and Trends. Greater Wellington Regional Council, Publication No. GW/EMI-T-12/137, Wellington, New Zealand.
- Morcillo M, Chico B, de la Fuente D and Simancas J. Looking Back on Contributions in the Field of Atmospheric Corrosion Offered by the MICAT Iberoamerican Testing Network. www.hindawi.com/journals/ijc/aip/824365.pdf
- Morcillo M, Chico B, Mariacab L and Oteroa E. 2000. Salinity in Marine Atmospheric Corrosion: Its Dependence on the Wind Regime Existing in the Site. *Corrosion Science* **42**(1):91-104
- Morcillo M, de la Fuente D, Díaz I and Cano H. 2011. Atmospheric Corrosion of Mild Steel. *Revista Metalurgia* **47**(5):426-444
- Moussa SO and Hocking MG. 2001. The Photo-inhibition of Localized Corrosion of 304 Stainless Steel in Sodium Chloride Environment. *Corrosion Science* **43**(11):2037-2047
- Mullan B, Burgess S, McKenzie R, Ramsay D, Reid S, Stephens S and Thompson C. 2006. Climate Change Scenarios for BRANZ Study of Built Environment Vulnerability. NIWA Client Report: WLG2006-54, New Zealand
- Mullan AB, Stuart SJ, Hadfield MG and Smith MJ. 2010. Report on the Review of NIWA's 'Seven-Station' Temperature Series. NIWA Information Series No.78. 175 p. NIWA, PO Box 14901, Kilbirnie, Wellington 6124, New Zealand. www.niwa.co.nz
- Natesan M, Palaniswamy N and Rengaswamy NS. 2006. Atmospheric Corrosivity Survey of India. *Materials Performance* **45**(1):52-56

- Natesan M, Venkatachari G, Palaniswamy N and Rajeswari A. 2008. A Novel Approach to Updating the Corrosiveness Maps of India. *Corrosion* **64**(2):92-100
- Nguyen MN, Wang XM and Leicester RH. 2012. Climate Change Impacts on Corrosion of Metal Fasteners in Timber Construction. Proceedings of the World Conference on Timber Engineering. 16-19 July 2012. Auckland, New Zealand
- Nyrkova LI, Polyakov SH, Osadchuk SO, Mel'nychuk SL and Hapula NO. 2012. Determination of the Rate of Atmospheric Corrosion of Metal Structures by the Method of Polarization Resistance. *Materials Science* **47**(5):683-688
- Oesch S and Faller M. 1997. Environmental Effects on Materials: The Effect of the Air Pollutants SO₂, NO₂, NO and O₃ on the Corrosion of Copper, Zinc and Aluminium. A Short Literature Survey and Results of Laboratory Exposures. *Corrosion Science* **39**(9):1505-1530
- Oesch S and Heimgartner P. 1996. Environmental Effects on Metallic Materials – Results of an Outdoor Exposure Programme Running in Switzerland. *Materials and Corrosion* **47**:425-438
- Oh SJ, Cook DC and Townsend HE. 1999. Atmospheric Corrosion of Different Steels in Marine, Rural and Industrial Environments. *Corrosion Science* **41**:1687-1702
- Olsson COA and Landolt D. 2005. Electrochemical Quartz Crystal Microbalance. In Analytical Methods in *Corrosion Science and Engineering*. Edited by P. Marcus and F. Mansfeld. CRC Press. pp733-751
- Parekh SP, Pandya AV and Kadiya HK. 2012. Progressive Atmospheric Corrosion Study of Metals like Mild Steel, Zinc and Aluminium in Urban Station of Ahmedabad District. *International Journal of ChemTech Research* **4**(4):1770-1774
- Qu Q, Yan CW, Zhang L, Wan Y and Cao CN. 2002a. Influence of NaCl Deposition on Atmospheric Corrosion of A3 Steel. *Journal of Materials Science and Technology* **18**(6):552-555
- Qu Q, Yan CW, Wan Y and Cao CN. 2002b. Effects of NaCl and SO₂ on the Initial Atmospheric Corrosion of Zinc. *Corrosion Science* **44**:2789-2803
- Qu Q, Yan CW, Li L, Zhang L, Liu GH and Cao CN. 2004. Initial Atmospheric Corrosion of Zinc in the Presence of NH₄Cl. *Acta Metallurgica Sinica (English Letters)* **17**(2):161-165
- Qu Q, Li L, Bai W, Yan CW and Cao CN. 2005. Effects of NaCl and NH₄Cl on the Initial Atmospheric Corrosion of Zinc. *Corrosion Science* **47**(11):2832-2840
- Reisinger A, Mullan B, Manning M, Wratt D and Nottage R. 2010. Global & Local Climate Change Scenarios to Support Adaptation in New Zealand. In *Climate Change Adaptation in New Zealand*, Edited by R.A.C. Nottage, D.S. Wratt, J.F. Bornman and K. Jones, New Zealand Climate Change Centre, Wellington, New Zealand
- Roberge PR. 1999. *Handbook of Corrosion Engineering*. McGraw-Hill, New York
- Roberge PR, Klassen RD and Tullmin M. 2000. Electrochemical Noise Analysis for Corrosivity Assessment. CORROSION 2000. NACE International. 26-31 March 2000. Orlando, FL., USA
- Roberge PR. 2010. Impact of Climate Change on Corrosion Risks. *Corrosion Engineering, Science and Technology* **45**(1):27-33
- Santana JJ, Santana J, Gonzalez JE, de la Fuente D, Chico B and Morcillo M. 2001. Atmospheric Corrosivity Map for Steel in Canary Isles. *British Corrosion Journal* **36**(4):266-271

- Santana Rodríguez JJ, Javier Santana Hernández and González González JE. 2003. The Effect of Environmental and Meteorological Variables on Atmospheric Corrosion of Carbon Steel, Copper, Zinc and Aluminium in a Limited Geographic Zone with Different Types of Environment. *Corrosion Science* **45**:799-815
- Schweitzer PA. 2006. Chapter 2 – Atmospheric Corrosion. In *Fundamentals of Metallic Corrosion – Atmospheric and Media Corrosion of Metals*. CRC Press. pp39-66
- Serreze MC. 2009. Understanding Recent Climate Change. *Conservation Biology* **24**(1):10-17
- Shalaby HM, Al-Hashem A, Al-Sabti F, Al-Muhanna K and Hussain BS. 2006. Atmospheric Corrosion of Carbon Steel, Galvanized Steel, Copper, and Anodized Aluminium in Kuwait. *Materials Performance* **45**(12):54-59
- Shaw WJD and Andersson JI. 2010. Atmospheric Corrosion of Carbon Steel in the Prairie Regions. NACE, Northern Area Western Conference, 15-18 February 2010. Calgary, Alberta
- Shitanda I, Okumura A, Itagaki M, Watanabe K and Asano Y. 2009. Screen-printed Atmospheric Corrosion Monitoring Sensor Based on Electrochemical Impedance Spectroscopy. *Sensors and Actuators B: Chemical* **139**(2):292-297
- Sica YC, Kenny ED, Portella KF and Campos Filho DF. 2007. Atmospheric Corrosion Performance of Carbon Steel, Galvanized Steel, Aluminium and Copper in the North Brazilian Coast. *Journal of the Brazilian Chemical Society* **18**(1):153-166
- Singh DDN, Yadav S and Saha JK. 2008. Role of Climatic Conditions on Corrosion Characteristics of Structural Steels. *Corrosion Science* **50**:93-110
- Slamova K, Glaser R, Schill C, Wiesmeier S and Köhl M. 2012. Mapping Atmospheric Corrosion in Coastal Regions: Methods and Results. *Journal of Photonics for Energy* **2**(1):022003. doi:10.1117/1.JPE.2.022003
- Standards Australia and Standards New Zealand. 2002. AS/NZS 2312 – Guide to the Protection of Structural Steel against Atmospheric Corrosion by the Use of Protective Coatings. SA, Sydney, NSW 2001, Australia; SNZ, Wellington 6140, New Zealand
- Standards Australia and Standards New Zealand. 2007. AS/NZS 2728 – Prefinished/prepainted Sheet Metal Products for Interior/exterior Building Applications - Performance Requirements. SA, Sydney, NSW 2001, Australia; SNZ, Wellington 6140, New Zealand
- Standards New Zealand. 1999. NZS 3604 – Timber Framed Buildings. SNZ, Wellington 6140, New Zealand
- Standards New Zealand. 2011. NZS 3604 – Timber Framed Buildings. SNZ, Wellington 6140, New Zealand
- Standards New Zealand. 2009. NZS 3404 – Steel Structures Standard, Part 1: Materials, fabrication, and construction. SNZ, Wellington 6140, New Zealand
- Suzuki K and Robertson IN. 2011. Atmospheric Chloride Deposition Rate for Corrosion Prediction on Oahu. Research Report UHM/CEE/11-02, University of Hawaii
- Svensson JE and Johansson LG. 1993a. A Laboratory Study of the Effect of Ozone, Nitrogen Dioxide, and Sulfur Dioxide on the Atmospheric Corrosion of Zinc. *Journal of the Electrochemical Society* **140**(8):2210-2216
- Svensson JE and Johansson LG. 1993b. A Laboratory Study of the Initial Stages of the Atmospheric Corrosion of Zinc in the Presence of NaCl; Influence of SO₂ and NO₂. *Corrosion Science* **34**(5):721-740

- Syed S. 2006. Atmospheric Corrosion of Materials. *Emirates Journal for Engineering Research* **11**(1):1-24
- Tidblad J, Kucera V and Mikhailov AA. 1998. UN/ECE International Co-Operative Programme on Effects on Materials, Including Historic and Cultural Monuments, Report No 30: Statistical analysis of 8 year materials exposure and acceptable deterioration and pollution levels. Swedish Corrosion Institute, Roslagsvägen 101, Hus 25, S - 104 05 Stockholm, Sweden
- Tran TTM, Fiaud C, Sutter EMM and Villanova A. 2003. The Atmospheric Corrosion of Copper by Hydrogen Sulphide in Underground Conditions. *Corrosion Science* **45**:2787-2802
- Tullmin M and Roberge PR. 2000. Atmospheric Corrosion. In *Uhlig's Corrosion Handbook*, 2nd edition, Edited by R. Winston Revie, John Wiley & Sons, Inc
- Vargel C. 2004. *Corrosion of Aluminium*. Elsevier, Amsterdam, Netherlands
- Vera R, Rosales BM and Tapia C. 2003. Effect of the Exposure Angle in the Corrosion Rate of Plain Carbon Steel in a Marine Atmosphere. *Corrosion Science* **45**:321-337
- Wall A. 1998. Zinc and its Uses. *Materials World* 6(4)
- WBK & Associates Inc. 2003. Sulphur Dioxide: Environmental Effects, Fate and Behaviour. Information Centre, Alberta Environment, Main Floor, Oxbridge Place, 9820 – 106th Street, Edmonton, Alberta T5K 2J6
- Wypych G. 2003. *Handbook of Material Weathering*, 3rd edition. ChemTec Publishing
- Xu NX, Zhao LY, Ding CH, Zhang CD, Li RS and Zhong QD. 2002. Laboratory Observation of Dew Formation at an Early Stage of Atmospheric Corrosion of Metals. *Corrosion Science* **44**(1):163-170
- Yamashita M, Miyuki H, Matsuda Y, Nagano H and Misawa T. 1994. The Long Term Growth of the Protective Rust Layer Formed on Weathering Steel by Atmospheric Corrosion during a Quarter of a Century. *Corrosion Science* **36**:283-299

APPENDIX A

A.1 Climate – Long Term Trend

A.1.1 Ambient Temperature

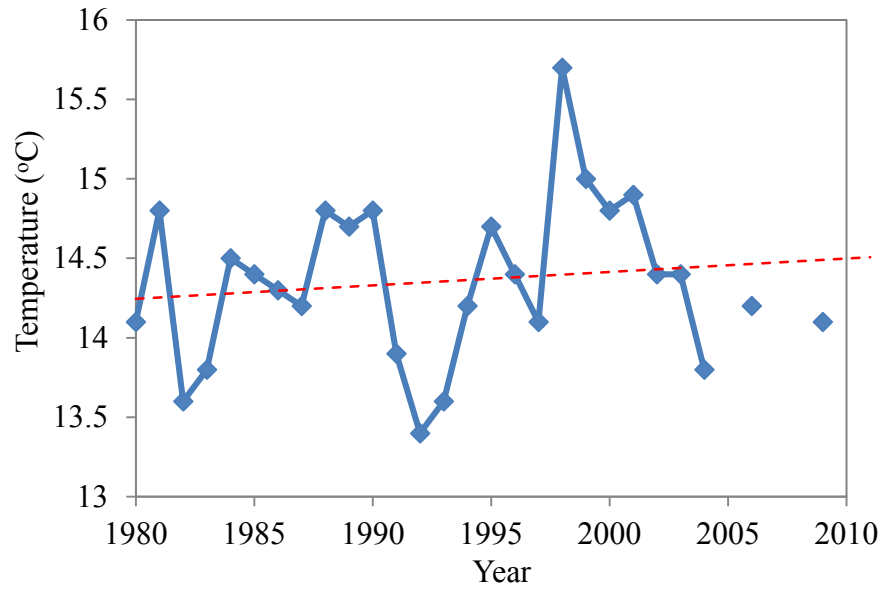


Figure A1. Annual mean ambient temperatures for Ardmore from 1980 to 2010 (Linear fitting to these data derived a temperature increase trend of 0.0084 °C/year)

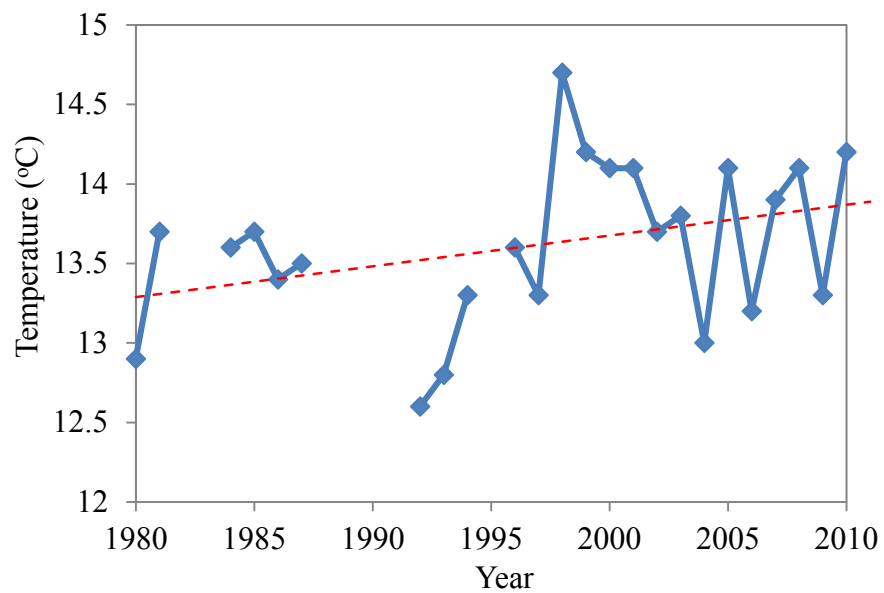


Figure A2. Annual mean ambient temperatures for Hamilton Airport from 1980 to 2010 (Linear fitting to these data derived a temperature increase trend of 0.0194 °C/year)

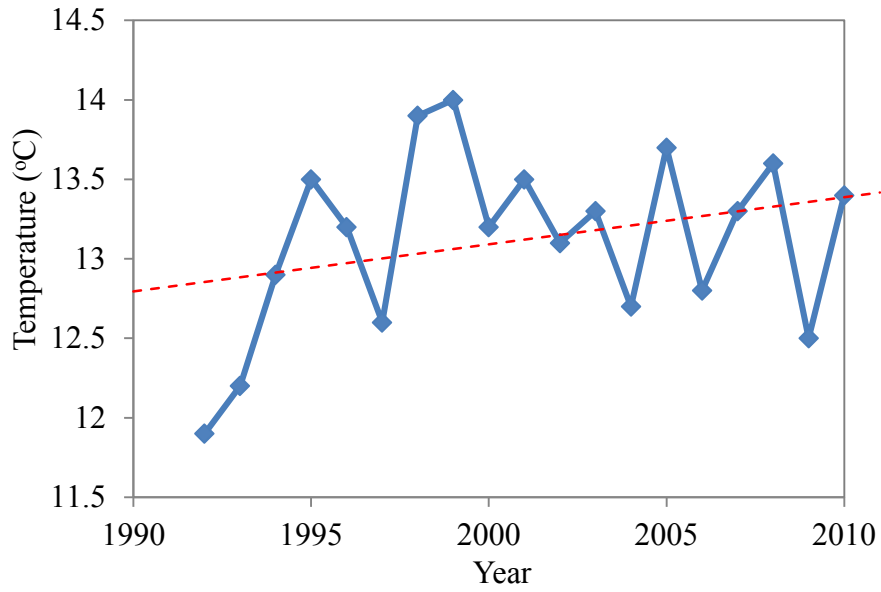


Figure A3. Annual mean ambient temperatures for Levin from 1992 to 2010 (Linear fitting to these data derived a temperature increase trend of 0.0296 °C/year)

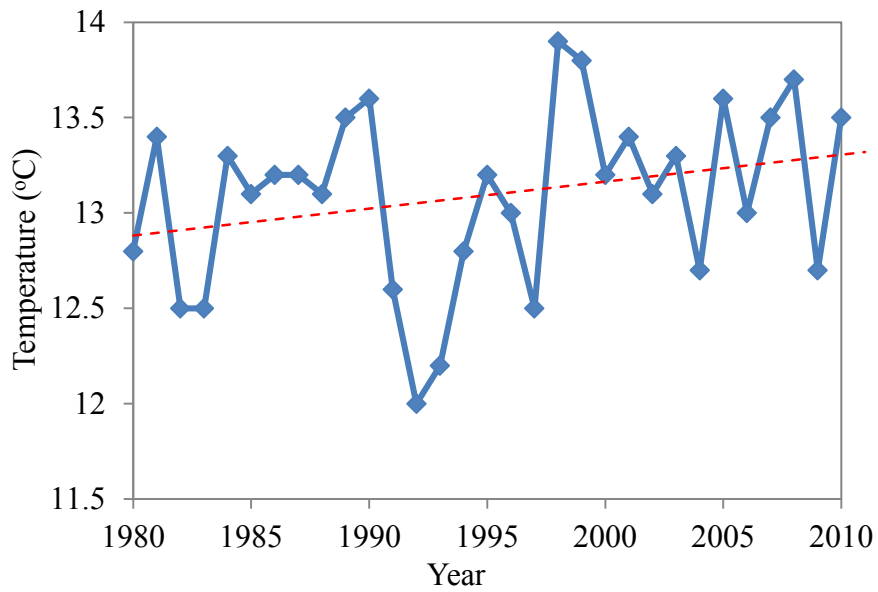


Figure A4. Annual mean ambient temperatures for Paraparaumu Airport from 1980 to 2010 (Linear fitting to these data derived a temperature increase trend of 0.0141 °C/year)

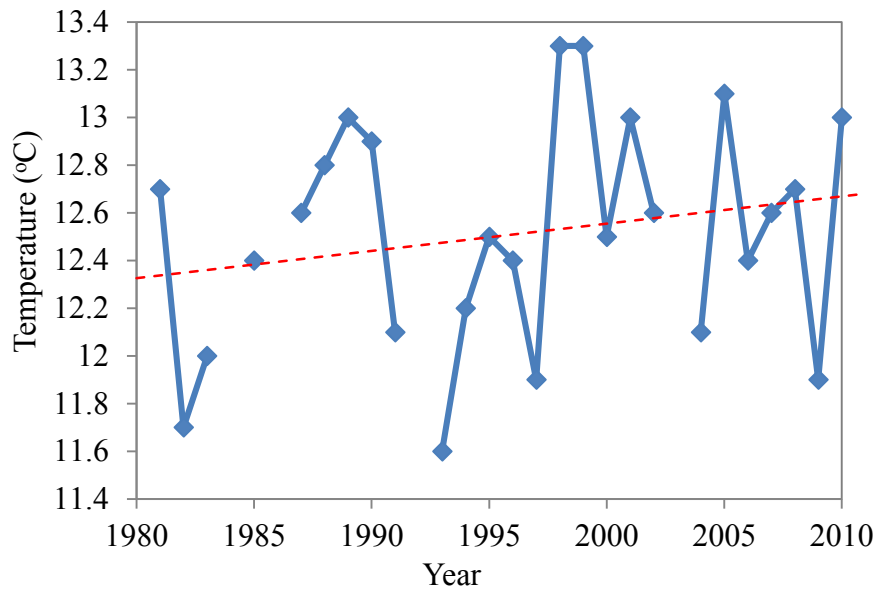


Figure A5. Annual mean ambient temperatures for Wallaceville from 1980 to 2010 (Linear fitting to these data derived a temperature increase trend of 0.0114 °C/year)

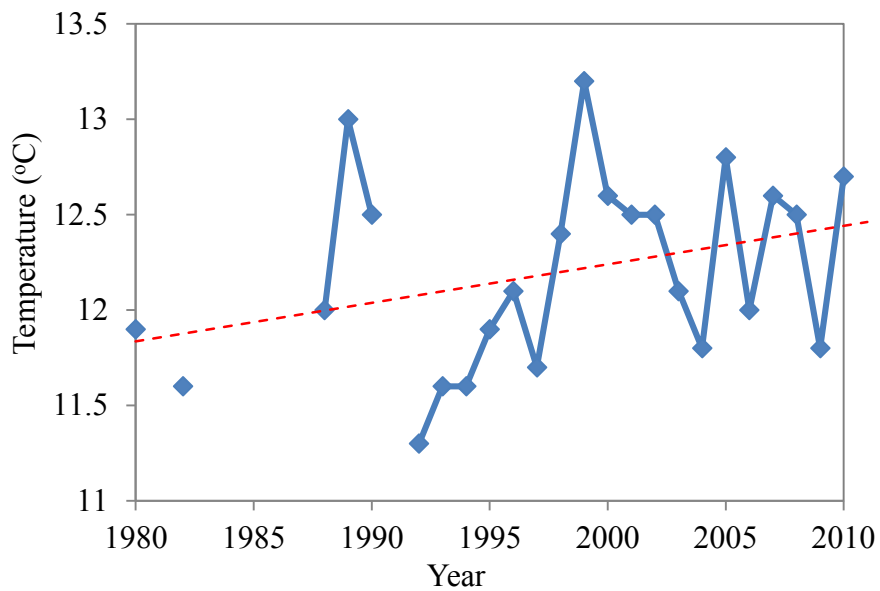


Figure A6. Annual mean ambient temperatures for Greymouth from 1980 to 2010 (Linear fitting to these data derived a temperature increase trend of 0.0202 °C/year)

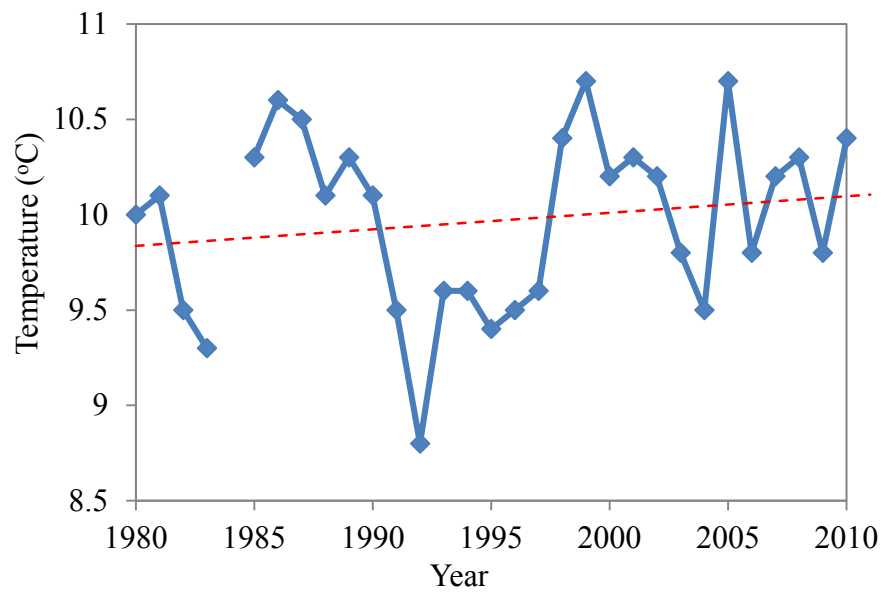


Figure A7. Annual mean ambient temperatures for Invercargill Airport from 1980 to 2010 (Linear fitting to these data derived a temperature increase trend of 0.0086 °C/year)

A.1.2 Rainfall and Wet Days

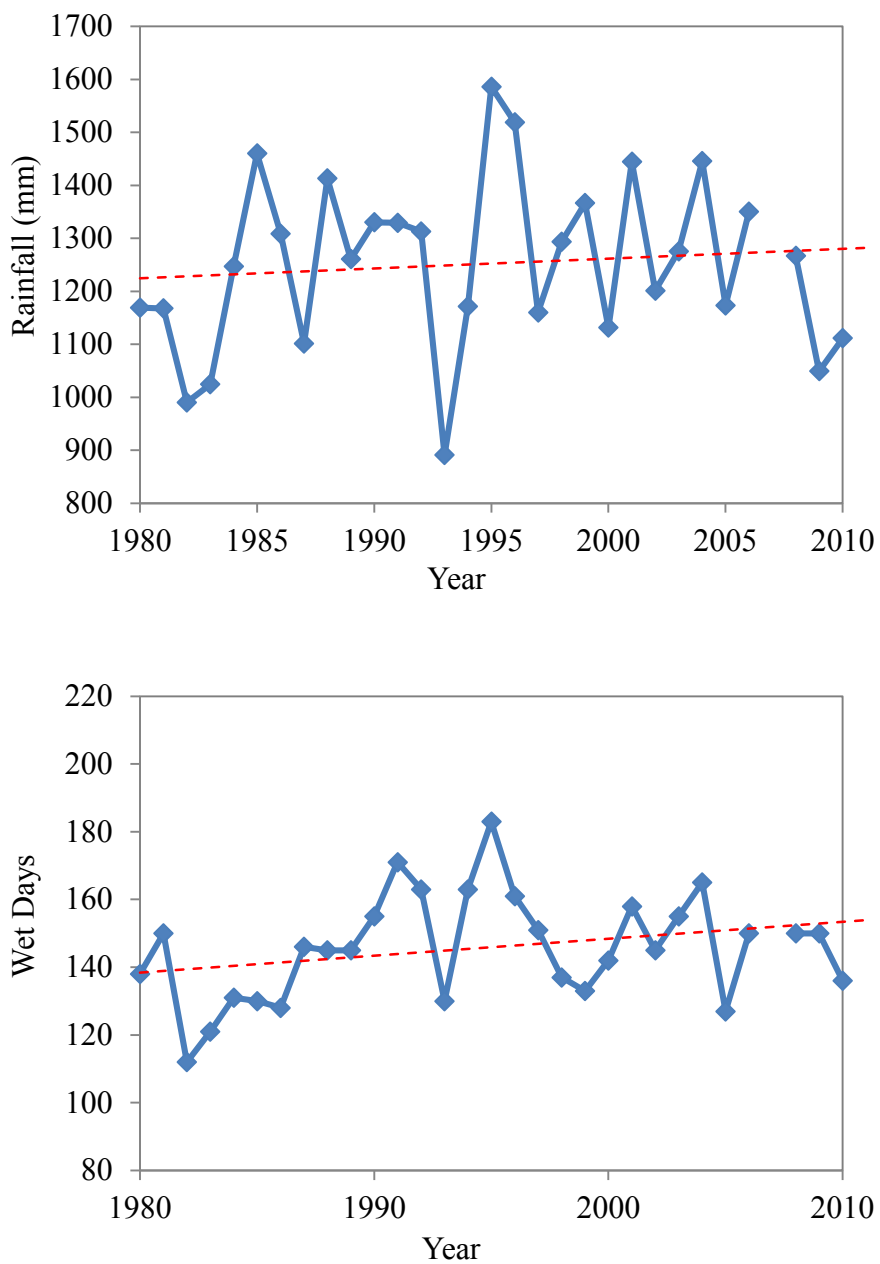


Figure A8. Annual rainfall and wet days at Ardmore from 1980 to 2010 (Linear fitting to these data showed an increasing trend for both rainfall and wet days)

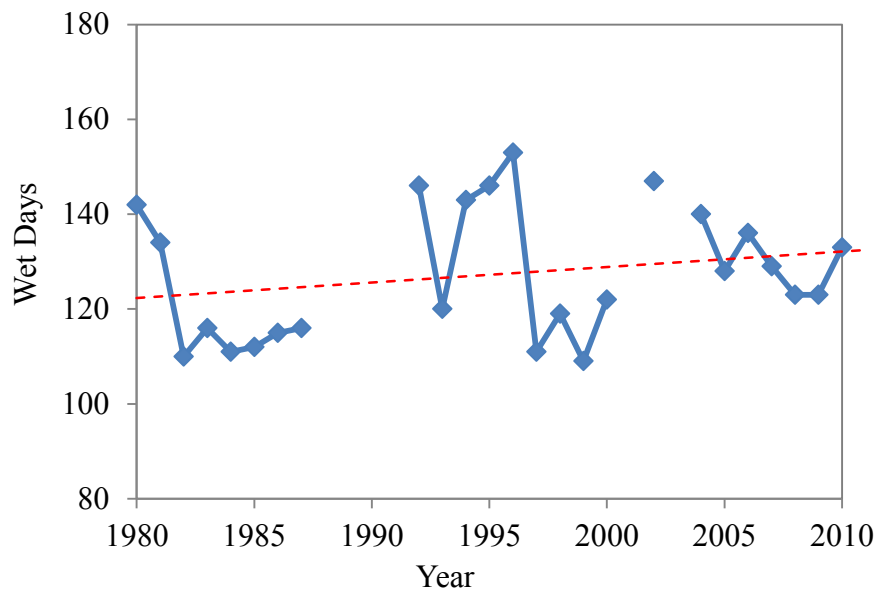
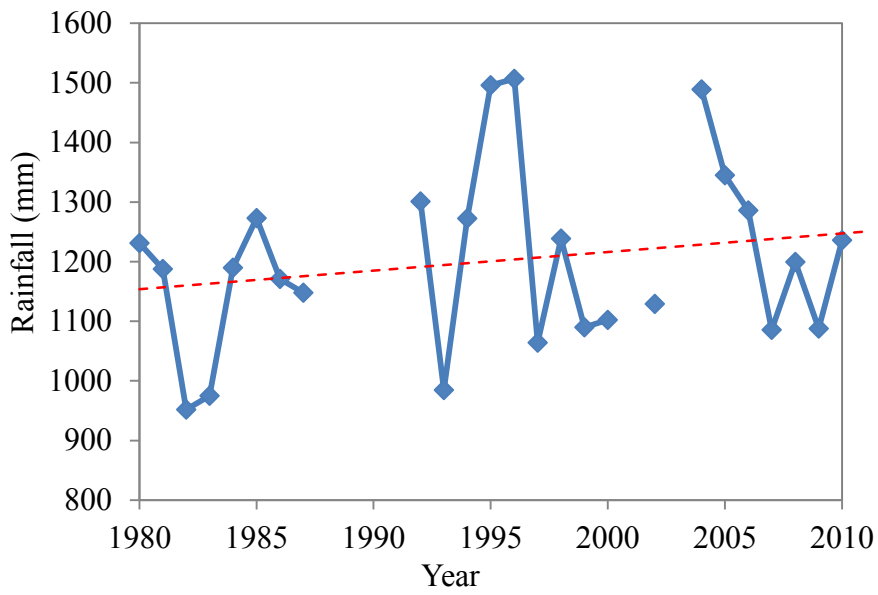


Figure A9. Annual rainfall and wet days at Hamilton Airport from 1980 to 2010 (Linear fitting to these data showed an increasing trend for both rainfall and wet days)

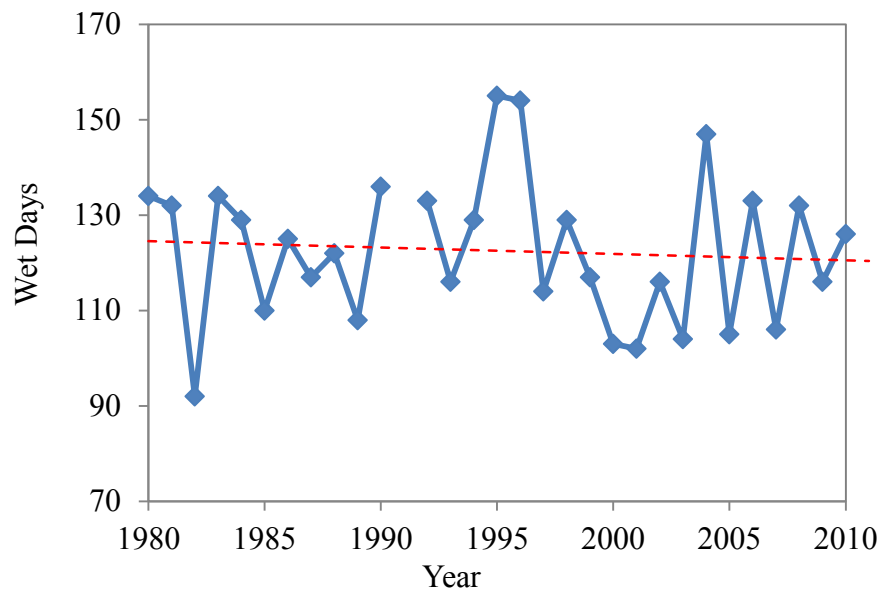
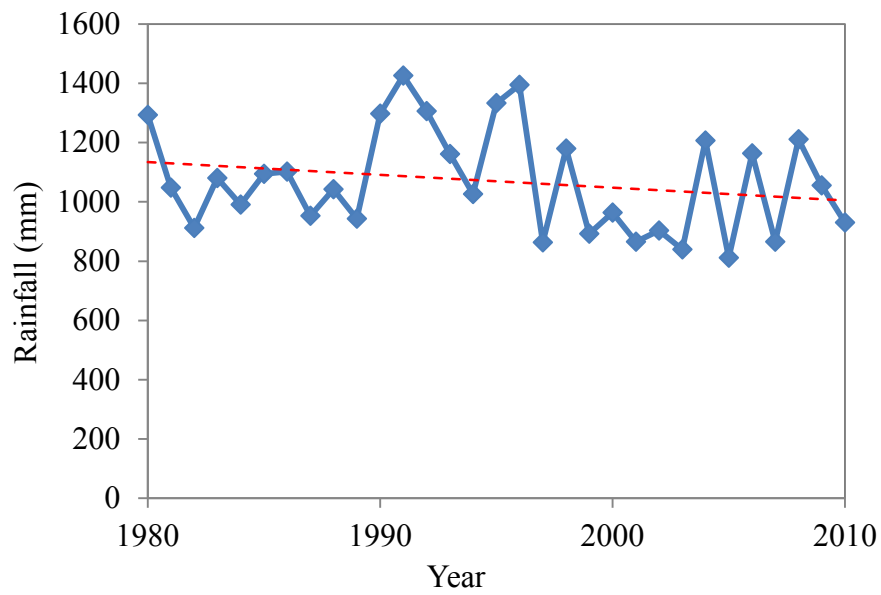


Figure A10. Annual rainfall at wet days at Levin from 1980 to 2010 (Linear fitting to these data showed a decreasing trend for both rainfall and wet days)

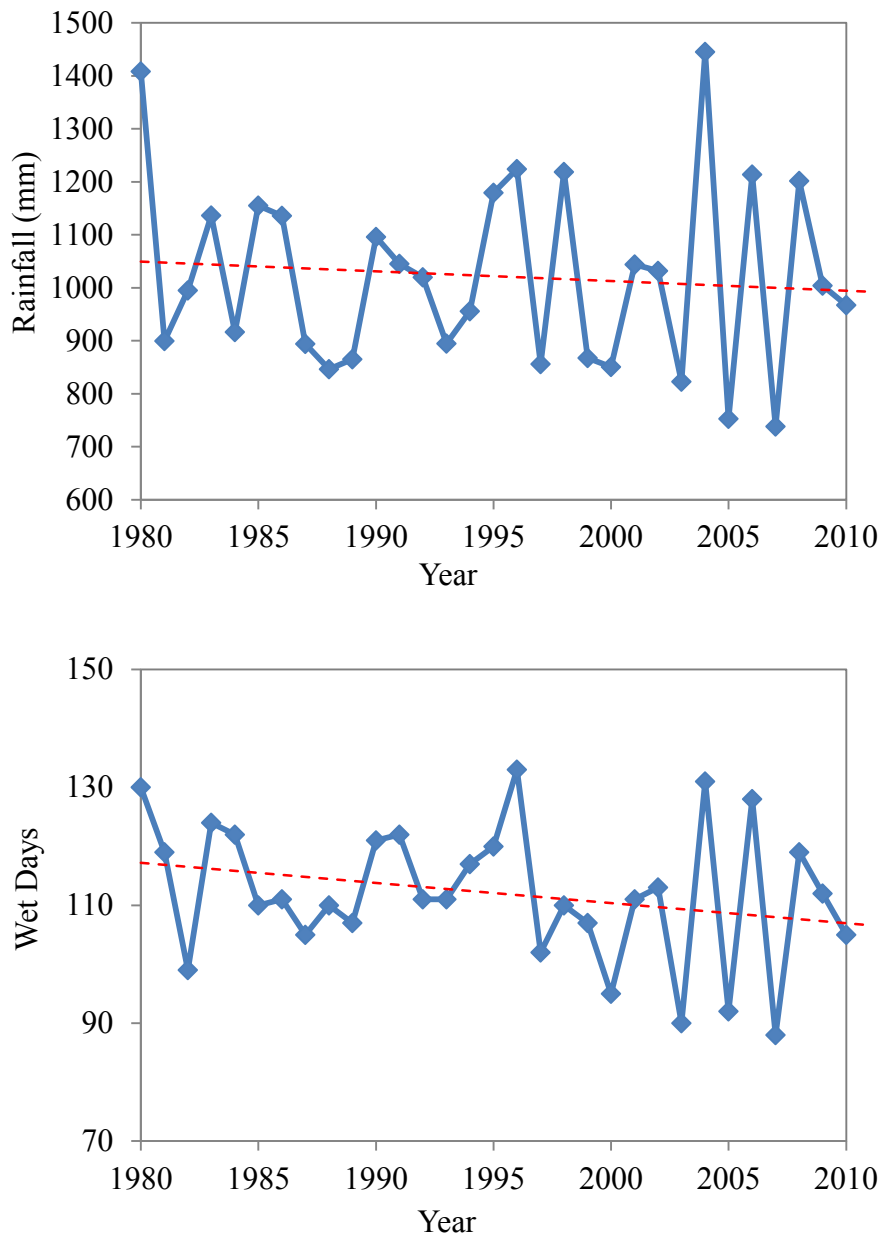


Figure A11. Annual rainfall and wet days at Paraparaumu Airport from 1980 to 2010 (Linear fitting to these data showed a decreasing trend for both rainfall and wet days)

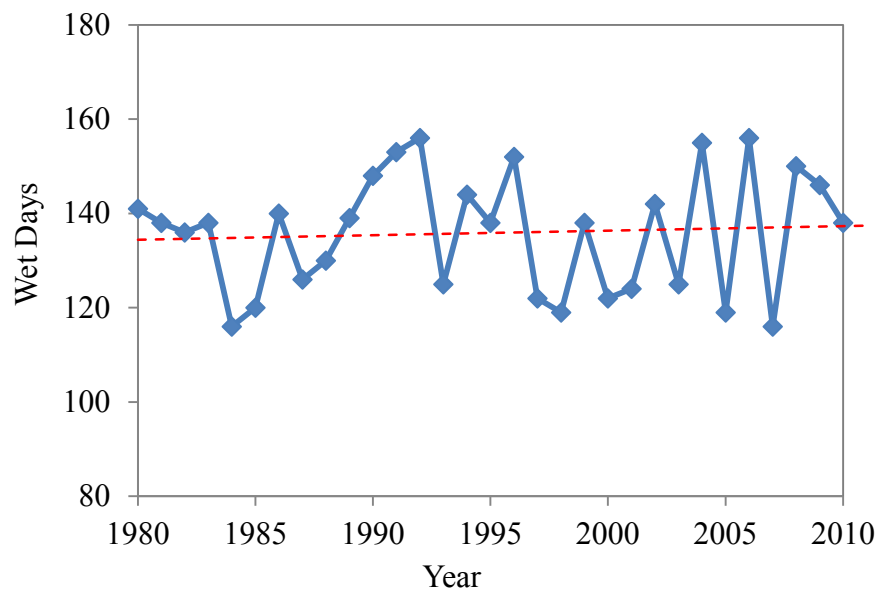
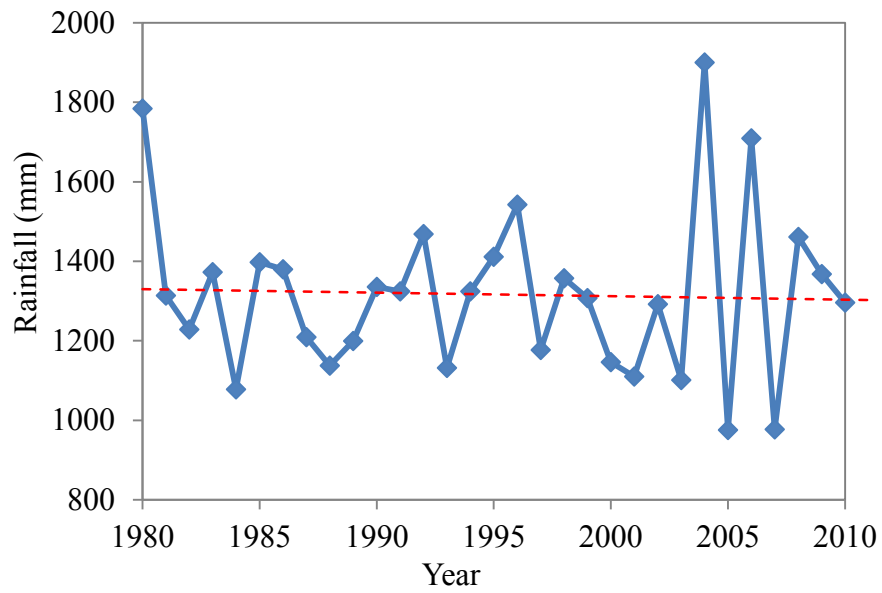


Figure A12. Annual rainfall and wet days at Wallaceville from 1980 to 2010 (Linear fitting to these data showed a very gentle decreasing trend for rainfall and a very small increasing trend for wet days)

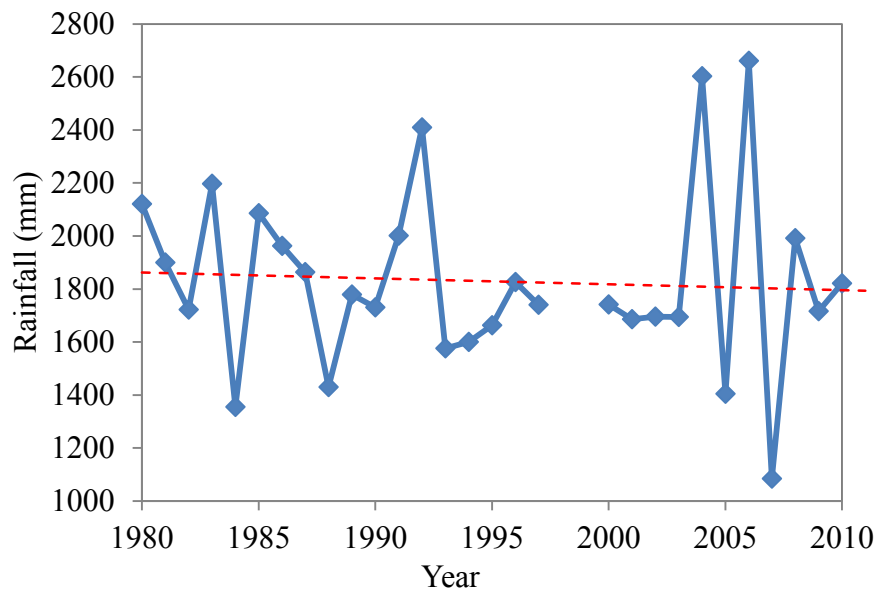


Figure A13. Annual rainfall for Wainuiomata from 1980 to 2010 (Linear fitting to these data showed a decreasing trend of rainfall)

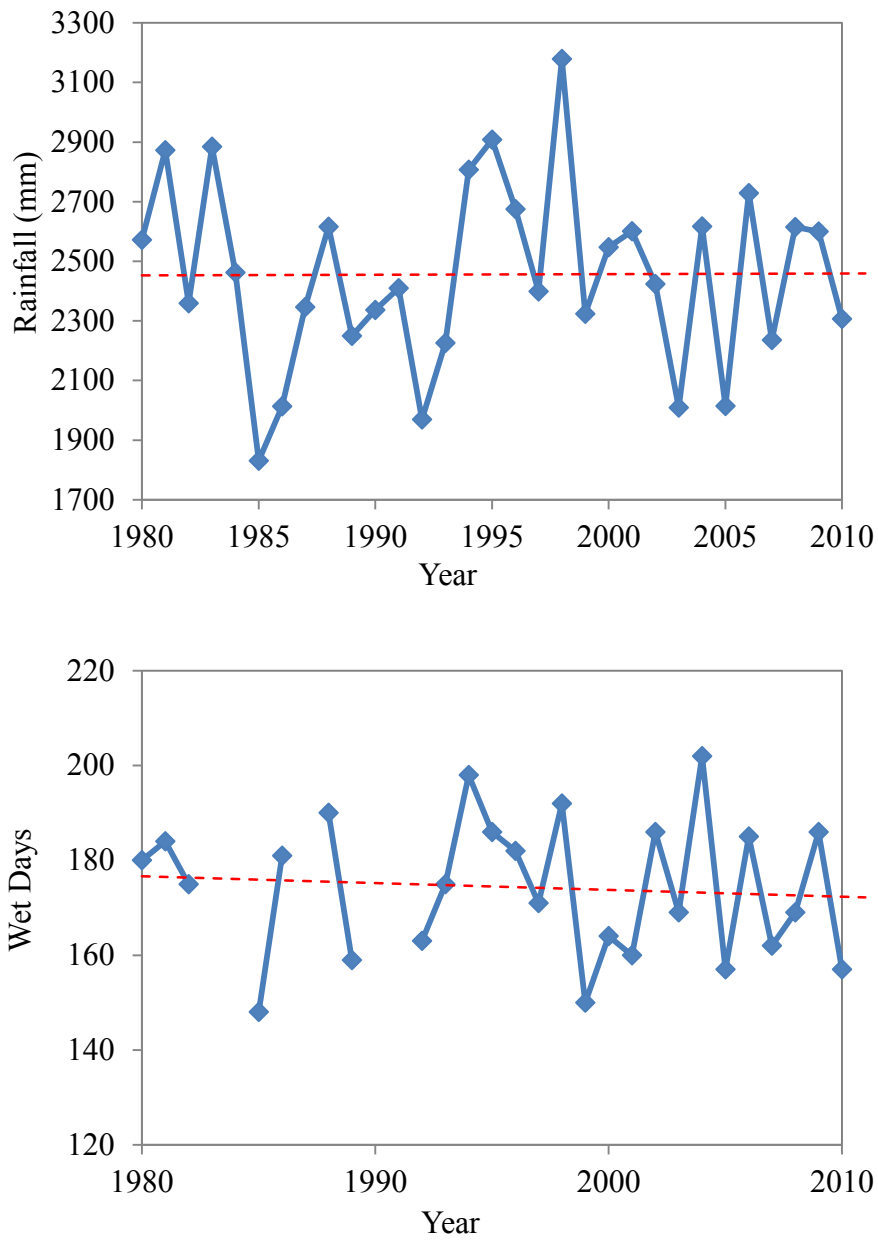


Figure A14. Annual rainfall and wet days at Greymouth from 1980 to 2010 (Linear fitting to these data showed that rainfall was relatively stable while wet days was decreasing slightly)

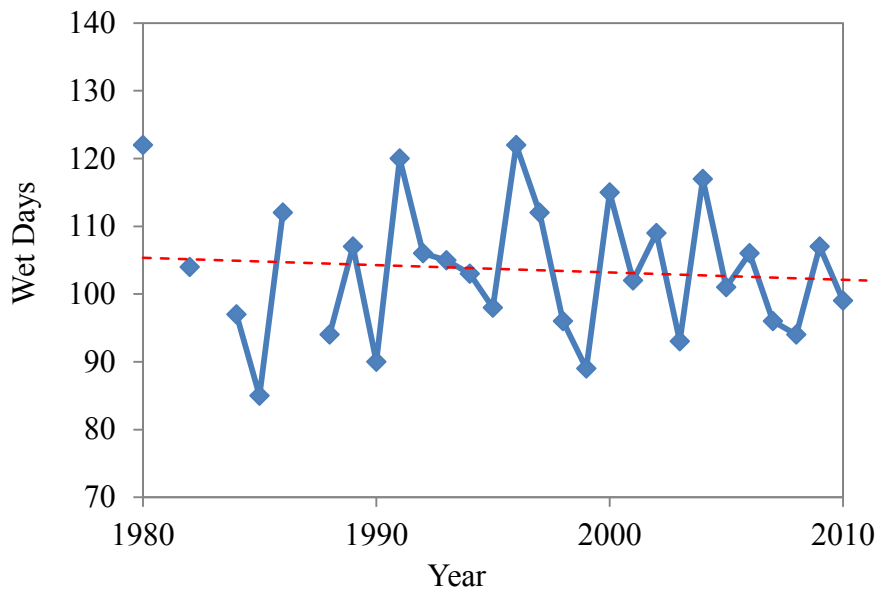
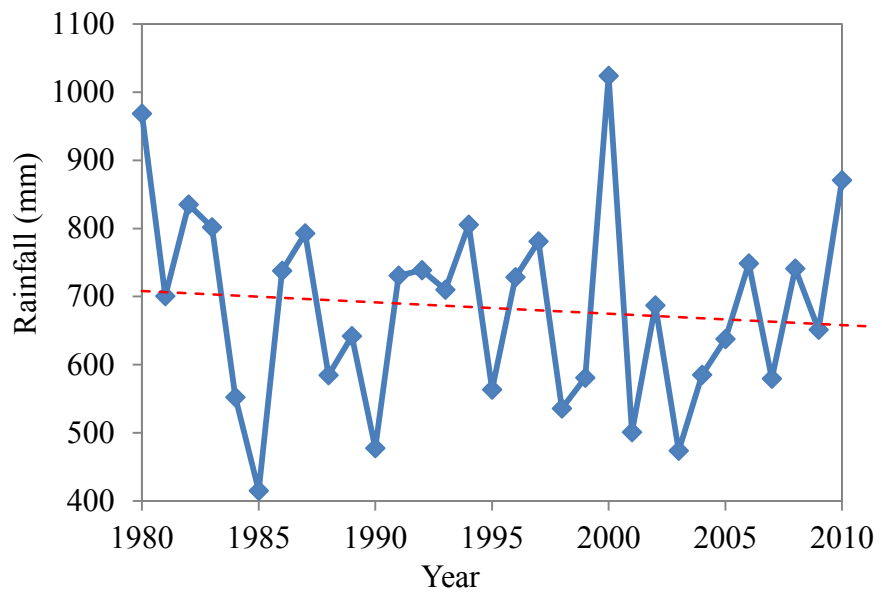


Figure A15. Annual rainfall and wet days at Mosgiel (Dunedin) from 1980 to 2010 (Linear fitting to these data showed a small decreasing trend for both rainfall and wet days)

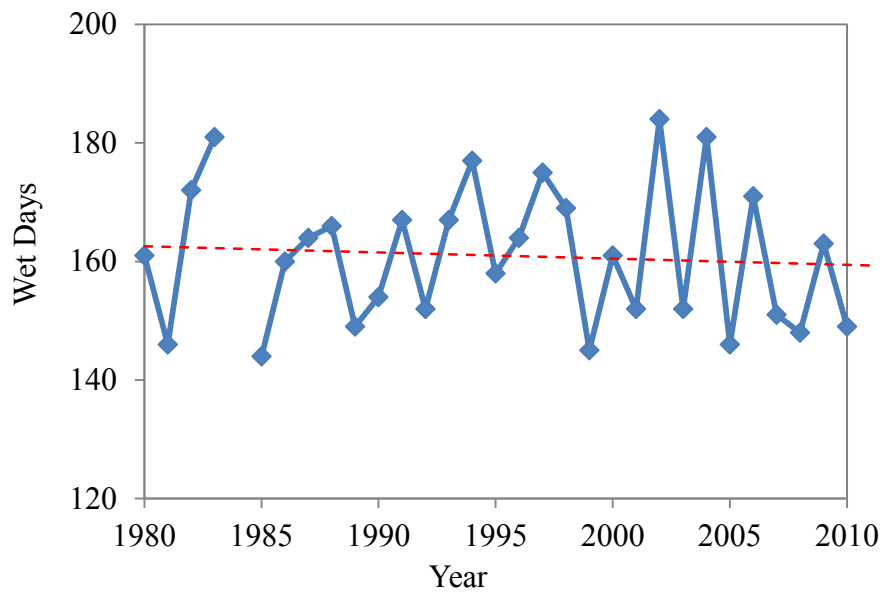
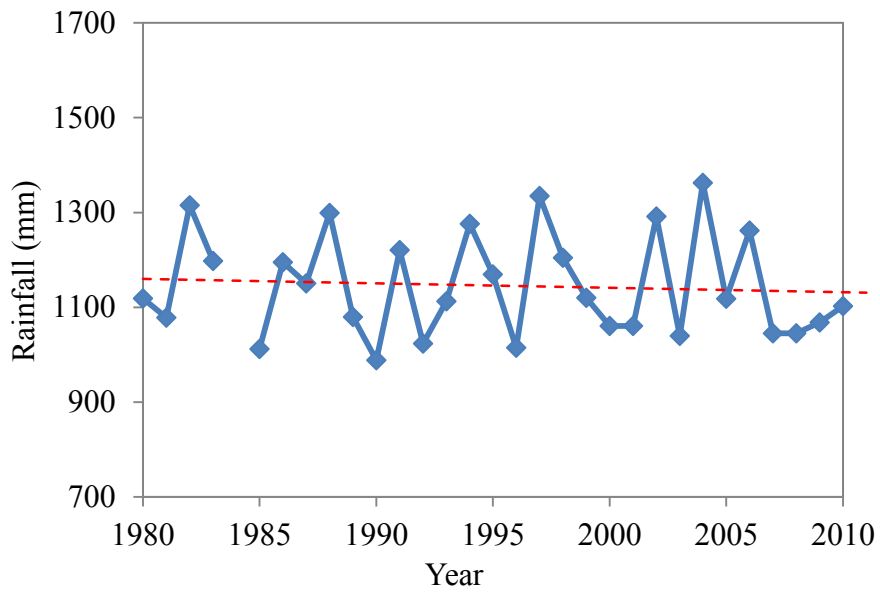


Figure A16. Annual rainfall and wet days at Invercargill Airport from 1980 to 2010 (Linear fitting to these data showed a very small decreasing trend for both rainfall and wet days)

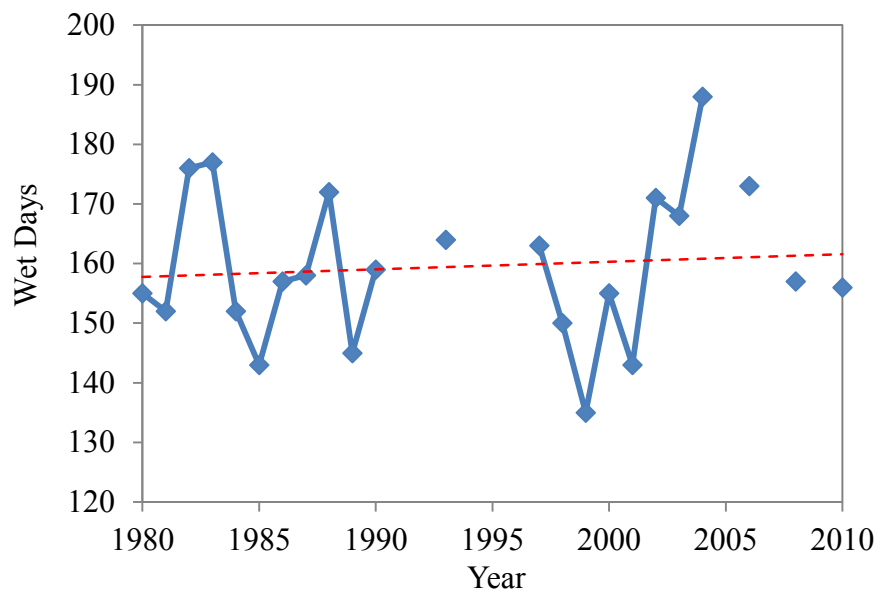
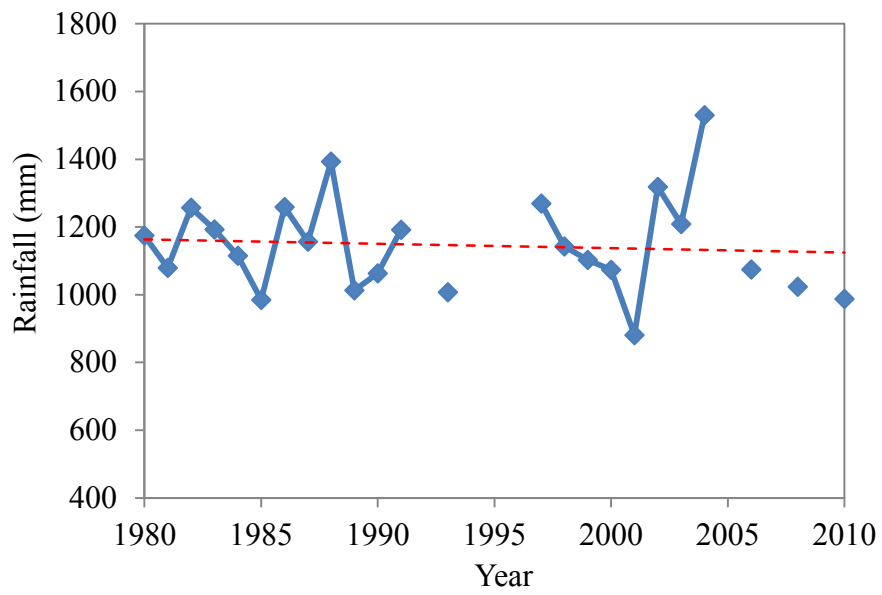


Figure A17. Annual rainfall and wet days at Tiwai Point from 1980 to 2010 (Linear fitting to these data showed a very small decreasing trend for rainfall and a very small increasing trend for wet days)

A.1.3 Relative Humidity

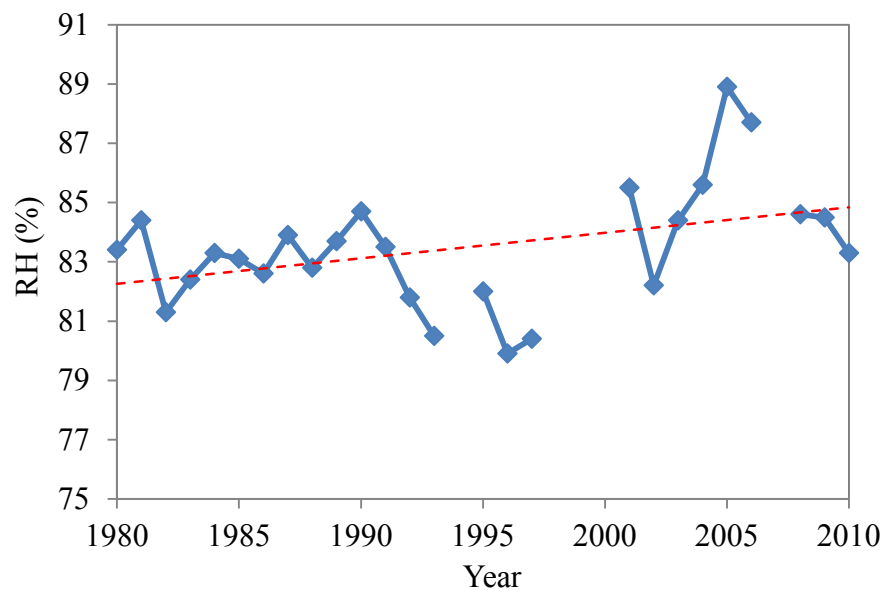


Figure A18. Mean 9am annual relative humidity for Warkworth from 1980 to 2010
Annual RH in 1980s and 1990s was around 83%. It increased in the early 2000s and then decreased. Linear fitting showed a small increasing trend in the last 30 years.

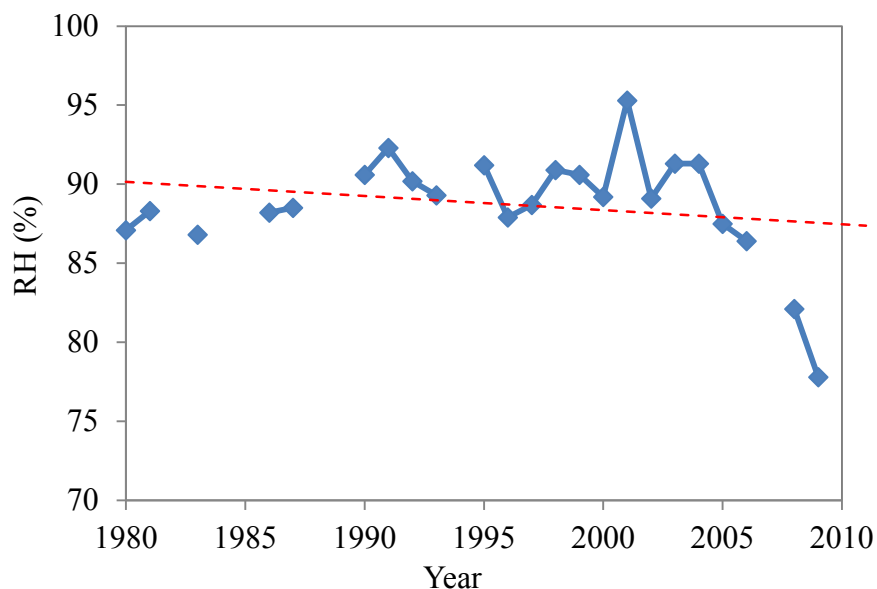


Figure A19. Mean 9am annual relative humidity for Ardmore from 1980 to 2010
From 1980 to 2001, RH was increasing slightly but after that it was decreasing sharply. Linear fitting showed a small decreasing trend of relative humidity in the last 30 years.

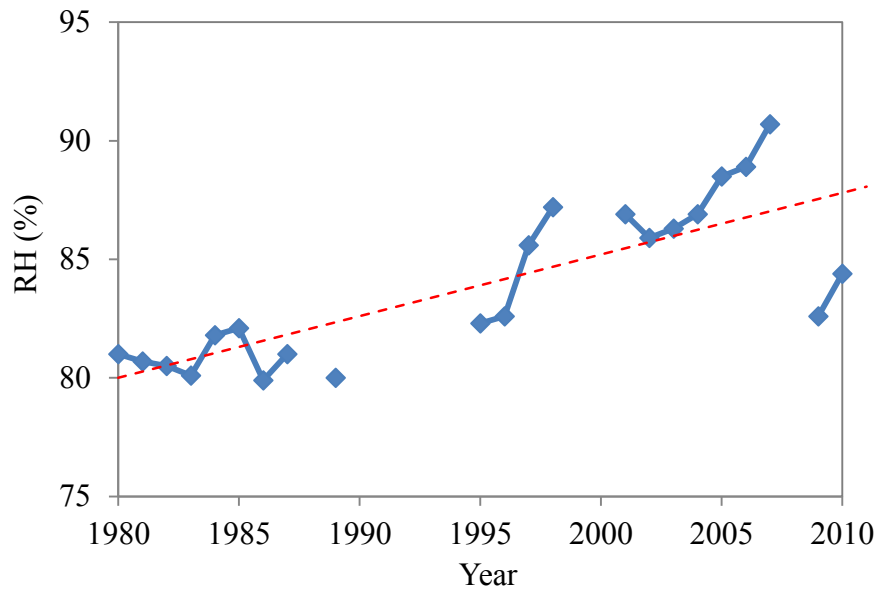


Figure A20. Mean 9am annual relative humidity for Pukekohe from 1980 to 2010
 The RH data record was incomplete for this site. Mean 9am annual RH was always higher 80% and showed an increasing trend in the past three decades.

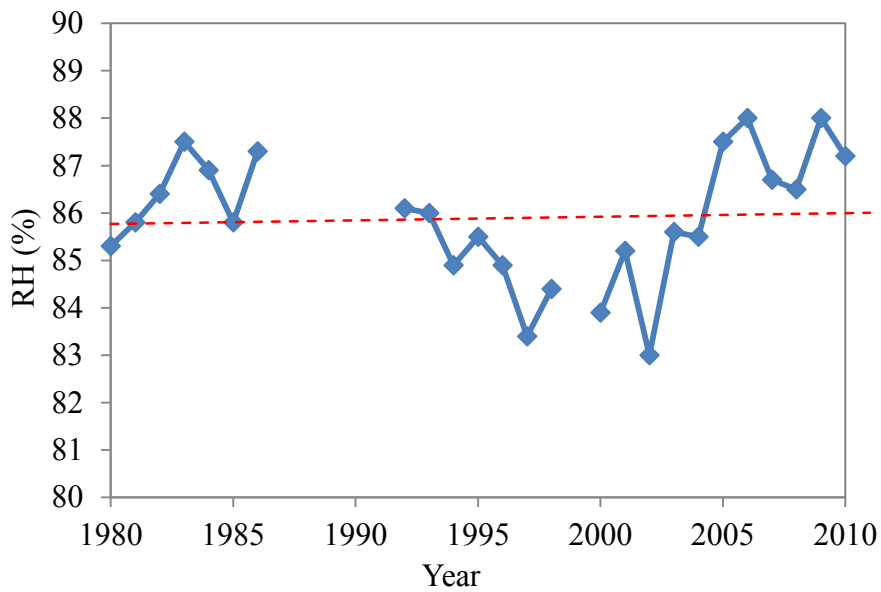


Figure A21. Mean 9am annual relative humidity for Hamilton Airport from 1980 to 2010
 The data record was incomplete. Mean 9am annual RH was high and typically ranging from 83% to 88%. It can be seen that RH during the period of 1992 to 2004 was lower than that in 1980s and the period after 2004. Linear fitting to these data showed a very small increasing trend in the past three decades.

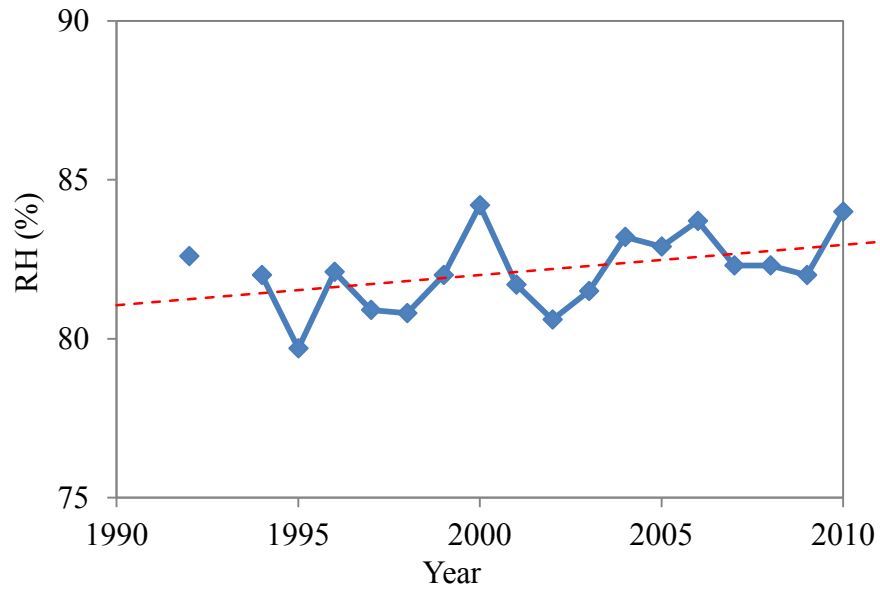


Figure A22. Mean 9am annual relative humidity for Levin from 1992 to 2010

The data record only covered the years from 1992. RH during this period was slightly increasing.

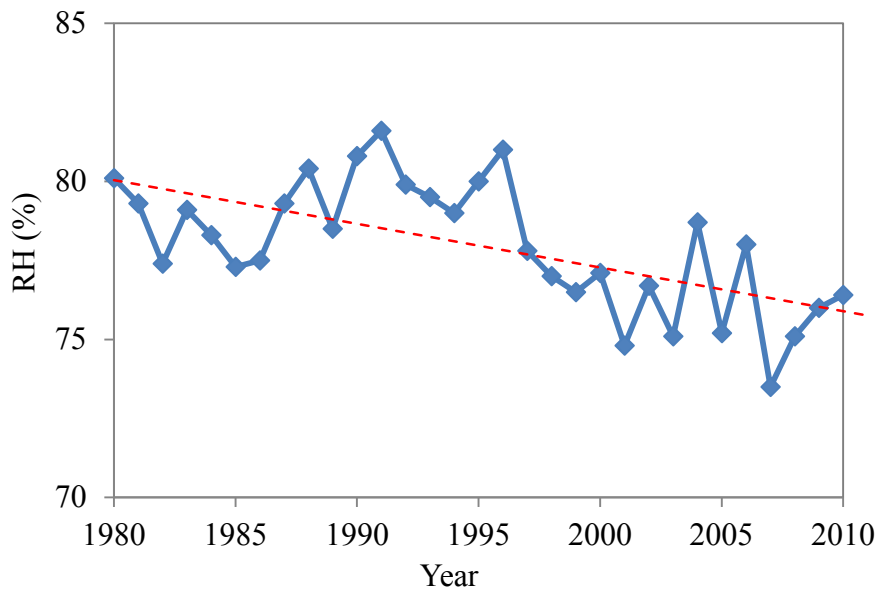


Figure A23. Mean 9am annual relative humidity for Paraparaumu Airport from 1980 to 2010

RH during the period of 1980 to 1996 was relatively steady with an average of 79-80%. After this, it was decreasing. Linear fitting showed a decreasing trend in the past three decades.

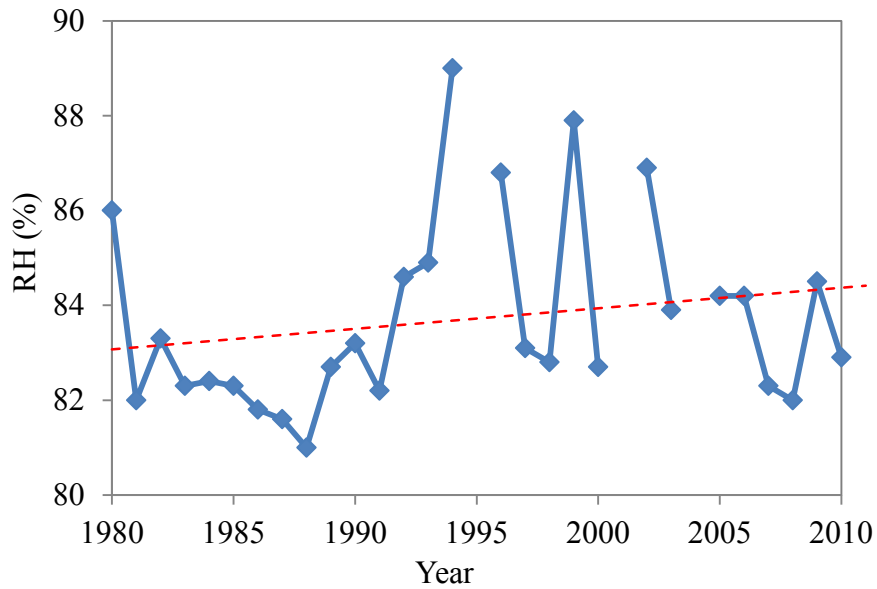


Figure A24. Mean 9am annual relative humidity for Wallaceville from 1980 to 2010
 RH records for several years were missing. The changing trend was complex though it appeared to be increasing in the past three decades. Mean 9am annual RH at this site was relatively high, all above 80%.

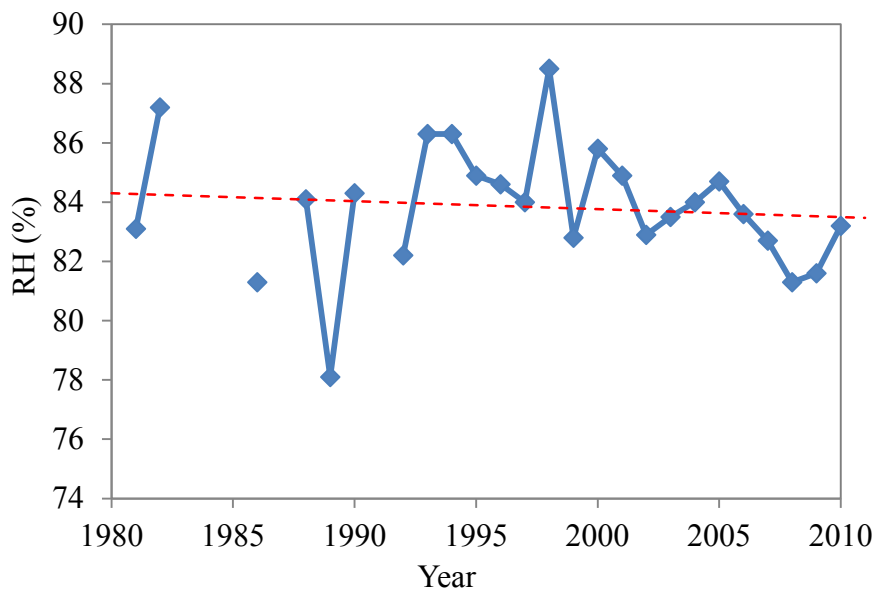


Figure A25. Mean 9am annual relative humidity for Greymouth from 1980 to 2010
 The RH data set was not complete. Linear fitting of the data available showing a decreasing trend of the mean 9am annual RH in the past three decades at this site.

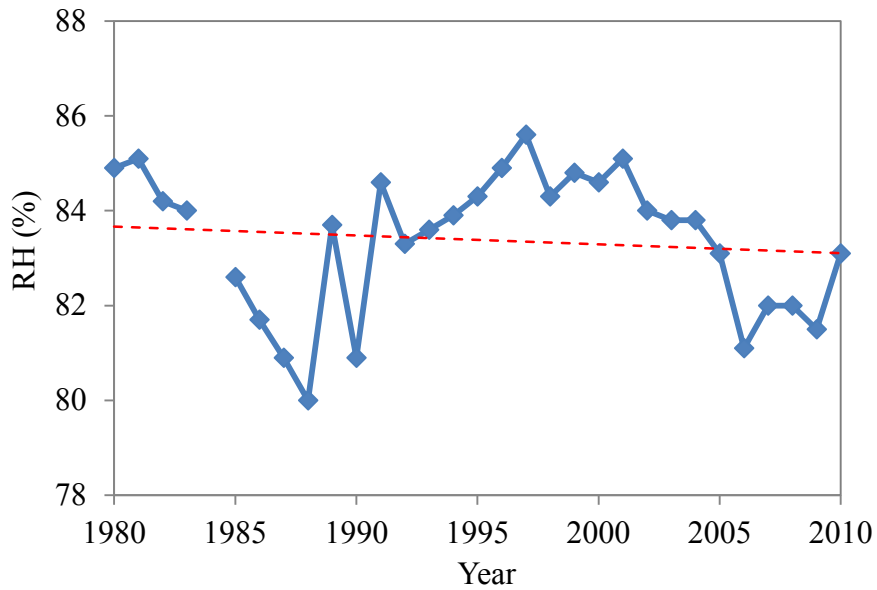


Figure A26. Mean 9am annual relative humidity for Invercargill Airport from 1980 to 2010

The mean 9am annual RH at this site was showing a complicated changing trend during the last 30 years. Before 1990, the RH was decreasing continuously. It was then increasing and staying at values higher than 84% before early 2000s. After this, the RH at this site was varying around 82%. Linear fitting of the data for the last 30 years exhibited a very small decreasing trend.

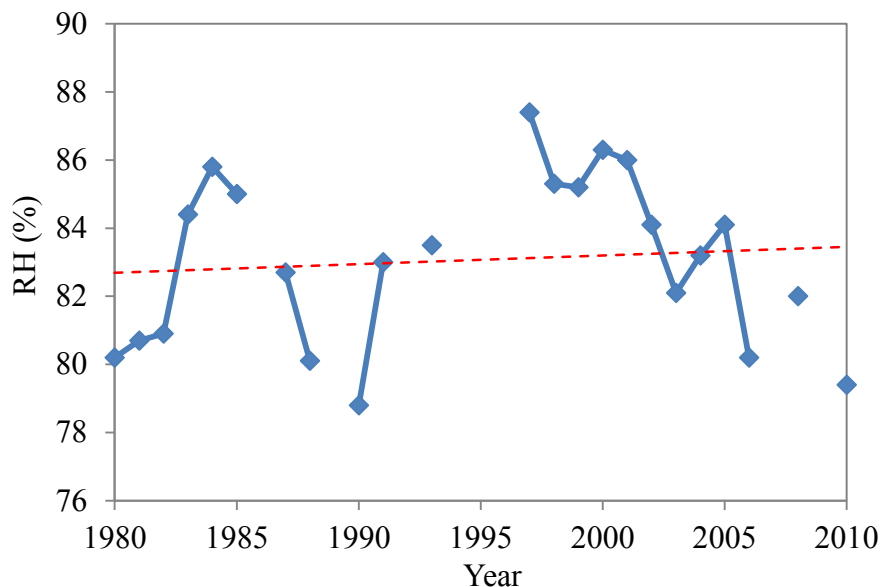


Figure A27. Mean 9am annual relative humidity for Tiwai Point from 1980 to 2010

The RH data set was not complete. A linear fitting of the data available was roughly made and a very small increasing trend of the mean 9am annual RH in the past three decades at this site was shown.

A.1.4 Wind Speed

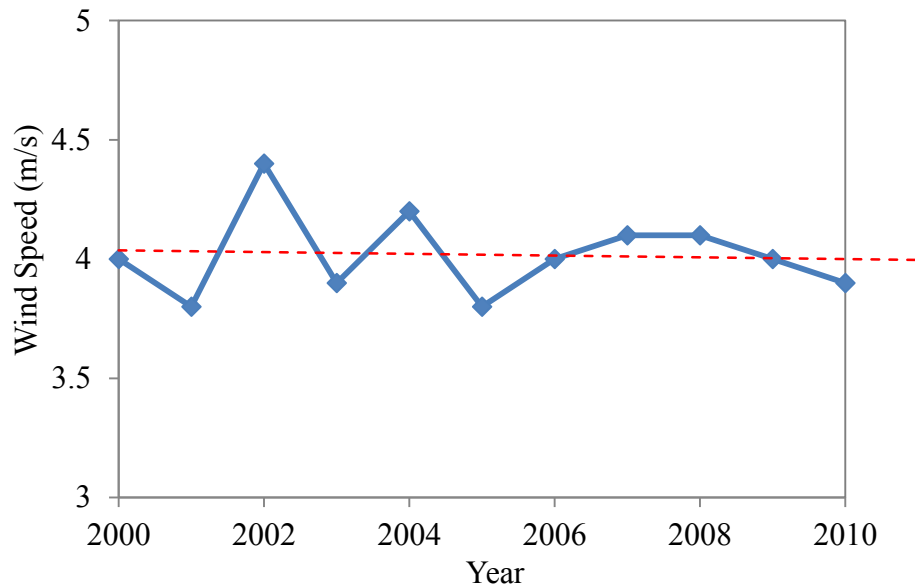


Figure A28. Mean annual wind speed at Warkworth from 2000 to 2010

Wind speed data for Warkworth weather station was only available after the year of 2000. In the past ten years, the annual wind speed at this site was averaged to be around 4 m/s and showing a relatively small decreasing trend.

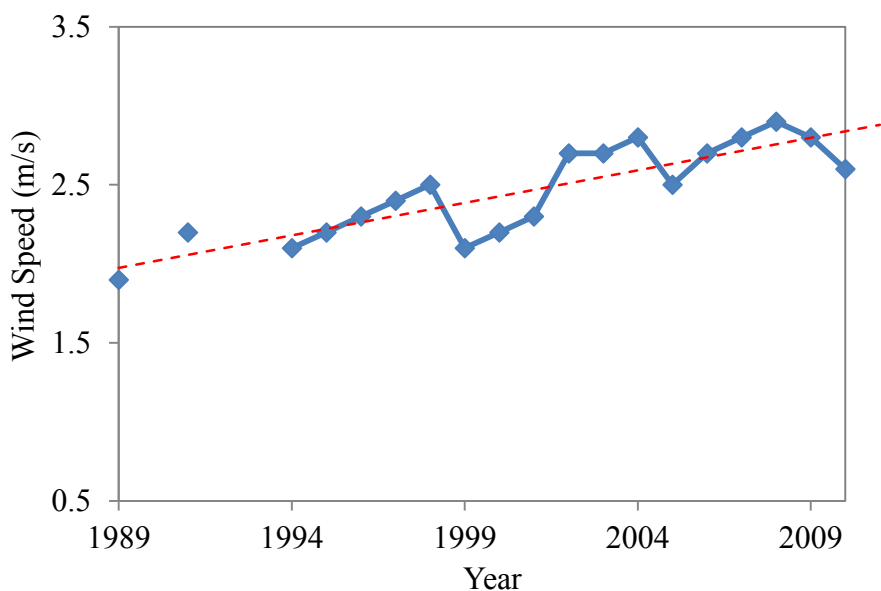


Figure A29. Mean annual wind speed at Pukekohe from 1989 to 2010

Wind speed at Pukekohe was generally less than 3 m/s. It was showing a pattern of step increase. However it is quite obvious that in the past 20 years, annual mean wind speed was increasing continuously.

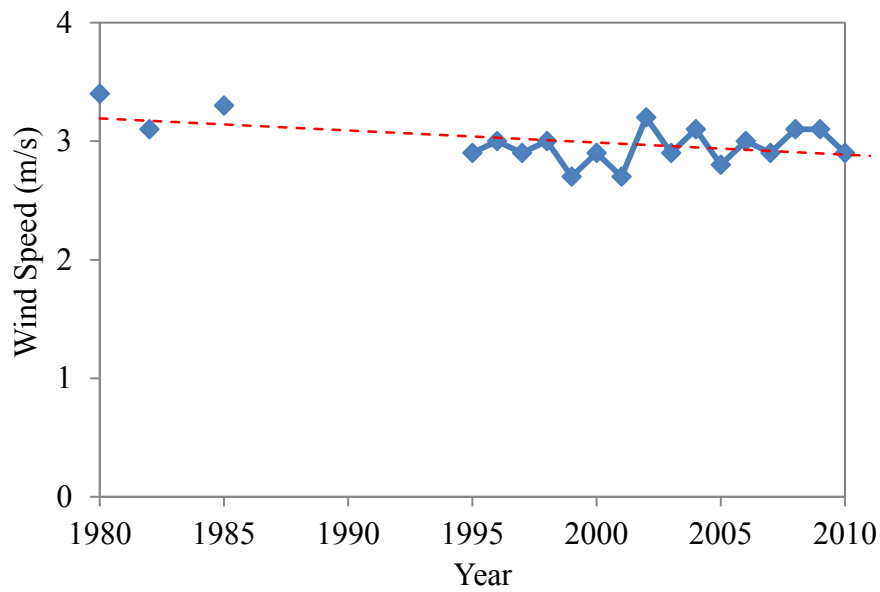


Figure A30. Mean annual wind speed at Hamilton Airport from 1980 to 2010

The data set for Hamilton Airport is incomplete. Wind speed at this site from 1995 to 2010 was around 3 m/s, with a very small variation year to year.

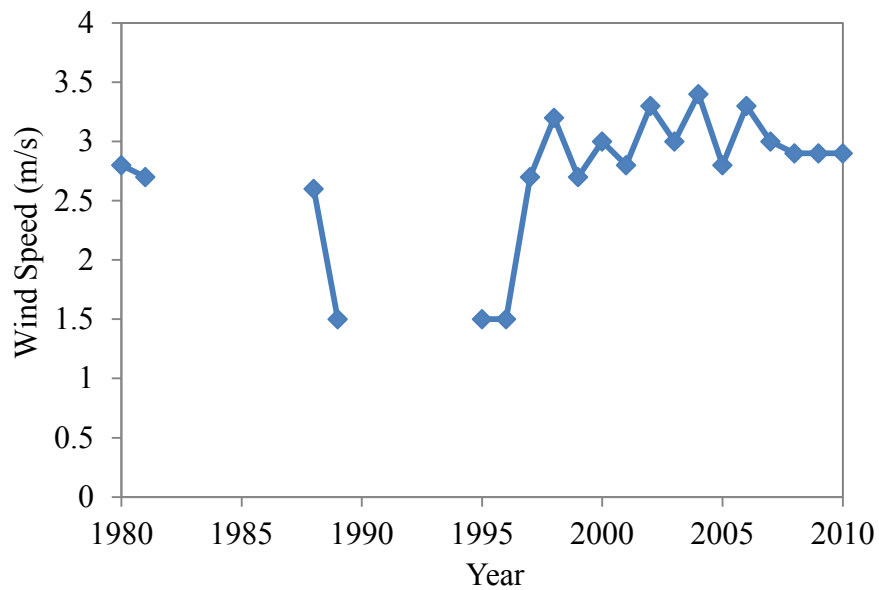


Figure A31. Mean annual wind speed at Levin from 1980 to 2010

From the incomplete data set, it appeared that wind speed was quite low but had a relatively large variation during the period of 1980 to 1990. From 1998 to 2010 wind speed at this site appeared to be reasonably stable, around 3 m/s.

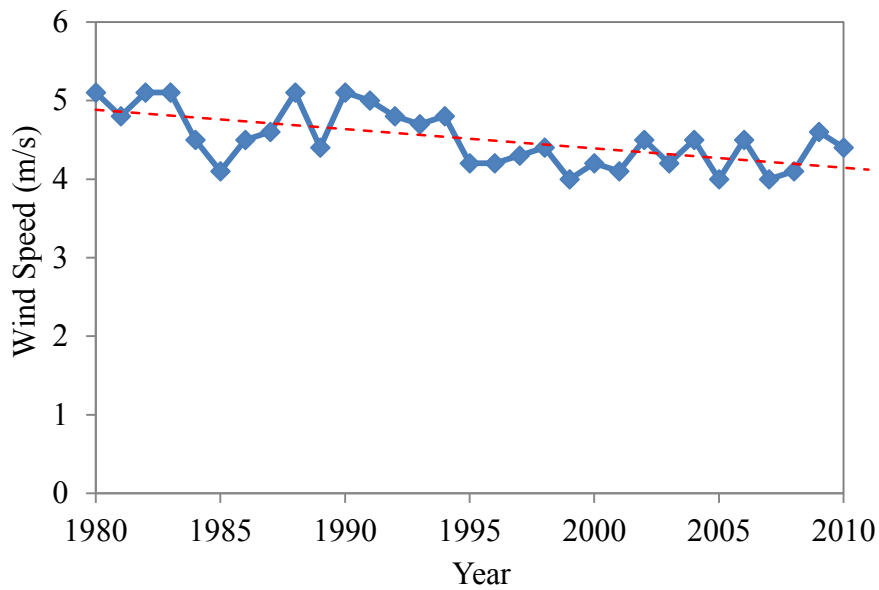


Figure A32. Mean annual wind speed at Paraparaumu Airport from 1980 to 2010

This data set could be roughly divided into two sections, i.e. 1980 to 1995 and 1995 to 2010. The former period had a slightly higher average annual mean wind speed than the latter. Though the linear fitting to the data collected for the past 30 years showed a decreasing trend, it appeared that the wind speed was relatively stable in the last 15 years and slightly higher than 4 m/s.

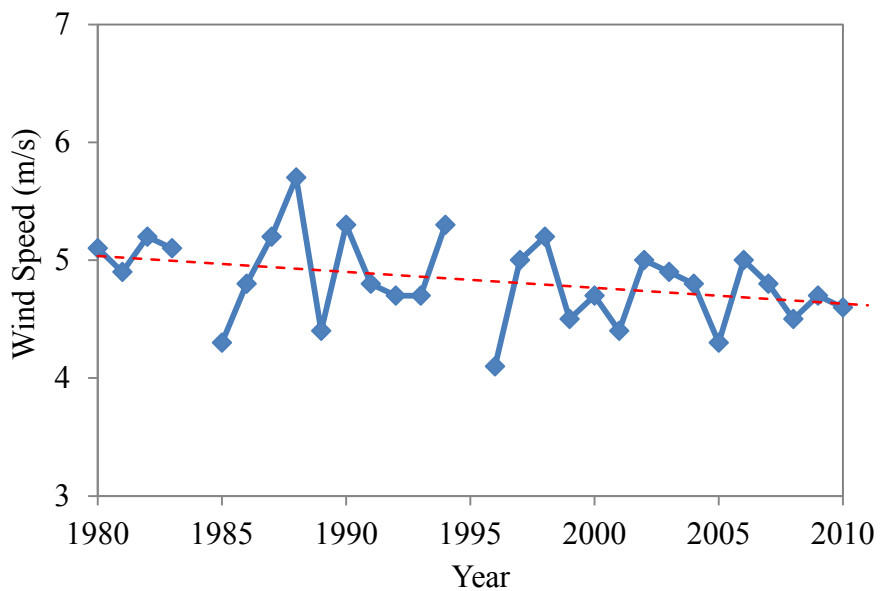


Figure A33. Mean annual wind speed at Invercargill Airport from 1980 to 2010

Wind speed at this site was high, around 5 m/s, however it was showing a slight decreasing trend in the past three decades.

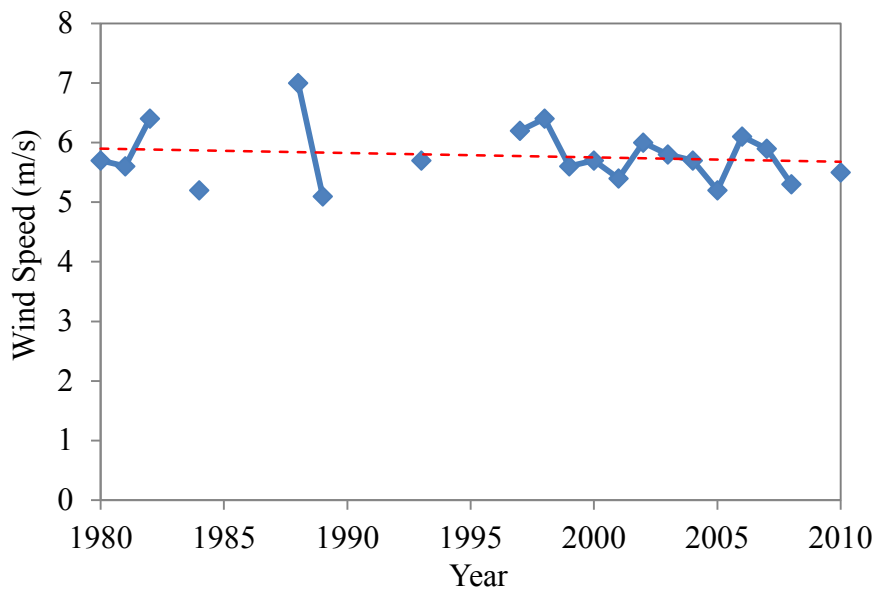


Figure A34. Mean annual wind speed at Tiwai Point from 1980 to 2010

Data record for wind speed at this site was incomplete. However, it appeared that typical wind speed was high, around 6 m/s. Linear fitting of the data available roughly indicated that wind speed was perhaps decreasing, very slowly, over the past three decades.

A.15 Mean Daily Global Radiation

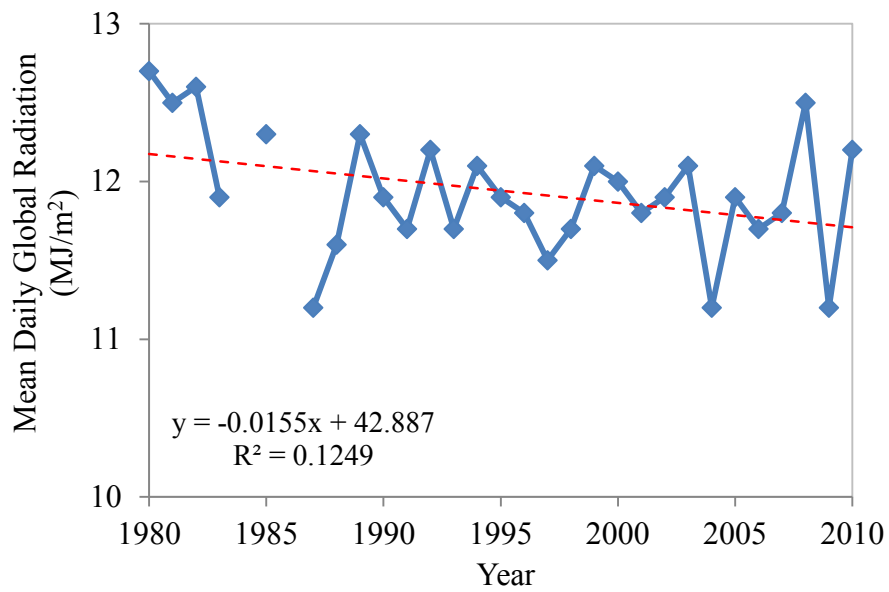


Figure A35. Mean daily global radiation at Invercargill Airport from 1980 to 2010

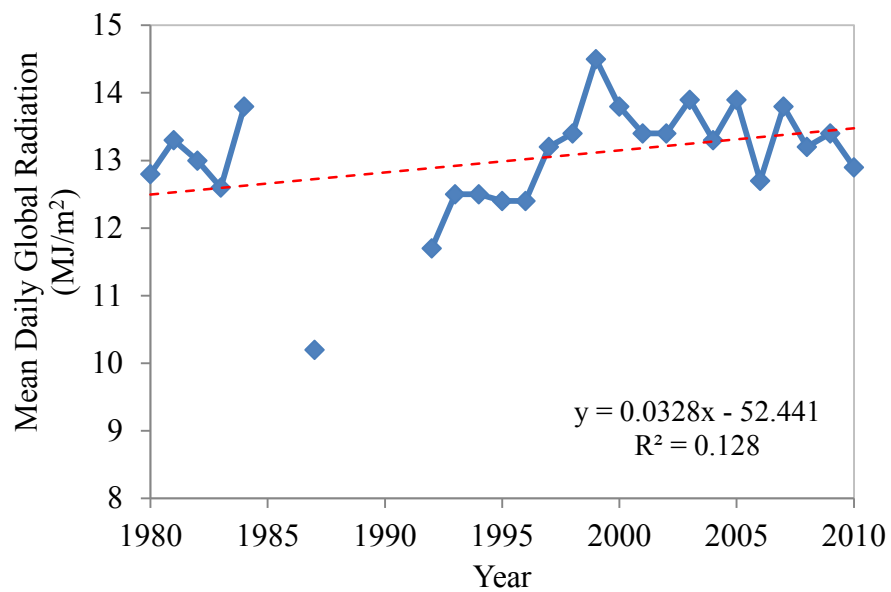


Figure A36. Mean daily global radiation at Levin from 1980 to 2010

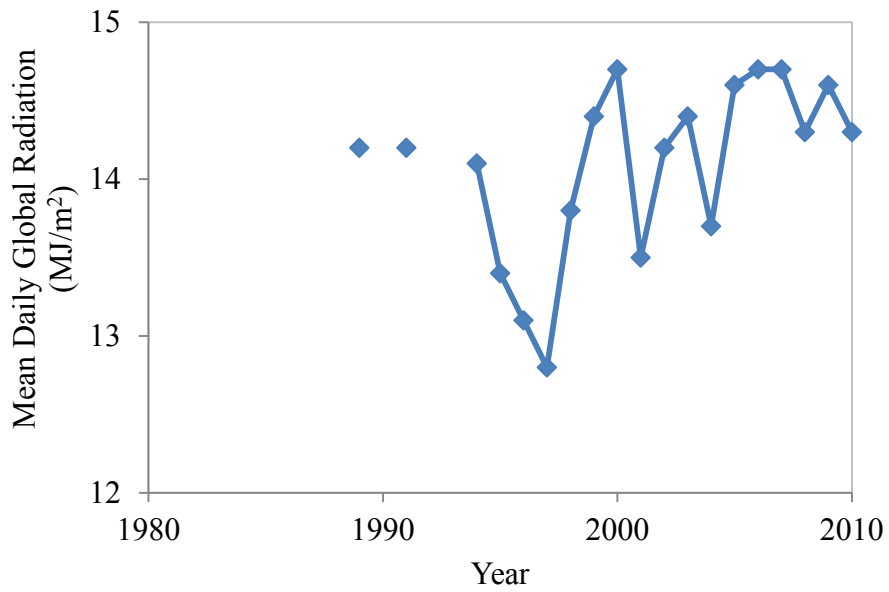


Figure A37. Mean daily global radiation at Pukekohe from 1980 to 2010

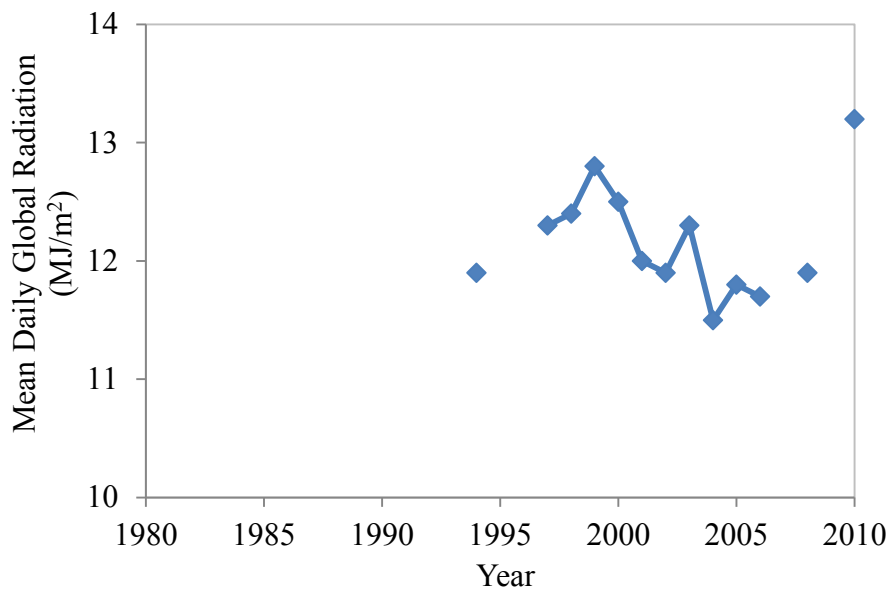


Figure A38. Mean daily global radiation at Tiwai Point from 1980 to 2010

A.2 Climate – Comparison between Short Term Data (2011 – 2012 vs. 1987 – 1988)

A.2.1 Ambient Temperature

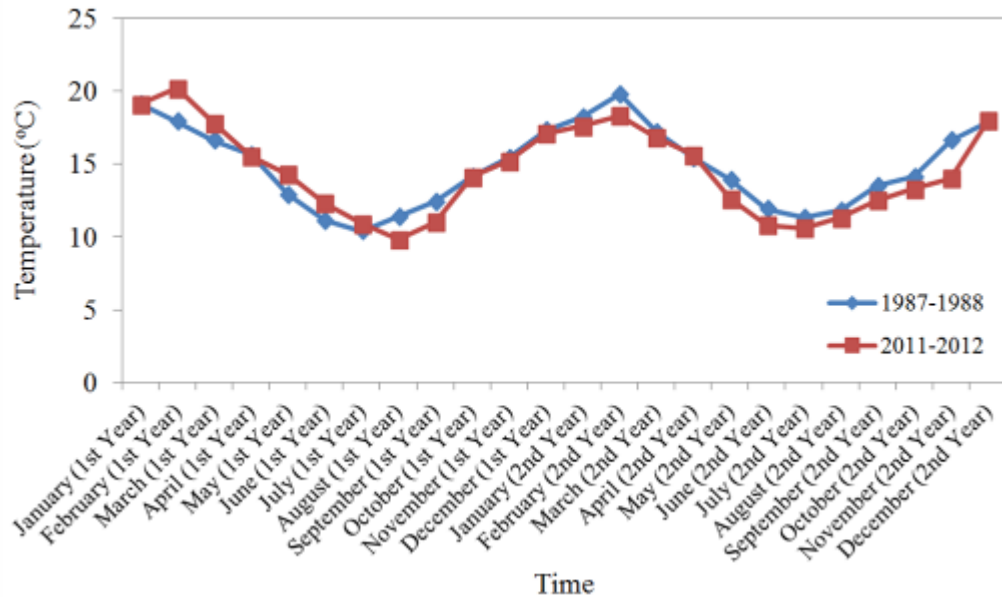


Figure A39. Comparison of ambient temperatures in the periods of 1987 – 1988 and 2011 – 2012 for Warkworth

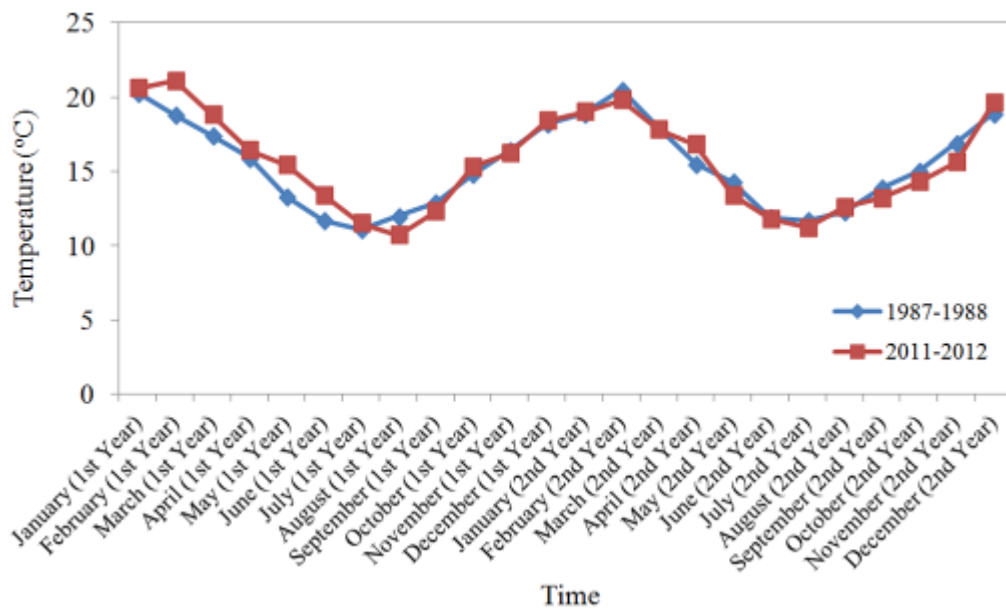


Figure A40. Comparison of ambient temperatures in the periods of 1987 – 1988 and 2011 – 2012 for Auckland Airport

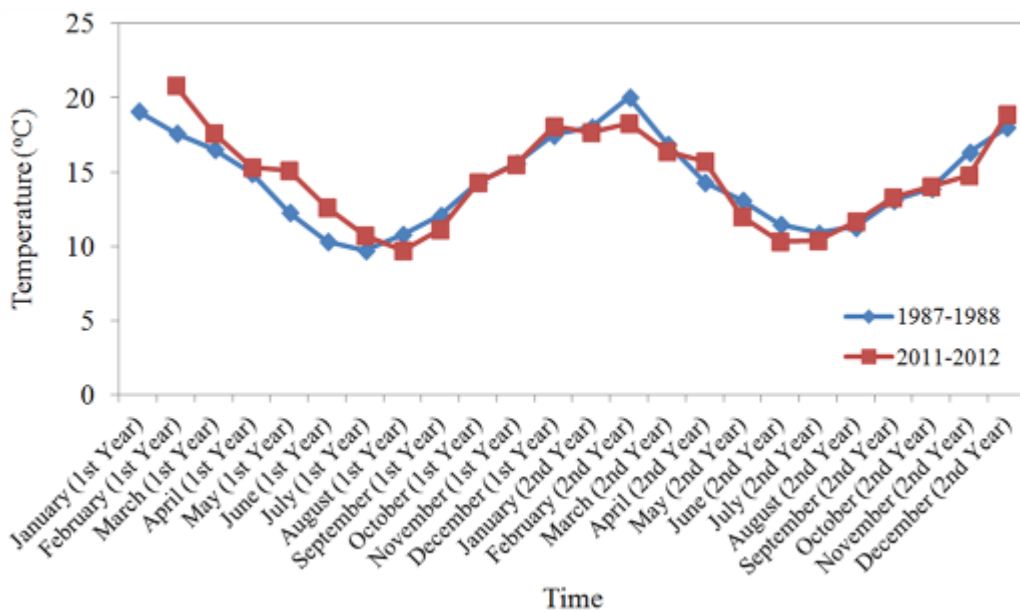


Figure A41. Comparison of ambient temperatures in the periods of 1987 – 1988 and 2011 – 2012 for Ardmore

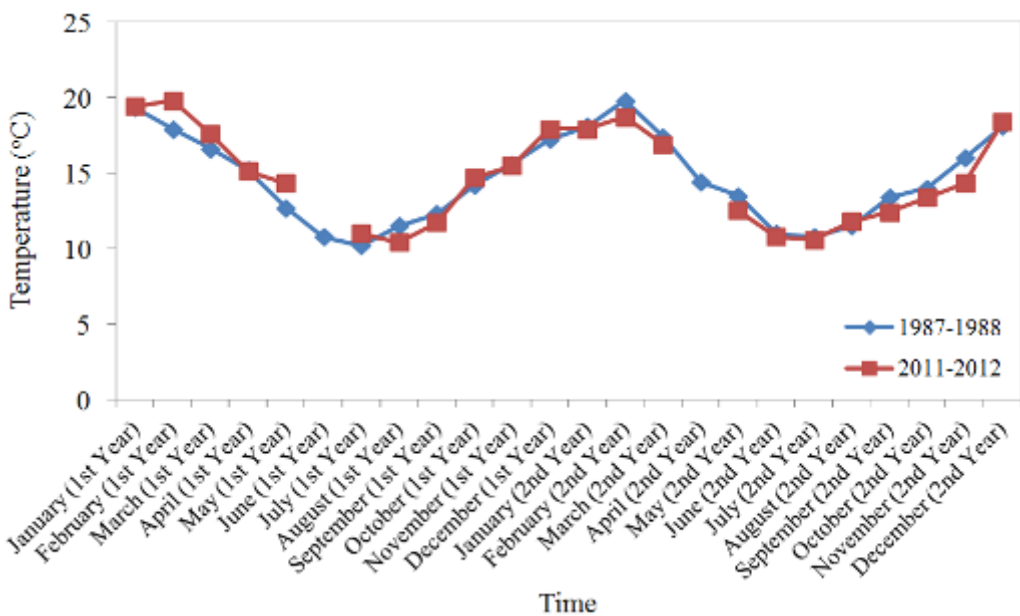


Figure A42. Comparison of ambient temperatures in the periods of 1987 – 1988 and 2011 – 2012 for Pukekohe

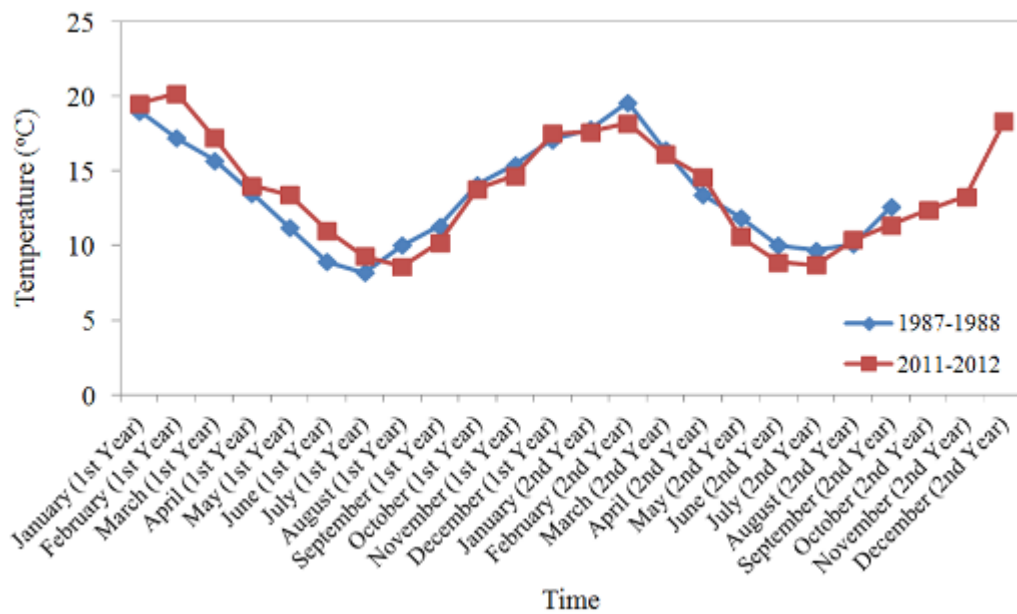


Figure A43. Comparison of ambient temperatures in the periods of 1987 – 1988 and 2011 – 2012 for Hamilton Airport

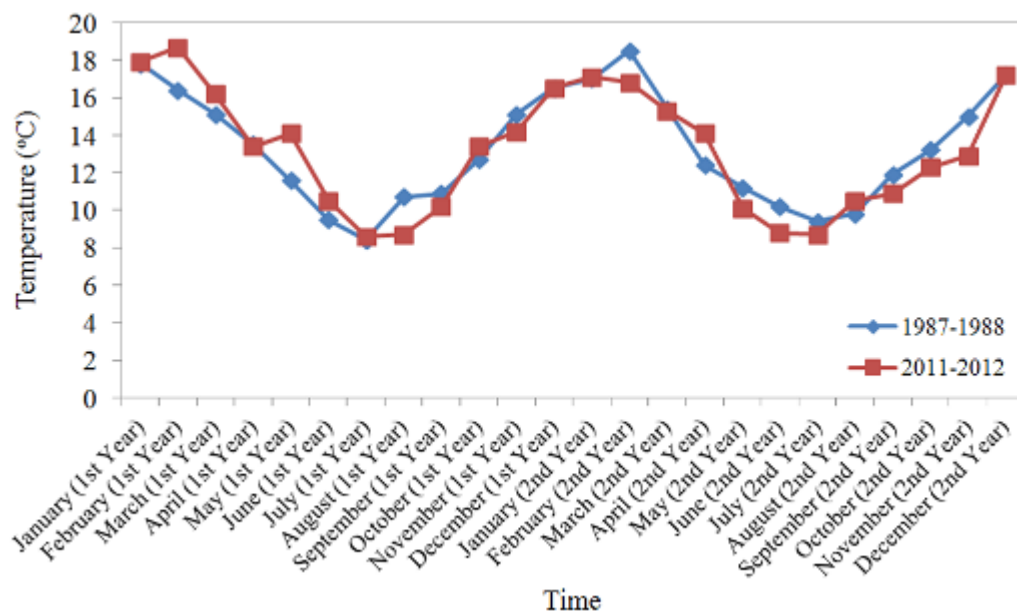


Figure A44. Comparison of ambient temperatures in the periods of 1987 – 1988 and 2011 – 2012 for Levin

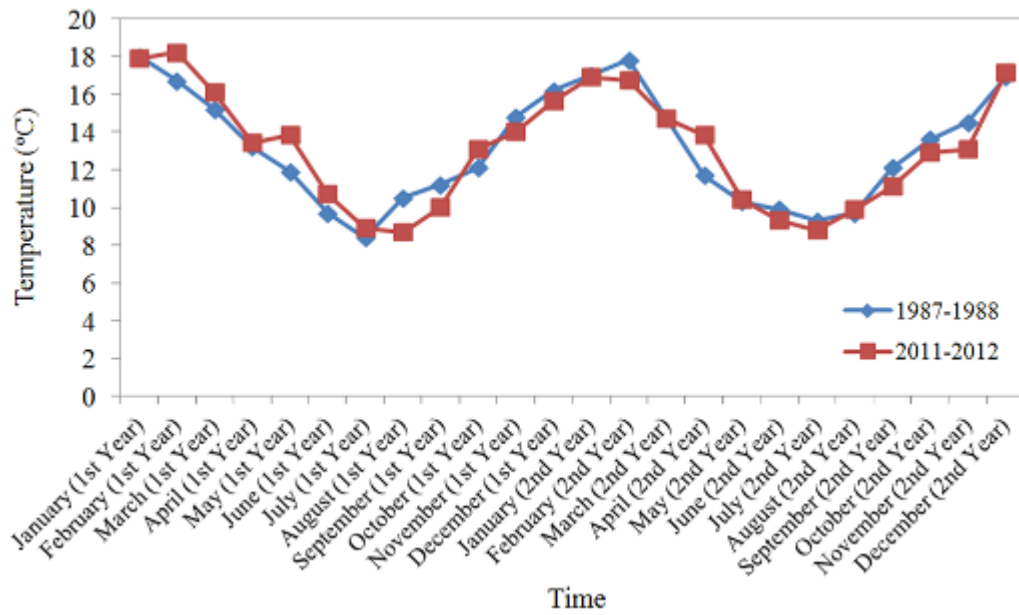


Figure A45. Comparison of ambient temperatures in the periods of 1987 – 1988 and 2011 – 2012 for Paraparaumu Airport

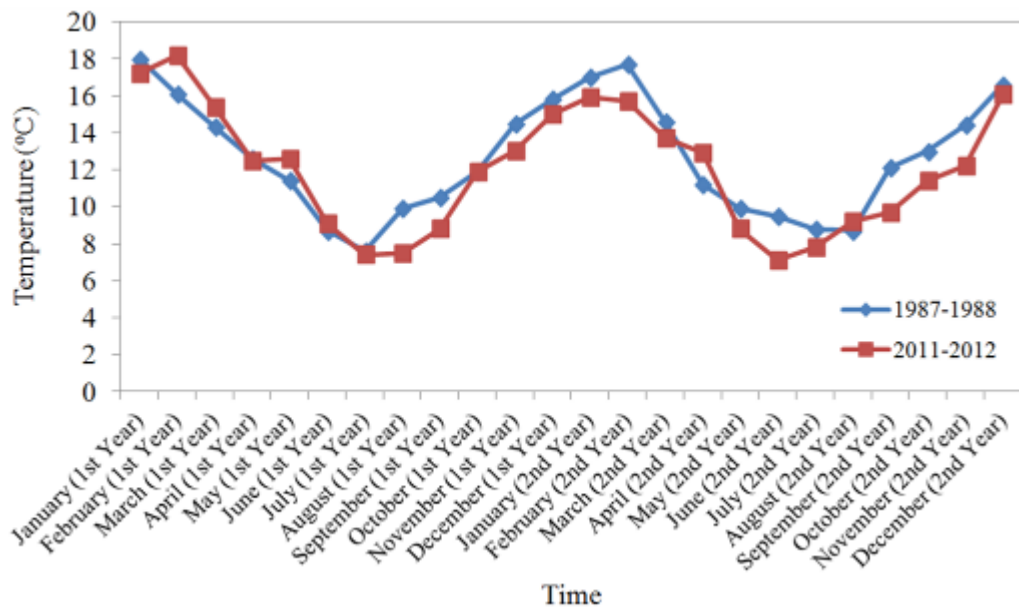


Figure A46. Comparison of ambient temperatures in the periods of 1987 – 1988 and 2011 – 2012 for Wallaceville

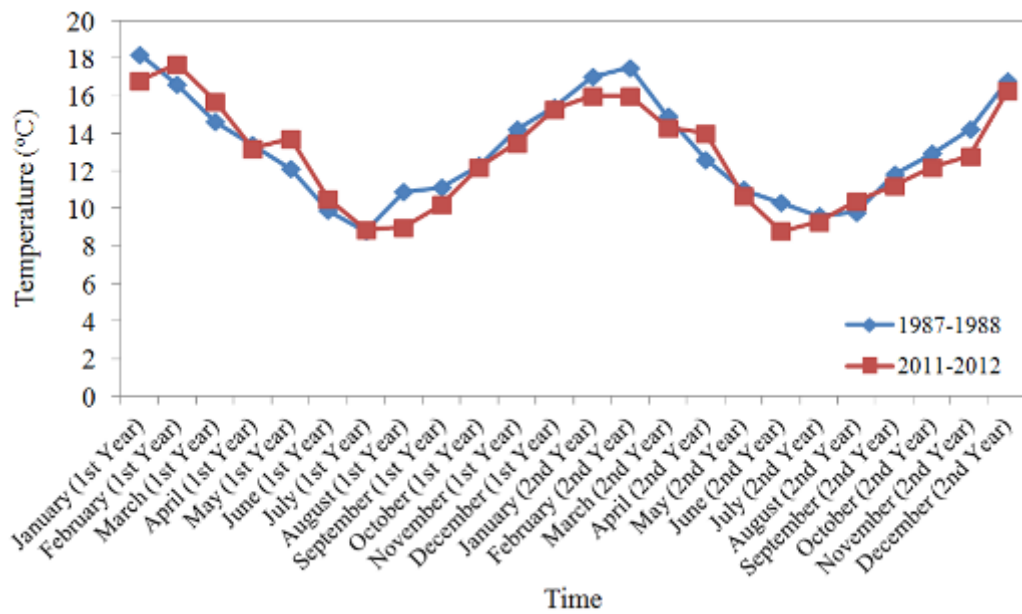


Figure A47. Comparison of ambient temperatures in the periods of 1987 – 1988 and 2011 – 2012 for Kelburn (Wellington)

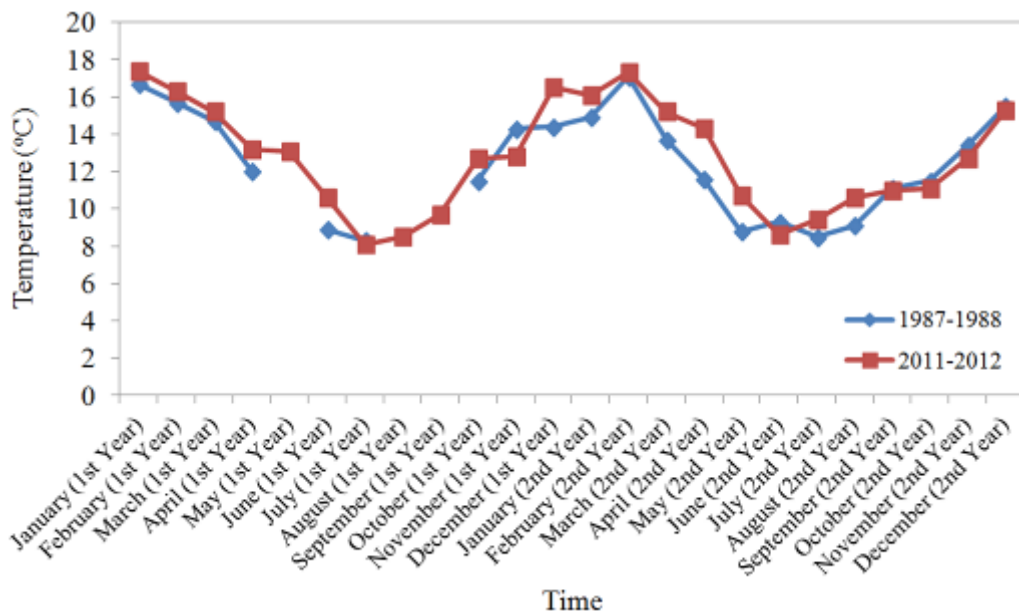


Figure A48. Comparison of ambient temperatures in the periods of 1987 – 1988 and 2011 – 2012 for Greymouth

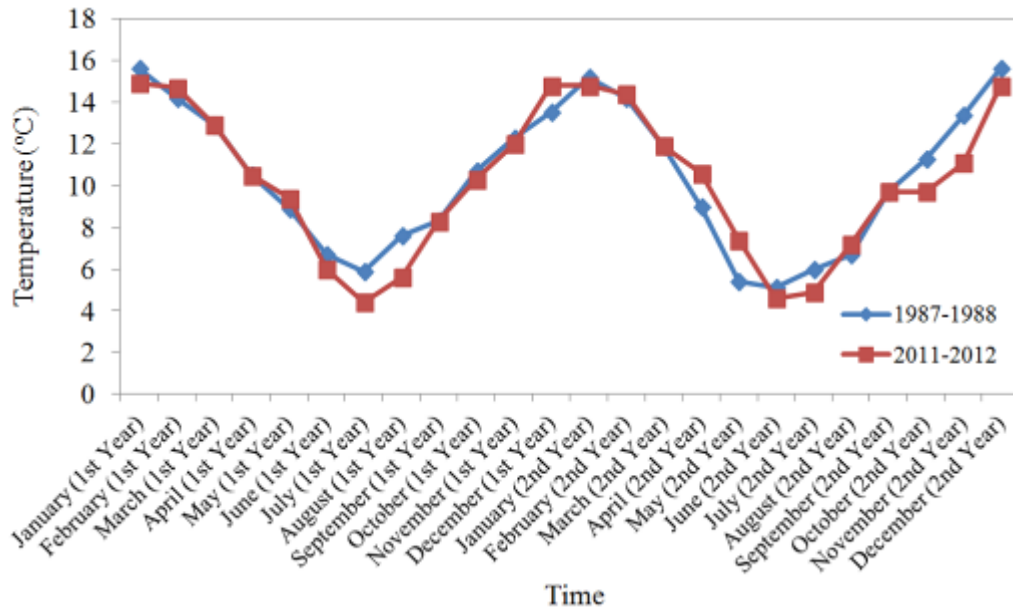


Figure A49. Comparison of ambient temperatures in the periods of 1987 – 1988 and 2011 – 2012 for Dunedin Airport

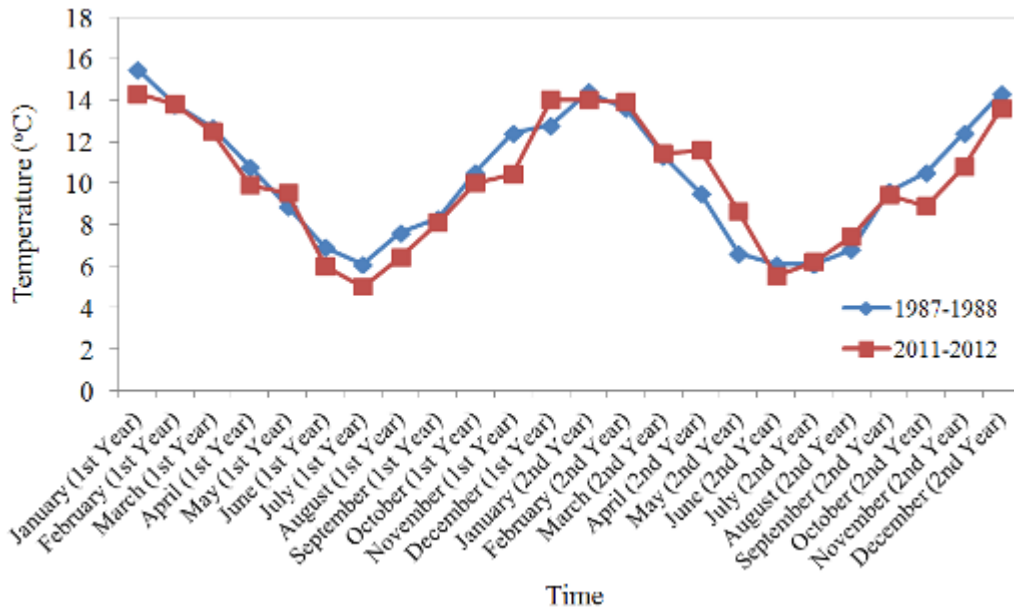


Figure A50. Comparison of ambient temperatures in the periods of 1987 – 1988 and 2011 – 2012 for Invercargill Airport

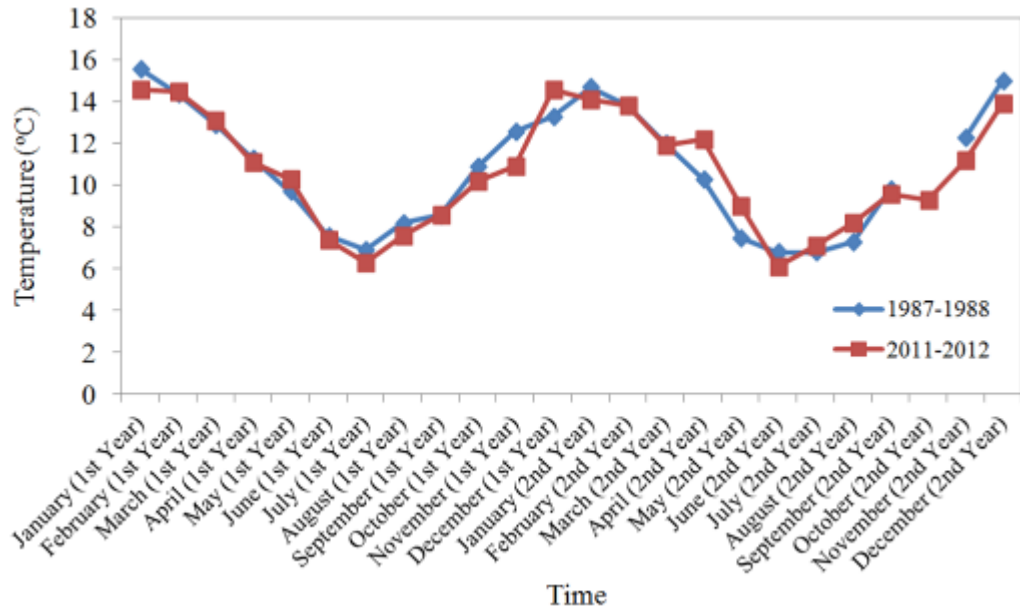


Figure A51. Comparison of ambient temperatures in the periods of 1987 – 1988 and 2011 – 2012 for Tiwai Point

A.2.2 Rainfall and Wet Days

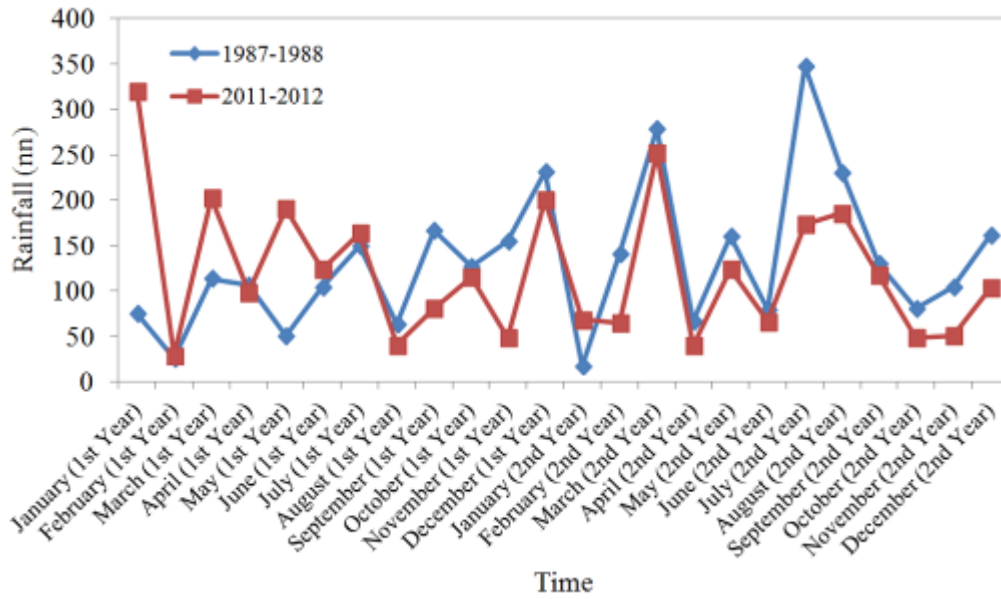


Figure A52. Comparison of rainfall in the periods of 1987 – 1988 and 2011 – 2012 for Warkworth

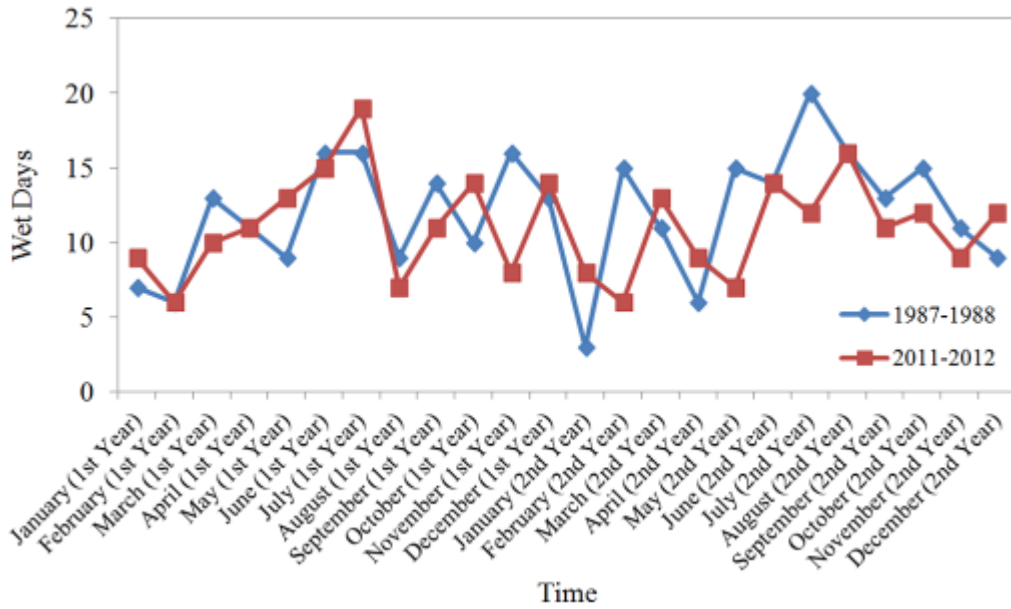


Figure A53. Comparison of wet days in the periods of 1987 – 1988 and 2011 – 2012 for Warkworth

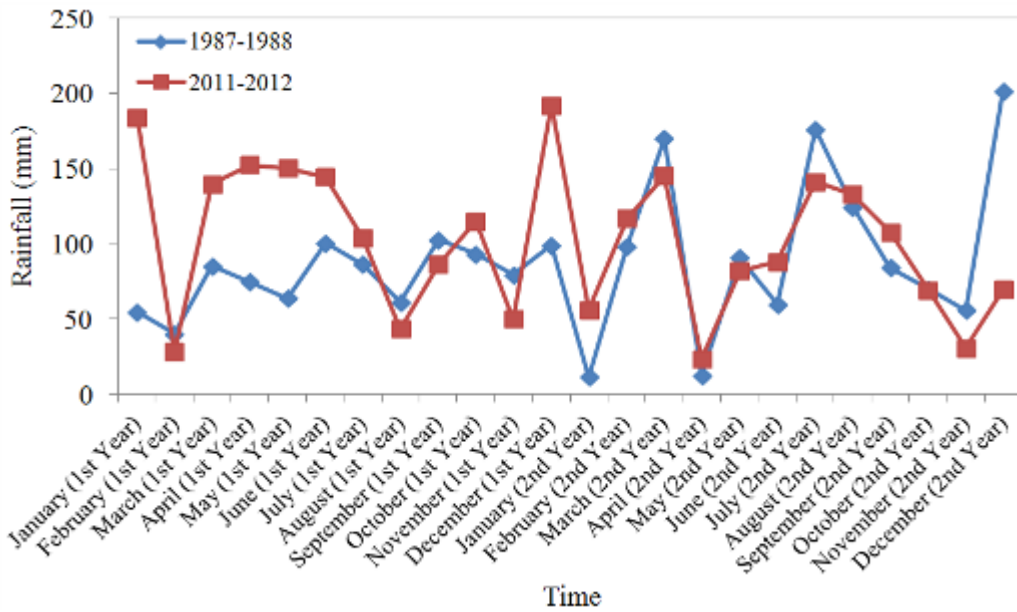


Figure A54. Comparison of rainfall in the periods of 1987 – 1988 and 2011 – 2012 for Auckland Airport

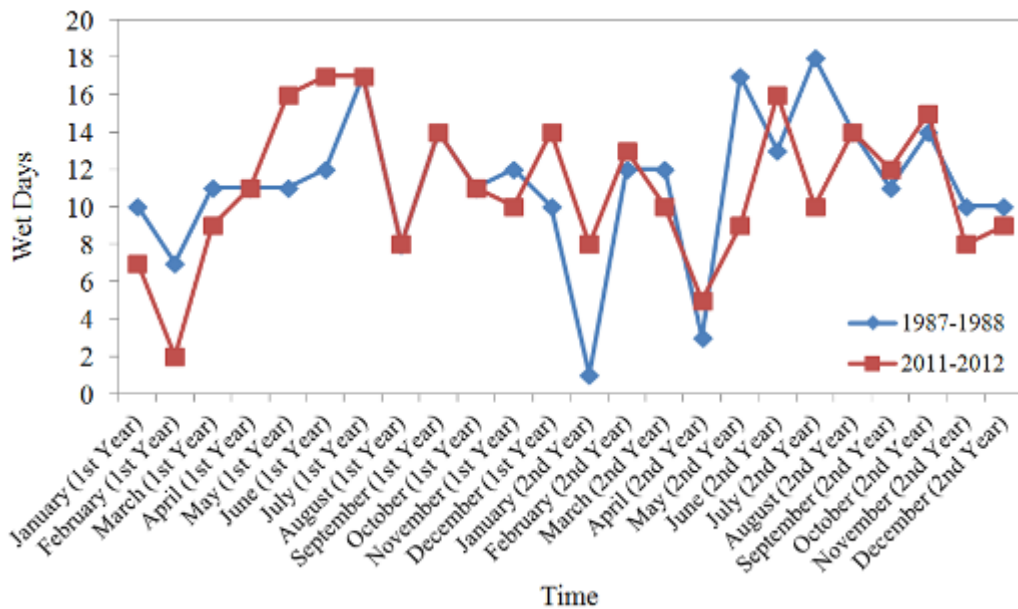


Figure A55. Comparison of wet days in the periods of 1987 – 1988 and 2011 – 2012 for Auckland Airport

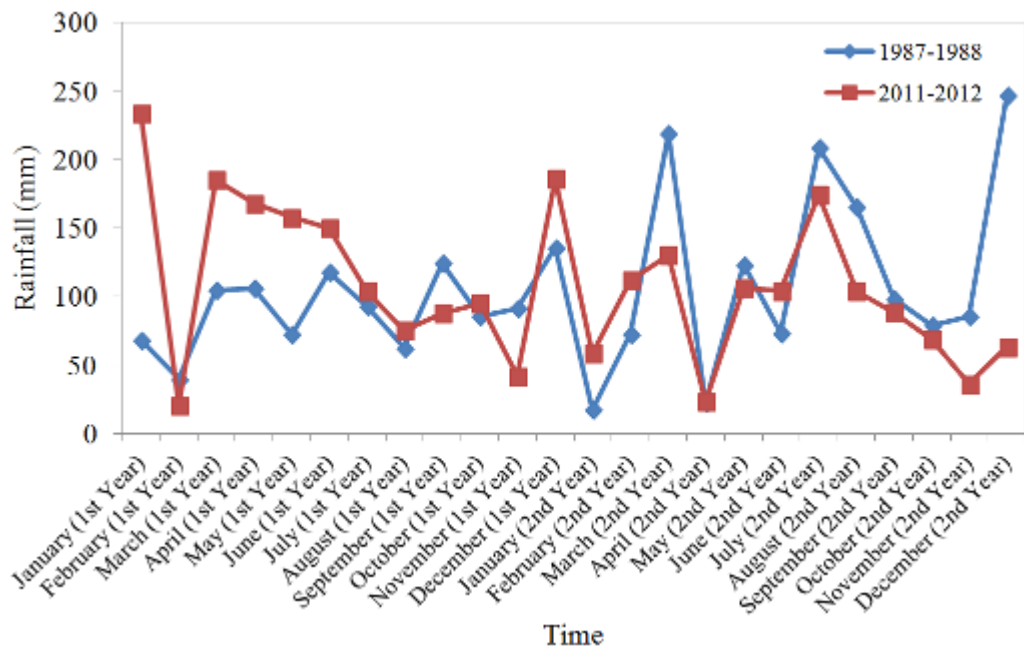


Figure A56. Comparison of rainfall in the periods of 1987 – 1988 and 2011 – 2012 for Ardmore

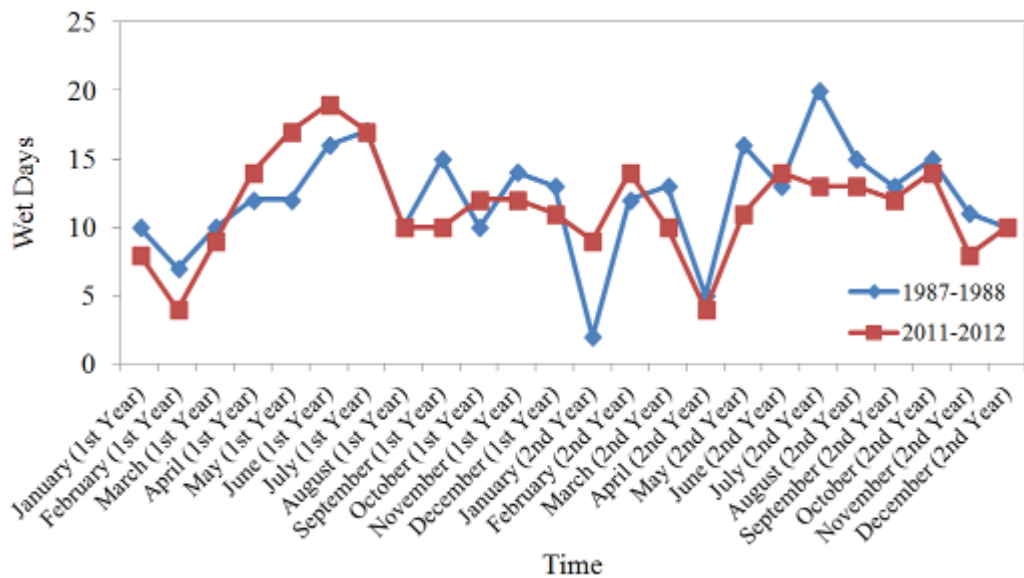


Figure A57. Comparison of wet days in the periods of 1987 – 1988 and 2011 – 2012 for Ardmore

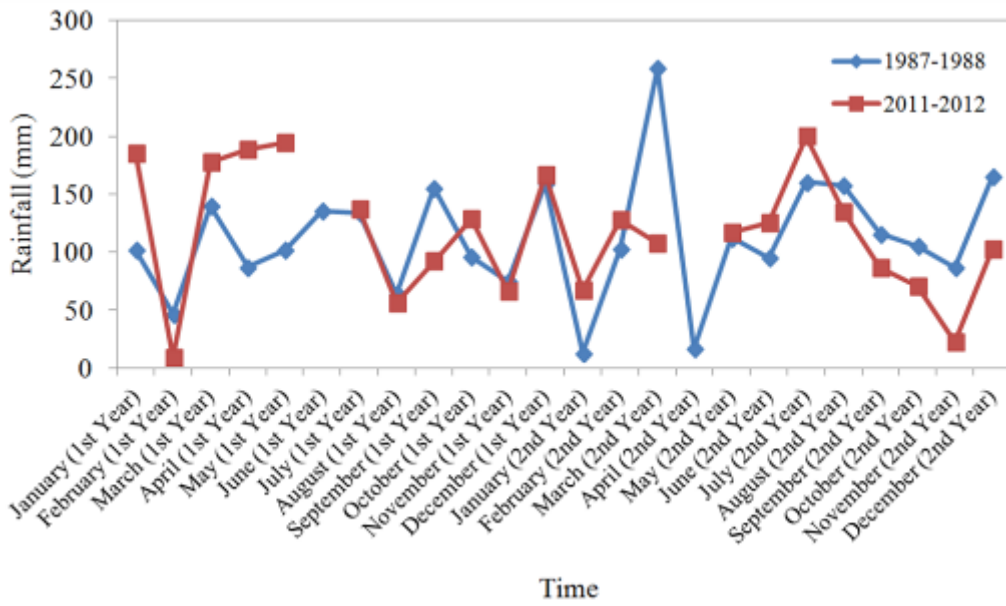


Figure A58. Comparison of rainfall in the periods of 1987 – 1988 and 2011 – 2012 for Pukekohe

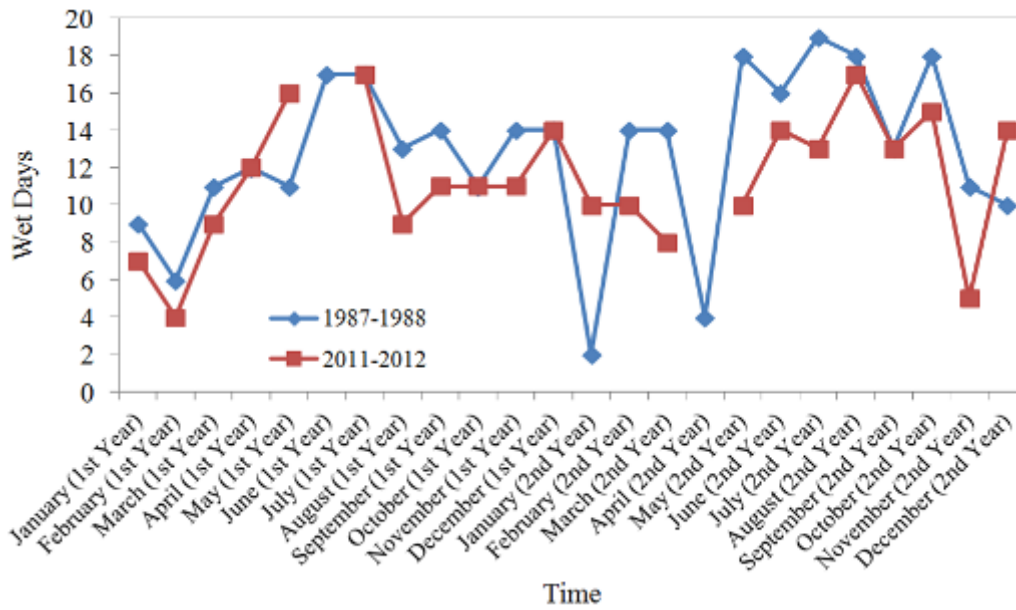


Figure A59. Comparison of wet days in the periods of 1987 – 1988 and 2011 – 2012 for Pukekohe

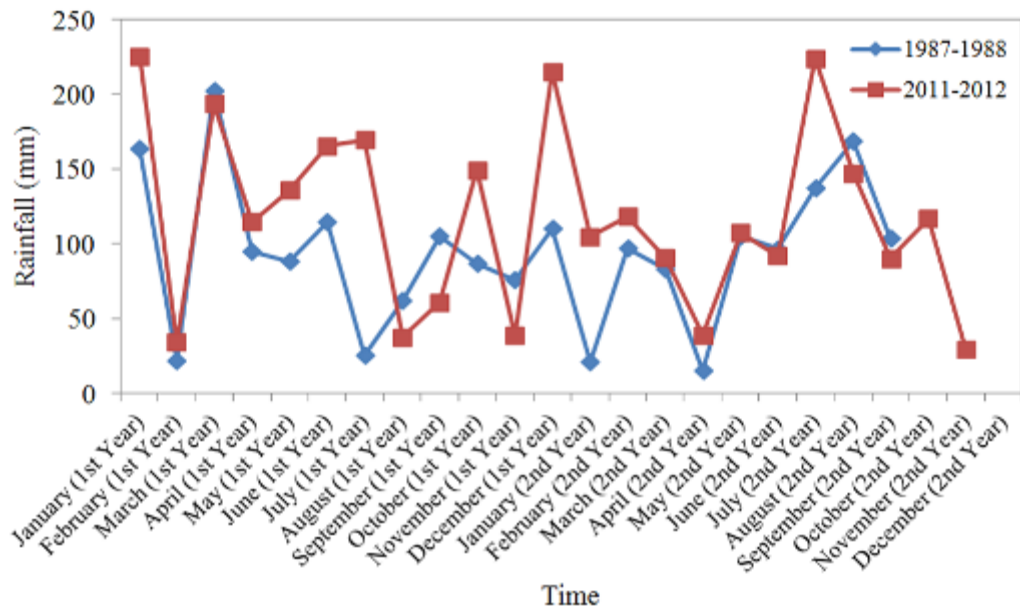


Figure A60. Comparison of rainfall in the periods of 1987 – 1988 and 2011 – 2012 for Hamilton Airport

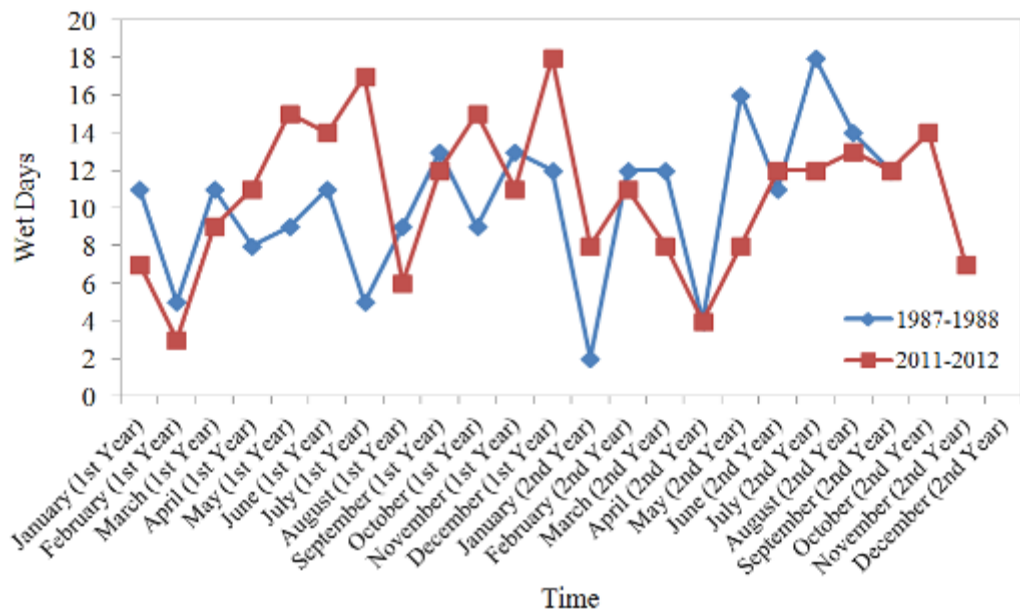


Figure A61. Comparison of wet days in the periods of 1987 – 1988 and 2011 – 2012 for Hamilton Airport

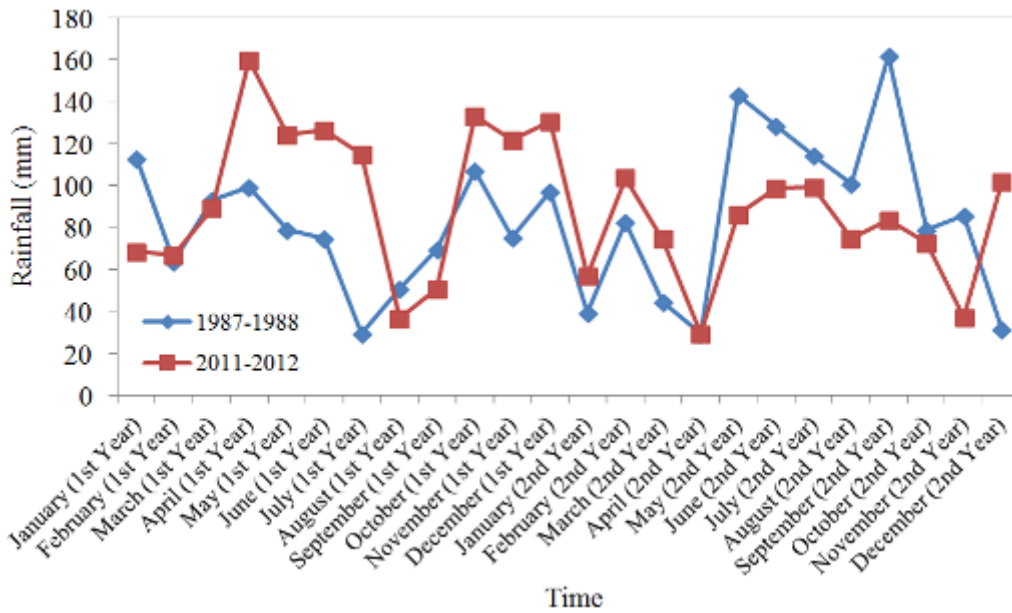


Figure A62. Comparison of rainfall in the periods of 1987 – 1988 and 2011 – 2012 for Levin

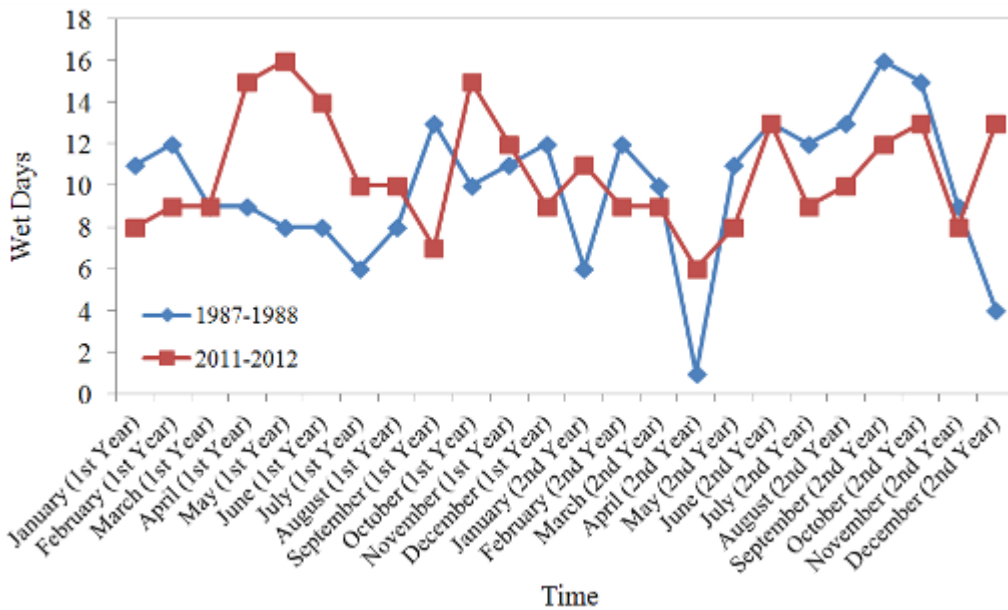


Figure A63. Comparison of wet days in the periods of 1987 – 1988 and 2011 – 2012 for Levin

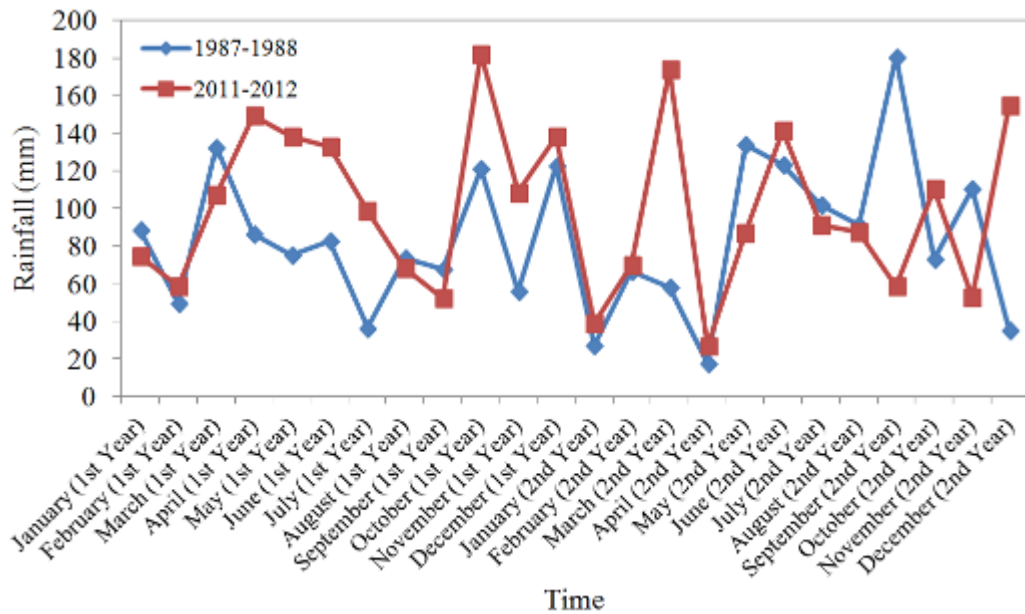


Figure A64. Comparison of rainfall in the periods of 1987 – 1988 and 2011 – 2012 for Waikanae

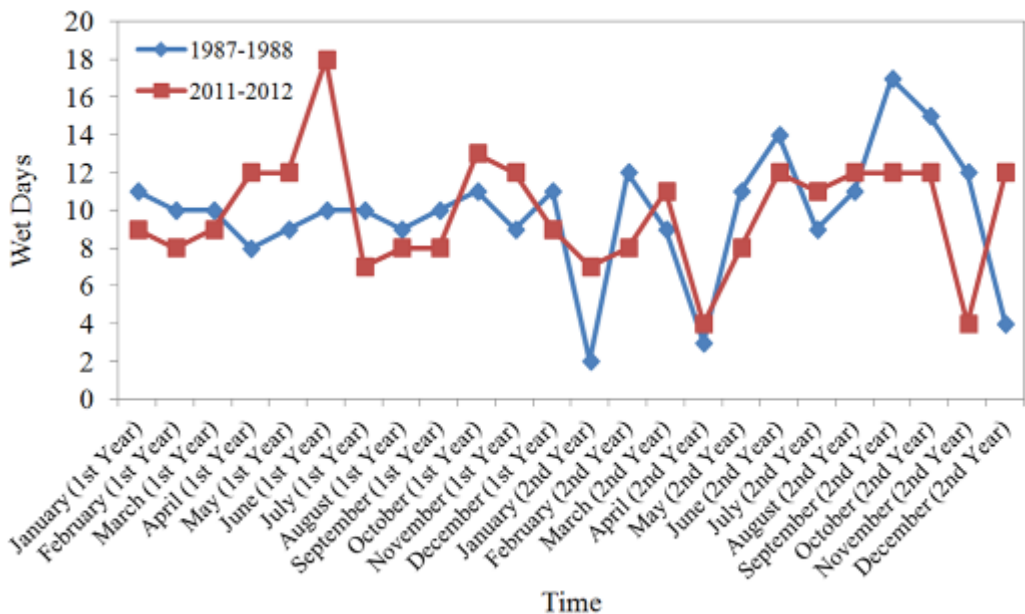


Figure A65. Comparison of wet days in the periods of 1987 – 1988 and 2011 – 2012 for Waikanae

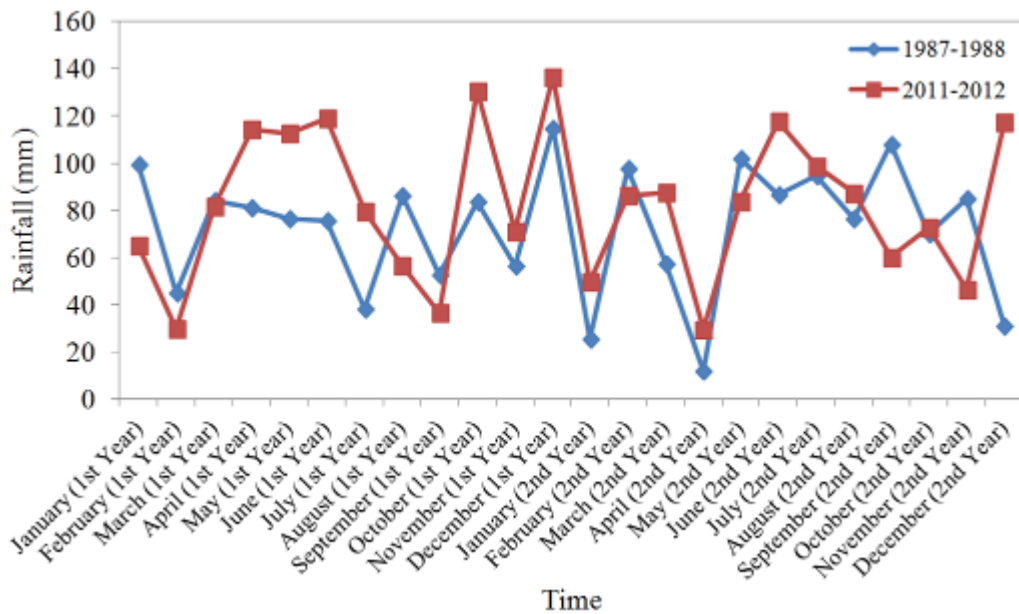


Figure A66. Comparison of rainfall in the periods of 1987 – 1988 and 2011 – 2012 for Paraparaumu Airport

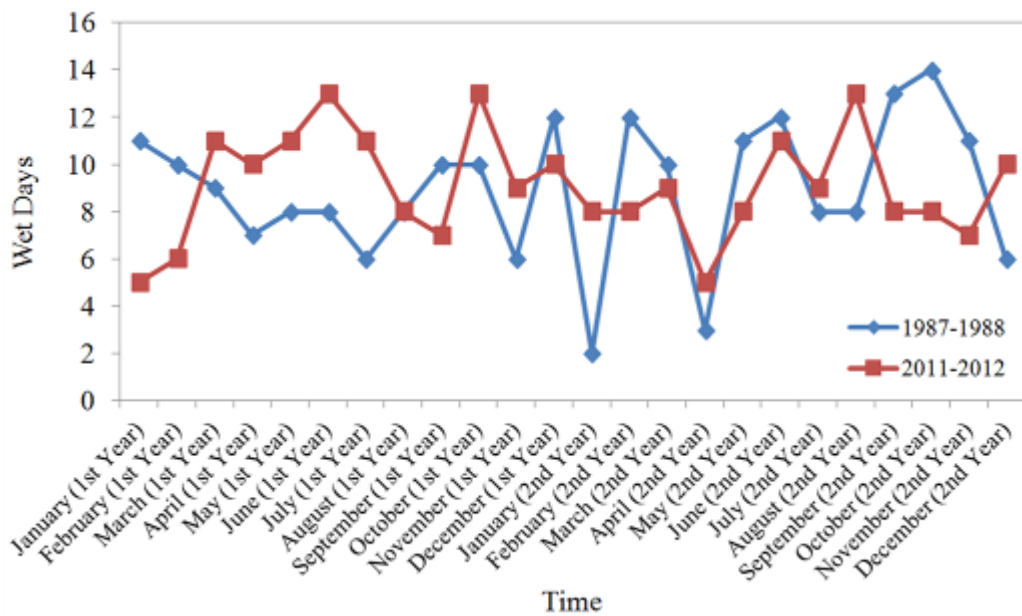


Figure A67. Comparison of wet days in the periods of 1987 – 1988 and 2011 – 2012 for Paraparaumu Airport

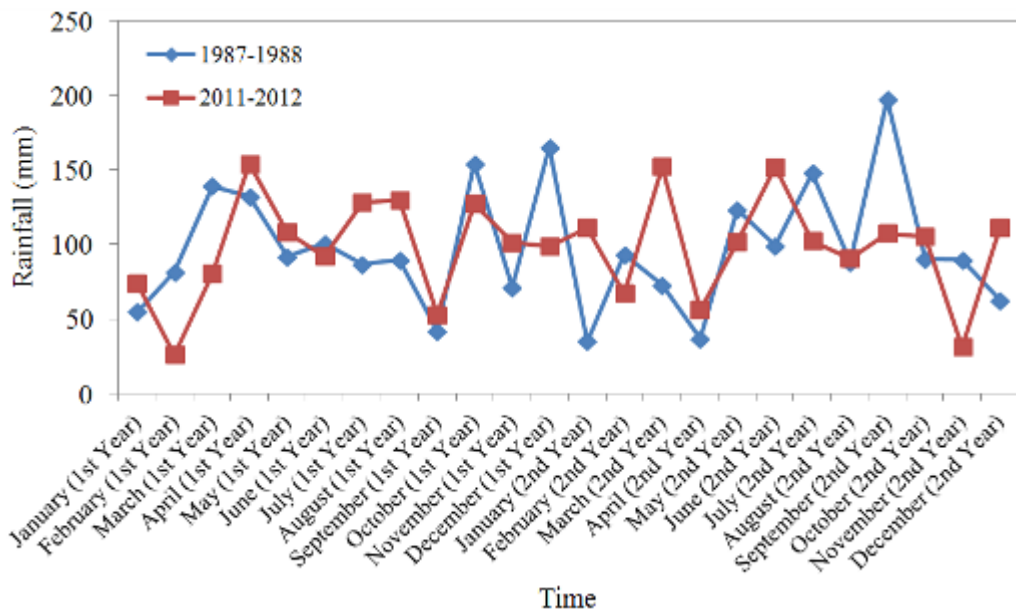


Figure A68. Comparison of rainfall in the periods of 1987 – 1988 and 2011 – 2012 for Wallaceville

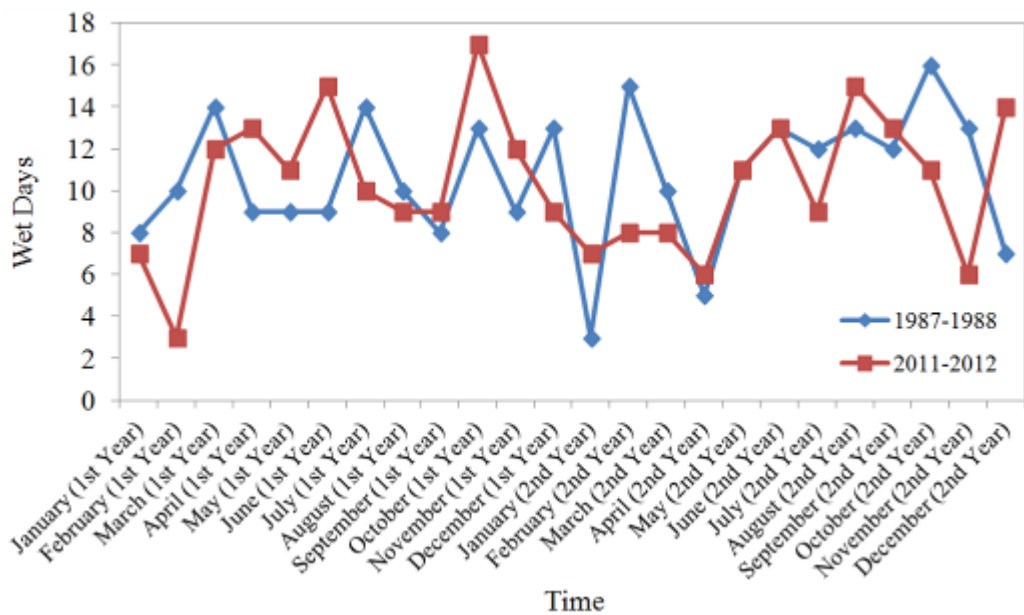


Figure A69. Comparison of wet days in the periods of 1987 – 1988 and 2011 – 2012 for Wallaceville

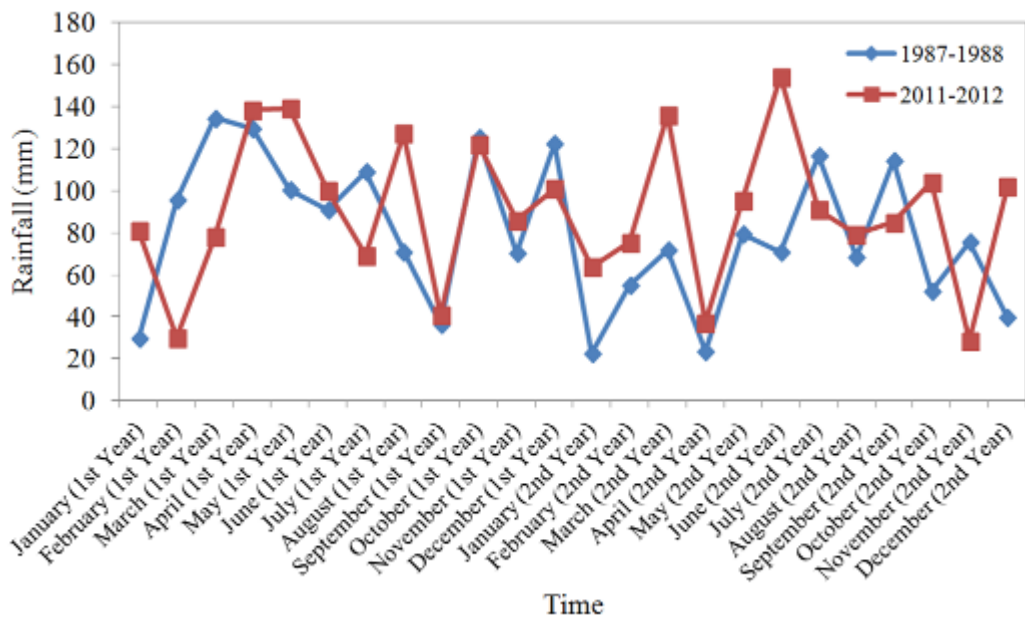


Figure A70. Comparison of rainfall in the periods of 1987 – 1988 and 2011 – 2012 for Judgeford (BRANZ)

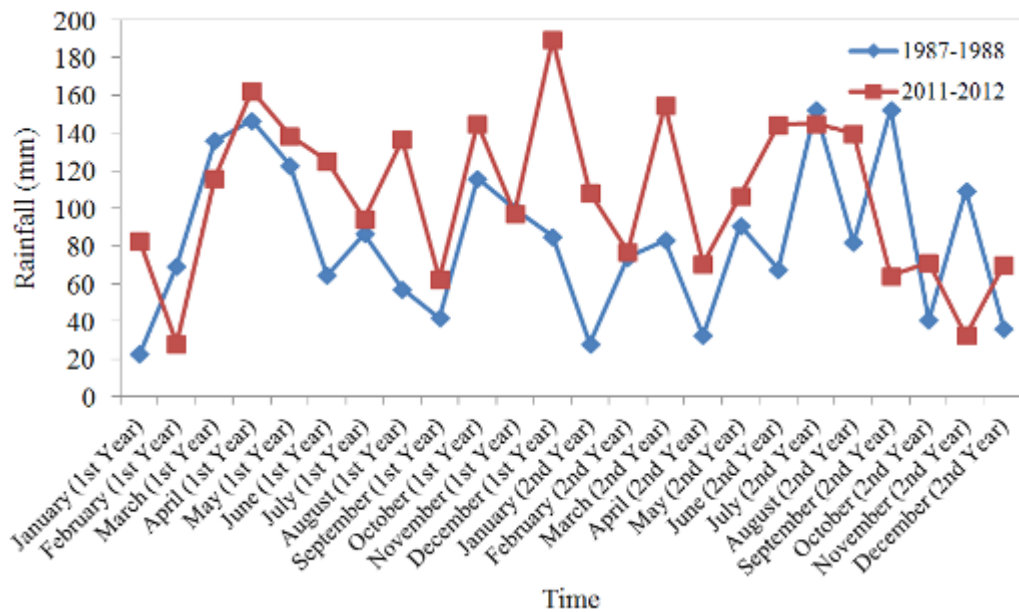


Figure A71. Comparison of rainfall in the periods of 1987 – 1988 and 2011 – 2012 for Kelburn (Wellington)

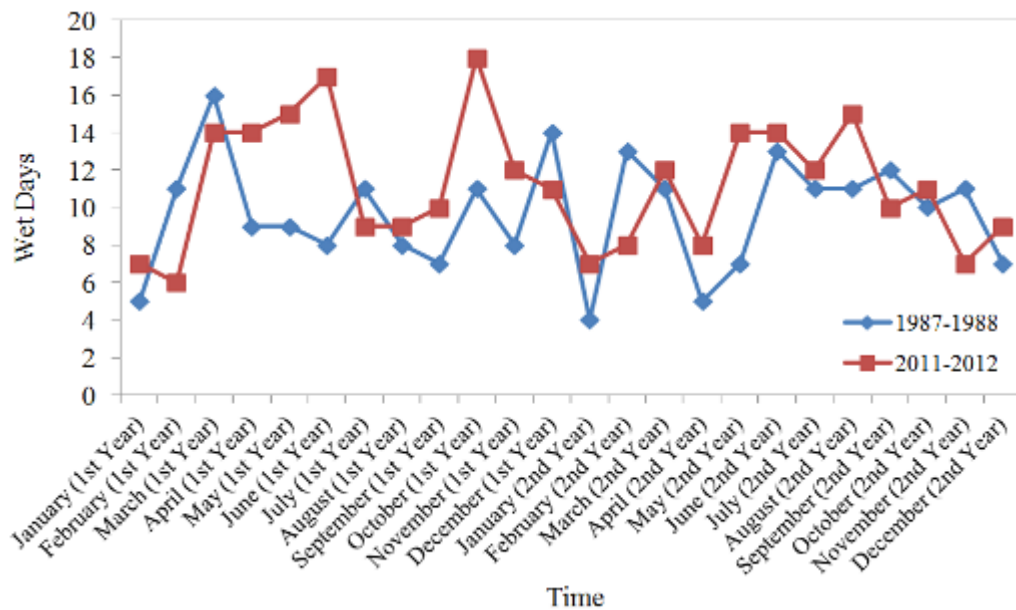


Figure A72. Comparison of wet days in the periods of 1987 – 1988 and 2011 – 2012 for Kelburn (Wellington)

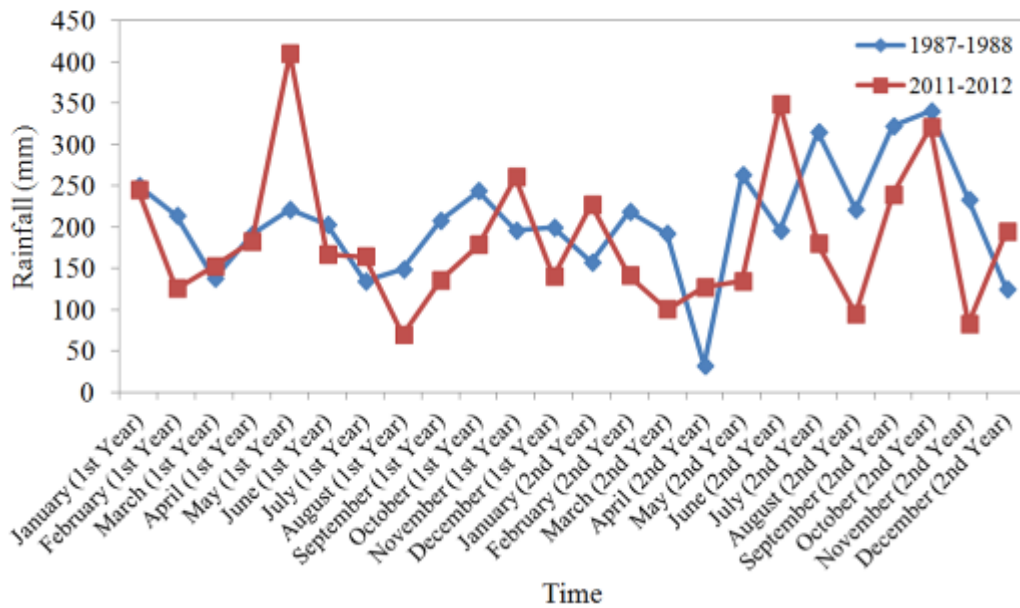


Figure A73. Comparison of rainfall in the periods of 1987 – 1988 and 2011 – 2012 for Greymouth

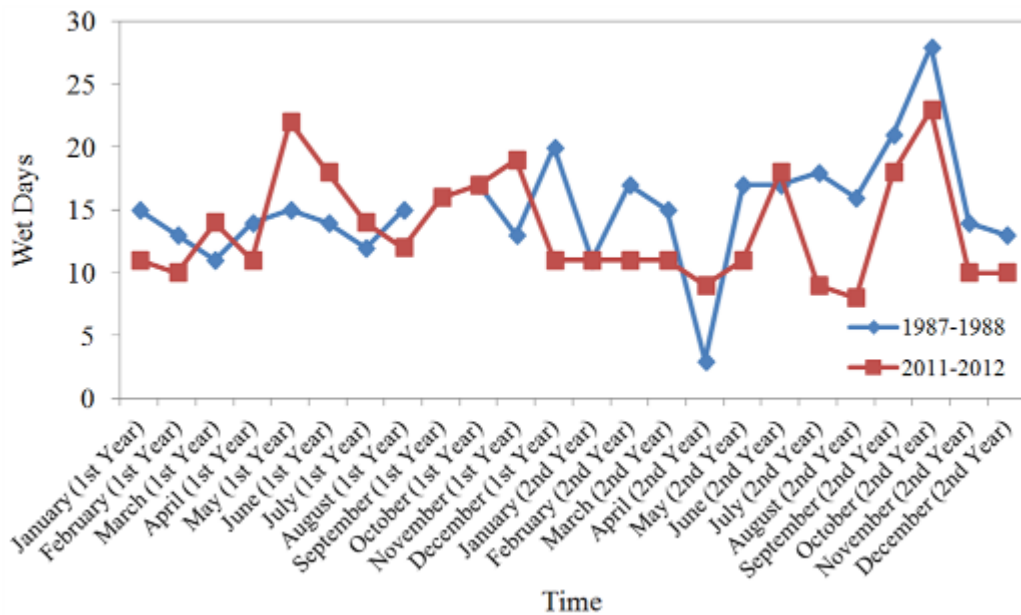


Figure A74. Comparison of wet days in the periods of 1987 – 1988 and 2011 – 2012 for Greymouth

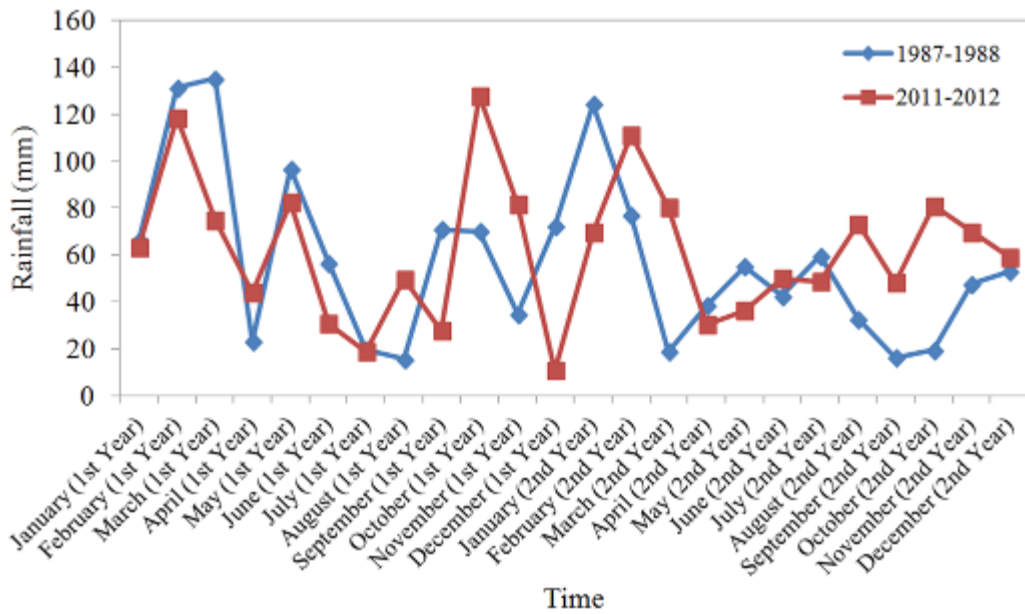


Figure A75. Comparison of rainfall in the periods of 1987 – 1988 and 2011 – 2012 for Mosgiel

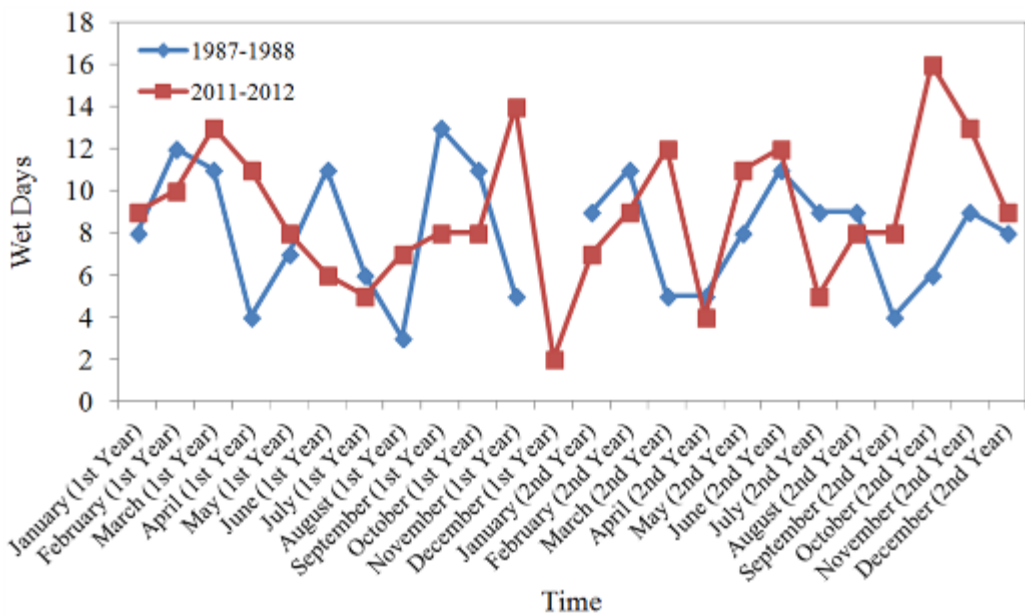


Figure A76. Comparison of wet days in the periods of 1987 – 1988 and 2011 – 2012 for Mosgiel

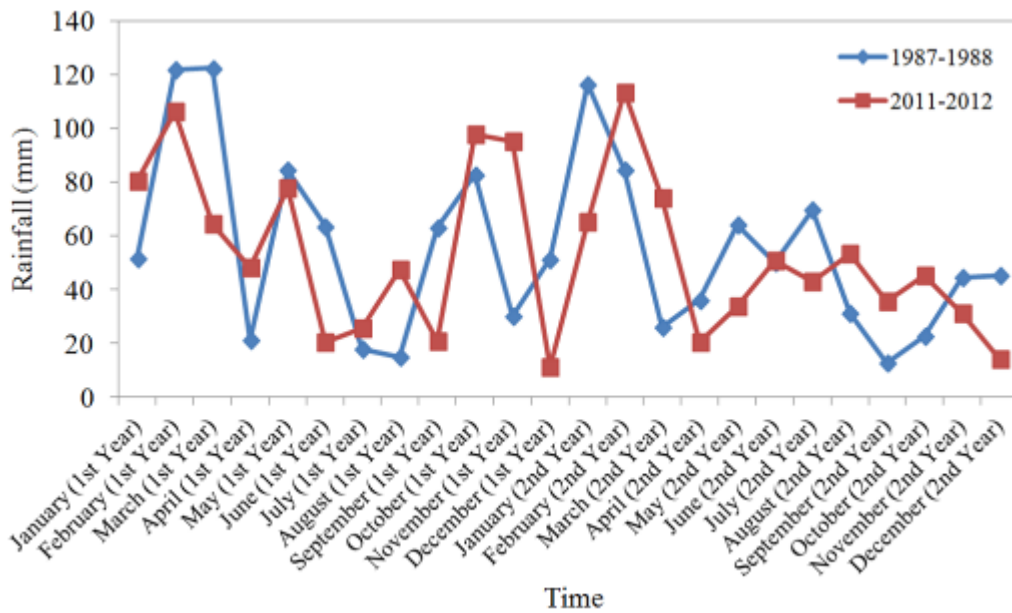


Figure A77. Comparison of rainfall in the periods of 1987 – 1988 and 2011 – 2012 for Dunedin Airport

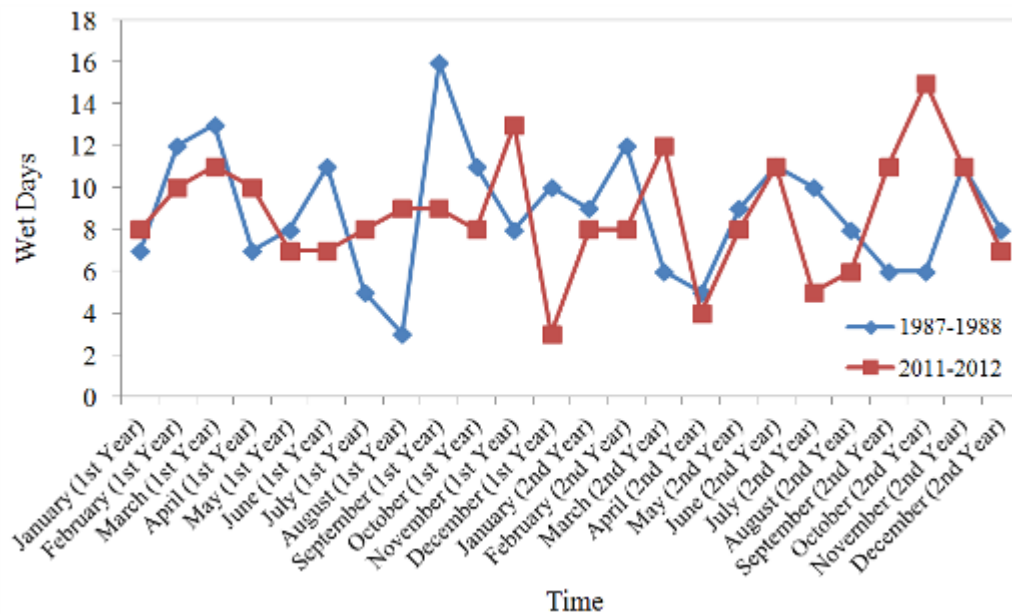


Figure A78. Comparison of wet days in the periods of 1987 – 1988 and 2011 – 2012 for Dunedin Airport

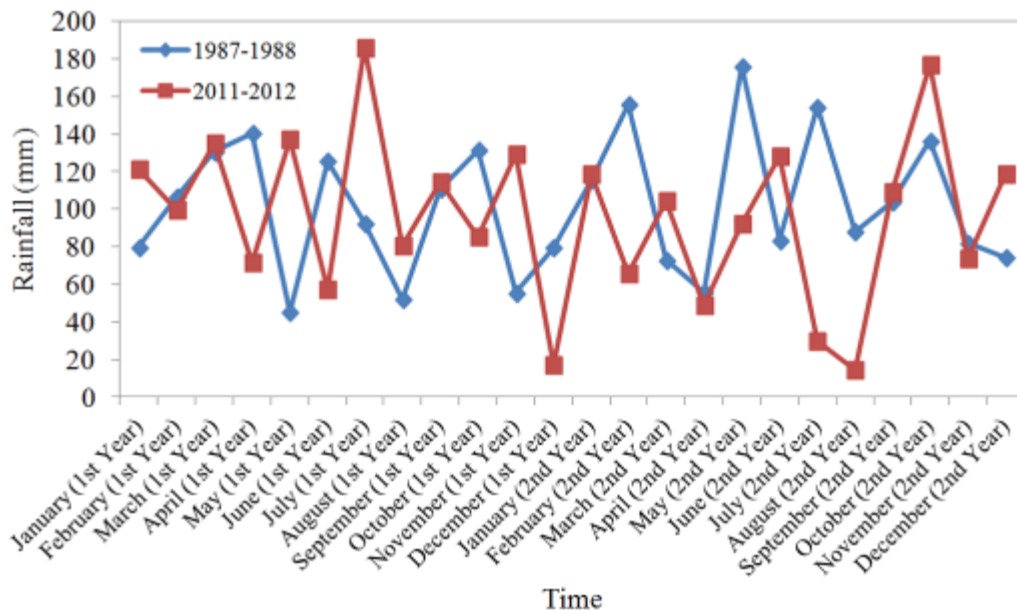


Figure A79. Comparison of rainfall in the periods of 1987 – 1988 and 2011 – 2012 for Invercargill Airport

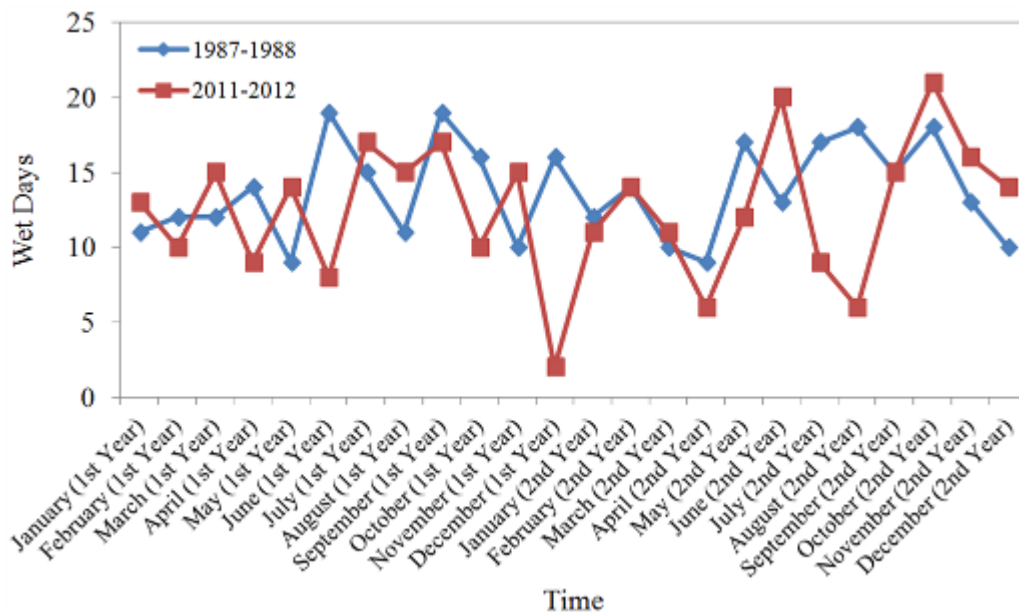


Figure A80. Comparison of wet days in the periods of 1987 – 1988 and 2011 – 2012 for Invercargill Airport

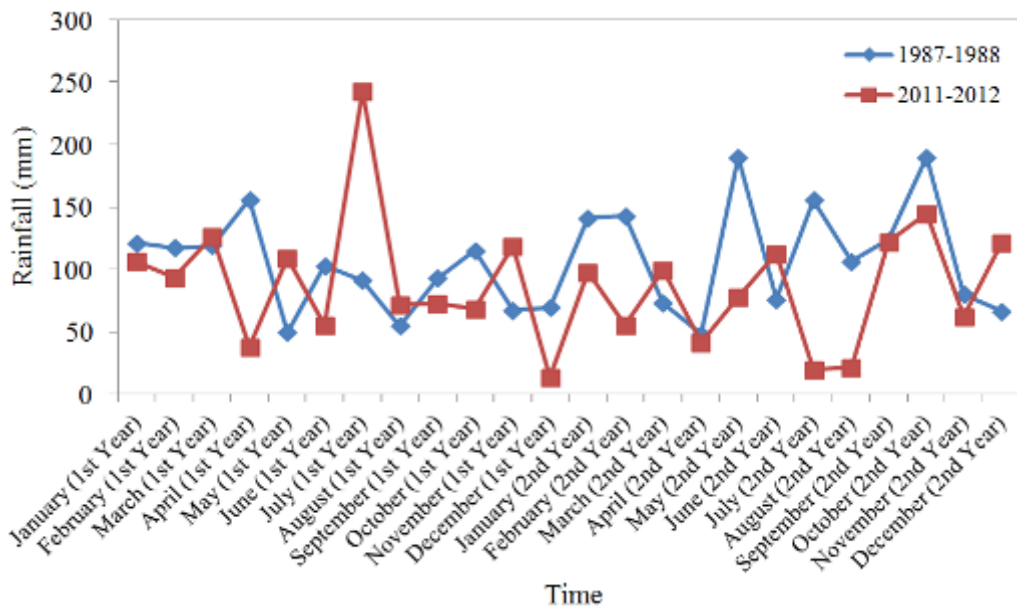


Figure A81. Comparison of rainfall in the periods of 1987 – 1988 and 2011 – 2012 for Tiwai Point

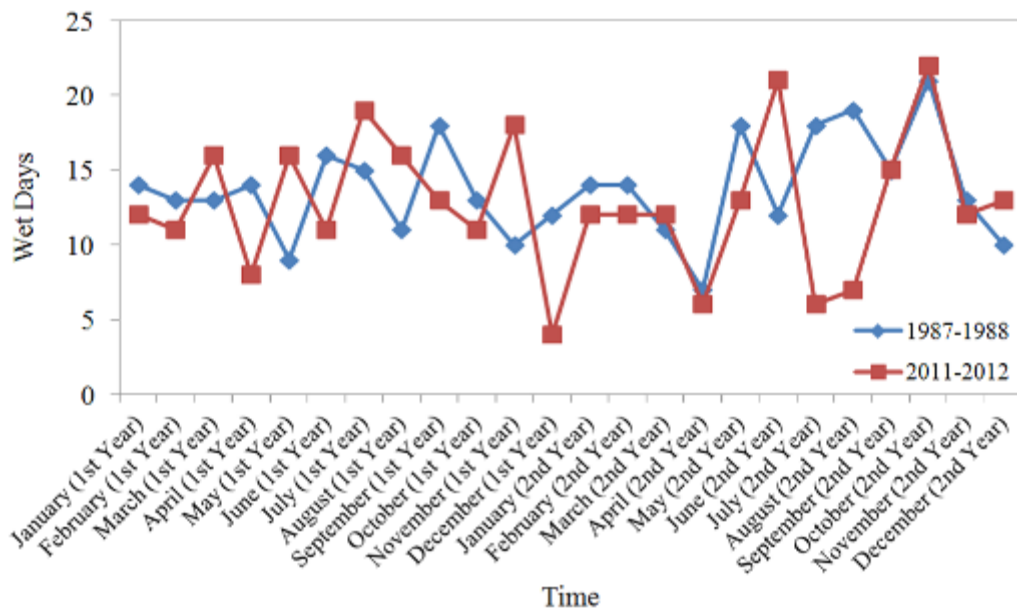


Figure A82. Comparison of wet days in the periods of 1987 – 1988 and 2011 – 2012 for Tiwai Point

A.2.3 Relative Humidity

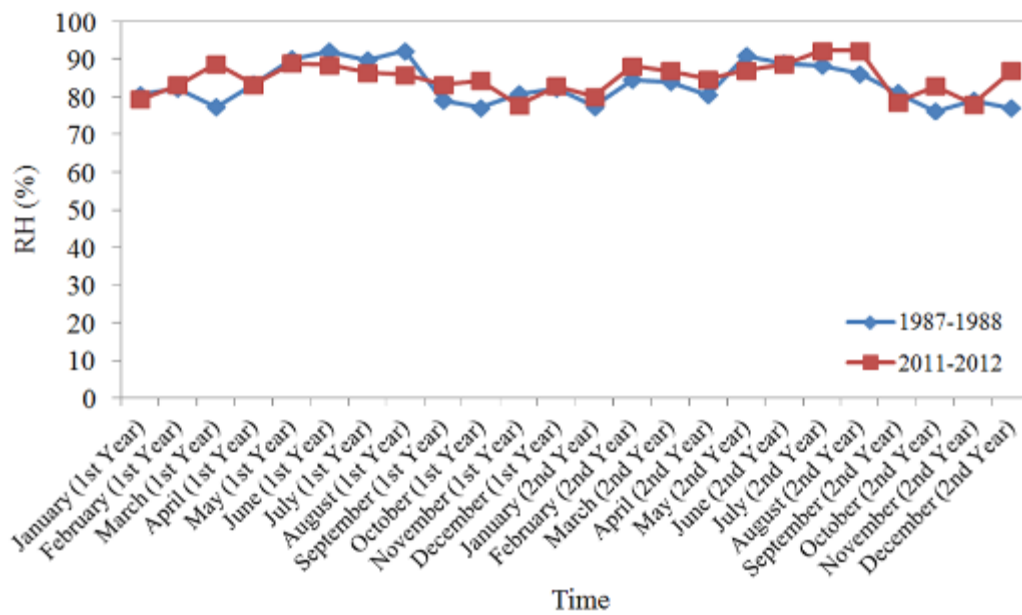


Figure A83. Comparison of relative humidity in the periods of 1987 – 1988 and 2011 – 2012 for Warkworth

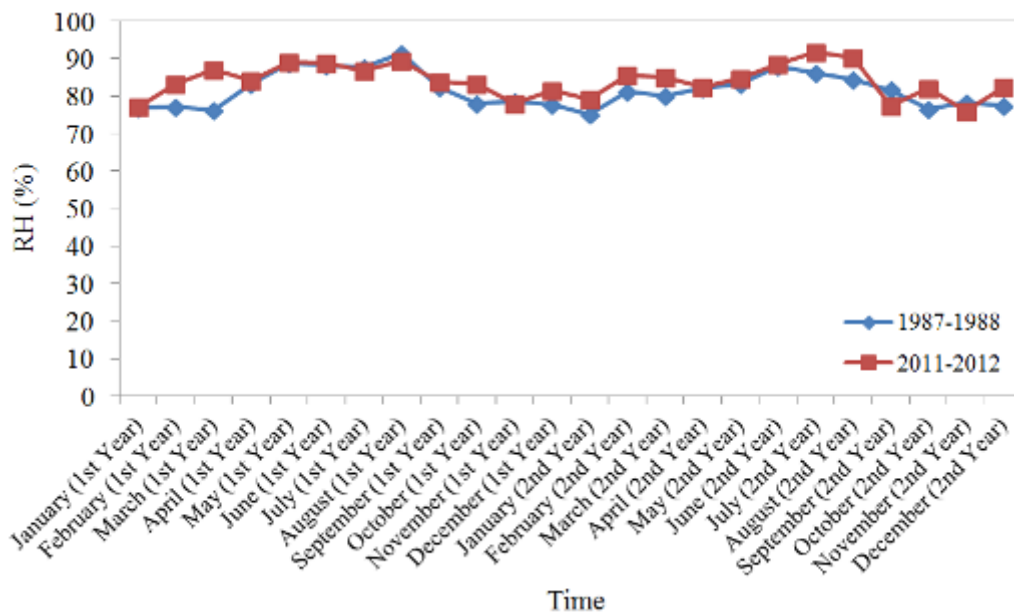


Figure A84. Comparison of relative humidity in the periods of 1987 – 1988 and 2011 – 2012 for Auckland Airport

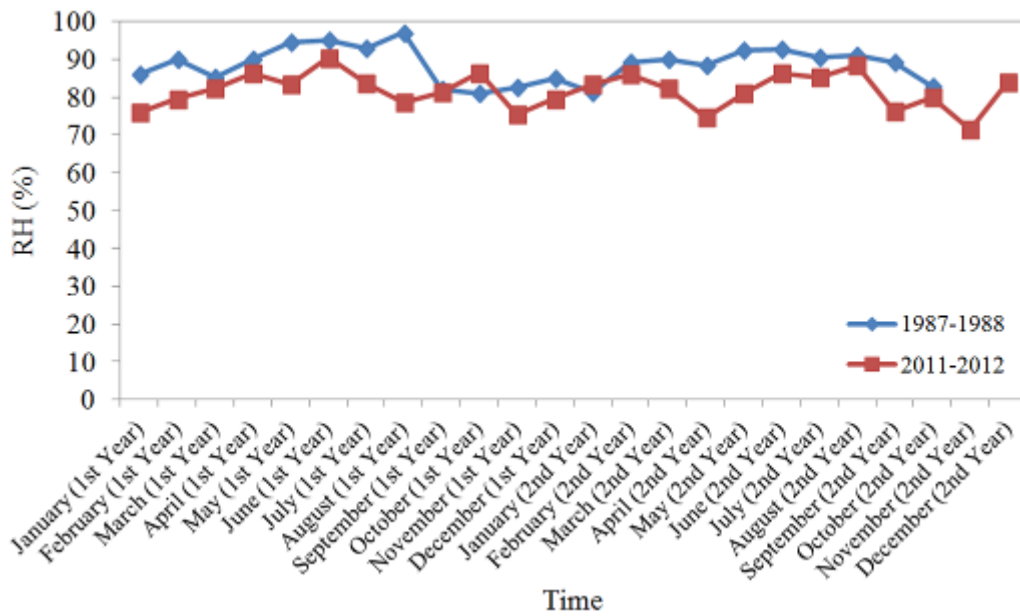


Figure A85. Comparison of relative humidity in the periods of 1987 – 1988 and 2011 – 2012 for Ardmore

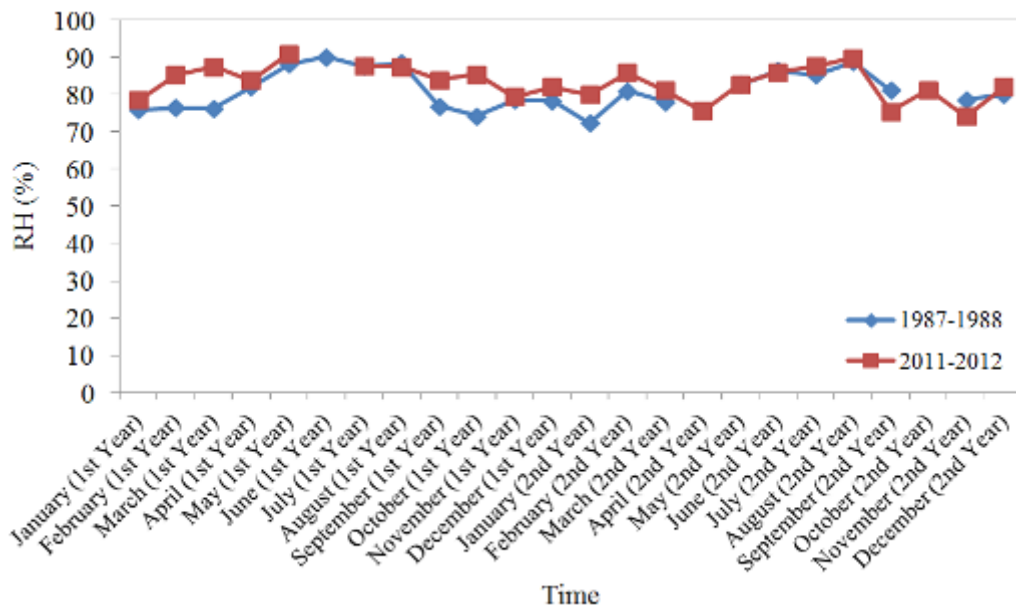


Figure A86. Comparison of relative humidity in the periods of 1987 – 1988 and 2011 – 2012 for Pukekohe

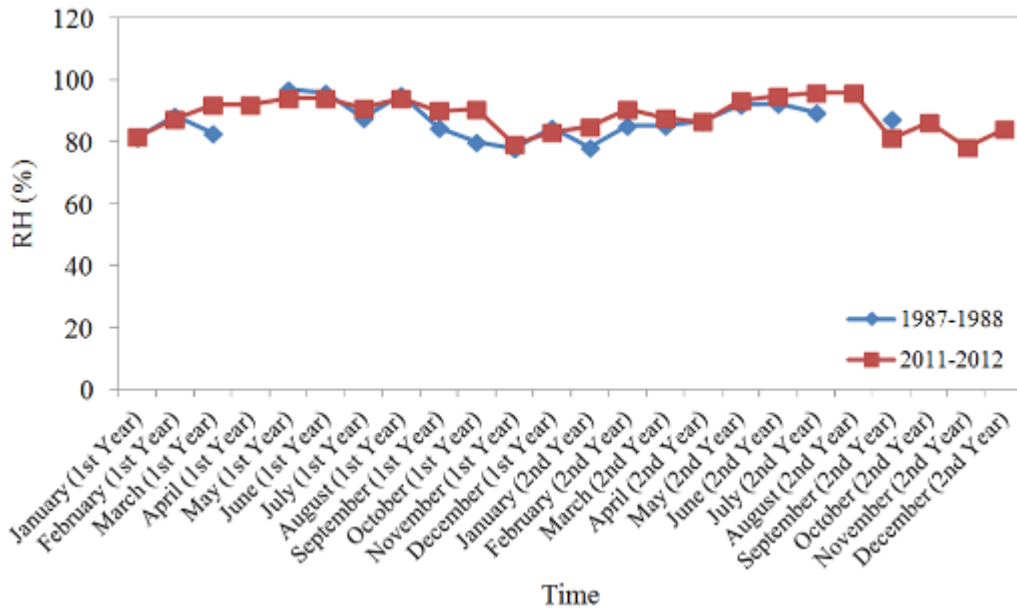


Figure A87. Comparison of relative humidity in the periods of 1987 – 1988 and 2011 – 2012 for Hamilton Airport

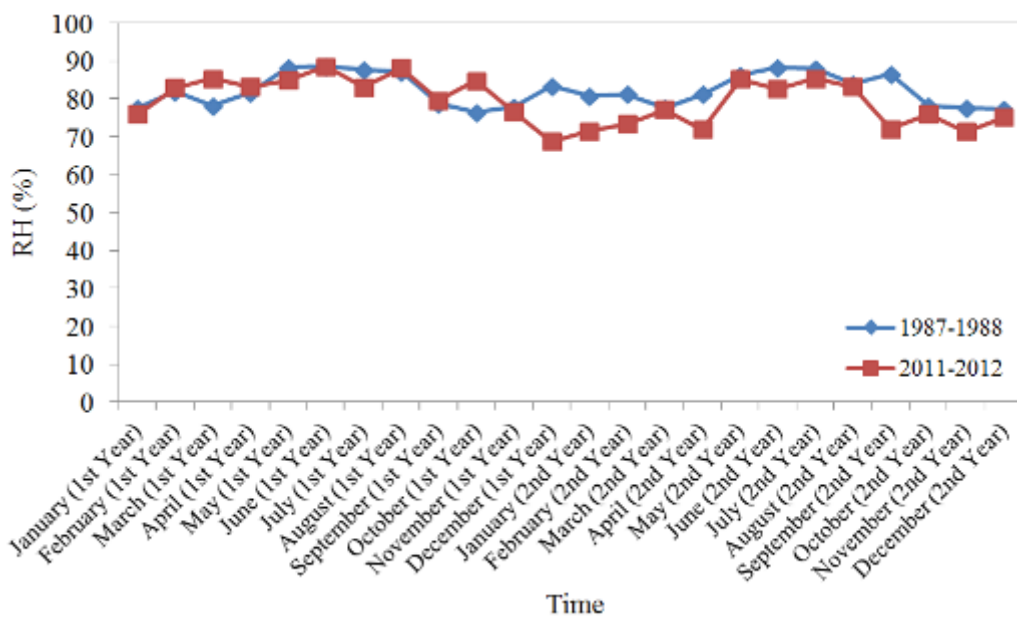


Figure A88. Comparison of relative humidity in the periods of 1987 – 1988 and 2011 – 2012 for Levin

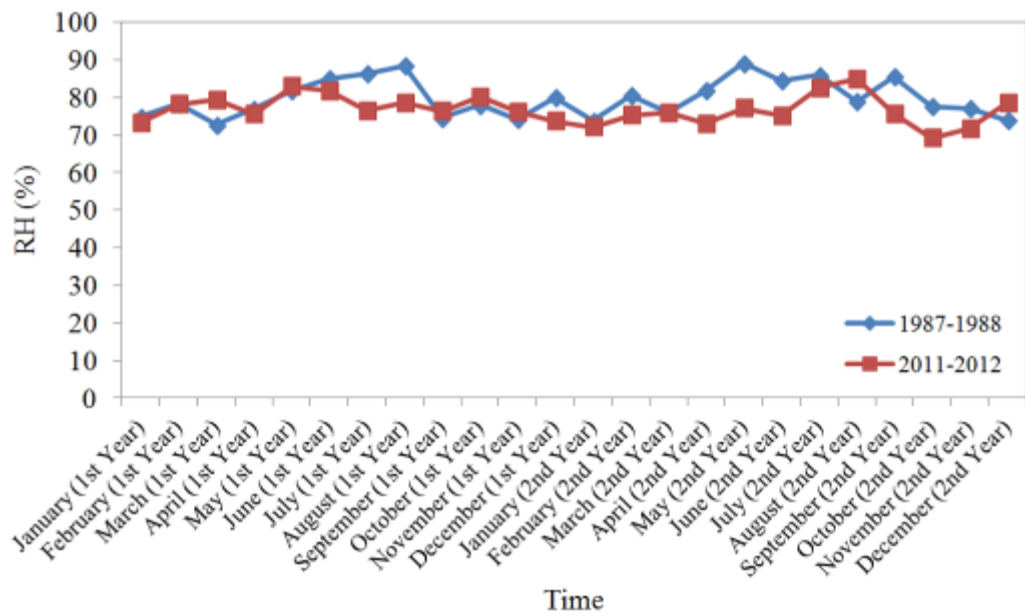


Figure A89. Comparison of relative humidity in the periods of 1987 – 1988 and 2011 – 2012 for Paraparaumu Airport

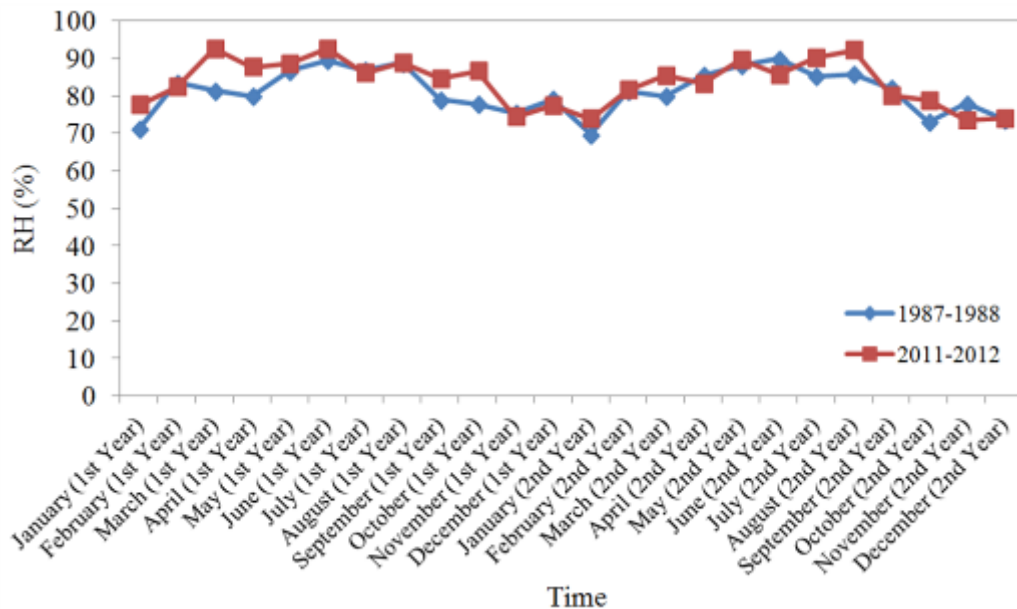


Figure A90. Comparison of relative humidity in the periods of 1987 – 1988 and 2011 – 2012 for Wallaceville

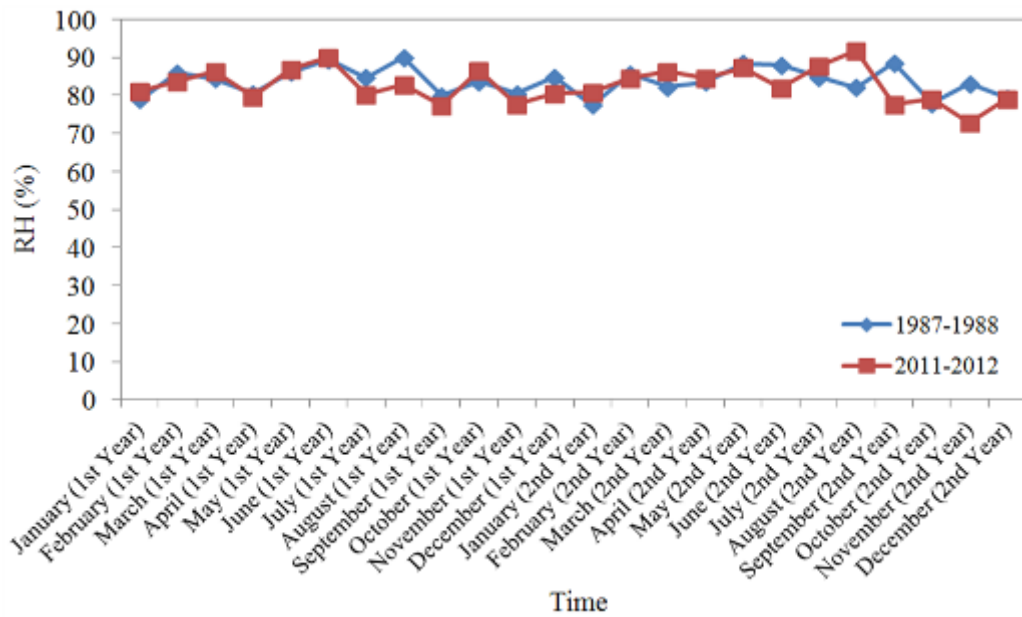


Figure A91. Comparison of relative humidity in the periods of 1987 – 1988 and 2011 – 2012 for Kelburn (Wellington)

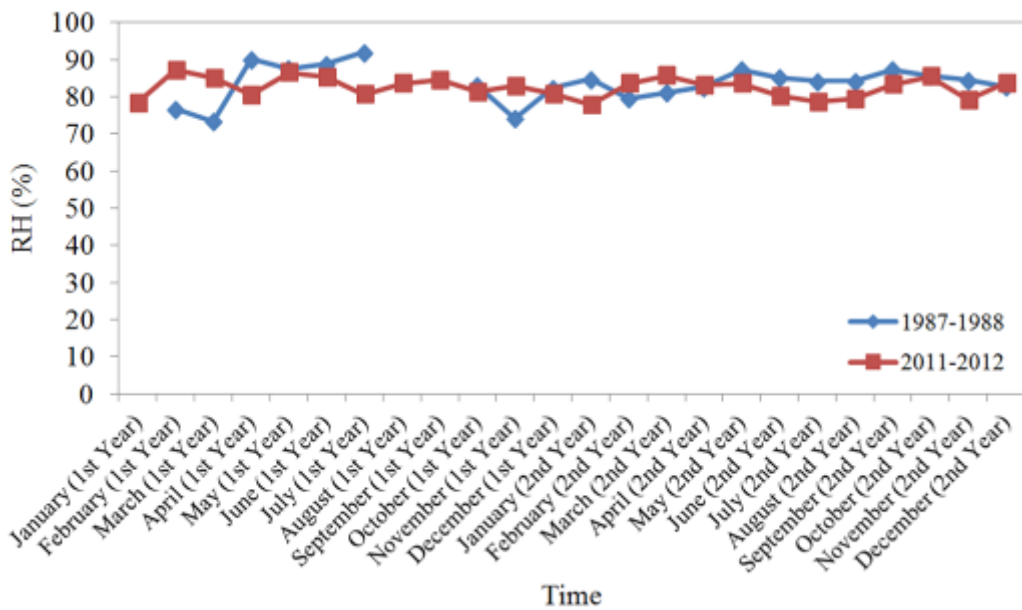


Figure A92. Comparison of relative humidity in the periods of 1987 – 1988 and 2011 – 2012 for Greymouth

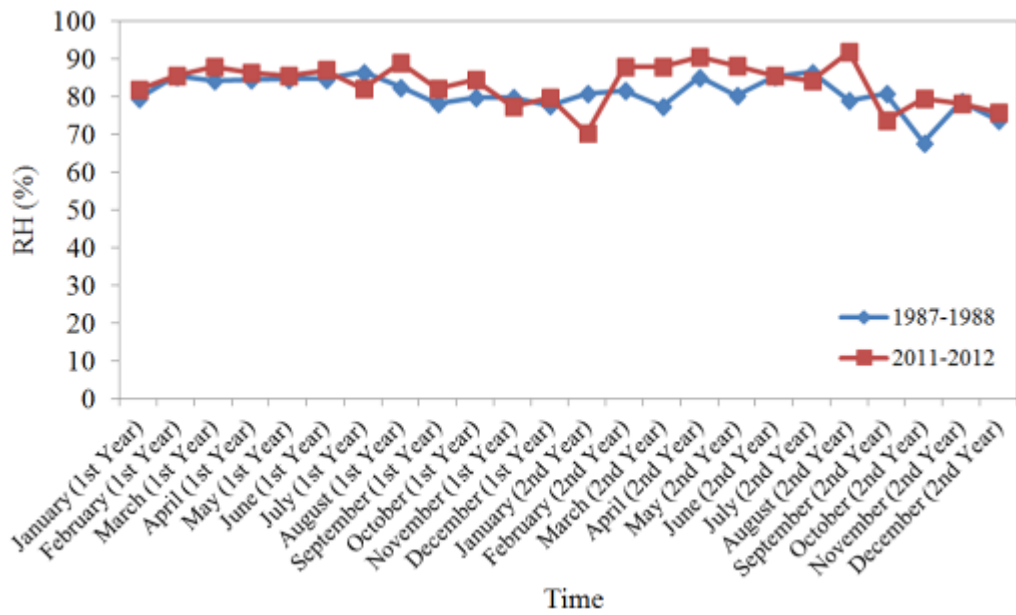


Figure A93. Comparison of relative humidity in the periods of 1987 – 1988 and 2011 – 2012 for Dunedin Airport

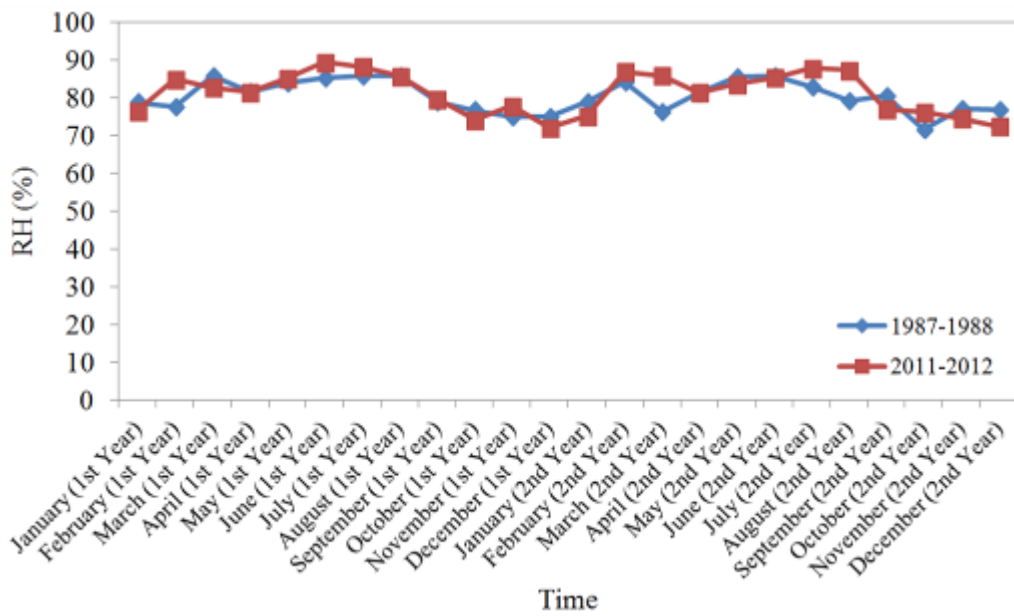


Figure A94. Comparison of relative humidity in the periods of 1987 – 1988 and 2011 – 2012 for Invercargill Airport

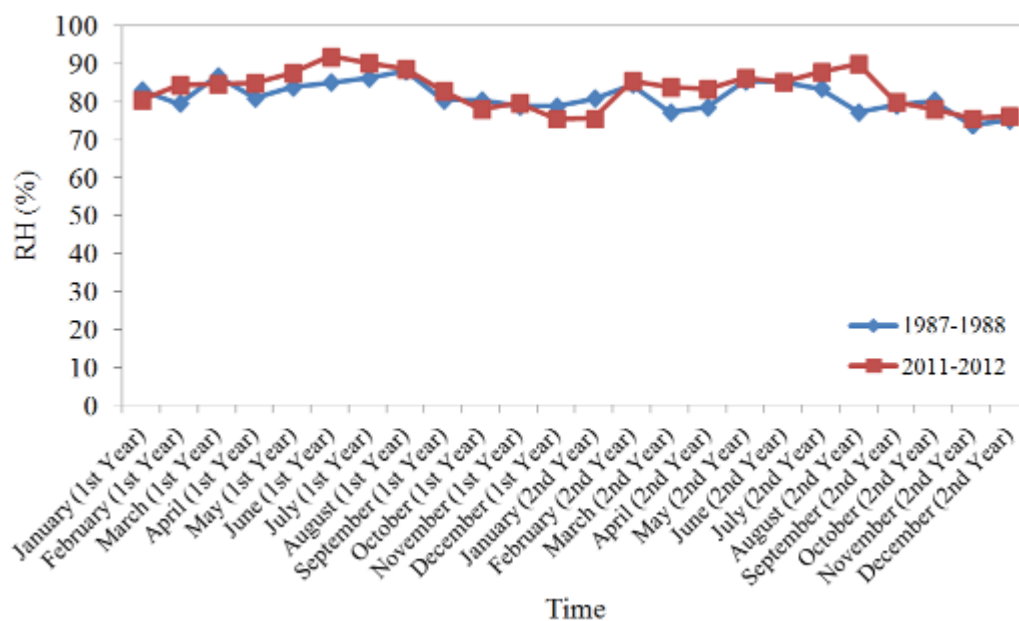


Figure A95. Comparison of relative humidity in the periods of 1987 – 1988 and 2011 – 2012 for Tiwai Point

A.2.4 Wind Speed

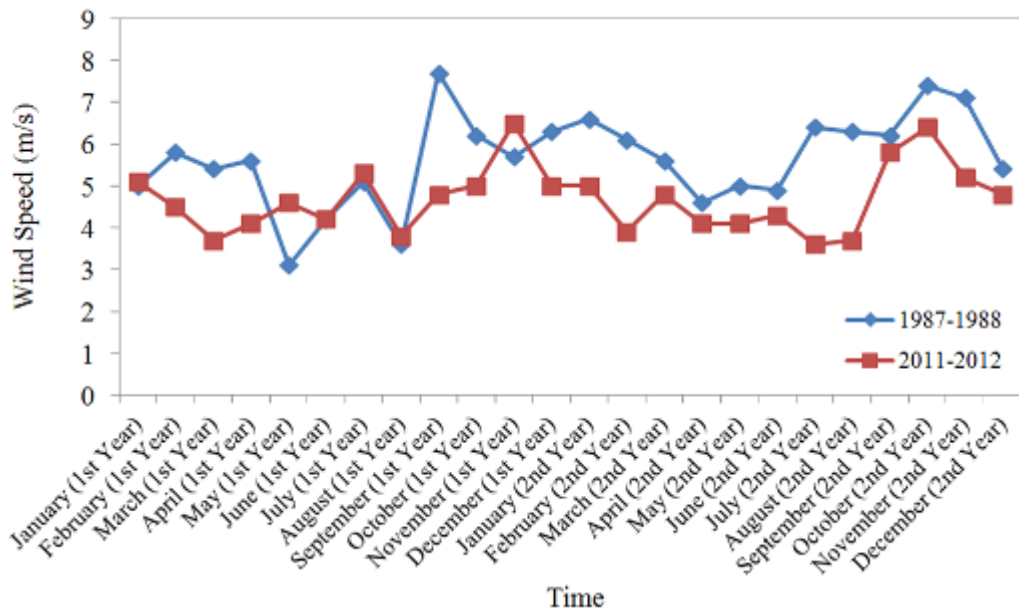


Figure A96. Comparison of wind speed in the periods of 1987 – 1988 and 2011 – 2012 for Auckland Airport

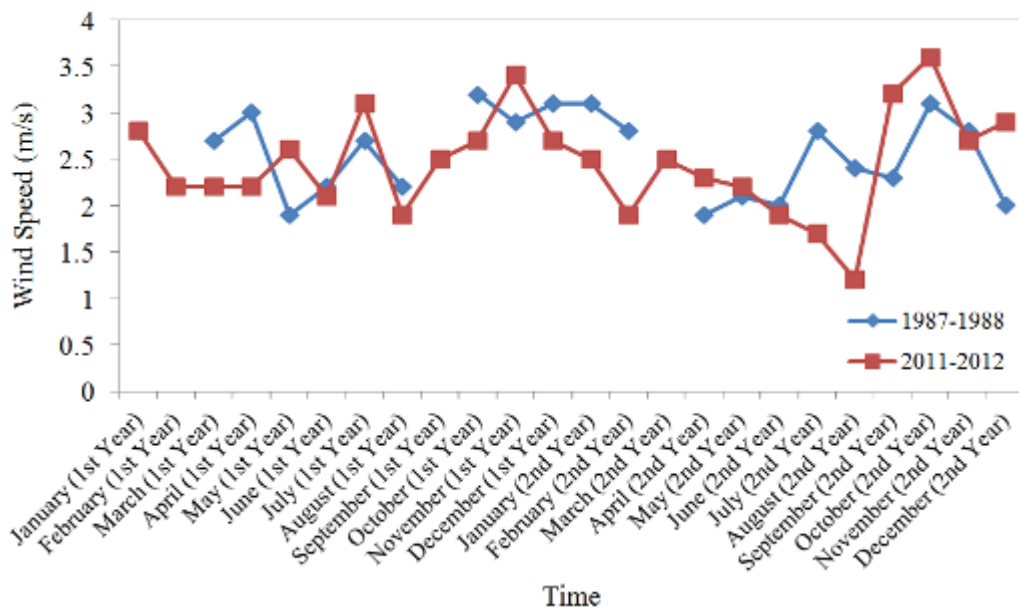


Figure A97. Comparison of wind speed in the periods of 1987 – 1988 and 2011 – 2012 for Pukekohe

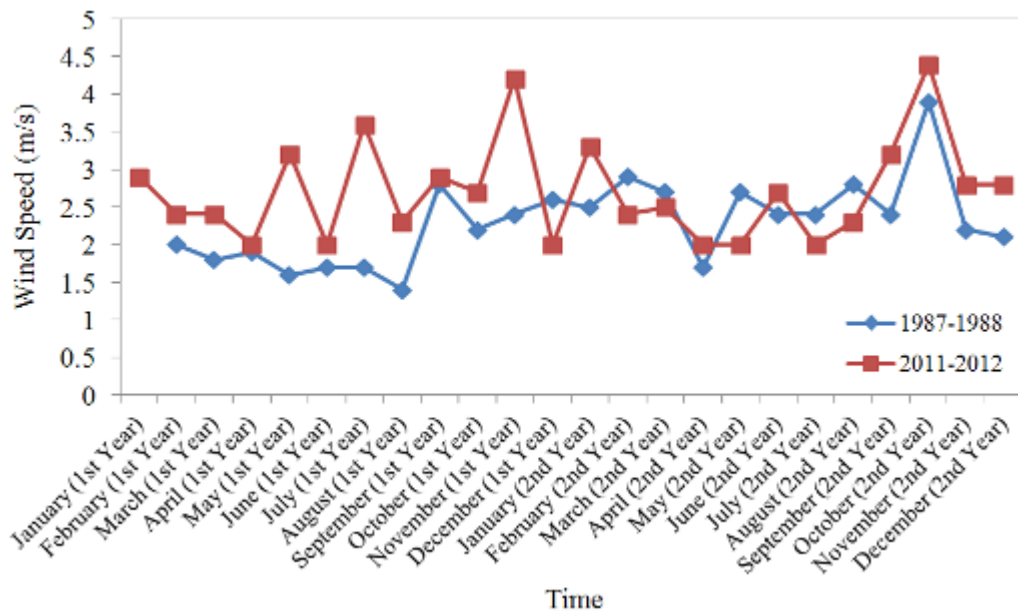


Figure A98. Comparison of wind speed in the periods of 1987 – 1988 and 2011 – 2012 for Levin

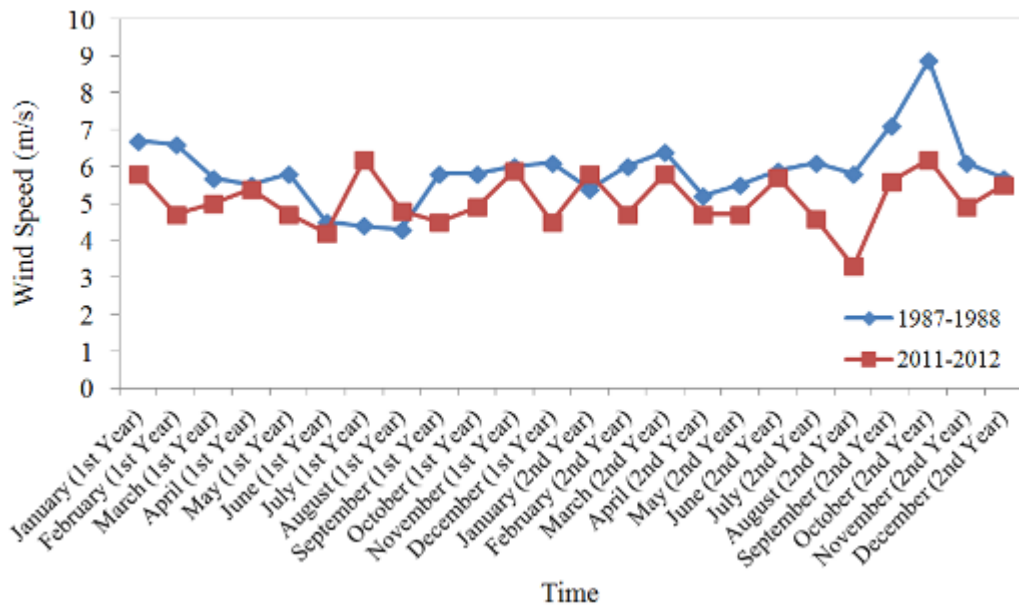


Figure A99. Comparison of wind speed in the periods of 1987 – 1988 and 2011 – 2012 for Kelburn (Wellington)

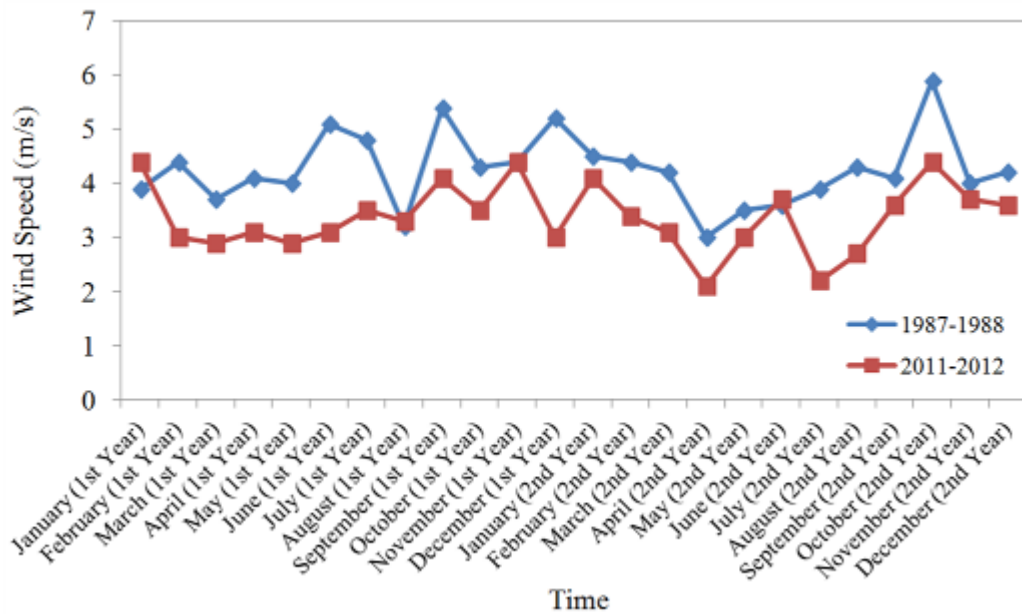


Figure A100. Comparison of wind speed in the periods of 1987 – 1988 and 2011 – 2012 for Dunedin Airport

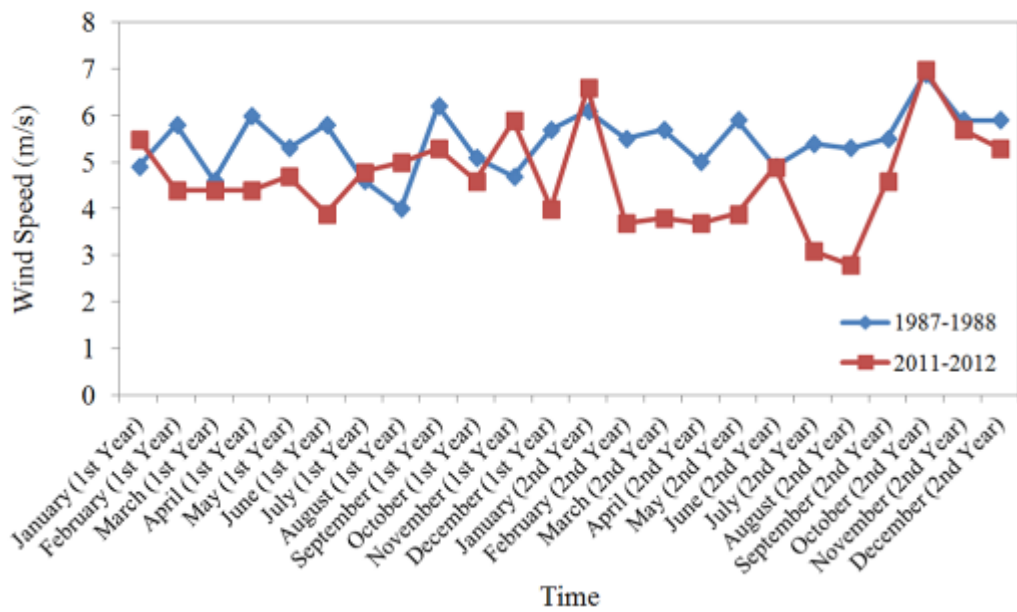


Figure A101. Comparison of wind speed in the periods of 1987-1988 and 2011-2012 for Invercargill Airport

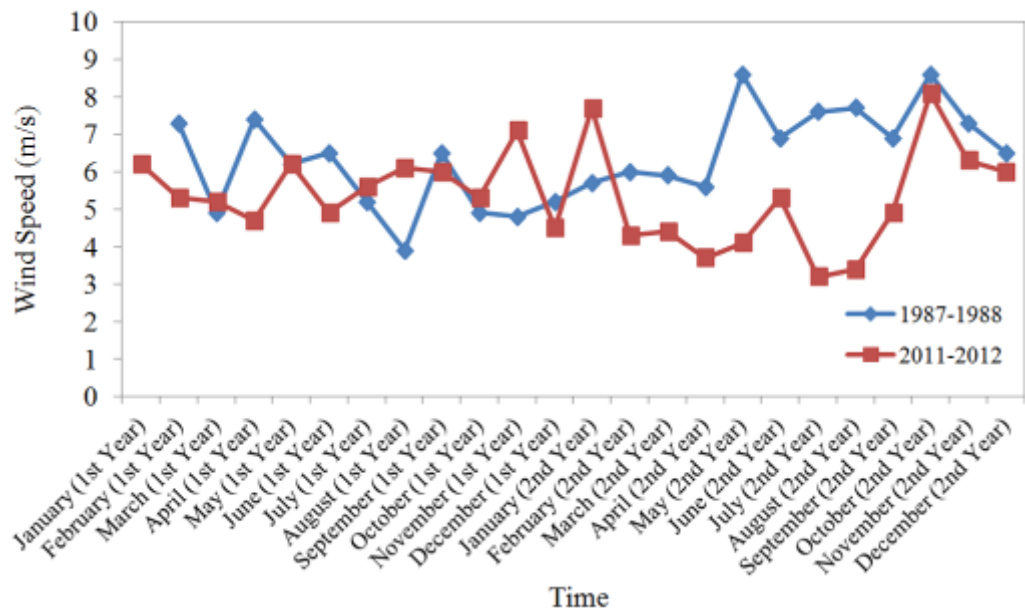


Figure A102. Comparison of wind speed in the periods of 1987 – 1988 and 2011 – 2012 for Tiwai Point